UNIVERSITEIT VAN PRETORIA
UNIVERSITY OF PRETORIA
YUNIBESITHI YA PRETORIA

RELIABILITY-BASED SLOPE STABILITY ANALYSIS AND ASSOCIATED SEVERITY OF FAILURE OF TAILINGS DAMS

SCOTT MARK GOVER

A project dissertation submitted in partial fulfilment for the requirements for the degree of

MASTER OF ENGINEERING (GEOTECHNICAL ENGINEERING)

In the

FACULTY OF ENGINEERING

UNIVERSITY OF PRETORIA

November 2014

© University of Pretoria

PROJECT DISSERTATION SUMMARY

RELIABILITY-BASED SLOPE STABILITY ANALYSIS AND ASSOCIATED SEVERITY OF FAILURE OF TAILINGS DAMS

SCOTT MARK GOVER

Supervisor: Professor G Heymann
Department: Civil Engineering
University: University of Pretoria
Degree: Master of Engineering (Geotechnical Engineering)

Slope stability analysis is crucial to the design of every new tailings storage facility, and while deterministic methods such as limit-equilibrium analysis are the most widely used method of analysis, the safety factors produced by them are ultimately difficult to comprehend for non-engineers and are often applied unknowingly to conditions involving widely varying degrees of uncertainty. There is, therefore, an increasing trend towards the determination of probabilities of failure in addition to safety factors to assess slope stability.

The most common method of statistical analysis within the engineering field has historically been the Monte-Carlo method due to its conceptual simplicity, and reliability-based analysis has up until recently had little practical usage due to its computational and conceptual barriers.

This dissertation compares pre-programmed probability methods available in “off-the-shelf” slope stability packages to various reliability-based analysis methods. Each of these methods is applied to several embankments/ waste facilities, specifically selected and configured to investigate a wide range of safety factors, probabilities of failure and the effect of material uncertainty.

Based on the results of the analysis, and the discussions in the literature review, a suitable reliability-based analysis method is selected to be implemented in the remaining analyses and experiments.

© University of Pretoria

Consequence of failure is not often thoroughly assessed in early stages of design and is usually only quantified by the engineering judgement of experienced practitioners. This is generally done using only the critical failure surface returned in the limit-equilibrium analysis, and while larger failure surfaces may indeed have higher safety factors, their associated probability of failure may be unacceptable for that specific size of failure.

Furthermore, the prescribed limits of acceptable probabilities of failure do not take into account the complex behaviour of tailings (such as the potential for liquefaction and flow to occur) and are, additionally, presented against the potential number of fatalities caused by failure which is considered inappropriate for the assessment of consequence of failure of tailings storage facilities.

This dissertation therefore also introduces the concept of measuring ‘severity’ of failure and ‘slope performance’, which takes into account the effect material uncertainty has on the probability of failure of slip surfaces smaller and larger than the critical slip surface, and limits of acceptable, intermediate and unacceptable probabilities of failure are proposed in order to provide a completely objective assessment of whether the performance of a facility is acceptable.

© University of Pretoria

UNIVERSITEIT VAN PRETORIA
UNIVERSITY OF PRETORIA
YUNIBESITHI YA PRETORIA

DECLARATION

I, the undersigned hereby declare that:

- I understand what plagiarism is and I am aware of the University's policy in this regard;
- The work contained in this thesis is my own original work;
- I did not refer to work of current or previous students, lecture notes, handbooks or any other study material without proper referencing;
- Where other people's work has been used this has been properly acknowledged and referenced;
- I have not allowed anyone to copy any part of my thesis;
- I have not previously in its entirety or in part submitted this thesis at any university for a degree.

DISCLAIMER:

The work presented in this report is that of the student alone. Students were encouraged to take ownership of their projects and to develop and execute their experiments with limited guidance and assistance. The content of the research does not necessarily represent the views of the supervisor or any staff member of the University of Pretoria, Department of Civil Engineering. The supervisor did not read or edit the final report and is not responsible for any technical inaccuracies, statements or errors. The conclusions and recommendations given in the report are also not necessarily that of the supervisor, sponsors or companies involved in the research.

Signature of student: _____

Name of student: Scott Gover

Student number: 10607596

Date: 19 March 2015

Number of words in report: 24 036 words

© University of Pretoria

ACKNOWLEDGEMENT

I wish to express my appreciation to the following organisations and persons who made this project dissertation possible:

a) Golder Associates Africa (Pty) Ltd for financial support and the provision of their slope stability application license during the course of the study.

b) Professor Gerhard Heymann, my supervisor, for his guidance and support. His enthusiasm for the field of geotechnical engineering is an inspiration and his ability to teach is second to none.

c) My family Clare, Zach, and Toby who are my motivation to better myself and put up with the long hours of study.

d) My parents and sister for their encouragement and support, particularly my dad who lets me talk his ear off about this so often.

e) Ronald Abbas for setting the bar of achievement so high for me to aim at.

© University of Pretoria

TABLE OF CONTENTS

1.0 INTRODUCTION 1-1
1.1 Background 1-1
1.2 Objectives of the Study 1-3
1.3 Scope of the Study 1-3
1.4 Methodology 1-5
1.5 Organisation of the Report 1-6
2.0 LITERATURE REVIEW 2-1
2.1 Principles of Tailings Dam Design 2-1
2.2 Probability Terminology 2-3
2.3 Geotechnical Materials Variability 2-5
2.4 Reliability-Based Analysis 2-8
2.4.1 History of Reliability-Based Analysis 2-8
2.4.2 Reliability Concept 2-9
2.4.3 The First Order Second Moment (FOSM) method 2-12
2.4.4 The Second Order Second Moment (SOSM) method 2-13
2.4.5 The Hasofer-Lind/ First Order Reliability Method (FORM) 2-13
2.4.6 Application of Reliability-Based Analysis to Slope Stability 2-17
2.5 Other Statistical Methods 2-18
2.5.1 The Point Estimate method 2-18
2.5.2 Monte Carlo Simulation 2-19
2.6 Consequence of Failure 2-21
2.6.1 Measurement of Consequence of Failure 2-21
2.6.2 Acceptable Probabilities of Failure 2-22
2.7 Summary of the Literature Review 2-25
3.0 EXPERIMENTAL DESIGN 3-1
3.1 Design Scope 3-1
3.2 Limit-Equilibrium Methodology and Assumptions 3-3
3.3 Probabilistic Analysis Methodology 3-6
3.3.1 Classical Monte Carlo Simulation 3-6
3.3.2 Modified Monte Carlo Analysis 3-7
3.3.3 FOSM Method 3-8
3.3.4 Simplified FOSM Method 3-9
3.3.5 Low and Tang (2004) FORM method 3-10
3.3.6 Low and Tang (2007) FORM method 3-11
3.3.7 Analysis Automation 3-13
3.4 Probabilistic Assumptions 3-13
4.0 APPLICATION OF RELIABILITY-BASED ANALYSIS METHODS 4-1
4.1 Stability Model Configurations 4-1
4.1.1 Case 1 - Embankment Dam on Clay Foundation No.1 4-1

© University of Pretoria

4.1.2 Case 2 - Embankment Dam on Clay Foundation No.2 4-2
4.1.3 Case 3 - Waste Rock Dump No.1 4-3
4.1.4 Case 4 - Waste Rock Dump No.2 4-4
4.1.5 Case 5 - Cycloned Slurry Dam No.1 4-5
4.1.6 Case 6 - Cycloned Slurry Dam No.2 4-6
4.1.7 Case 7 - Upstream Coal Rejects Facility 4-7
4.2 Analysis Results 4-8
4.3 Analysis Observations and Discussion 4-10
4.3.1 Safety Factors 4-10
4.3.2 Monte Carlo Methods 4-10
4.3.3 Reliability-Based Methods 4-11
4.3.4 Level of Uncertainty 4-12

5.0 'SEVERITY' OF FAILURE 5-1

5.1 'Severity' Concepts 5-2
5.2 Scope of the Analysis 5-4
5.3 Analysis Methodology 5-5
5.4 Analysis Results 5-8
5.5 Development of Performance Limits 5-9
5.6 Analysis Observations and Discussion 5-13
5.6.1 'Slope Performance' Curves 5-13
5.6.2 1:2 Slope Angle 5-13
5.6.3 1:2.5 Slope Angle 5-14
5.6.4 1:3 Slope Angle 5-14
5.6.5 Intermediate Zone 5-15

6.0 EXPERIMENT NO.1 – APPLICATION OF SEVERITY CHART 6-1

6.1 Scope of the Experiment 6-1
6.2 Experiment Methodology 6-1
6.3 Experiment Results 6-3
6.4 Experiment Observations and Discussion 6-5

7.0 EXPERIMENT NO.2 – RELATIONSHIP BETWEEN SAFETY FACTOR AND PROBABILITY OF FAILURE 7-1

7.1 Scope of the Experiment 7-1
7.2 Experiment Methodology 7-1
7.3 Experiment Results 7-3
7.4 Experiment Observations and Discussion 7-4
7.4.1 Results Analysis 7-4
7.4.2 Comparison to Published Data 7-6

8.0 DISCUSSION 8-1
9.0 CONCLUSIONS 9-1
10.0 REFERENCES 10-1

© University of Pretoria

LIST OF TABLES

Table 2.1: COV data for geotechnical materials pertinent to the study 2-7
Table 2.2: Properties of some typical residues (Chamber of Mines South Africa, 1996)..... 2-7
Table 4.1: Embankment dam on clay foundation No.1 - Material parameters 4-1
Table 4.2: Embankment dam on clay foundation No.1 - Material parameters 4-2
Table 4.3: Waste rock dump No.1 - Material parameters 4-3
Table 4.4: Waste rock dump No.2 - Material parameters 4-4
Table 4.5: Cycloned slurry dam No.1 - Material parameters 4-5
Table 4.6: Cycloned slurry dam No.2 - Material parameters 4-6
Table 4.7: Upstream coal rejects facility - Material parameters..... 4-7
Table 4.8: Summary of results - review of reliability-based analysis methods 4-8
Table 5.1: Material parameters used in the analysis..... 5-5
Table 5.2: Summary of results – severity of failure 5-8
Table 6.1: Experiment No.1 material properties – cycloned slurry facility V1 6-2
Table 6.2: Experiment No.1 material properties – cycloned slurry facility V2 6-2
Table 6.3: Summary of Experiment No.1 results 6-4
Table 7.1: Experiment No.2 material properties – uniform embankment 7-2
Table 7.2: Summary of Experiment No.2 results 7-3
Table 7.3: Chowdhury (1978) relationship of safety factor and probability of failure 7-7

© University of Pretoria

LIST OF FIGURES

Figure 1.1: Illustration of the effect of uncertainty on the distribution of safety factors 1-1
Figure 2.1: Upstream raising of a TSF 2-3
Figure 2.2: Centreline raising of a TSF 2-3
Figure 2.3: Downstream raising of a TSF 2-3
Figure 2.4: Probability density distribution for a safety margin (M) 2-10
Figure 2.5: Probability density function for safety factor (F) 2-10
Figure 2.6: Illustration of (Low & Tang, 1997) expanding ellipsoid perspective 2-15
Figure 2.7: Risk for selected engineering projects (Whitman, 1984) 2-22
Figure 2.8: Societal risk reference guideline (ANCOLD, 2003) 2-23
Figure 2.9: Risk tolerance chart for an engineered facility (Phoon, 2008) 2-24
Figure 3.1: Spreadsheet formulation of Low & Tang (2004) FORM method 3-10
Figure 3.2: Spreadsheet formulation of Low & Tang (2007) FORM method 3-12
Figure 4.1: Embankment dam on clay foundation No.1 - Model geometry 4-1
Figure 4.2: Embankment dam on clay foundation No.2 - Model geometry 4-2
Figure 4.3: Waste rock dump No.1 - Model geometry 4-3
Figure 4.4: Waste rock dump No.2 - Model geometry 4-4
Figure 4.5: Cycloned slurry dam No.1 - Model geometry 4-5
Figure 4.6: Cycloned slurry dam No.2 - Model geometry 4-6
Figure 4.7: Upstream coal rejects facility - Model geometry 4-7
Figure 4.8: Comparison of automated and reliability-based analysis methods 4-9
Figure 4.9: Extract of Figure 4.8 highlighting the increasing level of conservatism 4-11
Figure 4.10: Extract of Figure 4.8 highlighting the effect of uncertainty 4-12
Figure 5.1: Illustration of the measurement of 'severity' 5-3
Figure 5.2: Model construction - gold tailings dam at 1:2 slope 5-6
Figure 5.3: Model construction - gold tailings dam at 1:2.5 slope 5-6
Figure 5.4: Model construction - gold tailings dam at 1:3 slope 5-6
Figure 5.5: Organogram summarising the model configurations 5-7
Figure 5.6: Analysis results presented as severity versus probability of failure 5-9
Figure 5.7: Acceptability assessment of 1:3 slope with 10% COV - Small 5-11
Figure 5.8: Acceptability assessment of 1:3 slope with 10% COV - Global Minimum 5-11
Figure 5.9: Acceptability assessment of 1:3 slope with 10% COV - Medium 5-11
Figure 5.10: Acceptability assessment of 1:3 slope with 10% COV - Large 5-12
Figure 5.11: Analysis results on the Severity Chart 5-12
Figure 5.12: Extract of Figure 5.11 showing the 1:3 slope with 10% COV 5-15

© University of Pretoria

Figure 6.1: Experiment No.1 model configuration - cycloned slurry facility 6-2
Figure 6.2: Experiment No.1 results presented on severity chart 6-4
Figure 6.3: Critical deterministic and probabilistic failure surfaces 6-6
Figure 6.4: Critical probabilistic failure surface included in 'slope performance' curve 6-7
Figure 7.1: Experiment No.2 model configuration – uniform embankment 7-2
Figure 7.2: Experiment No.2 - uncertainty trend curves 7-4
Figure 7.3: Extract of Figure 7.2 highlighting slurry dam curves 7-5
Figure 7.4: Illustration of the effect of uncertainty on the distribution of safety factors 7-6
Figure 7.5: Extract of Figure 7.2 with published data superimposed 7-7
Figure 8.1: Illustration of the measurement of 'severity' 8-3
Figure 8.2: 'Severity' chart with proposed limits 8-5

© University of Pretoria

LIST OF SYMBOLS

SF	Safety Factor
pdf	Probability density function
p_f	Probability of failure
TSF	Tailings storage facility
COV	Coefficient of variation
σ	Standard deviation of the parameter
μ	Average, mean (also E[x])
SPT	Standard penetrometer test
Q	Load
R	Resistance
M	Safety margin
β	Reliability Index
g(x)	Performance function
$Cov(x_i,x_j)$	Covariance
$\rho(x_i,x_j)$	Correlation coefficient
$\boldsymbol{x}$	Vector representing the set of random variables, x_i
$\boldsymbol{\mu}$	Vector representing the set of mean values, μ_i
$\boldsymbol{C}$	Covariance matrix
$\boldsymbol{R}$	Correlation matrix
F	Failure region
R	Radius of the ellipsoid touching the failure surface
r	Radius of the one-standard-deviation dispersion ellipsoid
$\boldsymbol{n}$	Vector of n_i dimensionless variables
$\Phi(n_i)$	Standard normal cumulative distribution
c'	Effective cohesion
b	Slice width
W	Slice weight
u	Pore pressure
ϕ'	Effective friction angle
α	Angle of slice base
σ_{MC}	Standard deviation calculated from the Monte-Carlo data
x_i	ith value of the parameter
N	Number of Monte Carlo trials

© University of Pretoria

1.0 INTRODUCTION

1.1 BACKGROUND

Slope stability analysis is crucial to the design of every new tailings storage facility, whether carried out carried out using simple empirical methods, or through the use of more sophisticated techniques such as traditional limit-equilibrium methods and numerical methods (finite elements analysis, distinct element analysis etc.). Of these methods, limit-equilibrium analysis is still the most widely used method of analysis due to its simplicity and the level at which the theory/ mechanics are understood.

Notwithstanding this, the safety factors produced using the deterministic limit-equilibrium approach are ultimately difficult to comprehend for non-engineers and are often applied unknowingly to conditions involving widely varying degrees of uncertainty. This is best illustrated by Figure 1.1, where a distribution of safety factors calculated for a slope with high uncertainty in the input parameters has a higher mean safety factor, but also a higher probability of failure, than a second slope comprising lower uncertainty in the input parameters. There is, therefore, an increasing trend towards the determination of probabilities of failure in addition to safety factors to thoroughly assess slope stability.

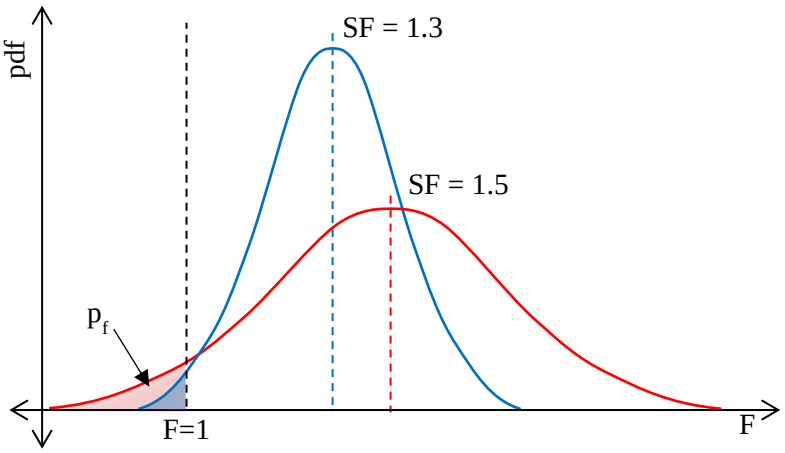


Figure 1.1: Illustration of the effect of uncertainty on the distribution of safety factors

The most common method of statistical analysis within the engineering field has historically been the Monte Carlo method due to its conceptual simplicity, and reliability-based analysis has until recently had little practical usage due to its computational and conceptual barriers. Put simply, reliability theory involves terms and concepts that are not familiar to most

© University of Pretoria

geotechnical engineers, and it is a common misperception that more data, time and effort is required for reliability-based analyses than is available in most instances.

Irrespective of the probabilistic method utilised in the slope stability analysis, increased computational effort is required to find the critical slip surface for each random simulation of shear strength parameters. This increased computational effort can be in the order of 2 hours per 10 000 simulations for a typical Monte Carlo analysis. A common simplification is, therefore, to use the critical deterministic failure surface only, but this evokes a philosophical contradiction since the shape of the surface is dependent on the combination of cohesion and friction angle (deeper surfaces for lower friction angle- higher cohesion- combinations, and visa-versa) and a high number of unlikely simulations are therefore performed, possibly skewing the result. A method of carrying out probabilistic slope stability analysis, which satisfies both the above philosophical issue and the computational requirements of practising engineers, is therefore required.

Consequence of failure is not often thoroughly assessed in early stages of design and is usually only quantified by the engineering judgement of experienced practitioners. This is generally done using only the critical failure surface returned in the limit-equilibrium analysis, and while larger failure surfaces may indeed have higher safety factors, their associated probability of failure may be unacceptable for that specific size of failure. These potential situations are often possible when analysing the stability of dams comprising cohesionless materials, i.e. the majority of tailings materials.

Furthermore, the limits which have been prescribed for acceptable probabilities of failure, by sources such as (ANCOLD, 2003), do not take into account the complex behaviour of tailings (such as the potential for liquefaction and flow to occur) and are, additionally, presented against the potential number of fatalities caused by failure which is considered inappropriate for the assessment of consequence of failure of tailings storage facilities.

An opportunity therefore exists to implement a completely objective assessment of the size of the failure, and how severe this failure is compared the size of the facility, before considering the many complex aspects affecting the consequence of failure, and using this information in the early decision making regarding the overall performance of the facility.

© University of Pretoria

1.2 OBJECTIVES OF THE STUDY

The objectives of this study are defined as follows:

- Review reliability-based analysis methods and their application to slope stability analysis;
- Select an appropriate reliability-based analysis method to investigate the effect uncertainty has on the probability of failure of slip surfaces smaller and larger than the critical failure surface determined in the limit-equilibrium analysis;
- Introduce the concept of 'severity' of failure as an alternative/ precursor to measuring consequence of failure of tailings storage facilities;
- Extend the 'severity' concept to the concept of 'slope performance' as a measure of the overall performance of a facility, and a possible alternative to the computationally extensive search for the critical probabilistic failure surface;
- Propose limits of acceptable performance for respective 'severities';
- Investigate the suitability, or application, of measuring 'severity' of failure and 'slope performance' using the proposed acceptable performance limits; and
- Explore whether a relationship between safety factors and probabilities of failure can be established for a certain level of uncertainty.

1.3 SCOPE OF THE STUDY

The dissertation reviews the available reliability-based analysis methods and applies them to slope stability analysis of tailings storage facilities. A literature study is carried out on the design of tailings storage facilities and the methods of reliability-based analysis, including the associated concepts of probability of failure, consequence of failure and geotechnical materials variability. Various reliability-based methods are programed into Microsoft Excel and applied to slope stability analysis using the Bishops Simplified Method of Slices. Based on the results of the analysis, reliability-based analyses are implemented to investigate key aspects of the analysis of tailings storage facilities, as well as introduce and apply the concept of 'severity' of failure and 'slope performance'.

This study is based on the theoretical application of reliability-based analysis concepts and slope stability analysis in order to propose a more thorough, or comprehensive, analysis of tailings storage facilities comprising predominantly cohesionless materials. A chart of 'severity' versus Probability of Failure is presented with suggested limits of acceptable,

© University of Pretoria

intermediate and unacceptable probabilities. This proposed method (and chart) is then applied to a more complex, cycloned tailings facility, with underflow and overflow materials with some cohesion, to illustrate and discuss its suitability/ application.

The proposed severity concept is intended to be an alternative/ precursor to a typical consequence of failure assessment, and is expected to act as a tool for decision making early in the design process.

The concept of investigating various sizes of failure and their associated probability of failure to plot 'slope performance' curves is expected to have synergy with the more traditional, but computationally extensive, procedure of searching for the critical probabilistic failure surface (whereby the slip surface is varied for each trial cohesion and friction angle in the probabilistic analysis), and a simple verification exercise is therefore performed in this study to investigate whether a similar failure surface is returned in both analyses.

A number of key assumptions are made in order to streamline the computational efforts in the study, as well as simplify the interpretation of the effect of uncertainty on resulting probabilities of failure, the most pertinent of which are as follows:

- Only the critical failure surface returned within the search limits of the limit-equilibrium analyses was analysed in the probabilistic analyses;
- The distribution of the shear strength parameters (cohesion and friction angle) are assumed to be normally distributed; and
- Only knowledge uncertainty is considered in the probabilistic analyses.

The above assumptions are discussed in more detail, together with the remaining assumptions applied in the analyses, in Section 2.0 and Section 3.0.

Time related (random) failure events, such as earthquakes and 1 in 100 year rainfall events, are not considered in the analysis as these obscure the interpretation of 'Probability of Failure'. Events such as these would, in practice, typically be considered when analysing the probability of failure for the full lifetime of a tailings storage facility. The analysis carried out in this study therefore considers only the post-operation/ pre-closure period of a tailings storage facility and probabilities of failure are presented per annum.

© University of Pretoria

1.4 METHODOLOGY

The methodology of the study is summarised as follows:

- Carry out a literature review of tailings design concepts, probability concepts, geotechnical materials variability, methods of reliability-based analysis (including the more common Monte Carlo and Point-Estimate methods) and consequence of failure.

- Review selected reliability-based methods programmed into Microsoft Excel and compare them to the Monte-Carlo and reliability methods pre-programmed into the Rocscience 2D limit-equilibrium analysis software, Slide 6.0.

- Using reliability-based analysis, investigate the effect material uncertainty has on the probability of failure of slip surfaces smaller and larger than the critical failure surface for a typical tailings storage facility (at various slope angles and varying uncertainty in the shear strength of the tailings);

- Introduce the concepts of ‘severity’ of failure and ‘slope performance’ in order to appropriately relate a size of failure to an acceptable probability of failure;

- Use the experiment data together with concepts presented in the literature review to propose limits of acceptable performance for the respective ‘severity’ of failure;

- Investigate and discuss the application of the suggested chart of ‘Severity’ versus Probability of Failure, and the proposed limits of acceptable performance, to a more complex, cycloned tailings storage facility;

- Verify whether the proposed concept of plotting ‘slope performance’ returns similar results to an overall probabilistic analysis (whereby the search for the critical probabilistic failure surface is carried out for each Monte Carlo simulation); and

- Explore whether a relationship between safety factors and probabilities of failure can be established for a certain level of uncertainty, regardless of the slope configurations and material properties.

© University of Pretoria

1.5 ORGANISATION OF THE REPORT

The dissertation consists of the following chapters:

- Chapter 1 serves as an introduction to the study;
- Chapter 2 entails the literature review and introduction to certain principles used in the dissertation;
- Chapter 3 presents the experimental design and outlines the methodology used in the various experiments;
- Chapter 4 reviews the different reliability-based methods and their application to slope stability analysis;
- Chapter 5 investigates the effect material uncertainty has on the probability of failure of slip surfaces smaller and larger than the critical failure surface, and introduces the concepts of 'severity' of failure and 'slope performance', and suggests limits of acceptable performance;
- Chapter 6 applies the concepts introduced in Chapter 5 to a cycloned tailings facility and serves as the discussion of the proposed concepts of 'severity' and 'slope performance';
- Chapter 7 explores whether a relationship between safety factors and probabilities of failure can be established for a certain level of uncertainty;
- Chapter 8 serves as a summary of the discussions presented in Chapters 4 to 7;
- Chapter 9 contains the conclusions and recommendations of the study; and
- Chapter 10 contains the references for the dissertation.

The appendices attached to the dissertation are summarised as follows:

- Appendix A contains the results of the analysis carried out in Chapter 4;
- Appendix B contains the results of the analysis carried out in Chapter 5;
- Appendix C contains the results of the analysis carried out in Chapter 6; and
- Appendix D contains the results of the analysis carried out in Chapter 7.

© University of Pretoria

2.0 LITERATURE REVIEW

2.1 PRINCIPLES OF TAILINGS DAM DESIGN

Tailings are a waste product consisting of ground rock and process effluents that are generated by the mine processing plant once the desired product/ commodity has been extracted from the ore. This process of product extraction is never 100% efficient, nor is it possible to recover all the processing reagents and chemicals. The unrecoverable metals, minerals, chemicals, organics and process water are therefore discharged, normally as slurry, to a final storage facility commonly known as a Tailings Storage Facility (TSF).

A typical TSF generally comprises the following components (McPhail & Wagner, 2002):

- Containment wall or toewall usually comprising engineered soils, to contain the tailings either as a total confining structure or during the early development of the facility.
- Underdrainage system of filter drains to control seepage within the facility and draw down the phreatic surface.
- Decant system to facilitate the removal of water accumulated on the facility. Examples are a penstock or floating barge.
- Delivery system comprising pipes, valves and discharge points to convey the slurry to the facility for deposition.
- Return water system consisting of dams, sumps, pumps and pipelines for holding and conveying excess effluent and water from the TSF back to the plant.
- Stormwater diversion system of trenches and bunds constructed around the facility to control and divert external stormwater.
- Stormwater catchment paddocks constructed around the toe of the facility to collect and store stormwater and sediment eroded from the facility.
- Ancillary system comprising access roads and power supply system.

The grain size distribution of tailings materials varies from fine sand to clay-sized particles depending on the characteristics of the ore and mill process (Messrs, et al., 1989). The method of disposal of hydraulically placed tailings is dependent on various aspects, such as solids content and density, but is particularly dependent on the distribution of the particle size fractions and the tendency of the tailings to segregate.

© University of Pretoria

A well-graded tailings material with a particle size distribution ranging from fine sand to clay, such as is common with copper and platinum tailings, will segregate rapidly while a uniform product such as gold tailings, which is predominantly silt sized, will have a much reduced tendency to segregate. Copper and platinum tailings would therefore be more suitable to being deposited by cycloning, while gold tailings would be more suitable to the paddock system of deposition. The most common tailings deposition methods are described below.

Paddock System:

The paddock system of tailings deposition involves raising the outer wall of the facility by controlled deposition of tailings, typically in layers not exceeding 150mm, which is carried out during the day to allow for evaporation and desiccation (and therefore densification and strengthening) of the tailings. During the night shift, the tailings are subsequently deposited into the interior of the dam behind the walls formed during the day. This method is particularly suited to semi-arid and temperate climates where evaporation is higher than precipitation. The impoundment wall (commonly referred to as the ‘day wall’) is raised in an upstream direction.

Cycloning:

The aim of cycloning is to segregate the tailings into coarse underflow materials with low water content, and fine overflow materials with high water content and good flow characteristics. The objective is to use the underflow to create the impoundment, within which the overflow is deposited. The lower moisture and fines content, as well as improved drainage characteristics, results in the underflow material having higher shear strength properties than the overflow materials. Using this method, the underflow impoundment can be developed in an upstream, centreline or downstream manner (or a combination thereof).

Spigotting:

Spigotting is another method of tailings deposition that aims to segregate the tailings material. This is achieved by discharging the tailings through multiple spigots along a delivery line, thereby increasing the discharge velocity which allows the coarse particles to settle under gravitation while the fine particles remain in suspension and are deposited in the pond. This method is limited to upstream development of the impoundment wall.

© University of Pretoria

Upstream, Centreline and Downstream Construction:

The impoundment walls described in the three deposition methods above are typically raised in an upstream, centreline or downstream method relative to the initial containment wall. This is depicted in Figures 2.1 to 2.3 below:

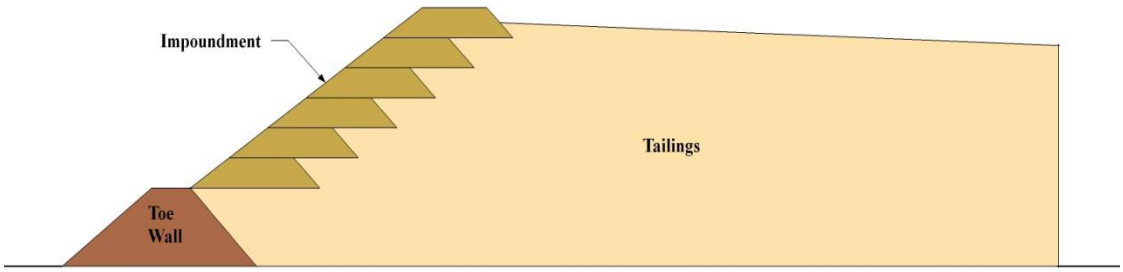


Figure 2.1: Upstream raising of a TSF

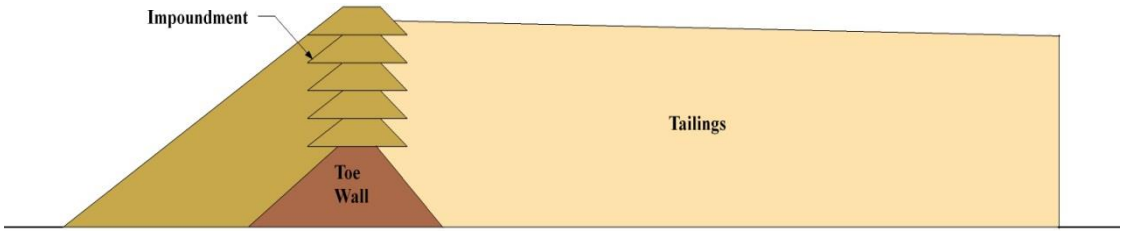


Figure 2.2: Centreline raising of a TSF

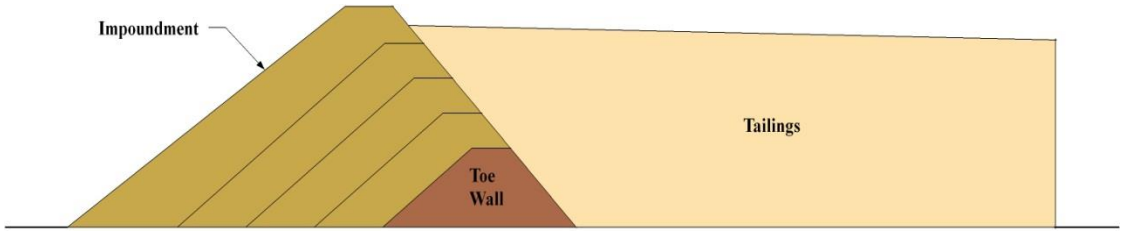


Figure 2.3: Downstream raising of a TSF

2.2 PROBABILITY TERMINOLOGY

When using terms such as ‘uncertainty’, ‘chance’, ‘random’ and ‘probability of failure’, the typical geotechnical engineer may implicitly believe they understand the definition of these terms, yet are unaware of some of the philosophical issues underlying them. It is only once more thought is put into their meaning that certain of these conflicting ideas become apparent, and it was therefore deemed necessary to define these terms in the context in which they have been applied in this dissertation.

© University of Pretoria

Randomness and uncertainty:

- Randomness, or a random event, is assumed to be caused by chance and is unpredictable. Examples of random events include natural processes such as earthquakes or severe rainfall events. Individual events such as these may be completely unpredictable, except in the relative frequencies in which they occur, i.e. the collective history of the events over a long period could have a regular pattern.

- Uncertainty is something unknown or unverified, but not unpredictable. It is the strength of opinion or degree of belief in something, and is dependent on qualitative assessment, reasoning and intuition. In geotechnical engineering, there are generally three categories of uncertainties, namely 'natural variability', 'knowledge uncertainty' and 'decision uncertainty' as described below.

Categories of uncertainty:

- Natural variability is the randomness of natural processes such as the spatial difference in ground conditions, geology or depth to the water table. In the context of this study, it could be the variability in the composition of the tailings material as a result of an inconsistent milling process.

- Knowledge uncertainty is the lack of data, information or understanding that limits our ability to model reality. In geotechnical engineering, this could be the uncertainty in the site investigation/ characterisation, the uncertainty in parameters derived from the inaccuracy in the testing procedure and limited sampling, and/ or the uncertainty in which the chosen model (mathematical or statistical) represents reality.

- Decision uncertainty is our inability to model social aspects such as the local community objectives, aversion to risk and/ or project planning timelines.

Note that for the purpose of this study, only knowledge uncertainty in the shear strength parameters of the tailings material is considered in the reliability-based analysis. Natural variability and decision uncertainty could, however, be included as an extension to the analyses.

© University of Pretoria

Probability of failure:

Just as uncertainty can be considered as both natural variability and degree of belief, so too can the concept of probability. Since the origin of modern probability theory in the 1600's, probability has been defined as either the relative frequency of occurrence in a large number of trials (commonly known as the Frequentist approach), or the degree of belief in the outcome of an event (commonly known as the Bayesian approach).

To illustrate this notion, consider a probability of failure of a tailings dam of 1%. This could be related to a 1% probability that the safety factors for the critical slip surface will be less than 1.0, or a probability of 1 out of every 100 similar tailings facilities failing. For engineering purposes, and particularly for the purpose of this dissertation, these two concepts, frequency and belief, complement one another and serve as a useful manner in which to conceptualise computed probabilities of failure.

Additionally, the effect of time is not explicitly referenced in calculated probabilities of failure, and is therefore expressed on an annual basis. Time-related probabilities of failure can, however, be included if the failure is assumed to apply for randomly occurring failure events such as earthquakes or 1:100 year rainfall events.

2.3 GEOTECHNICAL MATERIALS VARIABILITY

The evaluation of material properties is an important task of geotechnical engineering that differentiates it from other fields of engineering, particularly that of structural engineering. The variability of geotechnical materials is higher and more complex than, for example structural materials, and it therefore requires careful evaluation.

A useful means to represent variation in a parameter is by the coefficient of variation (COV), a dimensionless ratio that is independent of the units of the parameter and can therefore be used to compare the variations of many different parameters. The COV is calculated as follows:

$$COV = \frac{\sigma}{\mu}$$

Where,

σ = Standard deviation of the parameter

μ = Mean of the parameter

© University of Pretoria

An abundance of COV data for various geotechnical parameters has been gathered and published since the late 1960's; tabulated summaries of which can be found in (Baecher & Christian, 2003) for various soil types and based on various means of measurement (in-situ and laboratory testing methods).

A pertinent observation that is made from this data is that the COV for geotechnical materials is generally higher than for, say, structural materials, i.e. anything from 5% to 70% where structural materials generally have variations in the order of 10% to 20%. This can be attributed to both the natural variability present within the soil, and 'measurement error' which is a combination of factors such as sample disturbance, the accuracy of the testing method and equipment, and human error in the testing process.

To illustrate the impact 'measurement error' has on the uncertainty in geotechnical parameters, consider the degree of variation one might expect when evaluating the friction angle of a soil. Two extremes in accuracy exist whereby the friction angle could be determined by either triaxial testing or Standard Penetrometer Testing (SPT).

- Triaxial testing is understood to be highly accurate due to the controlled nature of the test and ability to accurately measure strains and pore pressures; whereas
- By virtue of the many factors affecting the energy transfer from the hammer to the soil in the SPT test (hammer type, sampler type, drill rod length, borehole diameter and overburden stress), the variation in the SPT N number achieved (which would be used to infer a friction angle) can be expected to vary by up to 100% between two separate SPT tests at the same location (CIRIA, 1995).

The COV for the friction angle could therefore be expected to be approximately 5% from the triaxial test and 15% to 20% from the SPT test.

For the purpose of this study, COV data for the cohesion and friction angle of geotechnical materials have been summarised from the available literature in Table 2.1 below:

© University of Pretoria

Table 2.1: COV data for geotechnical materials pertinent to the study

Property	Material	Source*	COV (%)
Friction angle for cohesionless materials	Sands	(Lumb, 1974), (Hoeg and Maruka, 1974), (Singh, 1971), (Schultze, 1975)	5 – 15
	Sands	(Lacasse and Nadim, 1996)	2 – 5
	Tailings	(Baecher et al., 1983)	5 – 20
Friction angle for cohesive materials		(Lumb, 1974), (Singh, 1971), (Schultze, 1975)	12 – 56
Cohesion		(Lumb, 1974), (Singh, 1971)	20 – 50

* Full information on the source references can be found in (Baecher & Christian, 2003)

Note that for the purpose of this study, the COV range for the friction angle of cohesive materials was not considered. Since the majority of materials modelled in the analyses are tailings materials, a COV range for the friction angle of 5% to 15% was generally considered.

Database of tailings shear strength parameters:

A statistical analysis of the properties of tailings materials in southern Africa was carried out by the Chamber of Mines in the 1970's. These were presented as average values for the strength and permeability parameters in Appendix XIV of "The Engineering Design, Operation and Closure of Matalliferous, Diamond and Coal Residue Deposits" (Chamber of Mines South Africa, 1996). Properties for the most common tailings materials in southern Africa are presented in Table 2.2 below:

Table 2.2: Properties of some typical residues (Chamber of Mines South Africa, 1996)

Residue	Classification according to grain size	Effective stress strength parameters	
		c' (kPa)	ϕ' (deg)
Coal duff	Gravelly sand	0	15°
Coal mine waste	Silty sand Gravel	0 8	28° 30°
Copper tailings	Clayey silt Sand	0	33° 33° to 37°
Gold tailings	Silt	0	35°
Kimberlite tailings	Clayey gravel Clayey silt	0 20	37° 22° to 32°
Platinum tailings	Silty sand to clayey silt	0	34° to 41°

© University of Pretoria

Distributions of material parameters:

The probability distribution within which the above materials exist in nature may be particular to each material type and could, additionally, differ from site to site. Given a sufficient amount of data, the correct distribution can be fitted using techniques such as the Maximum Likelihood method, but in the majority of geotechnical investigations there is insufficient data to fit an accurate distribution, and the distribution is therefore assumed.

There is some debate on which distributions best model different parameters, such as the lognormal distribution for cohesion which negates the possibility of negative values, but since assessing the effect of using certain distributions does not form part of the scope of this study, it assumed that the shear strength parameters can be suitably modelled using a Normal distribution, which is the most common distribution assumed in engineering.

(Phoon, 2015) suggested this be an acceptable assumption for a COV range of up to approximately 10%, and further studies would need to be undertaken to investigate the effect of assuming normality, or alternatively, the effect of modelling more accurate probabilistic distributions for the shear strength parameters.

For the purpose of this study, cohesion was modelled by careful selection of means and standard deviations to avoid simulating negative numbers during the probabilistic analysis.

2.4 RELIABILITY-BASED ANALYSIS

2.4.1 History of Reliability-Based Analysis

The initial concept of reliability-based analysis was introduced by Alfred Freudenthal in the 1950's and 1960's, and comprised the statistical description of material properties, state-space representation of failure conditions, and non-parametric reliability indices. Thereafter, major government programs and economic trends of the 1970's and 1980's (in particular the regulatory environment surrounding nuclear power generation, waste disposal and the energy crisis of the 1970's) resulted in increased focus on the topic by researchers such as A.H.-S. Ang, C.A. Cornell, O. Ditlevsen, A.M. Hasofer, N. Lind, and R. Rackwitz.

The majority of this initial research was focussed on the structural engineering field, as well surface mining, where rock slopes are designed to very low safety factors. By the 1980's

© University of Pretoria

however, through projects such as off-shore oil and gas production facilities, and various major dam failures, there was ever-increasing attention placed on quantifying uncertainties in site characterisation and geotechnical performance. As a consequence, the U.S. Bureau of Reclamation have since become leading exponents on the risk assessment of dams and the U.S Army Corps of Engineers have published numerous manuals and workshops on reliability theory.

In 2003, G.B. Baecher and J.T. Christian published their book, "*Reliability and Statistics in Geotechnical Engineering*" (©Wiley, 2003), collating the work done by the afore-mentioned researchers, themselves and others (for example H.H. Einstein, M.E. Harr, W.H. Tang and T.H. Wu) which relates the application of reliability-based analysis to Geotechnical Engineering. Subsequent contributions to the topic have since been collated and edited by K.K. Phoon in his book "*Reliability-based Design in Geotechnical Engineering*" (©Taylor & Francis, 2008) which advances reliability-based analysis into aspects of geotechnical design.

In addition to the afore-mentioned books, several technical papers were published by researchers such as B.K. Low and W.H. Tang which interpret the rather complex mathematics involved in reliability-based analysis and describe simplified techniques of carrying out reliability-analysis using matrix notation in the ubiquitous spreadsheet platform (for example, Microsoft Excel).

2.4.2 Reliability Concept

Reliability-based analysis uses the uncertainty present in the loads and resistance, or demand and capacity, of a particular system to evaluate the uncertainty in the resulting safety margin or safety factor. This uncertainty can be represented as a reliability index which can subsequently be related to a probability of failure using the standardised Normal distribution. It must be noted that failure in this context represents any "unacceptable difference between expected and observed performance" (Leonards, 1975).

If the load applied to an engineering system is defined as Q, and the available resistance as R, then the safety margin and safety factor, which are represented by M and SF respectively, can be defined as:

$$M = R - Q \qquad and \qquad SF = \frac{R}{Q}$$

© University of Pretoria

If failure occurs when M = 0 and SF = 1, then the *reliability index*, β expresses the distance of the mean value of M and F from its failure value in (dimensionless) units of standard deviation as follows:

$$\beta_M = \frac{E[M] - 0}{\sigma_M} \qquad and \qquad \beta_F = \frac{E[F] - 1}{\sigma_F} \qquad \text{(1a) and (1b)}$$

Where,

E[x] = Expected value/ mean, also μ[x]

σ_x = Standard deviation

This is shown graphically in Figure 2.4 and Figure 2.5 below:

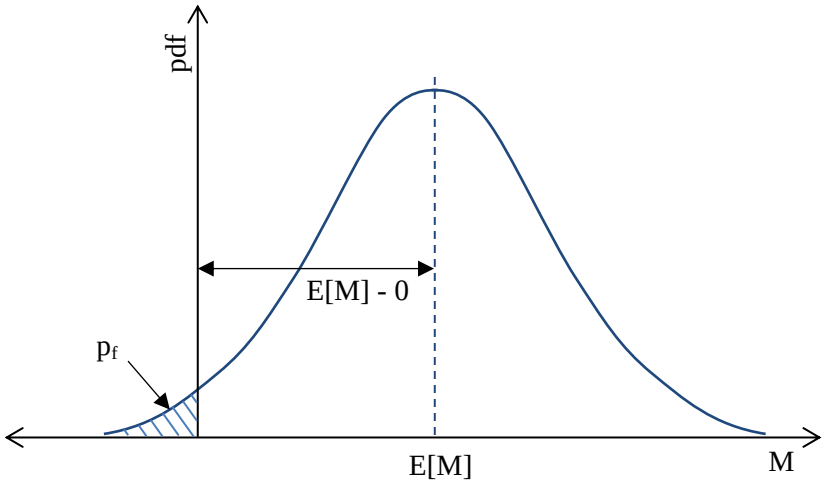


Figure 2.4: Probability density distribution for a safety margin (M)

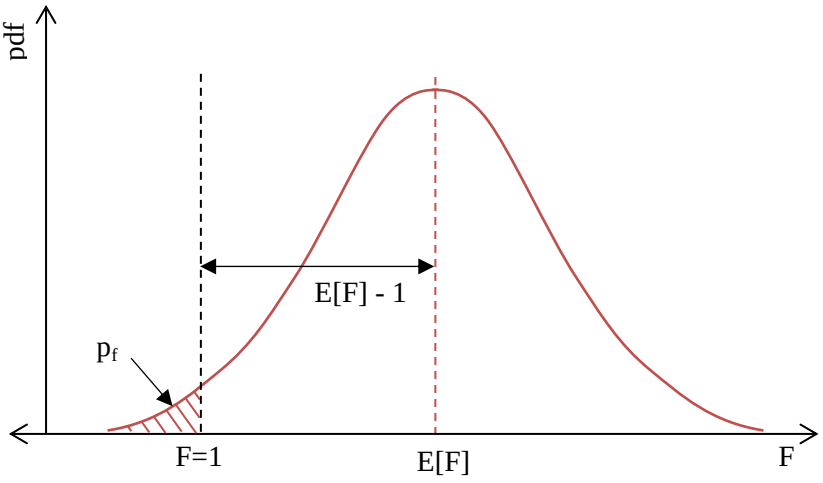


Figure 2.5: Probability density function for safety factor (F)

© University of Pretoria

The evaluation of the uncertainty in the calculated safety margin and safety factor is a special case of error propagation, in that the uncertainties in the input parameters are propagated through the calculation and affect the final result. This is more difficult when done for the safety factor than the safety margin, because F is the ratio of two uncertain parameters while M is the difference, and requires the solution of a Taylor series expansion of the performance function (the safety factor equation in our instance).

Error propagation is explained in (Baecher & Christian, 2003), and in greater detail in (Taylor, 1997), but the following is the basic formulation given by Baecher & Christian (2003) to setup the Taylor series expansion:

- Suppose the performance function we are evaluating is represented by the function g of the input parameters and variables (X_1, X_2, … , X_n) evaluated at some point (x_1, x_2, … , x_n), then:

$$g = g(x_1, x_2, \dots, x_n)$$

- If there is more than one independent variable and the initial value of each independent variable Xi is taken to be its mean value (μ_{xi}), then the following generalized Taylor series expansion can be used:

$$g(x_1, x_2, \dots, x_n) = g(\mu_{x1}, \mu_{x2}, \dots, \mu_{xn}) + \frac{1}{1!}\sum_{i=1}^{n}(x_i - \mu_{xi})\frac{\partial g}{\partial x_i}$$
$$+ \frac{1}{2!}\sum_{i=1}^{n}\sum_{j=1}^{n}(x_i - \mu_{xi})(x_j - \mu_{xj})\frac{\partial^2 g}{\partial x_i \partial x_j}$$
$$+ \frac{1}{3!}\sum_{i=1}^{n}\sum_{j=1}^{n}\sum_{k=1}^{n}(x_i - \mu_{xi})(x_j - \mu_{xj})(x_k - \mu_{xk})\frac{\partial^3 g}{\partial x_i \partial x_j \partial x_k} + \cdots$$

- Note that the partial derivatives are taken at μx1, μx2, …, etc., but the notation is left out to reduce clutter.

The methods, and/or the approximations, implemented to solve this Taylor series expansion form the basis of the various reliability-based methods described in the following three sections.

© University of Pretoria

2.4.3 The First Order Second Moment (FOSM) method

This method uses the first terms of the Taylor series expansion to estimate the mean and variance of the performance function, i.e. it assumes that all the ($x_i - \mu_{xi}$) terms are small, so their squares and higher powers are even smaller and can be ignored. It is called the second moment method because the variance is a form of the second moment and is the highest order statistical result used in the analysis.

The full derivation of the mean and variance for this method can be found in (Baecher & Christian, 2003), but the final result of the approximations to the Taylor series expansion leads to the following two equations:

$$\mu_g \approx g(\mu_{x1}, \mu_{x2}, \dots, \mu_{xn}) \tag{2}$$

And,

$$\sigma_g^2 \approx \sum_{i=1}^{n} \sigma_{Xi}^2 \left(\frac{\partial g}{\partial x_i}\right)^2 + \sum_{i=1}^{n}\sum_{j\neq i}^{n} Cov(X_i, X_j) \frac{\partial g}{\partial x_i}\frac{\partial g}{\partial x_j}$$

Where,

$Cov(X_i,X_j)$ = The covariance of the variables X_i and X_j

Or, if the correlation coefficient is expressed as the ratio of the covariance of two parameters to the square root of the product of the variances of those two parameters (using the correlation coefficients is easier to set up, and presents the correlation structure more explicitly than the covariance), then:

$$\sigma_g^2 \approx \sum_{i=1}^{n} \sigma_{Xi}^2 \left(\frac{\partial g}{\partial x_i}\right)^2 + \sum_{i=1}^{n}\sum_{j\neq i}^{n} \rho(X_i, X_j)\sigma_{Xi}\sigma_{Xj} \frac{\partial g}{\partial x_i}\frac{\partial g}{\partial x_j} \tag{3}$$

Where,

$\rho(X_i,X_j)$ = The correlation coefficient of the variables X_i and X_j

Note that the first equation implies that the expected value of a function of multiple variables is approximately equal to the function calculated with the mean values of all the variables.

© University of Pretoria

In practice, and particularly when the performance function is a limit-equilibrium safety factor equation, it is not practical to calculate the partial derivatives of the function g and it is simpler to solve them numerically. This can be done using central differences whereby the partial derivatives for each variable is found by increasing and decreasing the variable by a small increment, calculating the difference for the resulting values of g, and dividing the difference by twice the small increment. This increment should be as small as possible but without causing unacceptable rounding errors.

2.4.4 The Second Order Second Moment (SOSM) method

This technique uses the terms in the Taylor series up to the second order. The derivations of the mean and variance are complicated and can be found in various literatures, but the following is given in (Baecher & Christian, 2003) for the mean:

$$\mu_{\mathrm{g}} \approx \mathrm{g}(\mu_{x1}, \mu_{x2}, \ldots, \mu_{xn}) + \frac{1}{2}\sum_{i=1}^{n}\sum_{j\neq i}^{n} \sigma_{Xi}\sigma_{Xj}\rho_{XiXj}\frac{\partial^2 \mathrm{g}}{\partial x_i \partial x_j}$$

Where,

ρ_{XiXj} = correlation coefficient for the variables Xi and Xj

And (Ang & Tang, 1975) gives the variance when g is a function of one variable as follows:

$$\sigma_{\mathrm{g}}^2 \approx \sigma_{\mathrm{X}}^2\left(\frac{d\mathrm{g}}{dx}\right)^2 - \frac{1}{4}\left(\sigma_{\mathrm{X}}^2\right)^2\left(\frac{d^2\mathrm{g}}{dx^2}\right)^2 + E[(x-\mu_X)^3]\frac{d\mathrm{g}}{dx}\frac{d^2\mathrm{g}}{dx^2} + \frac{1}{4}E[(x-\mu_X)^4]\left(\frac{d^2\mathrm{g}}{dx^2}\right)^2$$

The computational difficulty is greater using SOSM and the improvement in accuracy is not always worth the extra effort. The SOSM method has therefore not found wide use in geotechnical applications.

2.4.5 The Hasofer-Lind/ First Order Reliability Method (FORM)

The reliability-based methods described in the previous two sections involve numerous assumptions or approximations which may not be acceptable in all situations. In particular, the resulting distribution of the safety factor is assumed to be Normal (which is most likely not the case), and the moments of the failure criterion are estimated using the mean values of the

© University of Pretoria

parameters and extrapolating linearly, i.e. this implies that it does not matter where the partial derivatives are evaluated. These methods do provide good results, but their accuracy is questionable when the analysis becomes more complicated (as is the case with slope stability calculations).

Hasofer & Lind (1974) therefore proposed an alternative approach based on a geometric interpretation of the reliability index as the distance in dimensionless space between the peak of the multivariate distribution and a function defining the failure criterion.

Baecher & Christian (2003) details the formulation of the problem into dimensionless space, and describes the approaches utilised to solve the reliability index, including the various modifications/ adjustments applied to the Hasofer-Lind method in order to deal with correlated and non-normal variables. These are not detailed herein, as the author made use of Low and Tang's 2004 and 2007 methods (described beneath) which superseded Baecher and Christian's book.

The following matrix formulation of the Hasofer-Lind (1974) reliability index is given in (Ditlevsen, 1981):

$$\beta = \min_{x \in F} \sqrt{(\boldsymbol{x}-\boldsymbol{\mu})^T \boldsymbol{C}^{-1} (\boldsymbol{x}-\boldsymbol{\mu})} \tag{4a}$$

Or equivalently,

$$\beta = \min_{x \in F} \sqrt{\left(\frac{x_i - \mu_i}{\sigma_i}\right)^T [\boldsymbol{R}]^{-1} \left(\frac{x_i - \mu_i}{\sigma_i}\right)} \tag{4b}$$

Where,

$\boldsymbol{x}$ = vector representing the set of random variables, x_i

$\boldsymbol{\mu}$ = vector representing the set of mean values, μ_i

σ_i = standard deviation values

$\boldsymbol{C}$ = Covariance matrix

$\boldsymbol{R}$ = Correlation matrix

F = Failure region

This method requires normalisation of the random variables, rotating the frame of reference (by carrying out an orthogonal transformation of the covariance matrix), and translation of the

© University of Pretoria

failure surface into the space of the reduced variables, so that the one-standard-deviation (1-σ) dispersion ellipsoid in the original space is represented by a unit sphere centred at the origin of the transformed space. Then the shortest distance from the origin to the transformed failure surface is the equivalent to the reliability index.

This method is conceptually and computationally difficult for the majority of engineers, and (Low & Tang, 1997), therefore, introduced an alternative interpretation of the Hasofer-Lind reliability index using the perspective of an expanding ellipsoid in the original space of the random variables. This method, and the subsequent extensions/ modification to it, are described below:

Low and Tang's (1997) Approach:

By this perspective, the quadratic form in Ditlevsen's equation (4a) $[(x-\mu)^T C^{-1}(x-\mu) = 1]$ represents an ellipsoid (which is tilted if the random variables are correlated) with failure occurring at the first point where the expanding ellipsoid touches tangent to the failure surface.

This is presented graphically in Figure 2.6 below. The expanding surfaces of the ellipsoid can be seen as decreasing probability values and the reliability index β is the axis ratio of the ellipsoid that touches the failure surface (R) and the one-standard-deviation dispersion ellipsoid (r).

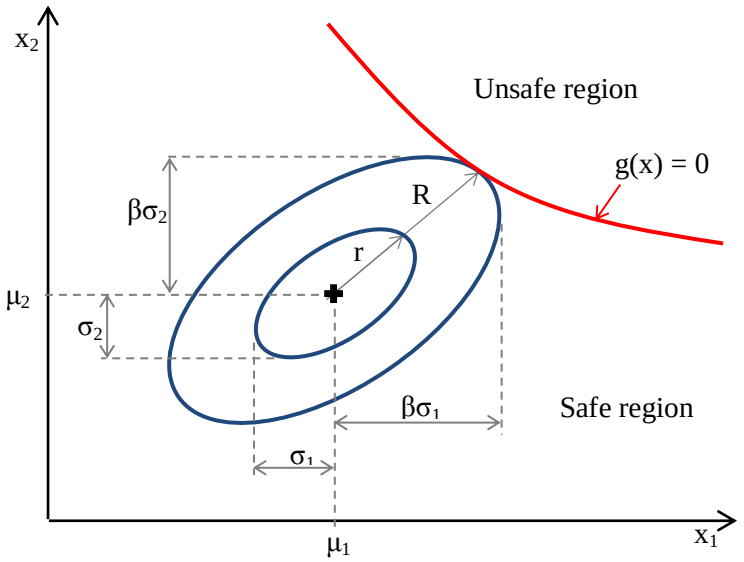


Figure 2.6: Illustration of (Low & Tang, 1997) expanding ellipsoid perspective

© University of Pretoria

The matrix formulation, based on equation (4a), is then solved by object-oriented constrained optimisation.

This method is far simpler and conceptually easier than the original (Ditlevsen, 1981) approach as it negates the use of transformed space, reduced variables and explicit partial derivatives. This is particularly useful when performance functions are either not explicit, or are lengthy and complicated, e.g. safety factor equations.

Low and Tang's (2004) Approach:

The approach presented in (Low & Tang, 1997) was applied to Normal and Log-Normal variables by conversion to equivalent normal parameters using the Rackwitz-Fiessler equivalent normal transformation entered directly into the spreadsheet equations. Low & Tang (2004), therefore, extended this method by applying the Rackwitz-Fiessler equivalent normal transformation in a user-created function, which is used to calculate the equivalent normal means and equivalent normal standard deviations for the various other non-normal variables (Gumbel, exponential, uniform, triangular, gamma, beta, PERT and Weibull) and provides enhanced operational advantage and versatility in the spreadsheet calculation.

Low and Tang's (2007) Approach:

A more efficient and robust method, which obviates the computation of equivalent normal parameters and reverses the parameters to be optimised, was subsequently presented by Low & Tang (2007). This method proposed varying the row and column vectors as dimensionless numbers and back-calculating values of x_i.

The matrix notation for this method is given as follows:

$$\beta = \min_{x \in F} \sqrt{(\boldsymbol{n})^T \boldsymbol{R}^{-1} (\boldsymbol{n})} \tag{5}$$

And,

$x_i = F^{-1}[\Phi(n_i)]$

Where,

$\boldsymbol{n}$ = vector of n_i dimensionless variables

© University of Pretoria

$\Phi(n_i)$ = standard normal cumulative distribution

The values for x_i are subsequently calculated as a function of n_i which is a straightforward process for the normal, lognormal, Gumbel, exponential, uniform, triangular and Weibull distributions, but the Newton–Raphson iteration method is required for the gamma, beta, and PERT distributions. A detailed explanation of this method is presented together with the coding of the user-created Excel function to back-calculate x_i in (Low & Tang, 2007).

The advantages of using this method over the 1997 and 2004 methods are, likewise, explained in depth in the paper, the most pertinent of which are summarised as follows:

- Obviates the need for computing equivalent standard normal parameters;
- Initial n_i are zero which negates the need for special calculations sometimes required for non-normal distributions when initial values are set equal to the mean values; and
- The solution process is faster and requires fewer iterations.

2.4.6 Application of Reliability-Based Analysis to Slope Stability

Two examples of the application of reliability-based analysis to slope stability are described below:

- The FOSM method of reliability-based analysis was applied with a central differences technique (to approximate the partial derivatives) by Christian, et al. (1994) in their analysis of the James Bay hydroelectric project. The project comprised the construction of approximately 50km of dikes on soft, sensitive clays and particular emphasis was therefore paid to the spatial variability of the foundation soils along the length of the dikes. This project set a benchmark for reliability-based analysis and has been quoted in many other sources.

- Low & Tang (2003) applied their 1997 method to the stability analysis of a 5m high embankment on a soft foundation by incorporating Spencer's method of slope stability analysis with a varying side force inclination. This method was found to be both out of the scope of this study (to include side force inclination in the probabilistic analysis) and not flexible enough to accommodate large changes in the slope configuration, i.e. changes made to the height of the embankment distorted the shape of the failure surface.

© University of Pretoria

A method whereby any slope configuration can be analysed using reliability-based analysis, as done deterministically with commercial slope stability packages, was not found in the author's literature survey. Packages such as Slide 6.0 can produce a reliability index, but this is done using the results of the Monte Carlo simulation (as described in Section 2.5.2 and its merits evaluated in Section 4.0). Since it is necessary to carry out several analyses for any particular slope, including for example variations in material uncertainty or evaluating various sizes of failure, a method to carry out reliability-based analysis as an extension of the limit-equilibrium analysis is required.

2.5 OTHER STATISTICAL METHODS

2.5.1 The Point Estimate method

Rosenblueth (1975) proposed a simple method of numerically obtaining the moments of the performance function by evaluating it at a set of specifically chosen discrete points, and in doing so, avoiding the often cumbersome calculation, or approximation, of partial derivatives in the Taylor series expansion of the performance function (as done in the afore-mentioned reliability methods). The point-estimate method is therefore a "*special case of the orthogonal polynomial approximation procedures leading to the Gaussian quadrature formulas*" (Baecher & Christian, 2003).

The derivation and details of the approach given by Rosenblueth can be found in (Baecher & Christian, 2003) as well as (Harr, 1987), but in summary, the point estimate method determines the change in the performance function for all the combinations of the variables, either plus or minus one standard deviation. The notation given for two random variables is as follows:

$$p_{++} = p_{--} = \frac{1 + \rho}{4}$$

$$p_{+-} = p_{-+} = \frac{1 - \rho}{4}$$

$$E[\mathrm{g}] = p_{++}\mathrm{g}_{++} + p_{+-}\mathrm{g}_{+-} + p_{-+}\mathrm{g}_{-+} + p_{--}\mathrm{g}_{--}$$

© University of Pretoria

$$E[g^2] = p_{++}g_{++}^2 + p_{+-}g_{+-}^2 + p_{-+}g_{-+}^2 + p_{--}g_{--}^2$$

$$Var[g] = E[g^2] - (E[g])^2$$

$$\sigma[g] = \sqrt{Var[g]}$$

Where,

Var(g) = The Variance of the performance function g

One of the disadvantages of the method is that it requires the performance function to be evaluated twice for each independent variable, and this can become a very large number when the number of uncertain parameters increases. Despite this, the simplicity and effectiveness of the method has made it popular amongst practitioners, and provided it is used for the right applications, it should return satisfactory results.

2.5.2 Monte Carlo Simulation

In this approach the analyst creates a large number of sets of randomly generated values for the uncertain parameters and computes the performance function for each set. The statistics of the resulting set of values of the function can be computed and the reliability index or probability of failure calculated directly. The method has the advantage of being conceptually simple, and is relatively easy to automate using a computer which renders it useful for a wide range of engineering applications.

The accuracy of the Monte Carlo method is highly dependent on the quality, or correctness, of the random numbers generated, and to achieve this, there are various methods in which these numbers can be generated (the most popular of which are linear congruentional), as well as various statistical tests of randomness which the generated set of random numbers should satisfy (such as the Kolmogorov-Smirnov test to determine whether the numbers are uniformly distributed).

In certain applications, the user employing a Monte Carlo simulation may want the set of random numbers generated to be repeatable so that the final result, for instance the probability of failure, can be reproducible for a particular analysis. This is carried out using computer

© University of Pretoria

algorithms to generate 'pseudo-random' numbers which are not truly random, but are determined by a small set of initial values called 'seed values'.

Additional techniques can be implemented to convert the uniformly distributed random numbers into any desired distribution, such as a normal or lognormal distribution, so that the numbers better represent the simulated parameters, which may exist in nature with that particular distribution.

In many applications the parameters to be simulated are correlated, and the Monte Carlo simulation must therefore be able to generate correlated sequences of random numbers. This is carried out by performing a Cholesky decomposition of the correlation matrix, the details of which can be found in (Baecher & Christian, 2003).

Monte Carlo Method Employed in Rocscience Slide 6.0:

The method of Monte Carlo simulation employed in Slide 6.0 (the slope stability analysis package used for certain of the analysis in this study), is based on the 'Latin Hypercube' method, which is a form of stratified sampling that can be applied to multiple variables. The method is commonly used to reduce the number or sets of random numbers necessary for a Monte Carlo simulation while still achieving a reasonably accurate random distribution.

The Latin Hypercube sampling method allows for variables to be sampled using an even sampling method, and then randomly combined sets of those variables are used for one calculation of the performance function. The sampling algorithm ensures that the distribution function is sampled evenly, but is still within the same probability trend.

Slide 6.0 combines the Monte Carlo method with reliability-based analysis by computing the standard deviation of the set of safety factors determined in the simulation, and calculating the reliability index using equation 1(b). This is discussed in more detail in Section 3.3.2.

Critical Deterministic- and Probabilistic- Failure Surfaces:

When carrying out a Monte Carlo analysis, increased computational effort is required to find the critical failure surface for each random simulation of shear strength parameters. This increased computational effort can be in the order of 2 hours per 10 000 simulations for a typical Monte Carlo analysis (measured using 2.8GHz processor and 8GB RAM).

© University of Pretoria

A common simplification is, therefore, to use the critical deterministic failure surface only (determined using the average of all the shear strength parameters), and calculate the probability of failure for each random simulation of shear strength parameters. This, however, evokes a philosophical contradiction since the shape of the surface is dependent on the combination of cohesion and friction angle (deeper surfaces for lower friction angle- higher cohesion- combinations, and shallower surfaces for higher friction angle- lower cohesion- combinations) and a high number of unlikely simulations are therefore performed, possibly skewing the result.

2.6 CONSEQUENCE OF FAILURE

2.6.1 Measurement of Consequence of Failure

A thorough assessment of consequence of failure, which is generally carried out in the design stages of a typical tailings project, typically comprises a combination of the following detailed studies (ANCOLD, 2003):

- Probabilistic slope stability analysis
- Analysis of topographical data
- Dam-break analysis
- Social and environmental risk assessments (population at risk)
- Event tree analysis
- Cost analysis (with a monetary value representing loss of life)

These studies are, however, cost-intensive and are therefore not feasible to carry out early in the project life-cycle. In early stages of design, measuring consequence of failure is an aspect of slope stability analysis that generally involves little science, or mathematics, and is usually only qualified by the engineering judgement of experienced practitioners. This is generally done by assessing whether the failure associated with the critical slip surface in the deterministic slope stability analysis has the potential to cause damage or loss of life downstream of the facility.

In fact, prior to certain major failures occurring in South Africa, such as Merriespruit and Bafokeng, little to no consideration was made of the potential damage that could occur downstream of tailings facilities, should a failure occur. Many of these old tailings facilities,

© University of Pretoria

some no longer operational, still pose a risk to the communities and infrastructure in close proximity to the facility and are, therefore, still monitored for signs of poor performance on a periodic basis.

2.6.2 Acceptable Probabilities of Failure

When carrying out a probabilistic slope stability assessment of a tailings storage facility with the purpose of assessing risk and measuring consequence of failure, the resulting probability of failure can be measured against prescribed limits to assess whether the performance of the facility is indeed acceptable. For the sake of brevity, three pertinent sources of acceptable limits are presented below.

Whitman (1984) presents the chart shown in Figure 2.7 which was modified from data published in (Baecher, 1982). The chart plots probabilities of failure of various engineering projects against costs that society, or at least some operating part of society, has implicitly found acceptable.

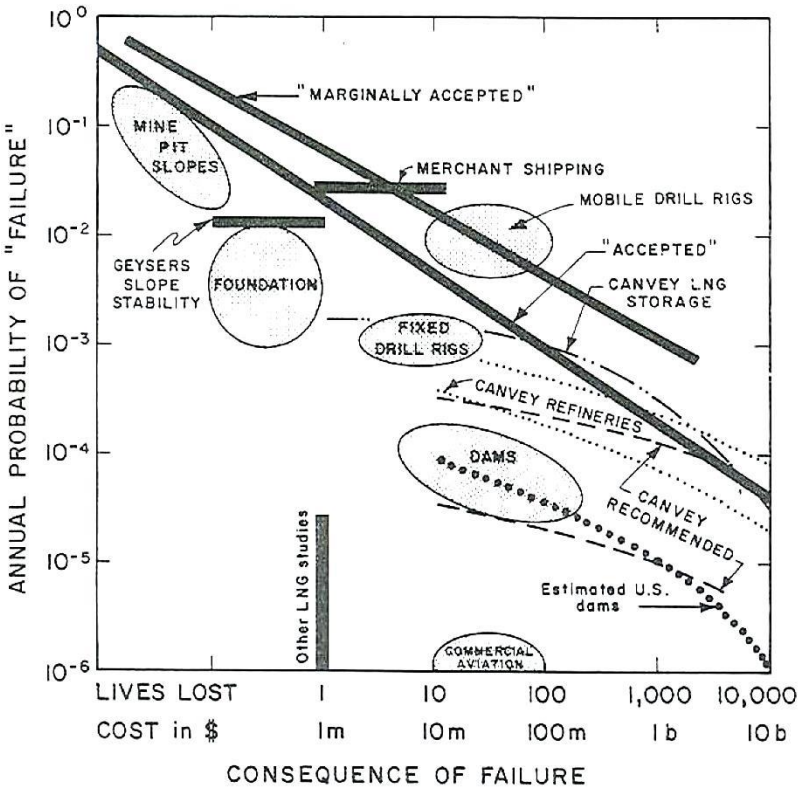


Figure 2.7: Risk for selected engineering projects (Whitman, 1984)

© University of Pretoria

The Australian Committee on Large Dams (ANCOLD) first commissioned their Guidelines on Risk Assessment in 1987 and has since published three versions, in 1994, 1998 and 2003. These were the result of working groups comprising numerous experts in the field of risk assessment and formed the collaboration of the then 'state of the art'. Figure 2.8 presents the combined chart of tolerable risk for new and existing dams given in (ANCOLD, 2003), the limits of which are defined as follows:

- Probabilities of failure above the respective limits for new and existing dams are defined as unacceptable, except in exceptional circumstances.
- Probabilities of failure below the respective limits for new and existing dams are defined as tolerable, only if they satisfy the ALARP principle.

The ALARP principle referred to is an assessment of whether the risk is "as low as reasonably practicable". No guidelines are provided on how to assess this but it should typically involve the weighing of the risk against the measures necessary for averting the risk (usually economic), and if the risk is insignificant in relation to the sacrifice, it is deemed to be acceptable.

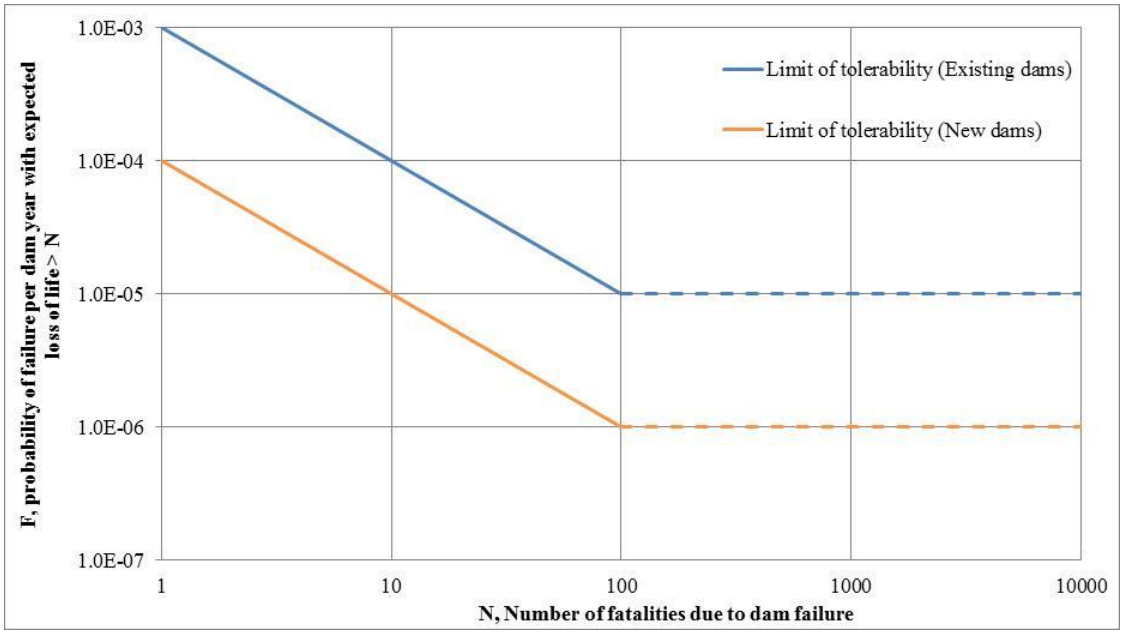


Figure 2.8: Societal risk reference guideline (ANCOLD, 2003)

Phoon (2008) considered the work done by Whitman (1984) and ANCOLD (1998) as well as others, and presented the upper and lower bound limits shown in Figure 2.9. These limits

© University of Pretoria

correspond to acceptable limits published for nuclear power plants (lower limit) and industrial facilities (upper limit) such as refineries and chemical plants.

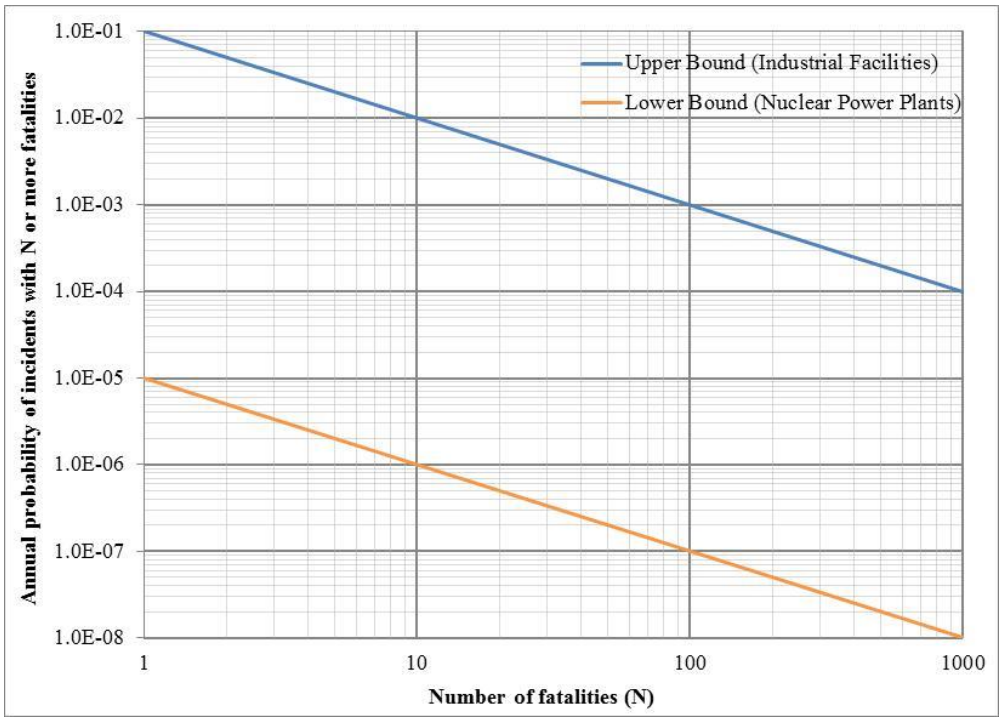


Figure 2.9: Risk tolerance chart for an engineered facility (Phoon, 2008)

Apart from having no direct reference to tailings storage facilities, the three sources presented above have a common feature which may not be appropriate for the risk assessment of tailings storage facilities. This is the measure of consequence by "potential number of fatalities" as this allows an element of subjectiveness into the assessment of how many lives are at risk for a particular size of failure.

Tailings materials, or at least those common in southern Africa, generally comprise cohesionless sandy silt- to silt- sized particles and exhibit complex behaviour depending on the pore pressure regime to which they are exposed, such as liquefaction potential and potential to flow, and it is therefore difficult to predict the behaviour of these materials on failure compared to that of general water retaining dams. For this reason, it is not always suitable to relate the size of failure of a tailings storage facility to a consequence (particularly in terms of potential fatalities) and an alternative approach is required.

© University of Pretoria

An additional observation from the three charts presented above, is that there seems to be a common "cut-off" for allowable probabilities of failure for dams of approximately 1.0E-06, i.e. probabilities less than this are generally perceived to be acceptable.

2.7 SUMMARY OF THE LITERATURE REVIEW

The following key points, which are pertinent to the dissertation going forward, are summarised from the literature review:

- Gold tailings in South Africa are deposited as an effectively uniform material using the paddock method of deposition (commonly referred to as the day-wall method);
- Deposition via the cycloning method segregates the tailings into a coarse 'underflow' material forming the impoundment wall, and fine 'overflow' material contained within the 'underflow' impoundment wall;
- The alternate interpretations of 'probability', i.e. frequency and belief, complement one another and serve as a useful manner in which to conceptualise computed probabilities of failure;
- The COV for geotechnical materials can vary from 5% to 70%, with the angle of friction for a cohesionless materials reported to be between 5% and 20%;
- The average friction angle of gold tailings is approximately 35° and could have a COV of between 5% and 20% depending the level of uncertainty;
- An efficient and robust method of reliability-based analysis, whereby the computations of equivalent normal parameters are alleviated completely, was presented by Low & Tang (2007). This method proposed varying the row and column vectors as dimensionless numbers and back-calculating values of x_i based on the user-created function "x_i";
- A method whereby any slope configuration can be analysed using reliability-based analysis, as done deterministically with commercial slope stability packages, was not found in the author's literature survey;

© University of Pretoria

- Consequence of failure is generally too expensive to measure extensively during early stages of the project and is therefore quantified only by the engineering judgement of experienced engineers; and

- The measure of consequence by "potential number of fatalities" allows an element of subjectiveness into the assessment of tailings facility failures. This is especially true since tailings material behaviour is complex and, therefore, difficult to predict compared to that of general water retaining dams.

© University of Pretoria

3.0 EXPERIMENTAL DESIGN

3.1 DESIGN SCOPE

The following four sections present the various analyses and experiments carried out in the study to review the application of reliability-based analysis to slope stability, as well as propose a method of applying the results to measure 'severity' of failure and 'slope performance' of tailings dams as an alternative to the typical consequence of failure.

Section 4.0 compares the pre-programmed probability methods available in "off-the-shelf" slope stability packages to various reliability-based analysis methods programed into Microsoft Excel. Each of these methods were applied to several embankments/ waste facilities, specifically selected and configured (by changing the slope geometry, shear strength parameters and the uncertainty in those parameters) to investigate a wide range of safety factors, probabilities of failure and material uncertainty. The results of these analyses are plotted on a graph of safety factor versus probability of failure in order to illustrate the effects of material uncertainty on the probability of failure, as well as identify any characteristics inherent to the different reliability-based analysis methods.

Based on the results of the above analysis, and the discussions in Section 2.4 of the literature review, a suitable reliability-based analysis method is selected to be implemented in the subsequent analyses and experiments.

The purpose of Section 5.0 is to apply the selected reliability-based analysis method to the analysis of a typical tailings storage facility, and investigate the effect material uncertainty has on the probability of failure of slip surfaces smaller and larger than the critical slip surface. The hypothesis is that, while surfaces larger and smaller than the critical slip surface may indeed have higher safety factors, they may not necessarily have acceptable probabilities of failure. Based on the reservations the author has with using consequence of failure for tailings dams (as discussed in Section 2.6), however, there appears to be uncertainty in what an acceptable probability of failure for a tailings storage facility is.

Section 5.0 therefore also serves as an introduction to the concept of measuring 'severity' of failure and 'slope performance', with an emphasis on what an owner of this type of facility and/ or the public, would deem as acceptable. This is done by analysing a uniform, cohesionless gold tailings facility at three different slope angles (1:2, 1:2.5 and 1:3), each with

© University of Pretoria

COV in the friction angle of the tailings material of 5%, 10% and 15%. Then for each model configuration, one failure smaller and two failures larger than the critical slip surface are analysed and their probabilities of failure plotted against a proposed measure of the relative size, or 'severity', of that failure.

The resulting chart of 'severity' versus probability of failure for the 36 analyses (3 slopes x 3 COV ranges x 4 failure sizes) are used, together with certain principles inherent to the various other proposed limits of acceptable probabilities of failure (see Section 2.6.2), to suggest limits of acceptable probability of failure for respective 'severities' of failure.

Having carried out the above analysis on a uniform, cohesionless gold tailings facility, and using the results to propose the limits of acceptable probability of failure, Section 6.0 presents an experiment to test the suitability of the proposed chart of 'severity' versus probability of failure for a slightly more complex tailings facility, namely a cycloned slurry dam comprising fine overflow material confined within a coarse underflow impoundment.

This cyclone facility was configured, by altering the geometry and position of the water table, to return a safety factor of exactly 1.5 for the critical slip surface. Failure surfaces bigger and smaller than the critical failure surface are then analysed for 10% COV in the shear strength parameters (cohesion and friction angle) of both the underflow and overflow materials. A second experiment is then carried out, and the results plotted on the same chart, to investigate the effect of using 15% COV in the shear strength parameters of the overflow material (a situation not unlikely considering the difficulty in accurately measuring the shear strength properties of these materials).

A simple verification exercise was subsequently undertaken, using the results of the above analyses, to compare the critical probabilistic failure surface returned from a typical overall probabilistic analysis in slope stability software, and the surface relating to the peak of the 'slope performance' curve. The purpose of this exercise is to assess whether the proposed method of plotting 'slope performance' can replace the computationally extensive search for the critical probabilistic failure surface, with a suitable level of accuracy.

Section 7.0 presents a reliability-based analysis experiment, specifically designed to further investigate an apparent trend observed in the curves of probability of failure versus safety factor presented in Section 4.0. This "trend" is that there appeared to be a fixed curve relating safety factors to probabilities of failure for a certain level of uncertainty, even though the

© University of Pretoria

embankments had very different geometries and configurations. A simple experiment was therefore carried out on a uniform, cohesionless embankment with a 1:3 slope angle, and friction angles varying in 5° increments from 25° to 40°, each with 5%, 10% and 15% COV. The three curves related to the level of uncertainty were then plotted on a chart of safety factor versus probability of failure, and the results of the various other analyses and experiments carried out in this study superimposed for comparative purposes.

3.2 LIMIT-EQUILIBRIUM METHODOLOGY AND ASSUMPTIONS

Limit-equilibrium slope stability analysis was used in the various analyses and experiments conducted in this study and was carried out with commercially available software for the following reasons:

- Commercial limit-equilibrium slope stability packages, such as Slide 6.0 and Geo-slope Slope/W, are common in engineering practice and familiar to the author;
- The results produced by these packages have been tested against specific verification slope stability problems such as those distributed by the Association for Computer Aided Design (Giam & Donald, 1989), as well as published examples in journals and conference proceedings;
- They are able to analyse virtually any slope geometry comprising hundreds of material types (the maximum in Slide 6.0 is 500) and using various material strength criteria (for example Mohr-Coulomb, Infinite Strength or Hoek-Brown); and
- The search for the critical surface is automated and efficient.

The pertinent assumptions used in the limit-equilibrium analysis, which define aspects such as the analysis method, water tables and material properties, are listed below:

- Bishop's simplified method of slices was selected due to the ease at which the method can be programmed into spreadsheet applications (which is required for the reliability-based analysis and described below);

© University of Pretoria

- The number of slices was increased from the default of 20 (which is generally accepted as the minimum) to 30. This does not increase the analysis duration but does improve the accuracy slightly;

- Convergence settings were kept at the default tolerance of 0.005 and a maximum of 50 iterations. These have been found to return satisfactory results without unnecessarily extending the analysis duration;

- Mohr-Coulomb strength parameters were used for all materials (also required in the reliability-based analysis), except where the foundations were modelled as 'infinite strength' to force failures through the embankment materials;

- For the purpose of this study, failure surfaces were assumed to be circular. Apart from certain embankments comprising complex geometries, which are out of the scope of this study, circular slip surfaces are understood to approximate the critical failure surface adequately;

- The slip centre grid, which defines the centre point for the slip surfaces analysed, was set to 40 x 40 intervals. The radius increment, which is the number of increments between the maximum and minimum radii possible for each grid centre, was set to 10. This results in a total of 18491 (41 x 41 x 11) slip surfaces evaluated per analysis;

- Saturated unit weights are generally difficult to estimate as they are dependent on the void ratio and specific gravity of the material which are generally not known. These were therefore assumed to be equal to the dry unit weights. This is neither a conservative nor unconservative assumption, as the unit weight has both failure-resisting and failure-causing effects on the safety factor, the ratio of which depends on the shape of the slip surface (i.e. the base inclination of the slices);

- Water tables were user-defined and the pore pressure coefficient (Hu) set to 1, i.e. simulating hydrostatic conditions. This is conservative and eliminates the rather complex task of estimating head loss due to seepage.

In the Low and Tang 2004 and 2007 reliability-based analysis methods programmed into Excel, which are detailed in Section 3.3, the performance function requires evaluating during

© University of Pretoria

the iterative solving of the matrices in the reliability equations. In this instance, the performance function is a limit-equilibrium equation, and it was therefore necessary to programme a Bishop's Simplified method of slices routine into the spreadsheet.

This was accomplished by importing the raw data from the Slide 6.0 analysis and computing the following (Bishop, 1955) simplified equation (in five iterations):

$$SF = \frac{\sum\{[c'b + (W - ub)\tan\phi']/m_\alpha\}}{\sum W \sin\alpha}$$

And,

$$m_\alpha = \left(1 + \frac{\tan\alpha \tan\emptyset'}{SF}\right)\cos\alpha$$

Where,

SF = Safety Factor
c' = Cohesion
b = Slice width
W = Slice weight
u = Pore pressure
ϕ' = Friction angle
α = Angle of slice base

Since SF appears on both sides of the equation, it is initially assumed to be equal to 1.0, and the equation is then solved iteratively. It was found during the analyses that convergence is achieved relatively quickly and only five iterations were therefore required.

The raw data from Slide comprises convenient tables of slice data from which the above parameters can be extracted and used directly in the equations. Only α is excluded from the slice data and was, therefore, calculated with basic trigonometry using the coordinates of the base of each slice.

© University of Pretoria

3.3 PROBABILISTIC ANALYSIS METHODOLOGY

Four reliability-based analysis methods were programed into a spreadsheet application for comparison with the automated procedures available in commercial slope stability packages. These, and the automated methods, are described below.

3.3.1 Classical Monte Carlo Simulation

Popular slope stability analysis packages, such as Rocscience Slide 6.0 and Geo-slope Slope/W, are fully automated to carry out probability analysis using the Monte-Carlo method and, in the case of the Slide 6.0, use the Monte-Carlo data to calculate a reliability index.

As mentioned in Section 2.5.2, the method of Monte Carlo simulation employed in Slide 6.0 is based on the 'Latin Hypercube' method, which is a form of stratified sampling that can be applied to multiple variables. The method is commonly used to reduce the number or sets of random numbers necessary for a Monte Carlo simulation while still achieving a reasonably accurate random distribution.

For the results of the analyses to be reproducible, pseudo-random numbers were generated using the (Park & Miller, 1983) number generator (the default method utilised by Slide 6.0) with a constant seed value set at 10116. The number of trials was set to 700 000, which was found to be the limit of the analysis package (anything more and the simulation failed to process).

Slide 6.0 also requires that limits be set for the minimum and maximum possible random numbers generated for each parameter. Assuming a normal distribution for all the parameters (as defined in the probabilistic assumptions listed in Section 3.4), this is done using the "Three sigma rule" which is a rule of thumb described in (Dai & Wang, 1992), based on the fact that 99.73% of all values of a normally distributed parameter fall within three standard deviations of the average value.

© University of Pretoria

3.3.2 Modified Monte Carlo Analysis

In a classical Monte Carlo simulation, many trials are analysed where the uncertain parameters are randomly selected according to a specified probability distribution. The number of cases where failure occurs (SF<1.0) is divided by the number of trials to obtain the probability of failure.

Slide 6.0 uses the results of the Monte Carlo simulation to calculate a reliability index in a different way, by first calculating the standard deviation of the distribution of safety factors determined in the Monte Carlo trials, and using this to compute the reliability index as follows:

$$\beta_F = \frac{E[F] - 1}{\sigma_{MC}}$$

And,

$$\sigma_{MC} = \sqrt{\frac{\sum[x_i - E[F]]}{N - 1}}$$

Where,

E[F] = Expected value/ mean calculated using the mean values of the input parameters

σ_{MC} = Standard deviation calculated from the Monte-Carlo data

x_i = ith value of the parameter (safety factor trial)

N = Number of Monte Carlo trials

Calculating the reliability index using the Modified Monte Carlo Analysis excludes some of the benefits of reliability-based methods defined in Section 2.4, and relies on the accuracy of the Monte-Carlo method to propagate the error through the analysis. The resulting probability of failure is therefore similar to that which is achieved with the Classical Monte Carlo Simulation, but has the added benefit of extrapolating probabilities of failure to orders of magnitude in excess of the number of trials carried out in the simulation. In a classical Monte Carlo analysis, if 10 000 trials are performed for example, the resulting probability of failure cannot be less than 0.0001.

© University of Pretoria

3.3.3 FOSM Method

This method is described in Section 2.4.3 and utilises equations (1b), (2) and (3) with the central differences method to obtain the partial derivatives. The method was selected as it does not require any additional safety factor calculations and can therefore be solved using the results of the sensitivity analysis alone. The equations are repeated below for ease of reference (note that the symbols have been altered for consistency between the three equations).

$$\beta = \frac{\mu_g - 1}{\sigma_g} \tag{1b}$$

$$\mu_g \approx g(\mu_{X1}, \mu_{X2}, \dots, \mu_{Xn}) \tag{2}$$

$$\sigma_g^2 \approx \sum_{i=1}^{n} \sigma_{Xi}^2 \left(\frac{\partial g}{\partial x_i}\right)^2 + \sum_{i=1}^{n}\sum_{j\neq i}^{n} \rho(X_i, X_j)\sigma_{Xi}\sigma_{Xj}\frac{\partial g}{\partial x_i}\frac{\partial g}{\partial x_j} \tag{3}$$

The central differences method was implemented to approximate $\partial g/\partial x_i$ by calculating $\Delta SF/2\Delta x$, with SF being the safety factor and x being a small increment set to approximately 5% of the standard deviation of each parameter. Equation (3) therefore becomes the following:

$$\sigma_g^2 \approx \sum_{i=1}^{n} \sigma_{Xi}^2 \left(\frac{\Delta SF}{2\Delta x_i}\right)^2 + \sum_{i=1}^{n}\sum_{j\neq i}^{n} \rho(X_i, X_j)\sigma_{Xi}\sigma_{Xj}\frac{\Delta SF}{2\Delta x_i}\frac{\Delta SF}{2\Delta x_j}$$

This was implemented by carrying out a sensitivity analysis in Slide 6.0, whereby each parameter was varied by plus and minus the small increment, while keeping the remaining parameters at their mean values, and recording the change in the safety factor. After running the analysis, the sensitivity data is imported into the spreadsheet application, and the reference values are extracted for solving the three reliability equations.

For the purpose of this study, whereby the analyses are limited to four uncertain parameters (c_1, c_2, ϕ_1 and ϕ_2), equation (3) was programmed into the spreadsheet application as follows:

© University of Pretoria

$$\sigma_g^2 \approx \sigma_{c_1}^2\left(\frac{\Delta SF}{2\Delta x_{c_1}}\right)^2 + \sigma_{\phi_1}^2\left(\frac{\Delta SF}{2\Delta x_{\phi_1}}\right)^2 + \sigma_{c_2}^2\left(\frac{\Delta SF}{2\Delta x_{c_2}}\right)^2 + \sigma_{\phi_2}^2\left(\frac{\Delta SF}{2\Delta x_{\phi_2}}\right)^2 + \rho(c_1,\phi_1)\sigma_{c_1}\sigma_{\phi_1}\frac{\Delta SF}{2\Delta x_{c_1}}\frac{\Delta SF}{2\Delta x_{\phi_1}} + \rho(c_2,\phi_2)\sigma_{c_2}\sigma_{\phi_2}\frac{\Delta SF}{2\Delta x_{c_2}}\frac{\Delta SF}{2\Delta x_{\phi_2}} \quad (6)$$

As stated in the literature review, this increment should be as small as possible but without causing unacceptable rounding errors. The value of 5% of the standard deviation was used in this instance as this was the smallest increment that could be extracted from the sensitivity analysis data (the minimum and maximum of which were set according to the "three sigma rule" for the Monte Carlo simulation). The opposite extreme, whereby a large increment is used in the FOSM analysis, forms the basis of the second reliability-based analysis method described below.

3.3.4 Simplified FOSM Method

In this 'simplified' FOSM method, central differences was again implemented to approximate $\partial g/\partial x_i$ by calculating $\Delta F/2\Delta x$, with x being set to three standard deviations of each parameter, i.e. the minimum and maximum limits of the Monte Carlo simulation. This was done to simplify the extraction of ΔF and $2\Delta x$ values from the sensitivity analysis data, and it eliminates the standard deviation terms from equation (6), simplifying it to the following:

$$\sigma_g^2 \approx \left(\frac{\Delta SF_{c_1}}{6}\right)^2 + \left(\frac{\Delta SF_{\phi_1}}{6}\right)^2 + \left(\frac{\Delta SF_{c_2}}{6}\right)^2 + \left(\frac{\Delta SF_{\phi_2}}{6}\right)^2 + \rho(c_1,\phi_1)\frac{\Delta SF_{c_1}}{6}\frac{\Delta SF_{\phi_1}}{6} + \rho(c_2,\phi_2)\frac{\Delta SF_{c_2}}{6}\frac{\Delta SF_{\phi_2}}{6}$$

The above simplified equation is one that can be programmed very easily into a spreadsheet and does not require many parameters to be solved, particularly if the parameters are assumed to be uncorrelated (i.e. $\rho = 0$) which is a slightly more conservative assumption (but not considered in this study).

To complete the method, equations (1b) and (2) are solved in exactly the same manner as for the previous FOSM method.

© University of Pretoria

3.3.5 Low and Tang (2004) FORM method

This method is described in Section 2.4.5 and utilises equations (1b), (2) and (4b), the latter of which is repeated below for ease of reference:

$$\beta = \min_{x \in F} \sqrt{\left(\frac{x_i - \mu_i}{\sigma_i}\right)^T [\boldsymbol{R}]^{-1} \left(\frac{x_i - \mu_i}{\sigma_i}\right)} \tag{4b}$$

Where,

x_i = vector representing the set of random variables

μ_i = equivalent normal mean values of the random variables

σ_i = equivalent normal standard deviation values of the random variables

$\boldsymbol{R}$ = Correlation matrix

F = Failure region

Note that equation (4b) is preferred over (4a) because the correlation matrix is easier to set up, and presents the correlation structure more explicitly than the covariance matrix.

The matrix notation given in equation (4b) was implemented in a spreadsheet application as illustrated in Figure 3.1:

	a	b	c	d	e	f	g	h	i	j	k	l	m
	Material	**Property**	**Distribution**	**μ**	**σ**	***x***	**μ^N**	**σ^N**	**$(x-\mu^N)/\sigma^N$**	**ϕ_1**	**c_1**	**ϕ_2**	**c_2**
1	Embankment	Phi	Normal	37.00	5.55	31.19	37.00	5.55	-1.047	1	-0.4	0	0
2	Embankment	Cohesion	Normal	5.00	1.00	5.37	5.00	1.00	0.365	-0.4	1	0	0
3	Clay	Phi	Normal	28.00	4.20	20.27	28.00	4.20	-1.840	0	0	1	-0.4
4	Clay	Cohesion	Normal	10.00	2.00	10.77	10.00	2.00	0.383	0	0	-0.4	1

Optimised vector — Correlation matrix [R]

=SQRT(MMULT(TRANSPOSE(i1:i4),MMULT(MINVERSE(j1:m4)),(i1:i4)))

g(x):	3E-08
β:	**2.152**
Prob.Fail:	**1.57E-02**

Figure 3.1: Spreadsheet formulation of Low & Tang (2004) FORM method

The matrix formulation was then solved by object-oriented constrained optimisation using the Solver tool in the spreadsheet application as follows:

© University of Pretoria

a) Formulas are programmed for the column vector (cells i1:i4 in Figure 3.1);
b) x values are set equal to the mean values initially (cells f1:f4);
c) The transpose of the column vector is calculated;
d) The inverse of the correlation matrix is calculated (cells j1:m4);
e) The matrix product of the vectors is computed;
f) The square root of the matrix product is calculated to solve for β based on x values;
g) The performance function is solved based on x values; and
h) Solver is invoked to minimise β by changing the x values (subject to g(x) = 0) and steps c) through g) are repeated.

In this instance the performance function is the Bishop's simplified limit-equilibrium equation programmed into the spreadsheet application (as described in Section 3.2), which was incorporated into the reliability-based analysis as follows:

- To solve for step g) above, the values for cohesion and friction angle at the base of each slice were adjusted to reference the x values for each probabilistic iteration; and
- The condition that g(x) = 0 was satisfied based on the assumption that failure occurs at SF=1, and therefore, g(x) = SF-1.

3.3.6 Low and Tang (2007) FORM method

This method is described in Section 2.4.5 and utilises equations (1b), (2) and (5), the latter of which is repeated below for ease of reference:

$$\beta = \min_{x \in F} \sqrt{(\boldsymbol{n})^T \boldsymbol{R}^{-1} (\boldsymbol{n})} \tag{5}$$

Where,

$\boldsymbol{n}$ = vector of n_i dimensionless variables

And,

$x_i = F^{-1}[\Phi(n_i)]$

The matrix notation given in equation (5) was implemented in a spreadsheet application as illustrated in Figure 3.2:

© University of Pretoria

	a	b	c	d	e	f	g	h	i	j	k
	Material	**Property**	**Distribution**	**μ**	**σ**	x_i	n_i	ϕ_1	c_1	ϕ_2	c_2
1	Embankment	Phi	Normal	37.00	5.55	31.19	-1.047	1	-0.4	0	0
2	Embankment	Cohesion	Normal	5.00	1.00	5.36	0.363	-0.4	1	0	0
3	Clay	Phi	Normal	28.00	4.20	20.27	-1.839	0	0	1	-0.4
4	Clay	Cohesion	Normal	10.00	2.00	10.76	0.381	0	0	-0.4	1

Optimised vector | Correlation matrix [R]

=SQRT(MMULT(TRANSPOSE(g1:g4),MMULT(MINVERSE(h1:k4)),(g1:g4)))

g(x):	2E-08
β:	**2.152**
Prob.Fail:	**1.57E-02**

Figure 3.2: Spreadsheet formulation of Low & Tang (2007) FORM method

The matrix formulation was then solved by object-oriented constrained optimisation using the Solver tool in the spreadsheet application as follows:

a) n_i values are set equal to zero initially (cells g1:g4 in Figure 3.2);
b) The transpose of the column vector is calculated;
c) The inverse of the correlation matrix is calculated (cells h1:k4);
d) The matrix product of the vectors is computed;
e) The square root of the matrix product is calculated to solve for β based on n_i values;
f) x_i values are back-calculated based on the n_i values and the user-created function "x_i";
g) The performance function is solved based on x_i values; and
h) Solver is invoked to minimise β by changing the n_i values (subject to g(x) = 0) and steps b) through g) are repeated.

The performance function, i.e. the Bishop's simplified limit-equilibrium equation programmed into the spreadsheet application, was solved in the same manner as for the Low & Tang (2004) method:

- To solve for step g) above, the values for cohesion and friction angle at the base of each slice were adjusted to reference the x_i values for each probabilistic iteration; and
- The condition that g(x) = 0 was satisfied based on the assumption that failure occurs at SF=1, and therefore, g(x) = SF-1.

© University of Pretoria

3.3.7 Analysis Automation

In order to streamline the procedure of carrying out the four reliability-based analyses described above, a VBA Macro was written to automate the Solver process and copy the results of all the analyses into a summary table. This was done by recording the entire analysis procedure into a Macro, and adding the reference to SOLVER.XLAM to the VBA module.

The total time for the full reliability-based analysis of each slope, i.e. to copy the raw data and sensitivity analysis data from Slide 6.0 into the spreadsheet and run the Macro, was subsequently less than a minute.

3.4 PROBABILISTIC ASSUMPTIONS

The assumptions used when carrying out the probabilistic analyses are summarised as follows:

- Only the shear strength parameters were considered as uncertain in the analyses. Unit weight generally has little effect on the safety factor, particularly on flat foundations, and was therefore assumed to be constant in all the analyses;

- A normal distribution was assumed for all uncertain material parameters. This is discussed in Section 2.3 and was selected to exclude the effect of using different probability distributions from the analyses;

- The correlation coefficient of c' and ϕ' was assumed to be equal to -0.4, which is in line with observed literature which ranges from -0.3 and -0.5 ((Low, 2003) and (Baecher & Christian, 2003) respectively);

- Only knowledge uncertainty in the shear strength parameters of the material was considered in the reliability-based analysis. Natural/ spatial variability and decision uncertainty have been excluded;

- The number of Monte Carlo trials was set to 700 000, which was found to be the limit of the analysis package used (anything more and the simulation failed to process);

© University of Pretoria

- Pseudo-random numbers were generated in the Monte Carlo simulation using a constant seed value of 10116 to give reproducible results;

- For the Monte Carlo simulation and sensitivity analysis in Slide 6.0, the minimum and maximum possible random numbers generated for each uncertain parameter were set to three standard deviations from the mean (according to the "Three-sigma" rule described in Section 3.3.1);

- The distribution of safety factors was assumed to be normally distributed in the FOSM and Simplified FOSM methods in order to extract a probability of failure from the reliability index;

- Only the deterministic critical failure surface returned within the search limits was analysed in the probabilistic analyses. This has some philosophical issues since a change in shear strength parameters should, subsequently, change the shape of the failure surface, but searching for the critical probabilistic failure surface was excluded for the following reasons:

  - The literature on reliability-based analysis was found to use the deterministic critical failure surface only ((Baecher & Christian, 2003) and (Low & Tang, 2007));

  - To search for a new failure surface for each Monte Carlo trial extends the analysis duration from a few seconds to over 2 hours (based on a number of trial runs using only 10 000 simulations); and

  - Failures smaller and larger than the critical failure surface are assessed as part of the study scope (defined as "slope performance") in Section 5.0 and Section 6.0 and this could be viewed as an alternative to the probabilistic analysis of the full slope.

© University of Pretoria

4.0 APPLICATION OF RELIABILITY-BASED ANALYSIS METHODS

In this section, the two Monte Carlo methods and four practical reliability-based methods (namely the FOSM, simplified FOSM, and both Low & Tang's 2004 and 2007 methods) were applied to seven embankments or waste facilities, specifically selected and configured to investigate a wide range of safety factors, probabilities of failure and the effect of material uncertainty. These are described in Section 4.1 below.

4.1 STABILITY MODEL CONFIGURATIONS

4.1.1 Case 1 - Embankment Dam on Clay Foundation No.1

This model comprised a 30m high, water retaining embankment dam on a soft clay foundation with relatively high uncertainty in the embankment and foundation materials, i.e. COV of 20% for the cohesion and 15% for the friction angle. The phreatic surface was assumed to extend from the upstream crest to the downstream toe with the foundation fully saturated throughout.

This model was selected and configured to return a deterministic safety factor of approximately 1.3, with high COV in the shear strength parameters. The model geometry is presented in Figure 4.1 and the material parameters follow in Table 4.1.

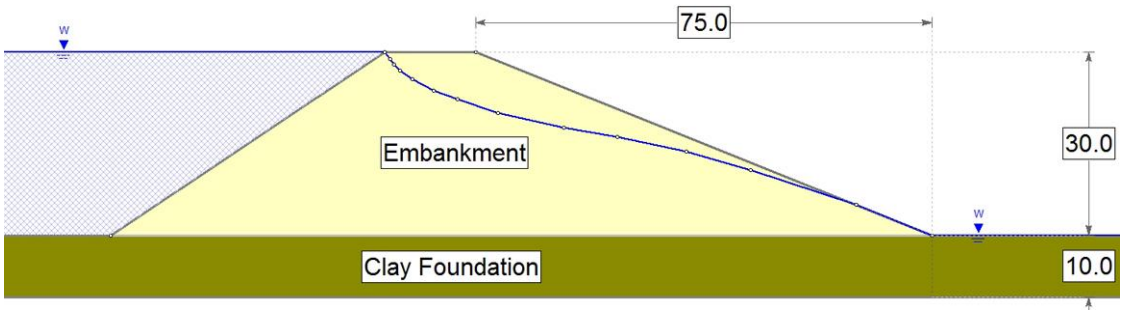


Figure 4.1: Embankment dam on clay foundation No.1 - Model geometry

Table 4.1: Embankment dam on clay foundation No.1 - Material parameters

Material Name	Unit Weight (kN/m^3)	Cohesion (kPa)		Friction Angle (deg)	
		μ	σ	μ	σ
Embankment	18	5	±1.0	37	±5.55
Clay Foundation	16	10	±2.0	28	±4.20

Key:
μ - Mean σ - Standard deviation

© University of Pretoria

4.1.2 Case 2 - Embankment Dam on Clay Foundation No.2

This model comprised the same 30m high, water retaining embankment dam on a soft clay foundation as in the previous model; however, the friction angle of the materials were reduced to return a deterministic safety factor of approximately 1.2, and the COV in the soil strength was reduced by 10%. This implies that although the soil is weaker than in Case 1, there is more certainty in these parameters.

This model was configured to investigate if, while a reduction in shear strength lowers the safety factor, reducing the COV in the shear strength parameters results in a lower probability of failure than in the previous, stronger, model.

The model geometry is presented in Figure 4.2 and the material parameters follow in Table 4.2.

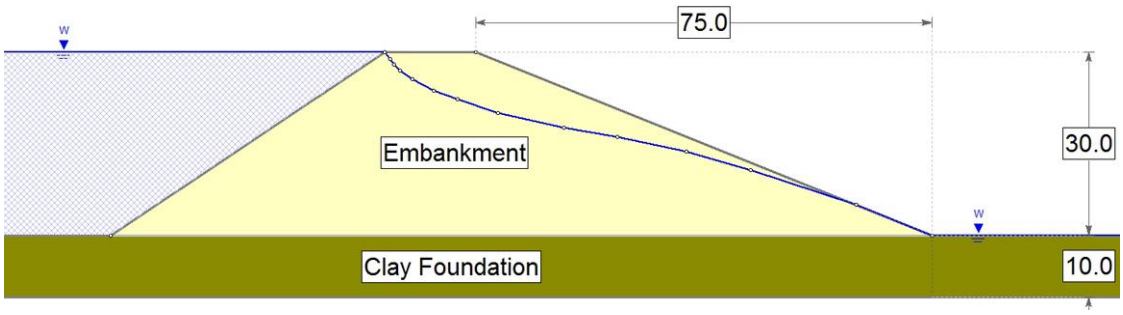


Figure 4.2: Embankment dam on clay foundation No.2 - Model geometry

Table 4.2: Embankment dam on clay foundation No.1 - Material parameters

Material Name	Unit Weight (kN/m^3)	Cohesion (kPa)		Friction Angle (degrees)	
		μ	σ	μ	σ
Embankment	18	5	±1.0	36	±3.6
Clay Foundation	16	10	±2.0	26	±2.6

Key:
μ - Mean
σ - Standard deviation

© University of Pretoria

4.1.3 Case 3 - Waste Rock Dump No.1

This model comprised a ±85m high waste rock embankment with approximately 1V:2.4H side slopes on a 4m to 6m thick clayey foundation underlain by bedrock, assumed for this purpose to be of infinite strength. COV in the material parameters was selected as 30% for the cohesion and 10% for the friction angle. No phreatic surface was included in the analysis.

This model was selected to investigate the difference in the probability of failures of the various methods for a high safety factor, and consequently, low probability of failure. The deterministic safety factor for the model is approximately 1.7

The model geometry is presented in Figure 4.3 and the material parameters follow in Table 4.3.

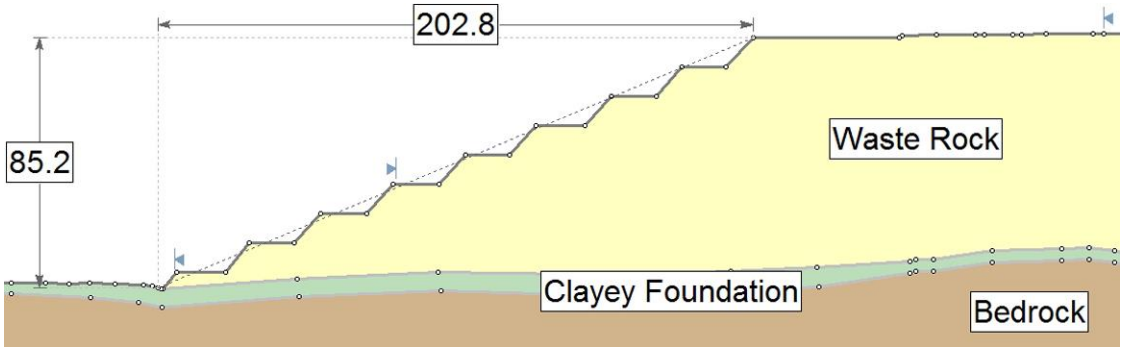


Figure 4.3: Waste rock dump No.1 - Model geometry

Table 4.3: Waste rock dump No.1 - Material parameters

Material Name	Unit Weight (kN/m^3)	Cohesion (kPa)		Friction Angle (degrees)	
		μ	σ	μ	σ
Waste Rock	24	0.1	±0.03	36	±3.6
Clayey Foundation	16	5.0	±1.5	26	±2.6
Bedrock	24	Infinite strength			

Key:
μ - Mean
σ - Standard deviation

Note that the waste rock was modelled as being effectively cohesionless, although the slight cohesion shown above is included to keep a consistent number of uncertain parameters in all the probabilistic analyses.

© University of Pretoria

4.1.4 Case 4 - Waste Rock Dump No.2

This model comprised a similar ±85m high waste rock embankment to the previous model except with approximately 1V:2.1H side slopes, and a reduction of the shear strength parameters (except the cohesion of the waste rock).

The model was configured, by steepening the slope and reducing the shear strength parameters of the previous model, to return a deterministic safety factor of approximately 1.5.

The model geometry is presented in Figure 4.4 and the material parameters follow in Table 4.4.

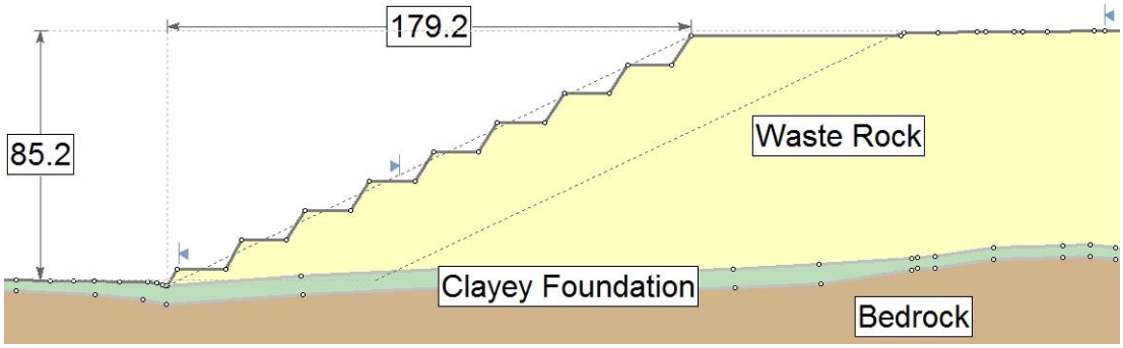


Figure 4.4: Waste rock dump No.2 - Model geometry

Table 4.4: Waste rock dump No.2 - Material parameters

Material Name	Unit Weight (kN/m^3)	Cohesion (kPa)		Friction Angle (degrees)	
		μ	σ	μ	σ
Waste Rock	24	0.1	±0.03	34	±3.4
Clayey Foundation	16	3.0	±1.0	25	±2.5
Bedrock	24	Infinite strength			

Key:
μ - Mean
σ - Standard deviation

Similarly to the previous model, the waste rock was modelled as being effectively cohesionless, although the slight cohesion shown above is included to keep a consistent number of uncertain parameters in all the probabilistic analyses.

© University of Pretoria

4.1.5 Case 5 - Cycloned Slurry Dam No.1

This model comprised a 30m cyclone slurry dam with 1V:3.0H side slopes on a competent sand foundation. COV in the material parameters was selected as 20% for the cohesion and 10% for the friction angle. The phreatic surface was assumed to extend arbitrarily from the underflow-overflow transition to the approximate middle of the base of the underflow.

This model was selected and configured to return a safety factor of approximately 1.4, with average uncertainty in the shear strength parameters.

The model geometry is presented in Figure 4.5 and the material parameters follow in Table 4.5.

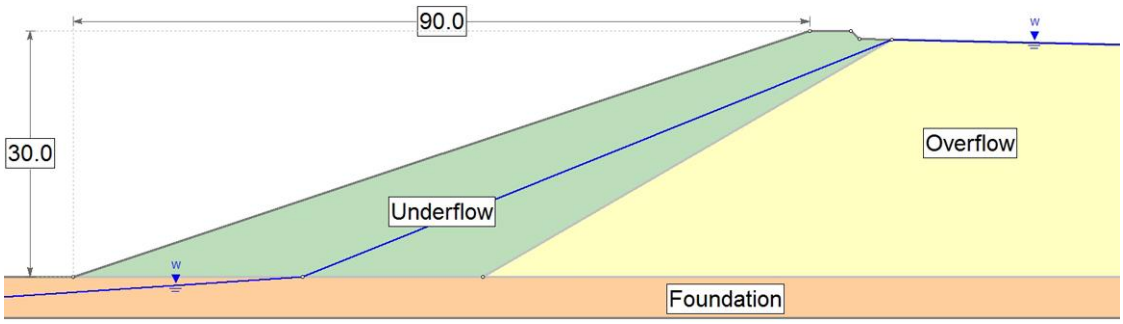


Figure 4.5: Cycloned slurry dam No.1 - Model geometry

Table 4.5: Cycloned slurry dam No.1 - Material parameters

Material Name	Unit Weight (kN/m^3)	Cohesion (kPa)		Friction Angle (degrees)	
		μ	σ	μ	σ
Underflow	16	2.0	±0.4	31.0	±3.1
Overflow	14	5.0	±1.0	23.0	±2.3
Foundation	18	0.0	-	36.0	-

Key:
μ - Mean
σ - Standard deviation

Note that the since the failure surface did not extent through the foundation there was no need to include uncertainty in the foundation properties in the probabilistic analysis.

© University of Pretoria

4.1.6 Case 6 - Cycloned Slurry Dam No.2

This model comprised a similar 30m cyclone slurry dam to the previous model with identical material properties and COV's, but with 1V:2.7H side slopes and a slightly steeper phreatic surface.

This model was configured to return a deterministic safety factor of approximately 1.35, and to investigate how only a change in geometry effects the probability of failure.

The model geometry is presented in Figure 4.6 and the material parameters follow in Table 4.6.

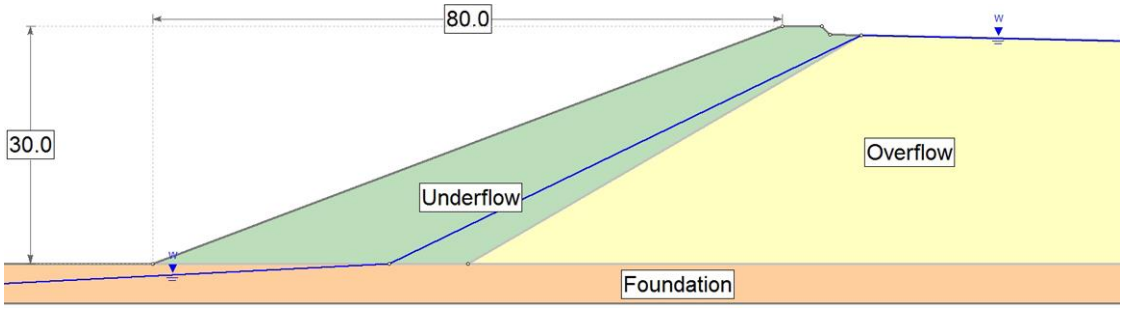


Figure 4.6: Cycloned slurry dam No.2 - Model geometry

Table 4.6: Cycloned slurry dam No.2 - Material parameters

Material Name	Unit Weight (kN/m^3)	Cohesion (kPa)		Friction Angle (degrees)	
		μ	σ	μ	σ
Underflow	16	2.0	±0.4	31.0	±3.1
Overflow	14	5.0	±1.0	23.0	±2.3
Foundation	18	0.0	-	36.0	-

Key:
μ - Mean
σ - Standard deviation

Similarly to the previous model, since the failure surface did not extent through the foundation there was no need to include uncertainty in the foundation properties in the probabilistic analysis.

© University of Pretoria

4.1.7 Case 7 - Upstream Coal Rejects Facility

This model comprised an approximately 115m high facility consisting of coal rejects contained within an upstream raised waste rock impoundment at 1V:2.1H side slopes on a silty sand foundation. COV in the friction angle was selected as 5% and all materials were modelled as being effectively cohesionless. No phreatic surface was included.

This model was selected and configured to return a safety factor of approximately 1.1, i.e. close to failure, with low COV in the shear strength parameters.

The model geometry is presented in Figure 4.7 and the material parameters follow in Table 4.7.

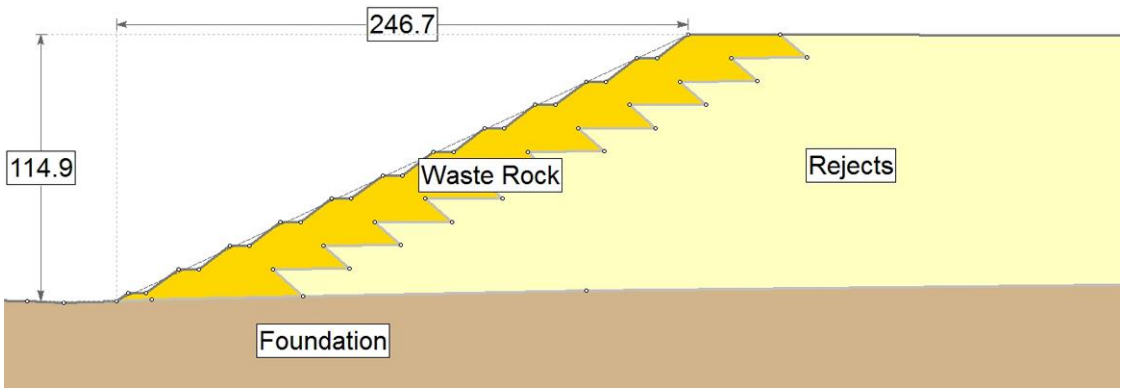


Figure 4.7: Upstream coal rejects facility - Model geometry

Table 4.7: Upstream coal rejects facility - Material parameters

Material Name	Unit Weight (kN/m^3)	Cohesion (kPa)		Friction Angle (degrees)	
		μ	σ	μ	σ
Rejects	18	0.1	±0.005	20.0	±1.0
Waste Rock	24	0.1	±0.005	40.0	±2.0
Foundation	18	0.0	-	36.0	-

Key:
μ - Mean
σ - Standard deviation

Note that since the failure surface did not extent through the foundation there was no need to include uncertainty in the foundation properties in the probabilistic analysis.

© University of Pretoria

4.2 ANALYSIS RESULTS

The probability of failure achieved using each of the six analysis methods applied to the seven embankments, is tabulated in Table 4.8 and plotted against safety factor in Figure 4.8:

Table 4.8: Summary of results - review of reliability-based analysis methods

Analysis	**Embankment on clay No.1**	**Embankment on clay No.2**	**Cycloned slurry dam No.1**	**Cycloned slurry dam No.2**	**Waste rock dump No.1**	**Waste rock dump No.2**	**Upstream coal rejects facility**
Analysis Reference	Case 1	Case 2	Case 3	Case 4	Case 5	Case 6	Case 7
Report Section Reference	4.1.1	4.1.2	4.1.3	4.1.4	4.1.5	4.1.6	4.1.7
Limit-Equilibrium Safety Factor Results							
Rocscience Slide 6.0	1.280	1.204	1.394	1.350	1.697	1.480	1.075
Microsoft Excel	1.300	1.220	1.400	1.360	1.710	1.500	1.080
Monte Carlo Results							
Classical - Monte Carlo Simulation	1.9E-02	6.2E-03	1.4E-06	2.6E-05	NR*	NR*	6.1E-02
Modified Monte Carlo Analysis	2.5E-02	8.7E-03	7.9E-05	1.9E-04	4.0E-07	3.5E-05	6.2E-02
Figure Number (Appendix A)	A1.1	A2.1	A3.1	A4.1	A5.1	A6.1	A7.1
Reliability-Based Analysis Results							
FOSM	2.4E-02	8.2E-03	1.1E-04	2.5E-04	4.4E-07	2.9E-05	4.6E-02
Simplified FOSM	2.9E-02	9.0E-03	1.4E-04	3.0E-04	7.2E-07	3.8E-05	4.7E-02
FORM (Low & Tang, 2004)	1.6E-02	4.3E-03	2.8E-05	8.7E-05	1.5E-08	7.0E-06	4.6E-02
FORM (Low & Tang, 2007)	1.6E-02	4.3E-03	2.8E-05	8.7E-05	1.5E-08	7.0E-06	4.6E-02
Figure Number (Appendix A)	A1.2	A2.2	A3.2	A4.2	A5.2	A6.2	A7.2

* NR – No Result (see notes below Figure 4.8)

© University of Pretoria

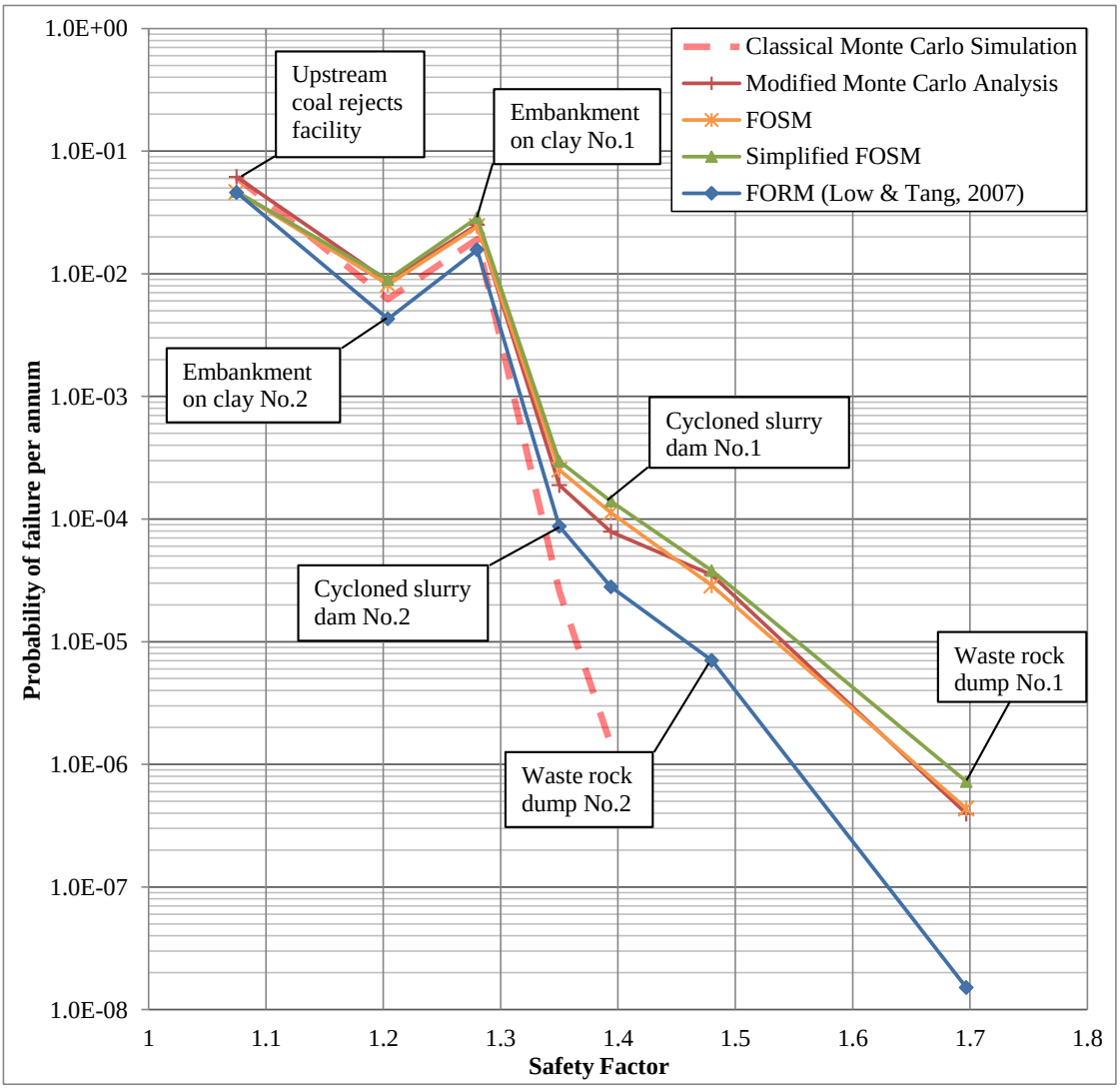


Figure 4.8: Comparison of automated and reliability-based analysis methods

Note 1: The results for each probabilistic method are connected by straight lines for visual purposes only.

Note 3: No results are possible below 1.43E-06 (i.e. 1 in 700 000) in the Monte Carlo analysis due to the 700 000 trials selected in the analyses (see Section 4.3).

Note 3: The results for the Low & Tang (2004) FORM method are not plotted on the above figure as these were found to be practically identical (to approximately six decimal places) to the Low & Tang (2007) FORM method and were, therefore, not visible.

The Slide 6.0 limit-equilibrium results, together with the results of the reliability-based analyses, are attached in Appendix A.

© University of Pretoria

4.3 ANALYSIS OBSERVATIONS AND DISCUSSION

The following observations were made from the comparison between the various probabilistic analysis methods. These are discussed in detail in this section, and the pertinent points summarised in Section 8.0 together with the remaining analyses/ experiments.

4.3.1 Safety Factors

The safety factors achieved in the spreadsheet calculation are within 0.4% to 1.5% of the safety factors determined using the analysis package. This verifies that the spreadsheet developed to calculate safety factors is sufficiently accurate. This slight error is carried through the Low & Tang FORM calculations but is considered negligible since the range of probabilities of failure assessed is large, i.e. up to eight orders of magnitude.

4.3.2 Monte Carlo Methods

No results are possible below 1.43E-06 in the Classical Monte Carlo Simulation due to the maximum of 700 000 trials selected in the analyses. This is a limitation of the Classical Monte Carlo Simulation, particularly for materials with low to average COV where this limit is already achieved at a safety factor of 1.4, i.e. less than the typical design standard of 1.5 used in South Africa. In order to achieve an additional order of magnitude, the number of trials would need to be increased correspondingly, which was found to be out of the computational capacity of the analysis package.

In this regard, it is expected that the probabilities of failure returned by the Monte Carlo analysis for Case 3 and Case 4 are of too low an accuracy to consider as correct solutions.

While the reliability-based methods are observed to have a set level of conservatism, i.e. there is no overlapping of curves, the Classical Monte Carlo Simulation is conversely inconsistent. This is particularly evident at lower probabilities of failure, i.e. near the limit of the Classical Monte Carlo Simulation (1 in 700 000 or 1.43E-06). This could be due to the “hit-or-miss” nature of the Monte Carlo method and should be less prevalent with more trials. The shape of these curves may possibly also change if different seed numbers were to be used.

The Modified Monte Carlo Analysis overcomes the limitation of the number of trials, and additionally returned consistently similar results to the Simplified FOSM methods. Since this

© University of Pretoria

method is based on the data from the Classical Monte Carlo Simulation, this would suggest that the number of failures recorded for the Cycloned slurry dam No.1 is perhaps not entirely representative.

4.3.3 Reliability-Based Methods

The results achieved with the two Low and Tang FORM methods are practically identical with differences only apparent at approximately six decimal places. This should be expected as both methods are based on the same concept, and mathematics, of an expanding ellipsoid. The difference between these two methods was reported in the literature to be associated to the robustness and efficiency of the Low & Tang (2007) method; however, apart from being slightly easier to set up and troubleshoot, there is almost no difference between the results.

The simplified FOSM method is the most conservative while the Low & Tang (2007) method is the least. There is also a consistent level of conservatism between the reliability-based methods, i.e. the curves do not overlap but the difference between them does appear to increase with a decrease in probability of failure.

The two analyses carried out on the cycloned slurry dam, whereby only the geometry of the facility was altered, illustrates this increase in conservatism as the difference between the two increased from 240% to 400% with the increase in safety factor (see Figure 4.9).

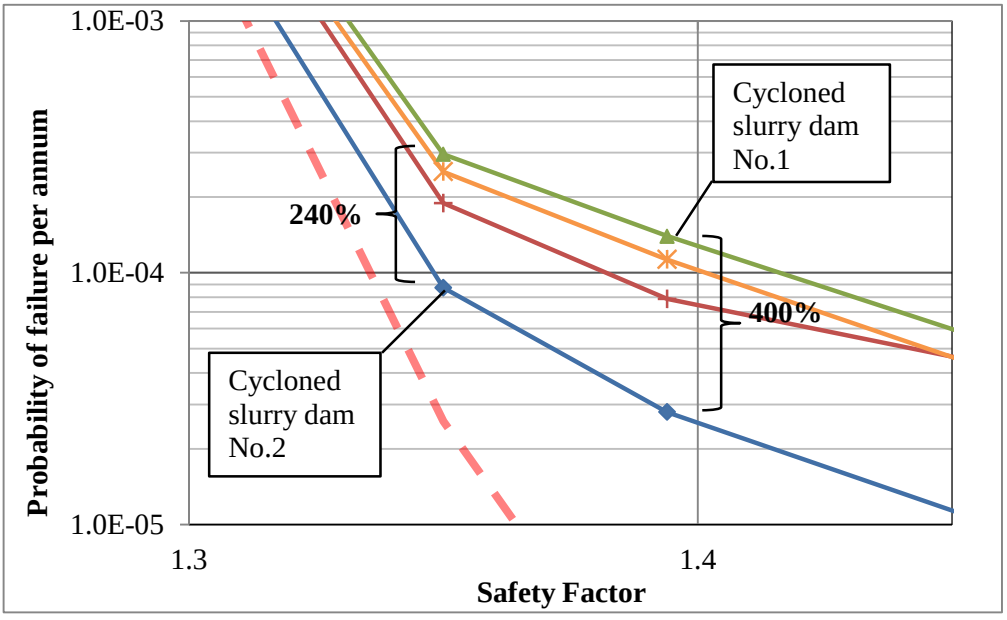


Figure 4.9: Extract of Figure 4.8 highlighting the increasing level of conservatism

© University of Pretoria

The conservatism of the FOSM and Simplified FOSM methods is understood to be due to the numerous assumptions or approximations involved in them. In particular, the resulting distribution of the safety factor is assumed to be Normal (which is most likely not the case), and the moments of the failure criterion are estimated using the mean values of the parameters and extrapolating linearly, i.e. this implies that it does not matter where the partial derivatives are evaluated.

Given that the Low & Tang (2007) method was generally found to be the least conservative, and therefore leading to more streamline design, and was computationally easier than the remaining reliability-based methods, this method was selected for use in the remaining analyses and experiments.

4.3.4 Level of Uncertainty

The effect of uncertainty is illustrated by the analyses on the embankment on soft clay, whereby the reduction in the shear strength properties reduced the safety factor, but the reduction in the COV in the shear strength reduced the probability of failure (see Figure 4.10). This is a significant observation as it illustrates that, even though the safety factor has reduced by 6% due to the friction angle of the materials being reduced by 1° or 2°, the probability of failure has reduced by 73% with only a 5% reduction in the COV.

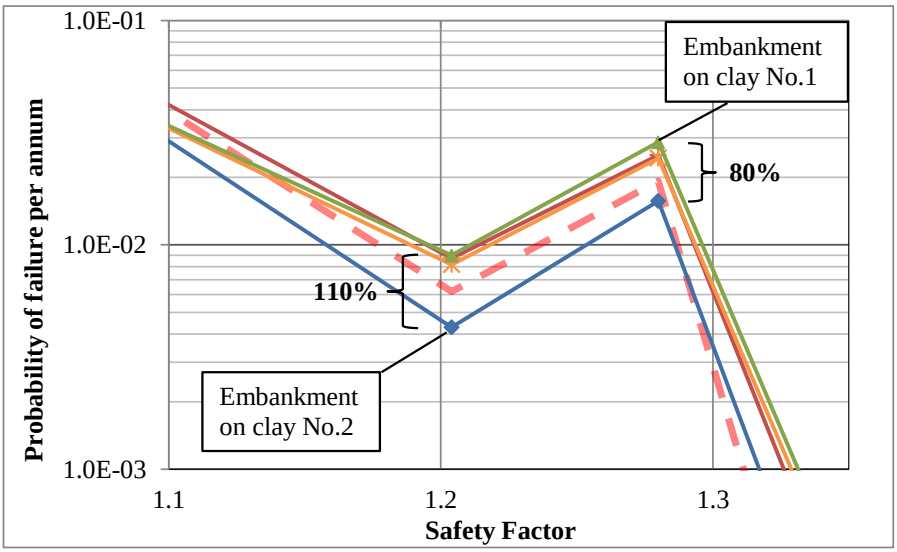


Figure 4.10: Extract of Figure 4.8 highlighting the effect of uncertainty

© University of Pretoria

Note: The difference between the Simplified FOSM and Low & Tang (2007), i.e. the most and least conservative respectively, is highlighted to reiterate the increasing difference in conservatism with decreasing probability of failure.

A further observation is that there appears to be a consistent relationship between safety factors to probabilities of failure for a certain level of uncertainty (COV), even though the embankments had very different geometries, configurations and material properties. Apart from the 'Embankment on clay No.1' and the 'Waste rock dump No.1', the uncertainty in the friction angle was modelled as a COV of 10% for the embankments and these subsequently follow a relatively consistent curve. If this is an inherent feature of reliability-based analysis, this could convey a very significant message regarding the level of uncertainty in material parameters and the resultant probability of failure. An experiment was therefore carried out to investigate this concept, the results of which are presented and discussed in Section 7.0.

© University of Pretoria

5.0 'SEVERITY' OF FAILURE

This section applies the Low & Tang (2007) FORM method (selected based on the results of the previous section) to the analysis of a typical tailings storage facility, and investigates the effect material uncertainty has on the probability of failure of slip surfaces smaller and larger than the critical slip surface. The hypothesis is that, while surfaces larger and smaller than the critical slip surface may indeed have higher safety factors, they may not necessarily have acceptable probabilities of failure.

In order to define what is acceptable, however, there are a number of issues that needed clarification prior to the onset of the analysis. These were the following:

- What is the probability of failure measured against?
- Given the reservations with using consequence of failure discussed in Section 2.6.1, what is the alternative?
- What is an acceptable probability of failure? Particularly if the published acceptable limits for consequence of failure are not applicable?

This section therefore introduces to the concept of measuring 'severity' of failure and 'slope performance', with an emphasis on what an owner of this type of facility and/ or the public, would deem as acceptable. The concept of 'severity' is defined in Section 5.1, following which, the various stability models are defined and the results presented and discussed.

This was done by analysing a uniform, cohesionless gold tailings facility at three different slope angles (1:2, 1:2.5 and 1:3), each with COV in the friction angle of the tailings material of 5%, 10% and 15%. Then for each model configuration, one failure smaller and two failures larger than the critical slip surface were analysed and their probabilities of failure judged against the proposed measure of relative size, or 'severity', of that failure.

The resulting chart of 'severity' versus probability of failure for the 36 (3 slopes x 3 uncertainties x 4 failure sizes) analyses were then used, together with certain principles inherent to the various proposed limits of acceptable probabilities of failure (see Section 2.6.2), to suggest limits of acceptable performance for respective 'severities' of failure.

© University of Pretoria

5.1 'SEVERITY' CONCEPTS

In the literature presented in Section 2.6.2, consequence of failure is measured against the "potential number of fatalities" caused by a particular failure event. This is understood to be an acceptable approach for water retaining embankments which, once a failure occurs, the flow of water can be predicted relatively well and the number of people in danger determined.

Tailings materials, or at least those common in southern Africa, generally comprise cohesionless sandy silt- to silt- sized particles and exhibit complex behaviour depending on the pore pressure regime to which they are exposed, such as liquefaction potential and potential to flow, and it is therefore difficult to predict the behaviour of these materials when failure occurs compared to that of general water retaining structures.

For example, a large failure of a tailings storage facility without flow potential would result in the material slumping and very little damage would occur. Conversely, a small failure in a facility comprising potentially liquefiable material could cause static liquefaction and result in large amounts of material flowing from the facility, which is what occurred in the Merriespruit failure in 1994.

Unless the prediction of whether the material will flow, how much of it will flow and how far, is appropriately assessed by detailed laboratory and/ or in-situ testing, this could lead to a particularly subjective assessment of how many lives are at risk (i.e. one engineers opinion could vary drastically from another). For this reason, it is perhaps not suitable to relate the size of failure of a tailings storage facility to a consequence, particularly in terms of potential fatalities, and a new approach is therefore presented herein.

'Severity' of failure is essentially defined as a measure of how severe a failure is, and is solely dependent on the size of the failure relative to the size of the facility. No consideration is given to the potential downstream damage and/ or loss of life; it is merely an assessment of whether a particular size of failure is within acceptable limits.

Note that it is anticipated that subsequent to this suggested procedure, the facility size, potential for flow and downstream infrastructure can be addressed in subsequent consequence/ risk analysis, such as with a decision/ event tree analysis. This is, however, not included in the scope of this study.

© University of Pretoria

In order to have a "universal" measurement of relative size of failure, i.e. consistent for all embankment sizes and configurations, the following criteria were considered:

- The measurement should be dimensionless;
- It should be consistent for any height of embankment;
- It should be consistent for any slope angle;
- It should be easily measureable; and
- It should be primarily applicable for materials with little cohesion, i.e. shallow failures.

The chosen approach was therefore taken as the ratio of the depth of the failure surface to the height of the embankment, as depicted in the equation and Figure 5.1 below, and referred to as the "Severity Index":

$$\text{Severity Index} = \frac{\text{Failure Surface Depth}}{\text{Height}} \tag{7}$$

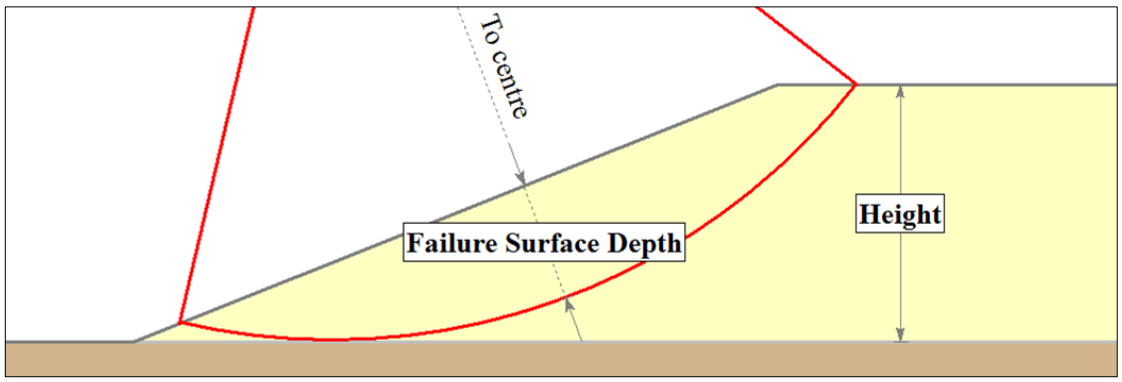


Figure 5.1: Illustration of the measurement of 'severity'

To better illustrate the applicability of the selected Severity Index, a brief description of the possible alternatives considered is discussed in short below:

- Using the area of the failed material surface is both a tedious calculation, and requires the division by a length squared (to be dimensionless), for example Height^2, which results in lower severity indexes for steeper embankments due to a higher height-to-width ratio;

© University of Pretoria

- Dividing the area of the failed material surface by the area of the embankment becomes complicated if the failure surface extends through the foundation or past the crest, or if the embankment is benched; and

- Using the arc length of the failure surface would give misleading (high) severities for the shallow failures common to cohesionless materials.

To illustrate the universal and objective nature of the proposed severity index, consider two tailings storage facilities with identical slope geometry, the first of which is 20m high and the second 80m high. If both facilities were impounding material with a potential to flow, it would likely take a failure through the crest of each facility of equivalent geometry (i.e. severity index) to cause a breach and release of the contained tailings material.

The final concept to define is that of 'slope performance', which is the term given to the curve produced by the various failure sizes plotted on a graph of 'Severity' versus Probability of Failure. This can be perceived as the overall performance of the facility, since certain failure sizes may fall within acceptable limits, while others may not.

The proposed procedure of plotting 'slope performance' curves is additionally considered as a possible alternative to the more typical, but computationally extensive, procedure of searching for the critical probabilistic failure surface. See verification exercise in Section 6.4.

5.2 SCOPE OF THE ANALYSIS

The scope of this analysis is to investigate the effect material uncertainty has on the probability of failure of slip surfaces smaller and larger than the critical failure surface, and introduce the concepts of 'severity' of failure and 'slope performance', as well as suggest limits of acceptable performance of failure

To constrain the analysis to the uncertainty in the tailings material only, the foundation materials were modelled as being highly competent, i.e. the cohesion was set to 100kPa and the friction angle 50°. This forces the failure through the tailings material only, and eliminates any effect that the foundation may have on the final outcome.

© University of Pretoria

Since the tailings material is cohesionless and the foundation materials were essentially not included in the analysis, there is effectively only one variable parameter. As the matrix notation was set up for four uncertain parameters in the previous section, to be consistent between the various other analyses/ experiments, the uncertainty in all the shear strength parameters (cohesion and friction angle for the tailings and foundation) were included by assigning negligible standard deviations where appropriate.

5.3 ANALYSIS METHODOLOGY

Three configurations of a typical cohesionless and uniform gold tailings dam were constructed to the following criteria/ assumptions:

- A total height of 30m;
- Uniform tailings material, i.e. there is no strength difference between the "day wall" and confined material;
- The slopes are continuous, i.e. no benches;
- Three slope variations of 1:2, 1:2.5 and 1:3; and
- A water table assumed to extend from the toe of the embankment to 30m from the crest.

Each of the three slopes were subsequently configured to model three degrees of COV in the tailings material. The material properties used in the analysis are listed in Table 5.1 below, including the three COV variations for the friction angle of the tailings material.

Table 5.1: Material parameters used in the analysis

Material Name	**Unit Weight (kN/m^3)**	**Cohesion (kPa)**		**Friction Angle (degrees)**		
		μ	**σ**	**μ**	**COV**	**σ**
Gold Tailings	16	0.01	±0.001	35*	5%	±1.75
					10%	±3.50
					15%	±5.25
Foundation	20	100	±0.001	50	NA	±0.001

Key:
μ - Mean
σ - Standard deviation
* - Selected from Table 2.2 in Section 2.3
COV - Coefficient of variation
NA - Not applicable

© University of Pretoria

Note that the negligible standard deviations of 0.001 were included to complete the matrix notation in the Low & Tang (2007) FORM analysis which was set up for four uncertain parameters.

The limit-equilibrium analysis was then carried out to locate the critical failure surface for each slope variation, and focus limits (which is a feature of the analysis package utilised to constrain the radii increments for each grid point to within a smaller "focus window") were then identified for the assessment of one failure smaller, and two larger, than the critical failure surface. Each of the slope configurations, together with their critical slip surface and selected focus limits, are presented in Figures 5.2, 5.3 and 5.4 below.

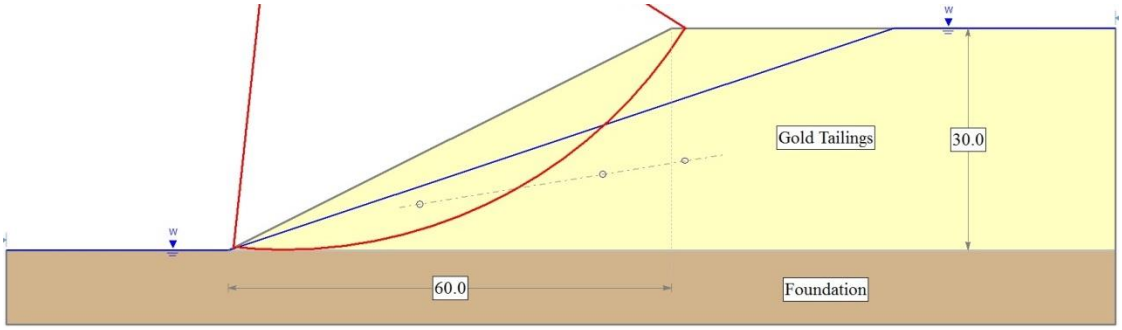


Figure 5.2: Model construction - gold tailings dam at 1:2 slope

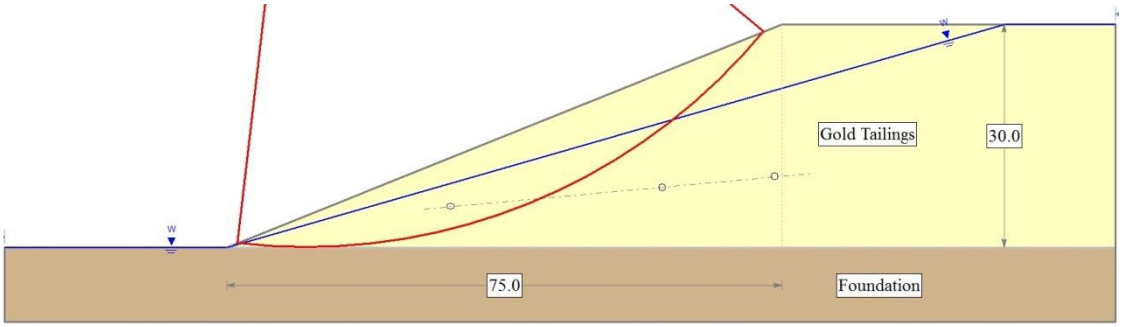


Figure 5.3: Model construction - gold tailings dam at 1:2.5 slope

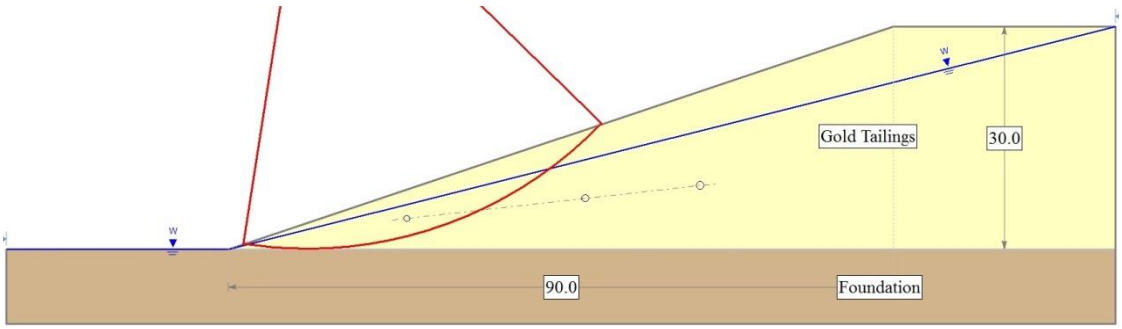


Figure 5.4: Model construction - gold tailings dam at 1:3 slope

© University of Pretoria

The focus limits were implemented by first, identifying the approximate locations relative to the critical failure surface (as shown by the circles in the figures above), and then duplicating the model three times with the respective "focus window" defined in each. This "focus window" limits the maximum and minimum radii of possible slip surfaces for each grid point to within this defined region.

For ease of reference, the various model configurations included in the analysis are summarised in the organogram shown in Figure 5.5.

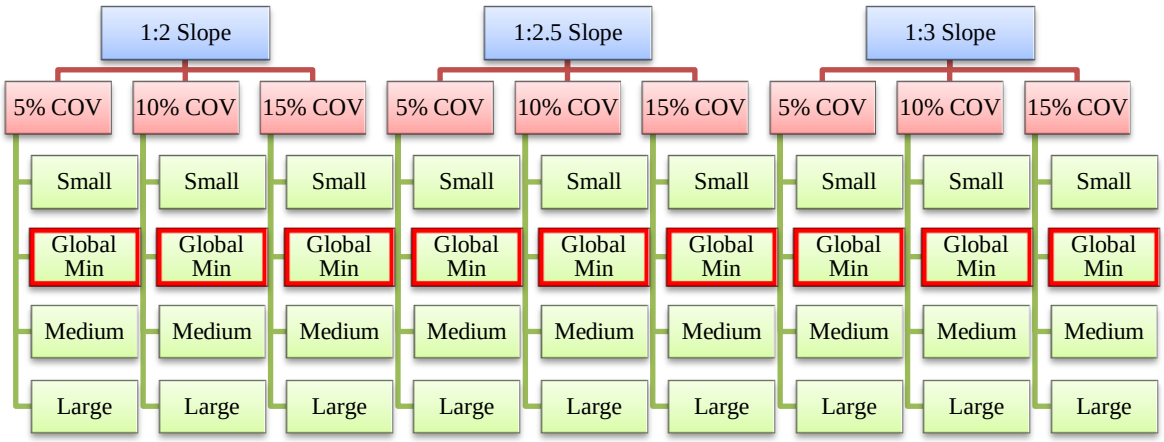


Figure 5.5: Organogram summarising the model configurations

The reliability-based analysis using the Low & Tang (2007) FORM method was subsequently carried out by importing the analysis data from the limit-equilibrium calculation, and running the macro created to automate the solution and tabulate the results. These methods are described in more detail in Sections 3.3.6 and 3.4.

© University of Pretoria

5.4 ANALYSIS RESULTS

The results of the limit-equilibrium and reliability-based analyses are summarised in Table 5.2 below and plotted on the Severity Chart in Figure 5.6. The limit-equilibrium results are attached in Appendix B:

Table 5.2: Summary of results – severity of failure

	Slope Angle:	1:2			1:2.5			1:3		
	COV:	5%	10%	15%	5%	10%	15%	5%	10%	15%
Small	Failure Surface Depth (m)	6.2			6.2			3.9		
	Safety Factor	1.135			1.288			1.439		
	Reliability Index	2.070	1.035	0.690	3.804	1.902	1.268	5.235	2.617	1.744
	Probability of Failure (%)	1.9E-02	1.5E-01	2.5E-01	7.1E-05	2.9E-02	1.0E-01	8.3E-08	4.4E-03	4.1E-02
	Severity Index	0.207			0.207			0.130		
Global Min	Failure Surface Depth (m)	9.3			9.7			6.2		
	Safety Factor	1.133			1.289			1.439		
	Reliability Index	2.055	1.028	0.685	3.796	1.898	1.265	5.230	2.615	1.743
	Probability of Failure (%)	2.0E-02	1.5E-01	2.5E-01	7.4E-05	2.9E-02	1.0E-01	8.5E-08	4.3E-03	4.1E-02
	Severity Index	0.310			0.323			0.207		
Medium	Failure Surface Depth (m)	12.9			14.0			8.9		
	Safety Factor	1.183			1.344			1.439		
	Reliability Index	2.654	1.327	0.885	4.382	2.191	1.461	5.231	2.615	1.743
	Probability of Failure (%)	4.0E-03	9.2E-02	1.9E-01	5.9E-06	1.4E-02	7.2E-02	8.4E-08	4.5E-03	4.1E-02
	Severity Index	0.430			0.467			0.297		
Large	Failure Surface Depth (m)	17.0			18.0			12.5		
	Safety Factor	1.305			1.482			1.449		
	Reliability Index	3.957	1.979	1.319	5.613	2.806	1.871	5.334	2.667	1.778
	Probability of Failure (%)	3.8E-05	2.4E-02	9.4E-02	1.0E-08	2.5E-03	3.1E-02	4.8E-08	3.8E-03	3.8E-02
	Severity Index	0.567			0.600			0.417		

© University of Pretoria

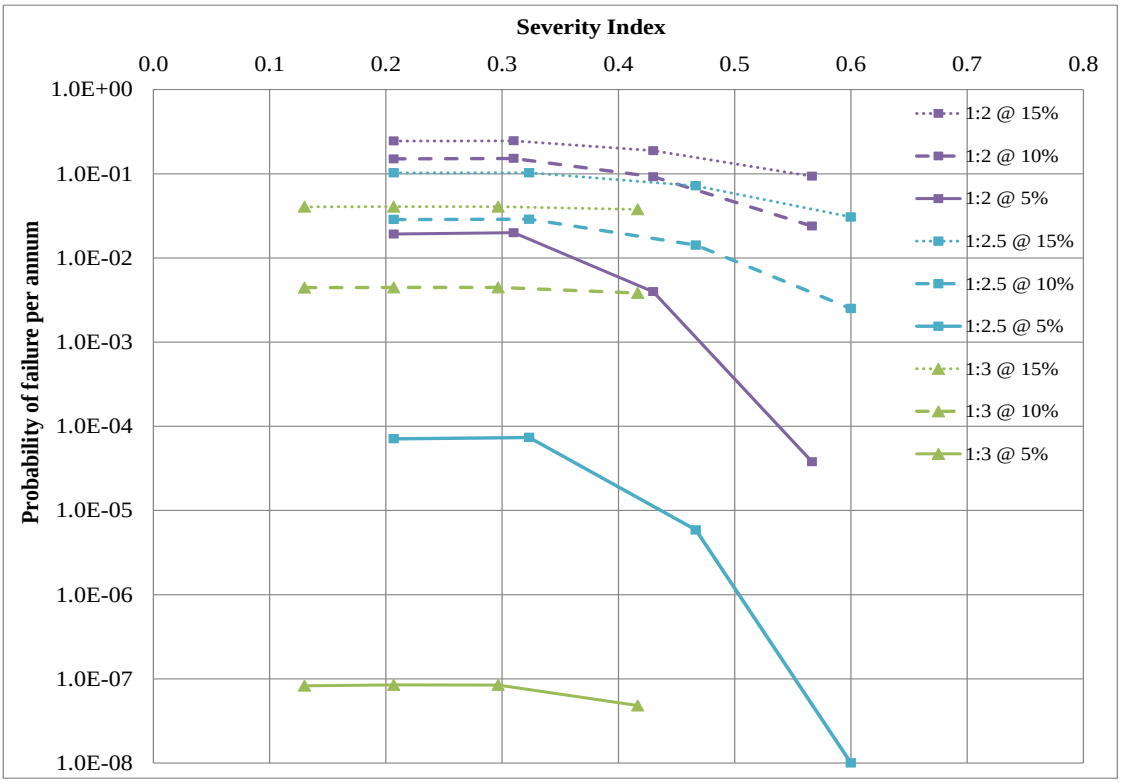


Figure 5.6: Analysis results presented as severity versus probability of failure

For the graphical representation of these results (or the "Severity Chart") to have tangible significance, i.e. form the basis of the analysis discussions, they need to be presented against limits of acceptable probabilities of failure which are, currently, undefined. A discussion of the development of the proposed acceptable limits is, therefore, included before the results are re-presented with the proposed acceptable limits superimposed.

Note that the development of the limits of acceptable probabilities of failure is presented in the section following, after which, the above figure is re-presented with the proposed limits of acceptable performance for detailed discussion.

5.5 DEVELOPMENT OF PERFORMANCE LIMITS

As stated on Section 5.3, in order for the results of the 36 analyses presented on Figure 5.6 to have tangible significance, they need to be presented against limits of acceptable performance. The following criteria were considered, and methodology followed, in the subsequent development of these proposed limits:

© University of Pretoria

a) A theoretical upper bound limit exists in that a severity index of zero should have an acceptable probability of failure of 100%;

b) The various methods discussed in Section 2.6.2, such as (ANCOLD, 2003), propose lower bound limits of acceptable probabilities of failure of approximately 1.0E-06, i.e. probabilities less than this are generally perceived to be acceptable, regardless of the consequence; and

c) Each of the slope stability results were reviewed by the author and supervisor to evaluate whether the failure size, or 'severity', and its associated probability of failure would be acceptable to an owner of this type of facility and/ or the public. This assessment was based partly on engineering judgement, as well as extrapolation from the ranges of probability of failure which society has implicitly found acceptable for various engineering projects, as presented by (Whitman, 1984).

It was found during this process that certain of the results were borderline between acceptable and unacceptable, and an intermediate performance zone was therefore included. The implication of this zone is discussed in Section 5.6.

The assessment given to each Slide 6.0 output result is shown on the respective figures attached in Appendix B, but for illustrative purposes, the assessment of the 1:3 slope with 10% COV is discussed below.

Figure 5.7 to Figure 5.10 present, from smallest to largest respectively, the results for the various 'severities' of the 1:3 slope with 10% COV. These were found to have very similar probabilities of failure of 4.4E-03 to 3.8E-03 (or approximately 1 in 250), i.e. the 'slope performance' curve was relatively flat, and the severity ranged from a small failure in the toe to a failure encompassing the entire slope. For the given probability of failure, the following assessments were made for the slope:

- The two smaller failures (Figure 5.7 and Figure 5.8) were deemed to be acceptable since the failure size is not expected to cause any major operational delays or stoppages to mine operations.

- The largest failure (Figure 5.10) is, however, expected to have unacceptable consequences since it encompasses the entire slope length and would likely cause

© University of Pretoria

operational stoppages for remediation work, and potentially damage to infrastructure and potential loss of life downstream of the facility (should the material flow). This is expected to be unacceptable at a probability of 1 in 250.

- The medium failure Figure 5.9 was deemed to be within the intermediate zone since, while the failure is relatively large, it is not expected to breach the containment of wet tailings but could result in substantial remediation work.

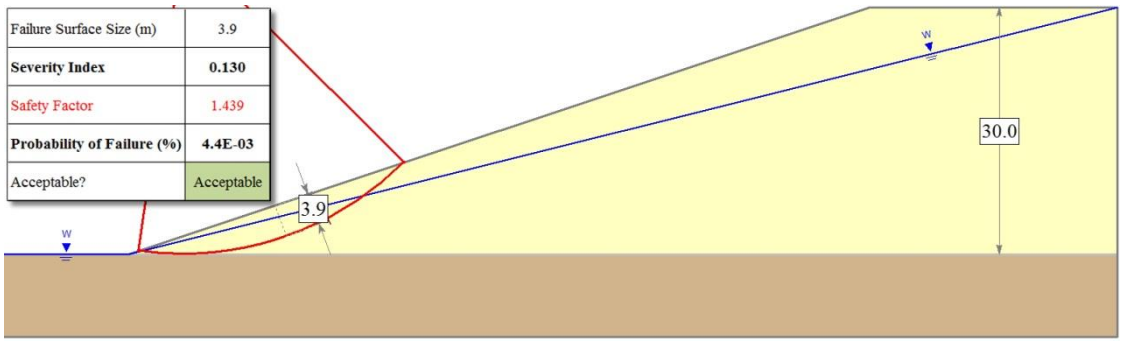


Figure 5.7: Acceptability assessment of 1:3 slope with 10% COV - Small

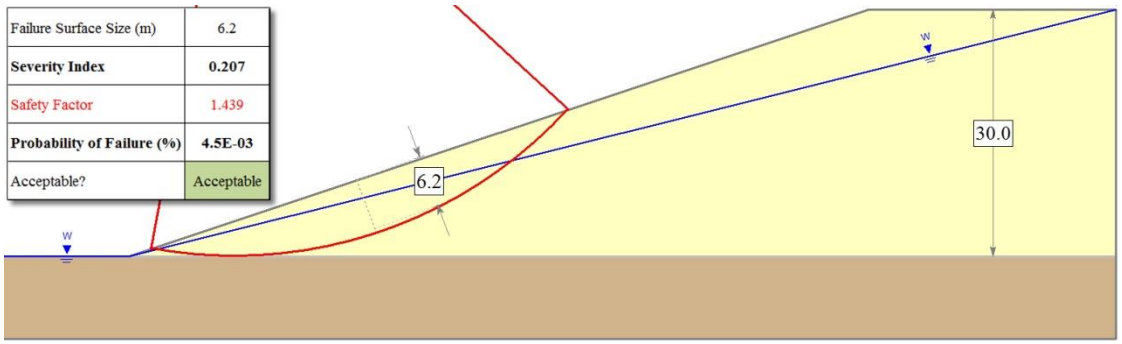


Figure 5.8: Acceptability assessment of 1:3 slope with 10% COV - Global Minimum

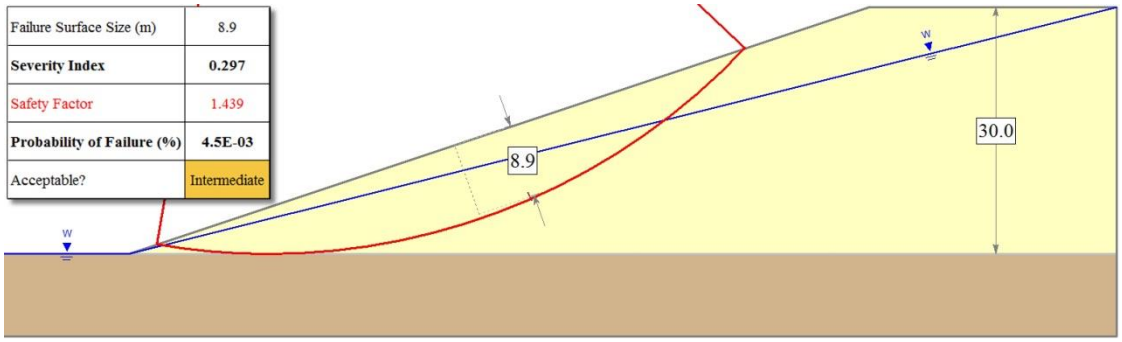


Figure 5.9: Acceptability assessment of 1:3 slope with 10% COV - Medium

© University of Pretoria

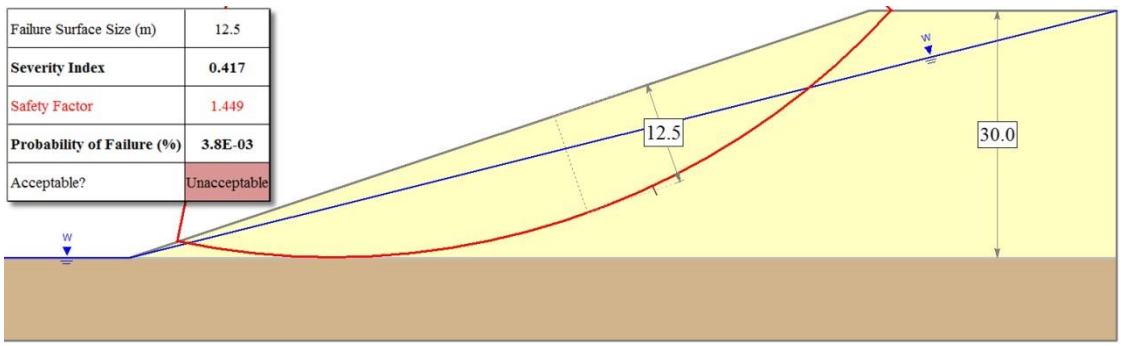


Figure 5.10: Acceptability assessment of 1:3 slope with 10% COV - Large

The limits joining the upper bound (p_f = 100% at S.I. = 0) and the lower bound (p_f = 1.0E-06), and separating the acceptable, intermediate and unacceptable performance zones, were arbitrarily selected as straight lines since these appeared to fit well for the data points available, i.e. for probabilities of failure of greater than 1.0E-03.

The results of the analyses are re-presented on Figure 5.11 below and discussed in Section 5.6:

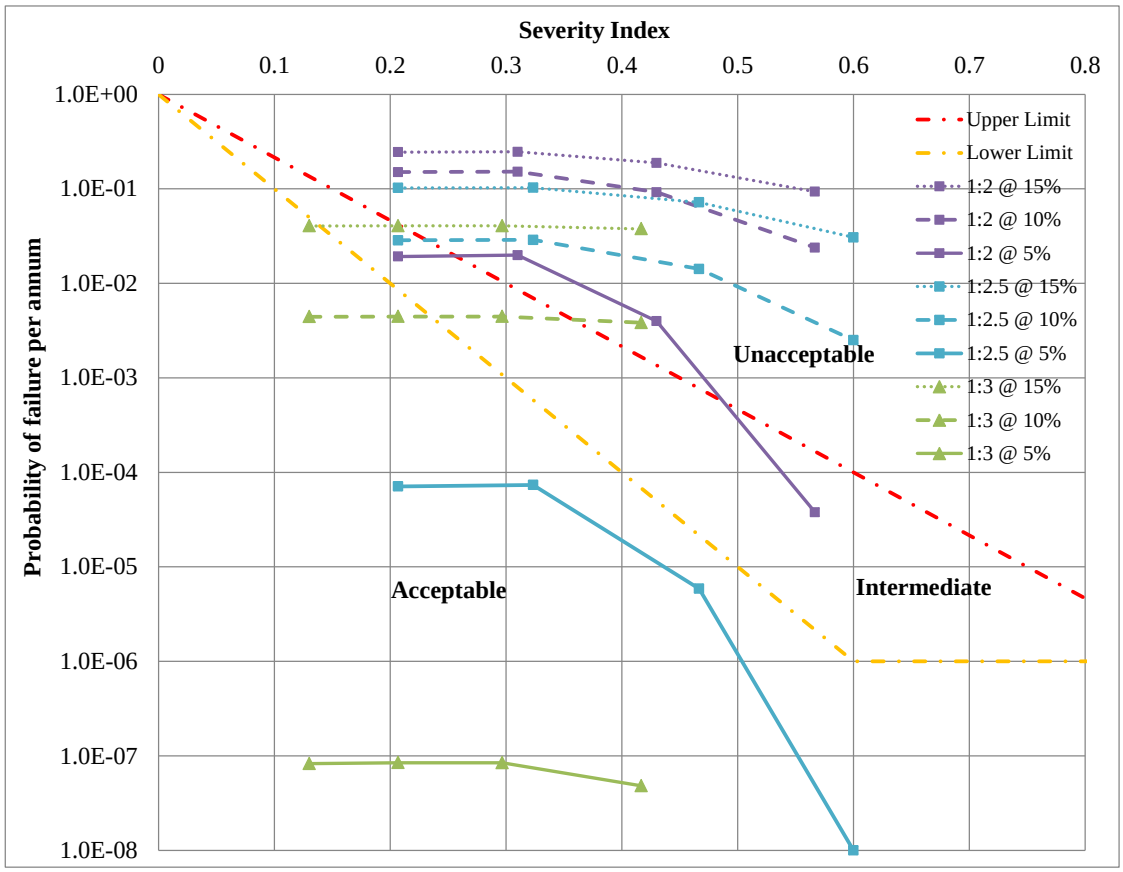


Figure 5.11: Analysis results on the Severity Chart

© University of Pretoria

5.6 ANALYSIS OBSERVATIONS AND DISCUSSION

The following observations were made from the results of the 36 analyses and their significance given the proposed limits of acceptable performance. These are discussed in detail in this section, and the pertinent points summarised in Section 8.0 together with the remaining analyses/ experiments. The limit-equilibrium results are attached in Appendix B.

5.6.1 'Slope Performance' Curves

The performance curves are relatively flat for severity indexes less than approximately 0.4. This is also reflected by the relatively consistent safety factors in Table 5.2 for severity indexes within approximately 30% to 40% of the severity index of critical failure surface. This is significant as it indicates that there is a range of failure sizes, or severities, near the critical surface at approximately the same safety factor and probability of failure. This is believed to be due to cohesionless nature of the tailings material and the influence of the (straight) water table assumed in the analysis, i.e. although the failure surface is a different size, it has the same ratio of forces causing and resisting failure.

This advocates that it is essential to investigate failure surface sizes larger than the critical failure surface returned in the limit-equilibrium analysis for cohesionless materials, as a much larger severity than that of the global minimum may exist with a very similar probability of failure.

The difference between the three slope performance curves (per slope) is greater at higher safety factors. This suggests that the relationship between the safety factor and probability of failure, if represented by a curve, may have an increasing negative gradient with increase in safety factor, i.e. the probability of failure reduces greatly further from the mean. This is investigated further in Section 7.0.

5.6.2 1:2 Slope Angle

Based on the proposed limits of acceptable probabilities of failure, none of the curves plot within the acceptable zone. Both the 10% and 15% COV variations of the 1:2 slope are deemed to be unacceptable, while the slope with 5% COV spans across the unacceptable zone and the intermediate zone. This could be expected as the safety factors ranged from 1.14 to 1.31 which is well below a target safety factor of approximately 1.4 to 1.5.

© University of Pretoria

5.6.3 1:2.5 Slope Angle

Based on the proposed limits of acceptable probabilities of failure, only the 1:2.5 slope with 5% COV is deemed to be acceptable. The safety factors for this slope ranged from 1.29 to 1.48, which, in typical deterministic engineering practices would be seen as unacceptable; particularly in South Africa where a typical design value for permanent water storage facilities is a safety factor of 1.5. In this instance, however, it is shown that the facility may be deemed as acceptable, provided the uncertainty (or variability) of the material is confirmed to be 5% or lower.

5.6.4 1:3 Slope Angle

Based on the proposed limits of acceptable probabilities of failure, only the 1:3 slope with 5% COV is deemed to be acceptable. The safety factors for this slope ranged from 1.44 to 1.45, which could be seen as borderline in South Arica, but acceptable in other countries where the requirement is a safety factor of only 1.4. Interpolation between the 5% COV curve and 10% COV curve suggests that a maximum material uncertainty of approximately 8% would return acceptable performance. Higher uncertainty would render the facility unacceptable.

The 1:3 slope with 10% COV, which is highlighted in Figure 5.12 below, is a particularly good example of a facility appearing to perform acceptably based on the safety factor of the critical failure surface. However, the severities of the failures are very different as shown in Figure 5.7 to Figure 5.10 and summarised in Figure 5.12. Clearly the performance of the facility is very different for the four cases. The significance of this is that an owner of this type of facility may be comfortable with the severity and associated probability of failure for the critical failure surface, but not with a similar probability of failure for failure surfaces larger than a severity index of 0.35. This may be the owners own implicit level of comfort, or it may be that the insurance costs associated with the size and probability of failure may be excessive.

© University of Pretoria

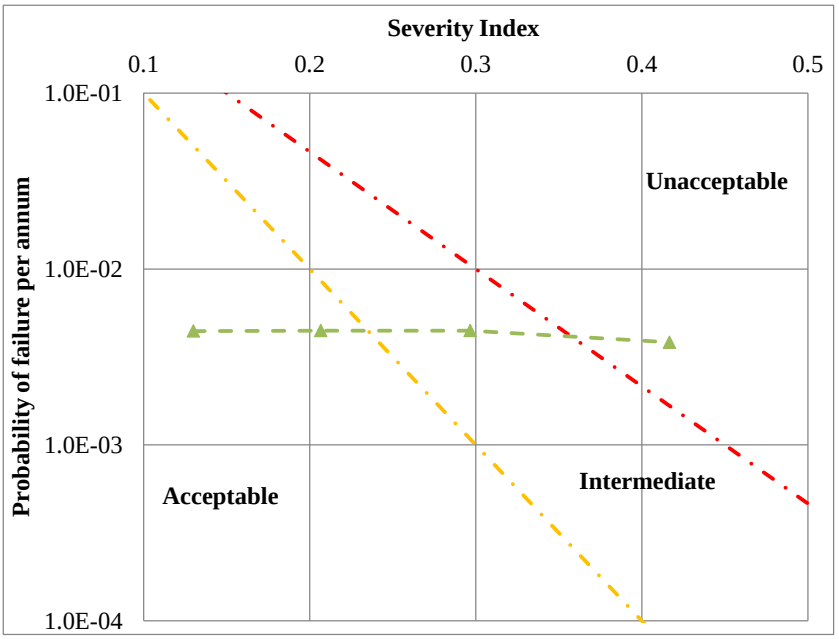


Figure 5.12: Extract of Figure 5.11 showing the 1:3 slope with 10% COV

5.6.5 Intermediate Zone

The intermediate zone was included because, as with many aspects of engineering, there is not always a clear boundary between what is acceptable and what is not, and the final decision is dependent on many other case-specific aspects (such as for example economics, site conditions, consequence or even politics).

In this instance it is suggested that a facility which has a slope performance curve extending from the acceptable zone into the intermediate zone, be treated in a manner similar to the ALARP principle used in (ANCOLD, 2003), i.e. by evaluating the following:

- the risk of failure;
- the potential consequence of failure; and
- the measures necessary for averting or mitigating the risk (usually economic),

If the risk and consequence is insignificant in relation to the sacrifice, it is deemed to be acceptable.

© University of Pretoria

6.0 EXPERIMENT NO.1 – APPLICATION OF SEVERITY CHART

Having carried out the above analysis on a uniform, cohesionless gold tailings facility, and using the results to propose the limits of acceptable probability of failure, this section presents an experiment carried out to test the suitability of the proposed 'severity' and 'slope performance' concepts, as well as the proposed limits of acceptable performance, for a more complex tailings storage facility, namely a cycloned slurry dam comprising fine overflow material confined within a coarse underflow impoundment.

6.1 SCOPE OF THE EXPERIMENT

The cyclone facility was configured, by positioning the water table, to return a safety factor of 1.5 for the critical slip surface. Failure surfaces bigger and smaller than the critical failure surface were then analysed assuming a 10% COV for the shear strength parameters (cohesion and friction angle) of both the underflow and overflow materials.

A second configuration of the facility was then analysed, and the results plotted on the same severity chart, to investigate the effect of using a 15% COV for the shear strength parameters of the overflow material (in-situ and laboratory testing is generally difficult in overflow materials, which leads to higher uncertainty, so a COV of 15% is not unrealistic).

The results of the above analyses were subsequently used in a verification exercise to compare the failure relating to the highest probability of failure, i.e. the peak of the 'slope performance' curve, to the critical probabilistic failure surface returned from a typical, but computationally extensive, overall probabilistic slope stability analysis whereby the critical failure surface is located for each simulation of shear strength parameters.

6.2 EXPERIMENT METHODOLOGY

The model comprised a 30m high cyclone slurry dam with approximately 1V:2.5H side slopes on a competent sand foundation. As stated above, the water table was configured to return a safety factor of 1.5. The model geometry is presented in Figure 6.1 and the material parameters for each analysis follow in Table 6.1.

© University of Pretoria

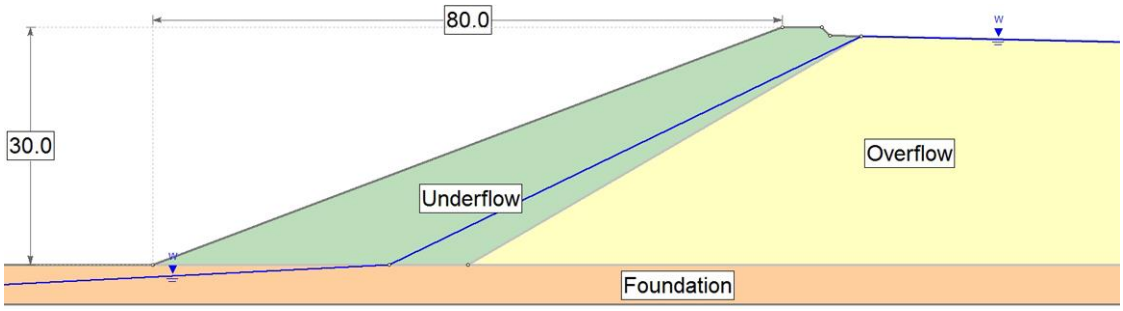


Figure 6.1: Experiment No.1 model configuration - cycloned slurry facility

Table 6.1: Experiment No.1 material properties – cycloned slurry facility V1

Material Name	Unit Weight (kN/m^3)	Shear Strength COV	Cohesion (kPa)		Friction Angle (degrees)	
			μ	σ	μ	σ
Overflow	14	**10%**	3.0	±0.30	22.5	±2.25
Underflow	16	10%	0.5	±0.05	31.0	±3.10
Foundation	18	NA	0.0	NA	36.0	NA

Key:
μ - Mean
σ - Standard deviation
COV - Coefficient of variation
NA - Not applicable

Table 6.2: Experiment No.1 material properties – cycloned slurry facility V2

Material Name	Unit Weight (kN/m^3)	Shear Strength COV	Cohesion (kPa)		Friction Angle (degrees)	
			μ	σ	μ	σ
Overflow	14	**15%**	3.0	±0.45	22.5	±3.375
Underflow	16	10%	0.5	±0.05	31.0	±3.100
Foundation	18	NA	0.0	NA	36.0	NA

Key:
μ - Mean
σ - Standard deviation
COV - Coefficient of variation
NA - Not applicable

Note that the since the failure surface did not extent through the foundation there was no need to include uncertainty in the foundation properties in the probabilistic analysis.

The following methodology was carried out in the analysis:

- The limit-equilibrium analysis was carried out to locate the critical deterministic failure surface for the first slope variation, and since the surface returned was relatively large,

© University of Pretoria

focus limits were identified for the assessment of two failures smaller, and one larger, than the critical failure surface.

- The focus limits were implemented by first, identifying the approximate locations relative to the critical failure surface, and then duplicating the model three times with the respective "focus window" defined in each. This "focus window" limits the maximum and minimum radii of possible slip surfaces for each grid point to within this defined region.

- The reliability-based analysis using the Low & Tang (2007) FORM method was subsequently carried out by importing the analysis data from the limit-equilibrium calculation, and running the macro created to automate the solution and tabulate the results. These methods are described in more detail in Sections 3.3.6 and 3.4.

- Once the analysis of the first slurry dam configuration was complete, the second was constructed by changing the COV of the overflow material (cohesion and friction angle) to 15%, and the limit-equilibrium and reliability-based analyses were rerun using the same focus limits.

The subsequent 'slope performance' verification exercise was carried out by running an overall probabilistic slope stability analysis (in the slope stability software) of the second slurry facility, and plotting the severity of the critical probabilistic failure surface returned on the 'slope performance' curve produced in the experiment analyses. The results of this verification exercise are presented and discussed in Section 6.4.

6.3 EXPERIMENT RESULTS

The results of the limit-equilibrium and reliability-based analyses are summarised in Table 6.3 below and plotted as probability of failure versus severity in Figure 6.2. The Slide 6.0 limit-equilibrium results are attached in Appendix C:

© University of Pretoria

Table 6.3: Summary of Experiment No.1 results

Failure Size	Failure Surface Depth (m)	Severity Index	Safety Factor	Reliability Index	Probability of Failure (%)	Appendix Figure No.
Slurry Dam V1						
Small	8.6	0.29	1.890	4.391	5.65E-06	Fig C1.1
Medium	11.4	0.38	1.678	4.573	2.40E-06	Fig C1.2
Global Min	15.5	0.52	1.500	4.484	3.66E-06	Fig C1.3
Large	19.5	0.65	1.532	4.740	1.07E-06	Fig C1.4
Slurry Dam V2						
Small	8.6	0.29	1.890	4.391	5.65E-06	Fig C2.1
Medium	11.4	0.38	1.678	4.432	4.67E-06	Fig C2.2
Global Min	15.5	0.52	1.500	3.712	1.03E-04	Fig C2.3
Large	19.5	0.65	1.532	3.606	1.56E-04	Fig C2.4

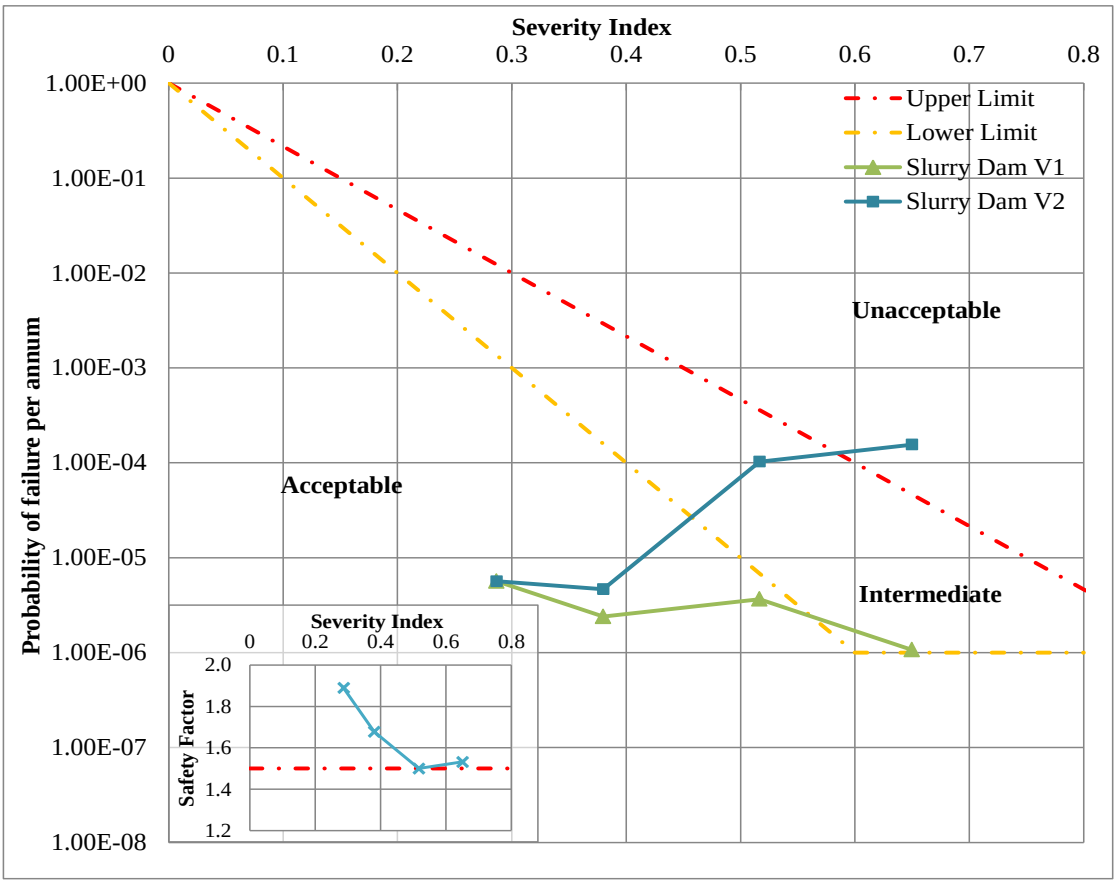


Figure 6.2: Experiment No.1 results presented on severity chart

Note that the insert showing the safety factor against severity index is included for illustrative purposes and is referred to in the discussions.

© University of Pretoria

6.4 EXPERIMENT OBSERVATIONS AND DISCUSSION

The following observations were made from the above experiment. These are discussed in detail in this section, and the pertinent points summarised in Section 8.0 together with the other analyses and experiments. The limit-equilibrium results are attached in Appendix C.

Based on the proposed limits of acceptable performance, the slope with 10% COV in both the underflow and overflow materials is deemed to be acceptable. Only a slight portion of the 'slope performance' curve intersects the intermediate zone, and extrapolating the curve suggests that larger severities than the largest analysis return back to the acceptable zone. Based on the safety factors presented in Table 6.3 and the insert in Figure 6.2, i.e. a critical safety factor of 1.5 and higher values for bigger and smaller failures, this facility would typically be deemed to be acceptable.

Based on the proposed limits of acceptable performance, the slope with a 10% COV in the underflow material and a 15% COV in the overflow materials is deemed to be unacceptable since the largest failure falls within the unacceptable zone. The 5% increase in COV for the overflow material resulted in increases in the probability of failure of approximately 1.5 orders of magnitude for the critical failure surface, and 2 orders of magnitude for the larger severity index. This causes the 'slope performance' curve to extend through the intermediate zone and into the unacceptable zone rendering the facility unacceptable.

This is significant as it illustrates how sensitive the probability of failure is to the uncertainty in the material parameters.

The results for the lowest severity index (0.29) are identical for both models. The failure surface in this instance extends through the underflow material only which has the same COV in both analyses. As the failure surface becomes bigger, more of the failure surface extends into the overflow material and the influence of the 15% COV becomes greater, causing the two curves to diverge.

The probability of failure for the lowest 'severity' (0.29) of Slurry Dam V1 is higher than the probability of failure of the critical failure surface. It is not clear why this occurred but is possibly due to either the distribution of safety factors, or the performance function representing the failure surface, changing shape as the slip surface becomes smaller and is influenced more by the underflow material. A method of plotting the multi-parameter

© University of Pretoria

distribution and failure surface is required in order to investigate this in more detail, and could form part of further research.

'Slope Performance' Verification Exercise

As discussed in Section 6.2, a subsequent 'slope performance' verification exercise was carried out by running an overall probabilistic slope stability analysis (in the slope stability software) for the second slurry facility, and plotting the severity of the critical probabilistic failure surface returned on the 'slope performance' curve produced in the experiment analyses.

This was undertaken since the concept of investigating various sizes of failure and their associated probability of failure to plot 'slope performance' curves is expected to have synergy with the more traditional, but computationally extensive, procedure of searching for the critical probabilistic failure surface (whereby the slip surface is varied for each trial cohesion and friction angle in the probabilistic analysis), and this verification exercise was therefore designed to investigate whether a similar failure surface is returned in both analyses.

The critical deterministic and probabilistic failure surfaces returned from a 5 hour long Monte Carlo analysis comprising 50 000 simulations, are presented in Figure 6.3 below:

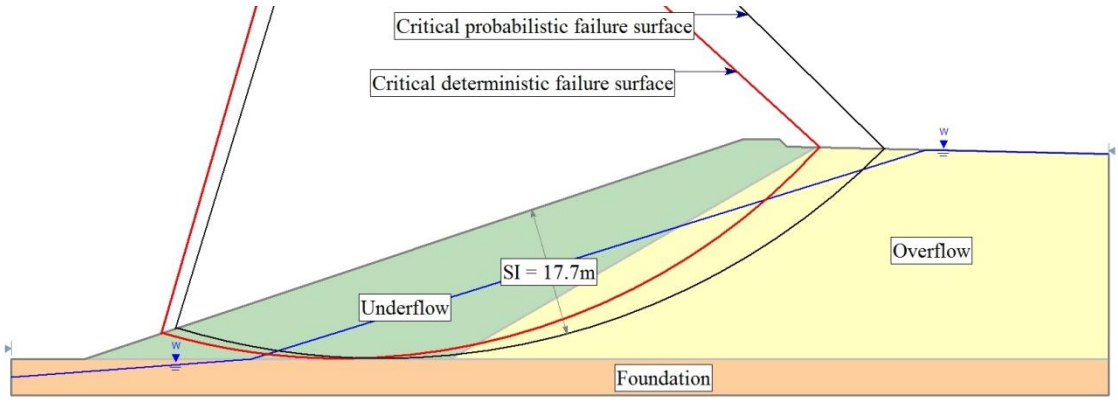


Figure 6.3: Critical deterministic and probabilistic failure surfaces

The severity index of 17.7m was then used as the focus limit, and the same methodology for the reliability-based analysis used in the remainder of the experiment was repeated. The resulting probability of failure was subsequently plotted together with the experiment results for the second slurry facility. The updated 'slope performance' curve is presented in Figure 6.4 below:

© University of Pretoria

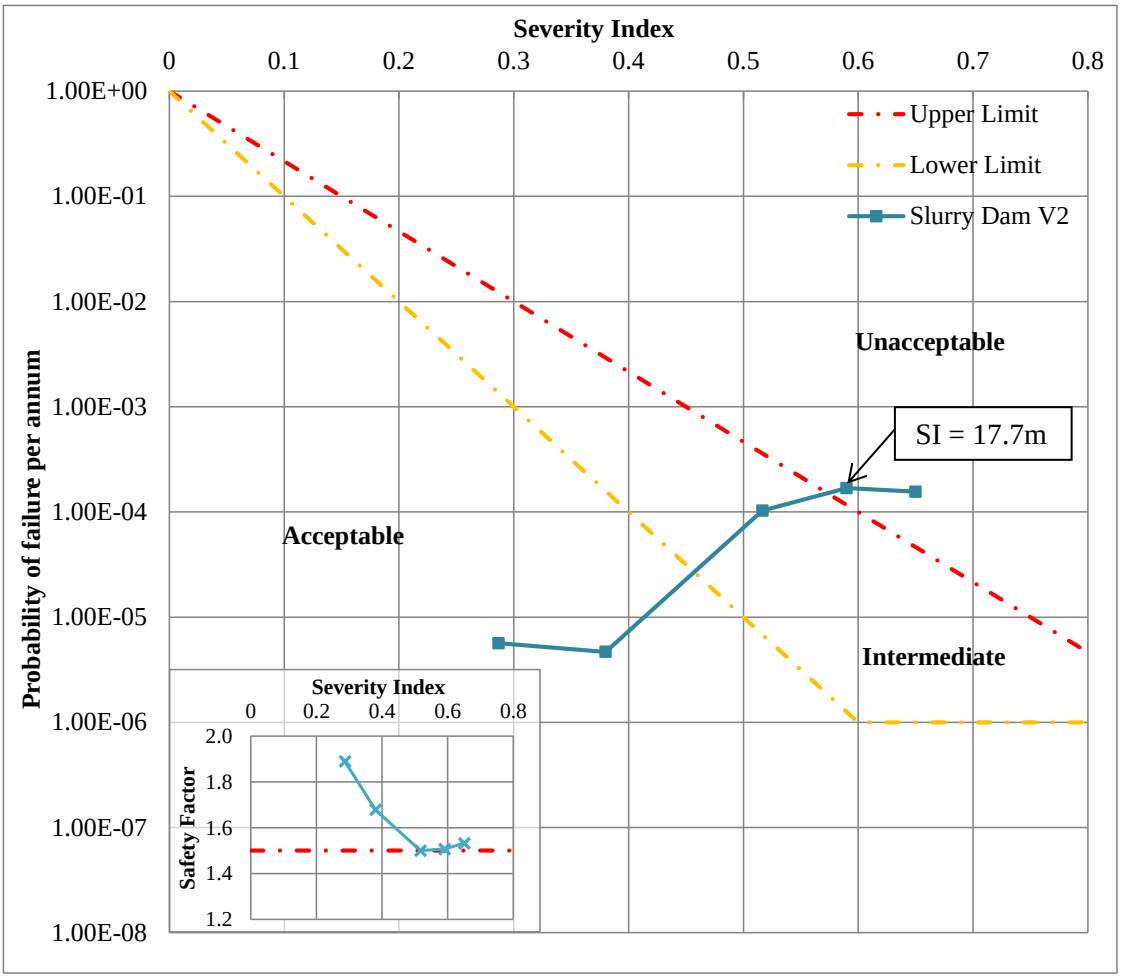


Figure 6.4: Critical probabilistic failure surface included in 'slope performance' curve

The results of the above verification exercise are significant since it suggest that, although the highest possible severity- probability of failure- combination was missed in the original experiment, the proposed 'slope performance' procedure was found to approximate the critical probabilistic failure surface with relatively good accuracy. This accuracy could be subsequently increased by the determination of more points on the 'slope performance' curve in the region where the peak is expected.

Given that a sufficient level of accuracy is achieved by this method, the primary significance to the practising engineer is the saving on computational effort to determine the critical probabilistic failure surface. Computational time to produce a slope performance curve with 5 points is approximately 30 minutes, i.e. 10% of the computational time it took to undertake the full Monte Carlo analysis above.

© University of Pretoria

7.0 EXPERIMENT NO.2 – RELATIONSHIP BETWEEN SAFETY FACTOR AND PROBABILITY OF FAILURE

This section presents a reliability-based analysis experiment, specifically designed to further investigate an apparent trend observed in the curves of probability of failure versus safety factor presented in Section 4.0. There appears to be a relationship between safety factors and probabilities of failure for a certain level of uncertainty, even though the embankments had very different geometries and configurations.

7.1 SCOPE OF THE EXPERIMENT

An experiment was carried out on a uniform, cohesionless embankment with a 1:3 slope angle, and friction angles varying in 5° increments from 25° to 40°, each with 5%, 10% and 15% COV. The three curves related to the level of uncertainty were then plotted on a chart of safety factor versus probability of failure, and the results of the various other analyses/ experiments carried out in this study were superimposed for comparative purposes.

7.2 EXPERIMENT METHODOLOGY

The model comprised a 30m high uniform, cohesionless embankment with 1V:3H side slopes on a competent foundation. The embankment material was modelled with a negligible cohesion (and associated COV) and the friction angle was varied in 5° increments from 25° to 40° with three variations in COV (5%, 10% and 15%) for each trial friction angle. Material properties for the foundation were modelled as being effectively infinite in strength, i.e. 100kPa cohesion and a friction angle of 50°, and negligible COV's were used to include this material in the reliability-based analysis (keeping to the norm of four uncertain parameters used in the remainder of the study). The phreatic surface was assumed to extend from the toe of the embankment to 30m from the crest.

The model geometry is presented in Figure 7.1 and the material parameters and uncertainties for each analysis follow in Table 7.1.

© University of Pretoria

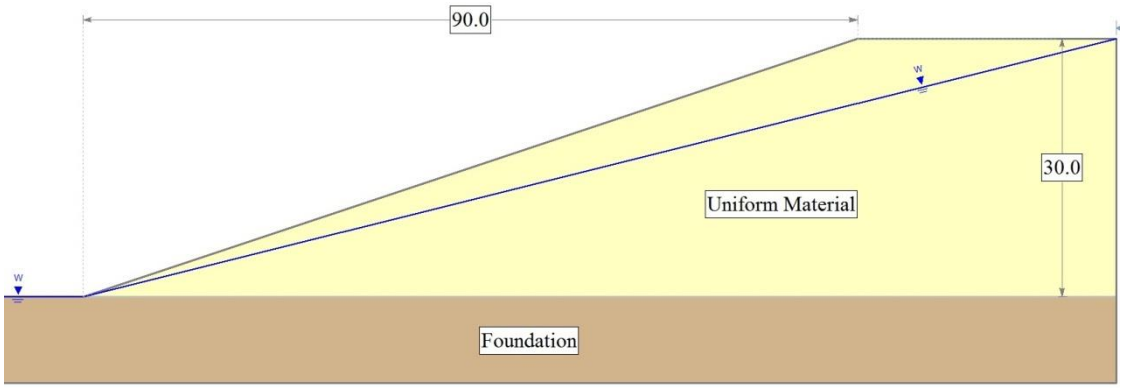


Figure 7.1: Experiment No.2 model configuration – uniform embankment

Table 7.1: Experiment No.2 material properties – uniform embankment

Model No.	COV Curve	Embankment				Foundation			
		Friction Angle (degrees)		Cohesion (kPa)		Friction Angle (degrees)		Cohesion (kPa)	
		μ	σ	μ	σ	μ	σ	μ	σ
1	5%	25	1.25	0.01	0.001	50	0.001	100	0.001
2		30	1.50						
3		35	1.75						
4		40	2.00						
5	10%	25	2.50	0.01	0.001	50	0.001	100	0.001
6		30	3.00						
7		35	3.50						
8		40	4.00						
9	15%	25	3.75	0.01	0.001	50	0.001	100	0.001
10		30	4.50						
11		35	5.25						
12		40	6.00						

Key:
μ - Mean
σ - Standard deviation
COV - Coefficient of variation

Note that the negligible standard deviations of 0.001 were included to complete the matrix in the Low & Tang (2007) FORM analysis which was set up for four uncertain parameters.

The experiment was carried out by first, computing the limit-equilibrium analysis to locate the critical failure surface for each model, and then importing the analysis data into the Low &

© University of Pretoria

Tang (2007) FORM spreadsheet to compute the reliability-based analysis. These methods are described in more detail in Sections 3.2, 3.3.6 and 3.4.

7.3 EXPERIMENT RESULTS

The results of the limit-equilibrium and reliability-based analyses are summarised in Table 7.2 below. The limit-equilibrium results are attached in Appendix D.

Table 7.2: Summary of Experiment No.2 results

Model No.	COV Curve	Friction Angle	Safety Factor	Reliability Index	Probability of Failure	Appendix Figure No.
1	5%	25°	0.959	0.679	2.49E-01	Fig D1.1
2		30°	1.186	2.768	2.82E-03	Fig D1.2
3		35°	1.439	5.230	8.46E-08	Fig D1.3
4		40°	1.724	7.077	7.37E-13	Fig D1.4
5	10%	25°	0.959	0.340	3.67E-01	Fig D2.1
6		30°	1.186	1.384	8.32E-02	Fig D2.2
7		35°	1.439	2.615	4.46E-03	Fig D2.3
8		40°	1.724	3.538	2.01E-04	Fig D2.4
9	15%	25°	0.959	0.226	4.10E-01	Fig D3.1
10		30°	1.186	0.923	1.78E-01	Fig D3.2
11		35°	1.439	1.743	4.06E-02	Fig D3.3
12		40°	1.724	2.359	9.17E-03	Fig D3.4

Key:
COV - Coefficient of variation

The above results are plotted in Figure 7.2 below, together with the results of the various other analyses and experiments carried out in the study.

© University of Pretoria

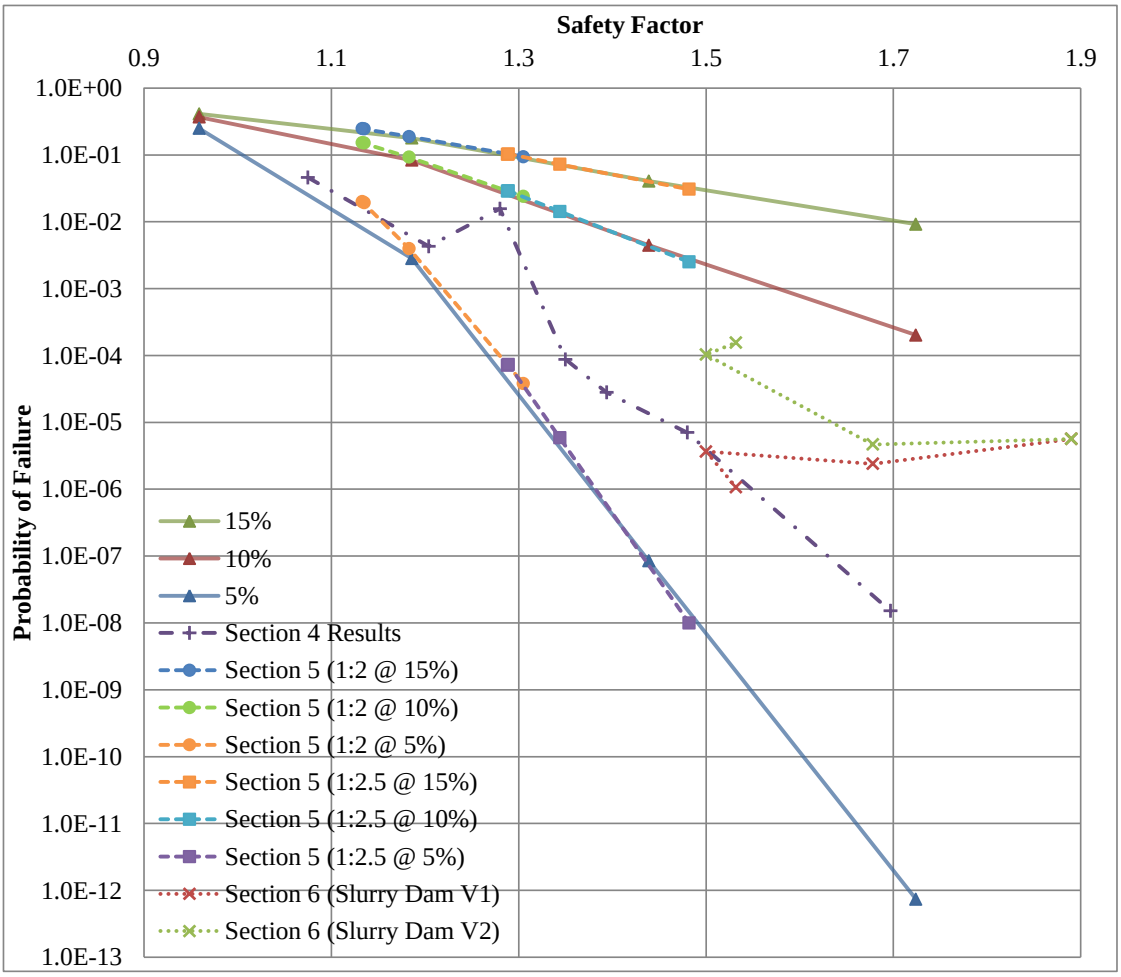


Figure 7.2: Experiment No.2 - uncertainty trend curves

7.4 EXPERIMENT OBSERVATIONS AND DISCUSSION

The following observations were made from the above experiment. These are discussed in detail in this section, and the pertinent points summarised in Section 8.0 together with the remaining analyses/ experiments. The limit-equilibrium results are attached in Appendix D.

7.4.1 Results Analysis

There are apparently consistent trend curves for varying COV values of uniform, cohesionless embankments. These trends are apparent even though the geometry (slope angle and phreatic surface) and material properties (friction angle) are different for the various facilities. This confirms the observation made in Section 4.0, that embankments with varying geometry and/ or material properties, but with similar uncertainty in the material properties could be found to fall on a specific "uncertainty curve".

© University of Pretoria

Increasing uncertainty in the cohesion, in addition to the friction angle, displaces the curves to regions of higher probabilities of failure. It is expected that, for uniform embankments, contours of cohesion COV could be included between the trend curves for the friction angle COV, i.e. given a safety factor for an embankment with known uncertainty in the friction angle and cohesion, the probability of failure could be extrapolated directly.

Complex geometries and differences in uncertainty between material zones results in more complex curves. This can be illustrated by the curves for the two slurry dams analysed in Section 6.0, where, material properties varied between the underflow and overflow, and the safety factor increased as the failure surface was reduced until it was consequently influenced less by the phreatic surface. The curves for the two slurry dams are highlighted in Figure 7.3 below.

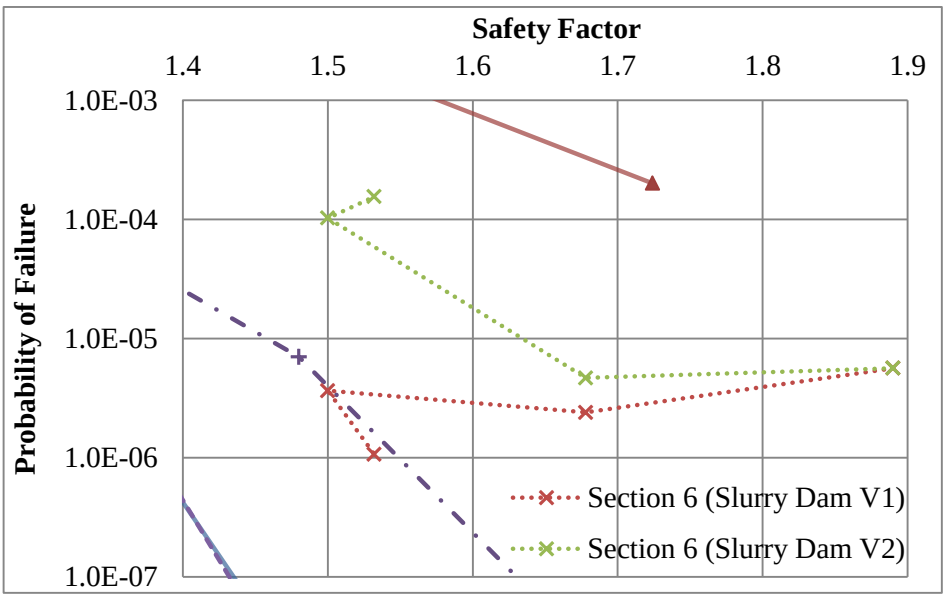


Figure 7.3: Extract of Figure 7.2 highlighting slurry dam curves

The difference between uncertainty curves is small at low safety factors and larger at higher safety factors. It is understood that this is related to the shape of the safety factor distributions, where, when the mean value is close to the failure value, the gradient of the distributions for varying COV values are similar. This is illustrated in Figure 7.4 below presenting sections of two arbitrary distributions.

© University of Pretoria

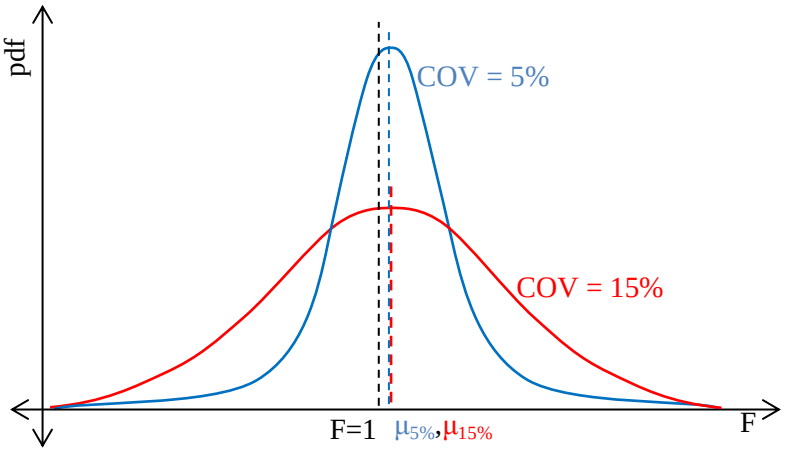


Figure 7.4: Illustration of the effect of uncertainty on the distribution of safety factors

There is a slight increasing negative gradient with increasing safety factor. This is again understood to be related to the shape of the safety factor distributions. Referring to Figure 7.4 above, this is represented by the region where the difference between the distributions increases further from the mean value.

The illustration does show the difference between the distributions to start decreasing closer to the tail, but this was phenomenon was not observed in any of the analyses and may be due to the complex shape of the multi-parameter distributions investigated. There is therefore scope to further investigate the nature of the distributions far from the mean values, and would entail plotting the multi-parameter distributions and failure surface in three dimensions (which was out of the scope of this study).

7.4.2 Comparison to Published Data

Two sources of published data were subsequently found regarding the relationship between safety factors and probabilities of failure. These are (Chowdhury, 1978), a straightforward relationship, and (Lambe, et al., 1988), which associates the relationship with the level of engineering achieved during design, construction and maintenance. These two sources are described below:

Chowdhury (1978) reported the following table for relating safety factors to probability of failure:

© University of Pretoria

Table 7.3: Chowdhury (1978) relationship of safety factor and probability of failure

Safety Factor	Probability of Failure
0.8	100%
1.0	50%
1.2	10%
1.5	2%

Lambe et. al. (1988) produced conceptual curves for four levels of engineering based on a numerical expression of their judgement (having very little data to work with at the time). These levels of engineering are summarised as follows:

I: Design by qualified engineer, full-time construction supervision and continuous maintenance by trained crew

II: Design by qualified engineer, part-time construction supervision and routine maintenance

III: Approximate design using inferred parameters, informal construction supervision and maintenance limited to emergency repairs

IV: No rational design, no construction supervision and no maintenance

The (Chowdhury, 1978) relationship, and the (Lambe, et al., 1988) conceptual curves for Levels I and III, have been superimposed on the experiment results in Figure 7.2 for discussion:

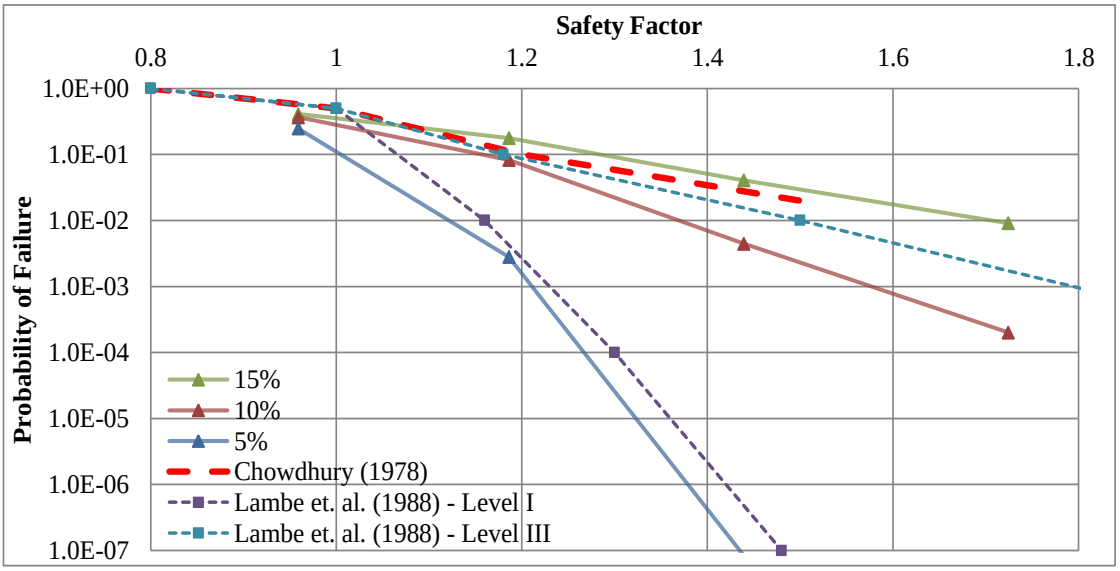


Figure 7.5: Extract of Figure 7.2 with published data superimposed

© University of Pretoria

The above figure suggests that the relationship reported by Chowdhury (1978) and the Lambe et. al. (1988) Level III curve implies a COV of approximately 15%, while the Lambe et. al. (1988) Level I curve implies a COV of approximately 5%. This supports the findings in this experiment and provides a useful guide to relate safety factors to probabilities of failure, provided there is an appreciation of the level of uncertainty in the material parameters.

© University of Pretoria

8.0 DISCUSSION

Reliability-Based Analysis Methods:

In Section 4.0, a comparison was made of a number of probability analysis methods. Each of these methods were applied to several embankments/ waste facilities, specifically selected and configured to investigate a wide range of safety factors, probabilities of failure and the effect of material uncertainty.

The probabilities of failure calculated with the Classical Monte Carlo method was found to be slightly irregular due to the "hit or miss" nature of the method, as well as limited to the orders of magnitude selected for the number of trials (and were therefore only valid for safety factors of up to approximately 1.4, as well as apparently inaccurate at safety factors between 1.3 and 1.4). The Modified Monte Carlo Analysis used to calculate reliability indices does overcome this limitation, and were found to give consistently similar results to those of the reliability-based analysis methods.

The simplified FOSM method was found to be the most conservative while the two Low & Tang methods were the least conservative. There was also a consistent, but increasing, level of discrepancy between the reliability-based methods with decreasing probability of failure. The conservatism of the FOSM and Simplified FOSM methods is understood to be due to the numerous assumptions or approximations involved in them. In particular, the resulting distribution of the safety factor is assumed to be Normal, and the moments of the failure criterion are estimated using the mean values of the parameters and extrapolating linearly, i.e. this implies that it does not matter where the partial derivatives are evaluated.

Given that the Low & Tang (2007) method was generally found to be the least conservative, and therefore leading to more streamline design, and was computationally easier than the remaining reliability-based methods, this method was selected for use in the remaining analyses and experiments.

Effect of Uncertainty:

The effect uncertainty has on the resulting probability of failure was highlighted in the two analyses on the embankment on soft clay (see Sections 4.1.1 and 4.1.2), whereby the shear strength of the materials were reduced, but so was the COV in the shear strength. This had a

© University of Pretoria

significant effect since, even though the safety factor reduced by 6% due to the lower friction angle, the probability of failure reduced by 73% with only a 5% reduction in the material COV (Figure 4.10).

This has important implications for geotechnical design. Clearly, if resources are used to determine soil strength parameters to a high level of certainty, lower probabilities of failure can be proven leading to more streamline designs of geotechnical structures.

Figure 4.8 also appeared to show a trend relating safety factors to probabilities of failure for a certain level of uncertainty (COV), even though the embankments had very different geometries, configurations and material properties. This was investigated further in Section 7.0 by carrying out a relatively simple experiment on a uniform, cohesionless embankment with friction angles varying in 5° increments from 25° to 40°, each with 5%, 10% and 15% COV and plotting the results (together with the results of the various other analyses and experiments carried out in the study) on a chart of safety factor versus probability of failure.

Figure 7.2 confirms the observation made in Section 4.0, in that embankments with varying geometry and/ or material properties, but with similar COV in the material properties have a specific "uncertainty curve". These curves appear to be consistent for cohesionless materials, and increasing COV in the cohesion displaces the curves to regions of higher probabilities of failure.

The relationship between safety factors and probabilities of failure given by Chowdhury (1978) and Lambe et. al. (1988) were also discussed, and it was found that the “uncertainty curves” produced in the experiment correlate well with different levels of engineering.

It was also observed that the difference between the uncertainty curves is small at low safety factors and large at higher safety factors. This is understood to be related to the shape of the safety factor distributions, where, when the mean value is close to the failure value, the gradient of the distributions for varying COV values are similar (Figure 7.4).

Other distribution “shape effects”, such as the increasing negative gradient of the curves were noted, but would entail detailed analysis of the multi-parameter distributions, i.e. plotting them in three dimensions, to fully investigate their significance. This was out of the scope of this study and therefore presents an opportunity for further research.

© University of Pretoria

Severity of Failure:

Section 5.0 applied the selected reliability-based analysis method (Low & Tang, 2007) to the analysis of a typical gold tailings storage facility to investigate the effect material uncertainty has on the probability of failure of slip surfaces smaller and larger than the critical slip surface. The concepts of 'severity' of failure and 'slope performance', with an emphasis on what an owner and/ or the public would deem as acceptable, were introduced.

The method selected for measuring 'severity' was taken as the ratio of the depth of the failure surface to the height of the embankment, as depicted in the equation below and Figure 8.1. This is referred to as the "Severity Index":

$$\text{Severity Index} = \frac{\text{Failure Surface Depth}}{\text{Height}}$$

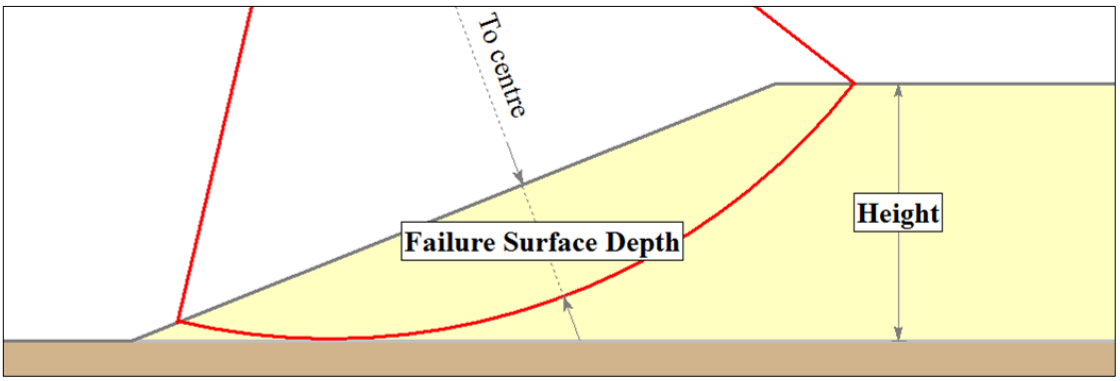


Figure 8.1: Illustration of the measurement of 'severity'

This method was found to be have a number of advantages over other methods considered since it is easy to measure, dimensionless, the most applicable to cohesionless materials and is consistent for any embankment height or slope angle.

The 'slope performance' curve is the term given to the curve produced by the various failure sizes plotted on a graph of 'Severity Index' versus Probability of Failure. This can be perceived as the overall performance of the facility, since certain failure sizes may fall within acceptable limits, while others may not. Plotting 'slope performance' curves can additionally be considered as a possible alternative to the more typical, but computationally extensive, procedure of searching for the critical probabilistic failure surface.

© University of Pretoria

The 'slope performance' curves were found to be relatively flat for severity indexes less than approximately 0.4, which was reflected by the relatively constant safety factors in Table 5.2 for severity indexes within approximately 30% to 40% of the severity index of critical failure surface. This is believed to be due to cohesionless nature of the tailings material and the influence of the (straight) water table assumed in the analysis, i.e. although the failure surface is a different size, it has the same ratio of forces causing and resisting failure. This advocates that it is essential to investigate failure surface sizes larger than the critical failure surface returned in the limit-equilibrium analysis for cohesionless materials, as a much larger severity than the global minimum may exist with a similar probability of failure.

Limits of Acceptable Performance:

In order for the results of the 36 analyses presented on Figure 5.6 to have tangible significance, they needed to be presented against limits of acceptable performance and these were therefore developed in Section 5.5. The methodology followed in developing these limits was based on theoretical considerations, learnings gathered from other proposed limits and engineering judgement.

The proposed limits are presented on Figure 8.2 (on the following page) and include zones of acceptable, unacceptable and intermediate performance; which are separated with straight lines and include a lower bound limit of 1E-06.

The intermediate zone was included because, as with many aspects of engineering, there is not always a clear boundary between what is acceptable and what is not, and the final decision is dependent on many other case-specific aspects (such as for example economics, site conditions, consequence or even politics).

In this instance it is suggested that a facility which has a slope performance curve extending from the acceptable zone into the intermediate zone, be treated in a manner similar to the ALARP principle used in (ANCOLD, 2003), i.e. by evaluating the following:

- the risk of failure;
- the potential consequence of failure; and
- the measures necessary for averting or mitigating the risk (usually economic),

If the risk and consequence is insignificant in relation to the sacrifice, it is deemed to be acceptable.

© University of Pretoria

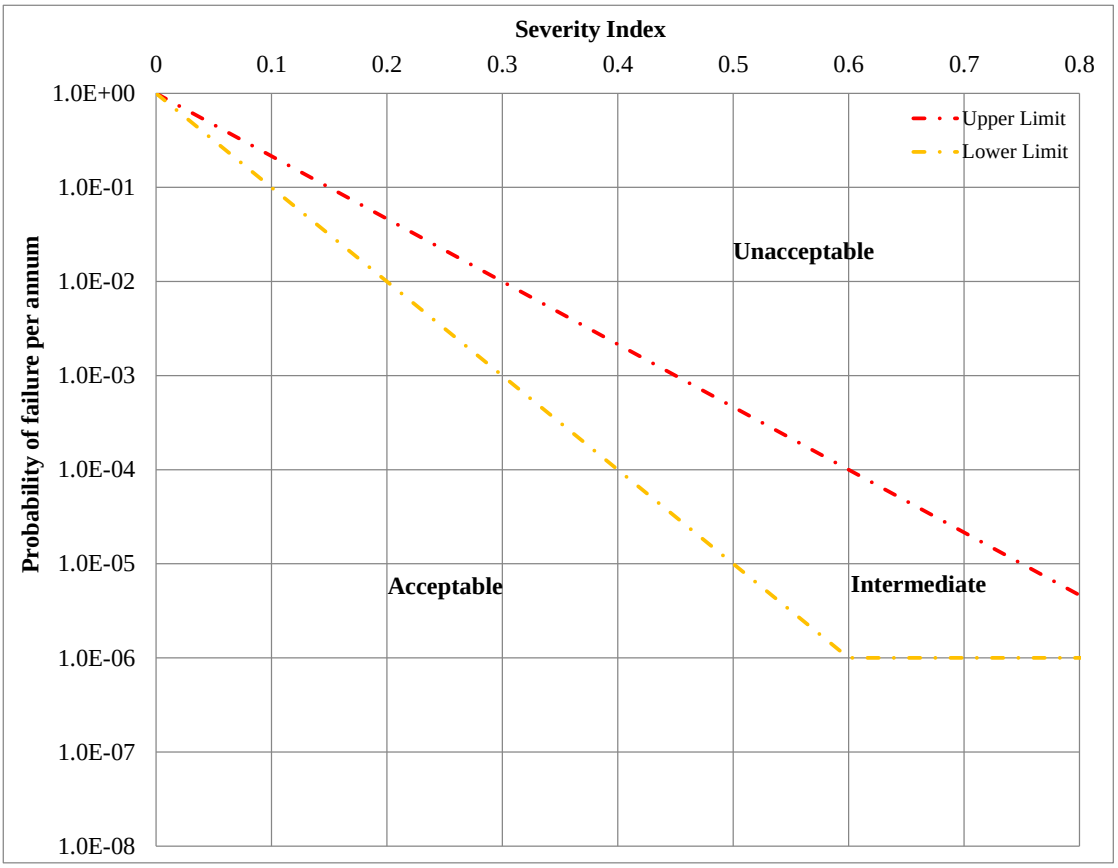


Figure 8.2: 'Severity' chart with proposed limits

Based on the limits presented in Figure 5.11, the 1:2 slope was deemed to be unacceptable for all COV trials, and only the 1:2.5 and 1:3 slopes with 5% COV fell completely within the acceptable zone. This emphasises the effect uncertainty has on the stability of tailings dams, as it implies that either:

- A 1:2.5 slope, which appears unacceptable based on the deterministic safety factors, could be proven to be acceptable if the material uncertainty is 5% or less; or
- A 1:3 slope, which would generally be considered acceptable in most situations (and appears stable based on the deterministic safety factors), could be proven to be unacceptable if the material uncertainty is approximately 8% or above.

Suitability of the Proposed Concepts and Severity Chart:

Having carried out the analyses on a uniform, cohesionless gold tailings facility, and using the results to propose the limits of acceptable performance, an experiment was carried out to test the suitability of the proposed ‘severity’ and ‘slope performance’ concepts, as well the

© University of Pretoria

proposed severity chart, for a slightly more complex tailings facility, namely a cycloned slurry dam comprising fine overflow material confined within a coarse underflow impoundment.

Two configurations of a (deterministically) stable cyclone facility were analysed for various 'severities', i.e. to produce 'slope performance' curves, and with different COV values in the shear strength of the overflow material, i.e. 10% and 15% respectively.

The resulting 'slope performance' curves were presented on the severity chart in Figure 6.2 and indicated that the facility with 10% COV in the shear strength parameters would be deemed as performing acceptably, but the increase in COV of the overflow to 15% causes the slope performance curve to extend through the intermediate zone and into the unacceptable zone for larger 'severities'.

The results of the above experiment were subsequently used in a verification exercise to compare the failure relating to the highest severity, i.e. the peak of the 'slope performance' curve, to the critical probabilistic failure surface returned from a typical, but computationally extensive, overall probabilistic slope stability analysis whereby the critical failure surface is located for each simulation of shear strength parameters.

Although the highest possible severity- probability of failure- combination was missed in the original experiment, the proposed 'slope performance' procedure was found to approximate the critical probabilistic failure surface with relatively good accuracy. The primary significance of this is the saving on computation effort to determine the critical probabilistic failure surface.

© University of Pretoria

9.0 CONCLUSIONS

The following conclusions are drawn from the dissertation:

1) The literature review indicated that geotechnical materials are highly variable, with potential COV's of between 5% and 70%, and these are therefore expected to have a significant effect of the reliability of the geotechnical structure in which they are utilised.

2) The Classical Monte Carlo Simulation was found to be slightly irregular and generally more conservative (producing higher probabilities of failure) than the reliability-based analysis methods, in particular more than the Low & Tang 2004 and 2007 FORM methods.

3) The Low & Tang (2007) method was generally found to be the least conservative, therefore leading to more streamline design, and was computationally easier than the remaining reliability-based methods. It was therefore used in the remaining analyses and experiments. The method is robust and conceptually simple, and since very little additional information and effort is required to carry out the analysis, it is considered to be an invaluable tool for engineers investigating the reliability of their designs.

4) Uncertainty has a significant effect on the resulting probability of failure in reliability-based analysis of tailings storage facilities. It was demonstrated in this dissertation that facilities with the same, or even higher, material shear strengths can have higher probabilities of failure if there is higher uncertainty in the shear strength parameters.

5) The relationship between safety factors and probabilities of failure is not direct, but is dependent on the level of uncertainty in the material parameters. This dependency is large for higher safety factors as the mean value of the distribution of safety factors moves further from the failure value.

6) It was additionally found that the "uncertainty curves" produced in the experiment correlate well with different levels of engineering.

7) The concept of assessing failures smaller and larger than the global minimum failure surface returned from the limit-equilibrium analyses, and plotting them as a 'slope

© University of Pretoria

performance' curve, is necessary for the analysis of cohesionless tailings materials as it was shown in this dissertation that much larger 'severities' may exist within the facility with very similar safety factors and probabilities of failure.

8) The above concept is additionally a suitable replacement for the more typical, but computationally extensive, search for the critical probabilistic failure surface.

9) Limits of acceptable, intermediate and unacceptable performance are proposed for use with the 'severity' and 'slope performance' concepts. This provides a consistent means of assessing the stability of a tailings storage facility, taking into account the uncertainty in the material parameters, and results in a completely objective assessment of whether the performance of the facility is indeed acceptable.

© University of Pretoria

10.0 REFERENCES

ANCOLD, 2003. *Guidelines on Risk Assessment,* Sydney: Australian Committee on Large Dams Inc..

Ang, A. H.-S. & Tang, W. H., 1975. *Probability Concepts in Engineering Planning and Design.* Vol.1 ed. New York: John Wiley & Sons.

Baecher, G. B., 1982. *Simplified Geotechnical Data Analysis.* Bornholm: s.n.

Baecher, G. B. & Christian, J. T., 2003. *Reliability and Statistics in Geotechnical Engineering.* West Sussex: Wiley.

Bishop, A. W., 1955. The use of the slip circle in the stability analysis of slopes. *Geotechnique,* 5(1), pp. 7-17.

Chamber of Mines South Africa, 1996. The Engineering Design, Operation and Closure of Matalliferous, Diamond and Coal Residue Deposits. *Guidelines for Environmental Protection,* March.Volume 1/1979.

Chowdhury, R. N., 1978. *Slope analysis.* 2 ed. Michigan: Elsevier Scientific Pub. Co., 1978.

Christian, J. T., Ladd, C. C. & Baecher, G. B., 1994. Reliability Applied to Slope Stability Analysis. *Journal of Geotechnical Engineering,* Volume 120, pp. 2180-2207.

CIRIA, 1995. *Report 143 - The Standard Penetration Test (SPT): methods and use,* London: Construction Industry Research and Information Association.

Dai, S. -H. & Wang, M. -O., 1992. *Reliability analysis in engineering.* New York: Van Nostrand Reinhold.

Ditlevsen, O., 1981. *Uncertainty Modelling: with Applications to Multidimensional Civil Engineering Systems.* New York: McGraw-Hill.

Giam, P. & Donald, I., 1989. Example problems for testing soil slope stability programs. *Civil Engineering Research Report No. 8/1989,* ISBN 0867469218(ISSN 01556282).

© University of Pretoria

Harr, M. E., 1987. *Reliability-Based Design in Civil Engineering.* New York: McGraw-Hill.

Hasofer, A. M. & Lind, N. C., 1974. Exact and invariant second-moment code format. *Journal of Engineering Mechanics,* 100(1), pp. 111-121.

Lambe, T. W., Silva, F. & Lambe, P. C., 1988. Expressing the level of stability of a slope. *The Art of Science of Geotechnical Engineering at the Dawn of the Twenty-First Century: A Volume Honoring Ralph B. Peck.*, Prentice-Hall, pp. 558-588.

Leonards, G. A., 1975. Investigation of Failures. *Journal of the Geotechnical Engineering Division,* 108(GT2), pp. 187-246.

Low, B. K. & Tang, W. H., 1997. Efficient reliability evaluation using spreadsheet. *Journal of Engineering Mechanics, ASCE, New York,* 123(7), pp. 749-752.

Low, B. K., 2003. *Practical Probabilistic Slope Stability Analysis.* Massachusetts, s.n., pp. 2777-2784.

Low, B. K. & Tang, W. H., 2004. Reliability Analysis Using Object-oriented Constrained Optimization. *Structural Safety, Elsevier Science Ltd.*, 26(1), pp. 69-89.

Low, B. K. & Tang, W. H., 2007. Efficient Spreadsheet Algorithm for First-order Reliability Method. *Journal of Engineering Mechanics, ASCE,* 133(12), pp. 1378-1387.

McPhail, G. I. & Wagner, J. C., 2002. *Disposal of Residues.* Fort Collins, Colorado, CRC Press.

Messrs, G. H. H., Legge, G. L., Penman, A. D. M. & Wahler, W. A., 1989. Tailings Dam Safety. *Guidelines,* Volume Bulletin 74, pp. 15-23.

Phoon, K. K., 2008. *Reliability-based Design in Geotechnical Engineering.* 1st ed. New York: Taylor & Francis.

Phoon, K. K., 2015. Personal communication.

© University of Pretoria

Rosenblueth, E., 1975. Point Estimate for Probability Methods. *Proceedings of the National Academy of Sciences,* 72(10), pp. 3812-3814.

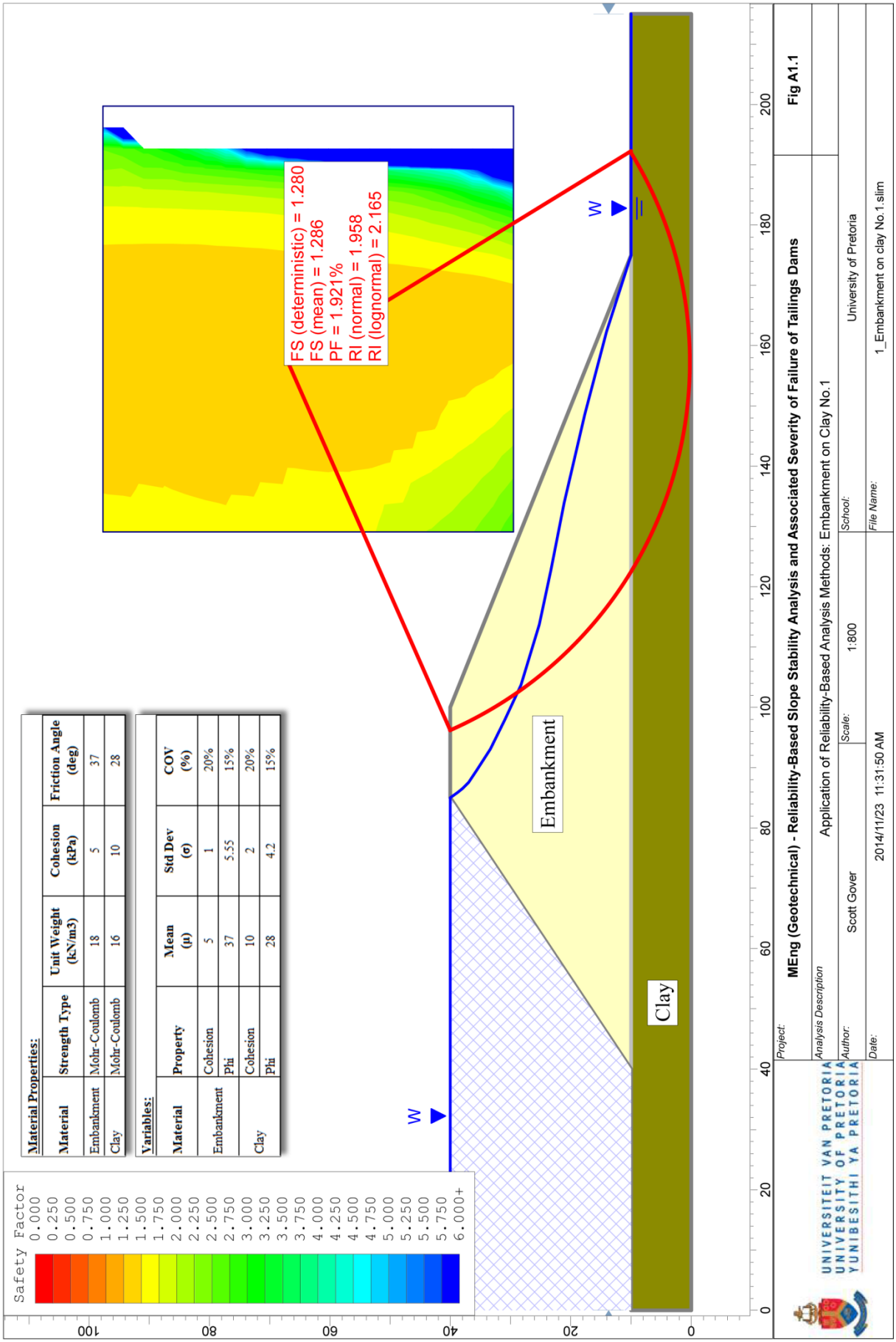
Taylor, J. R., 1997. *An Introduction to Error Analysis.* California: University Science Books.

Whitman, R. V., 1984. Evaluating Risk in Geotechnical Engineering. *Journal of Geotechnical Engineering, ASCE,* 110(2), pp. 145-188.

© University of Pretoria

APPENDIX A

© University of Pretoria



© University of Pretoria

Analysis: **Application of Reliability-Based Analysis Methods: Embankment on Clay No.1** **Fig A1.2**

1. FOSM Method (Report Section 3.3.3):

Material	Embankment		Clay	
Property	Cohesion	Phi	Cohesion	Phi
Std Dev (σ)	1.00	5.55	2.00	4.20
2Δx	0.12244	0.67960	0.24485	0.51420
ΔSF	0.00050	0.00919	0.00313	0.01651
$\sigma_{Xi}^2\left(\frac{\Delta SF}{2\Delta x_i}\right)^2$	1.668E-05	5.633E-03	6.537E-04	1.819E-02
$\rho(X_i,X_j)\sigma_{Xi}\sigma_{Xj}\frac{\Delta SF}{2\Delta x_i}\frac{\Delta SF}{2\Delta x_j}$	-0.0001226		-0.0013791	
Total	2.30E-02			
$\sigma=\sqrt{\text{Total}}$	0.152			
μ_g	1.299			
β	**1.971**			
p_f	**2.43E-02**			

2. Simplified FOSM Method (Report Section 3.3.4):

Material	**Property**	**Mean (μ)**	**Std Dev (σ)**	**Min SF**	**Max SF**	**ΔSF**
Embankment	Cohesion	5.00	1.00	1.26797	1.29253	0.02456
Embankment	Phi	37.00	5.55	1.06928	1.54489	0.47561
Clay	Cohesion	10.00	2.00	1.20268	1.35615	0.15347
Clay	Phi	28.00	4.20	0.89535	1.72963	0.83429

σ*	0.157
μ_g	1.299
β	**1.900**
p_f	**2.87E-02**

* See equation in Section 3.3.4 of the report

3. Low & Tang (2004) FORM analysis in the normalised space of correlated nonnormals (Report section 3.3.5):

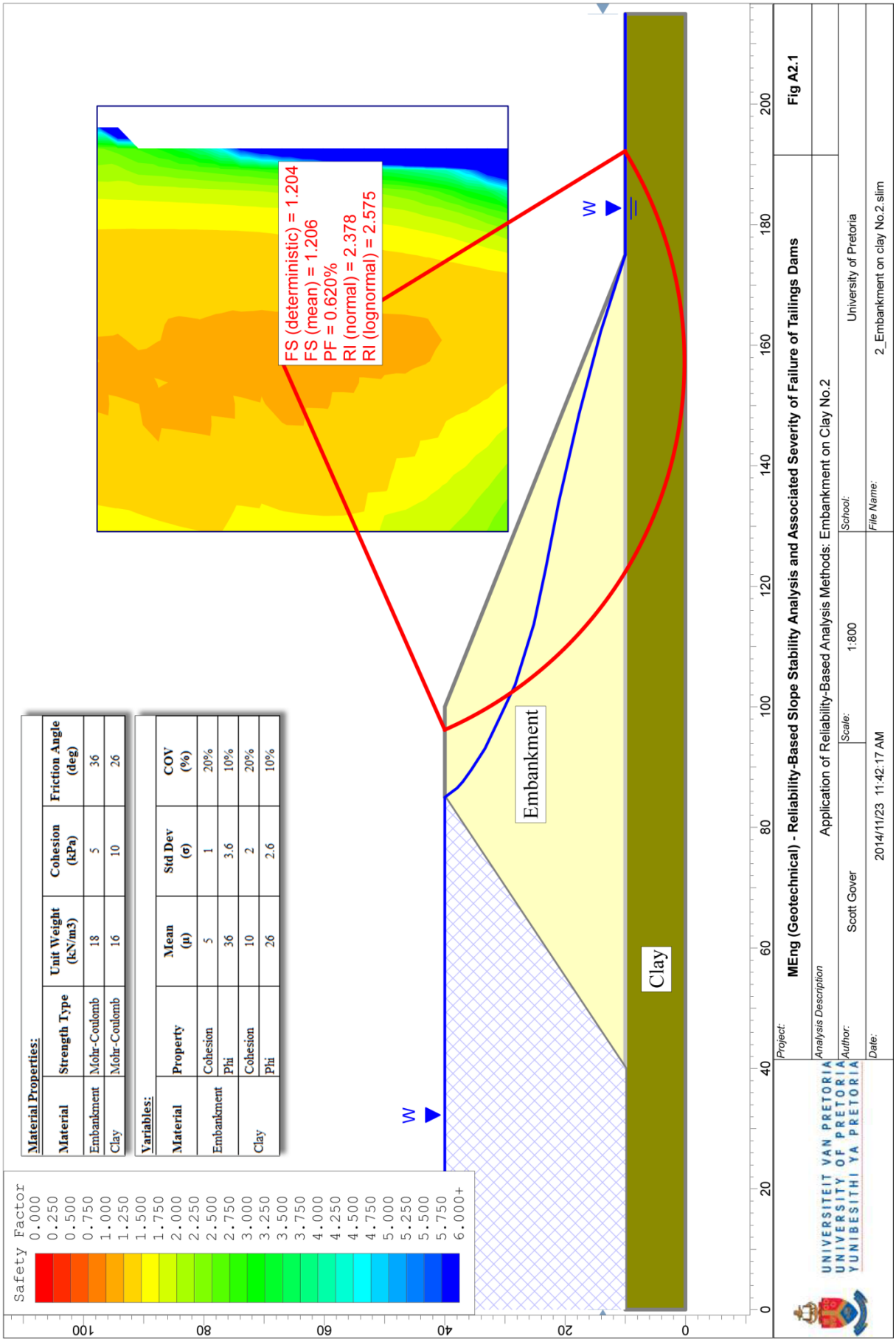
Material	**Property**	**Distribution**	**μ**	**σ**	***x***	**μ^N**	**σ^N**	**$(x-\mu^N)/\sigma^N$**	**ϕ_1**	**c_1**	**ϕ_2**	**c_2**	**g(x)**	**β**
Embankment	Phi	Normal	37.00	5.55	31.19	37.00	5.55	-1.047	1	-0.4	0	0	3E-08	**2.152**
Embankment	Cohesion	Normal	5.00	1.00	5.37	5.00	1.00	0.365	-0.4	1	0	0		
Clay	Phi	Normal	28.00	4.20	20.27	28.00	4.20	-1.840	0	0	1	-0.4		**Prob.Fail**
Clay	Cohesion	Normal	10.00	2.00	10.77	10.00	2.00	0.383	0	0	-0.4	1		**1.57E-02**
						Equivalent parameters		Optimised	Correlation matrix [R]					

4. Low & Tang (2007) FORM analysis in the original space of correlated nonnormals (Report section 3.3.6):

Material	**Property**	**Distribution**	**μ**	**σ**	**Para3**	**Para4**	**xi***	**ni**	**ϕ_1**	**c_1**	**ϕ_2**	**c_2**	**g(x)**	**β**
Embankment	Phi	Normal	37.00	5.55			31.19	-1.047	1	-0.4	0	0	2E-08	**2.152**
Embankment	Cohesion	Normal	5.00	1.00			5.36	0.363	-0.4	1	0	0		
Clay	Phi	Normal	28.00	4.20			20.27	-1.839	0	0	1	-0.4		**Prob.Fail**
Clay	Cohesion	Normal	10.00	2.00			10.76	0.381	0	0	-0.4	1		**1.57E-02**
								Optimised	Correlation matrix [R]					

© University of Pretoria

UNIVERSITEIT VAN PRETORIA
UNIVERSITY OF PRETORIA
YUNIBESITHI YA PRETORIA



© University of Pretoria

Analysis: **Application of Reliability-Based Analysis Methods: Embankment on Clay No.2** **Fig A2.2**

1. FOSM Method (Report Section 3.3.3):

Material	Embankment		Clay	
Property	Cohesion	Phi	Cohesion	Phi
Std Dev (σ)	1.00	3.60	2.00	2.60
2Δx	0.12244	0.44080	0.24485	0.31840
ΔSF	0.00050	0.00571	0.00314	0.00993
$\sigma_{Xi}^2\left(\frac{\Delta SF}{2\Delta x_i}\right)^2$	1.668E-05	2.175E-03	6.578E-04	6.575E-03
$\rho(X_i,X_j)\sigma_{Xi}\sigma_{Xj}\frac{\Delta SF}{2\Delta x_i}\frac{\Delta SF}{2\Delta x_j}$	-0.0000762		-0.0008319	
Total	8.52E-03			
$\sigma=\sqrt{\text{Total}}$	0.092			
μ_g	1.222			
β	**2.401**			
p_f	**8.17E-03**			

2. Simplified FOSM Method (Report Section 3.3.4):

Material	**Property**	**Mean (μ)**	**Std Dev (σ)**	**Min SF**	**Max SF**	**ΔSF**
Embankment	Cohesion	5.00	1.00	1.19154	1.21594	0.02440
Embankment	Phi	36.00	3.60	1.07005	1.35674	0.28669
Clay	Cohesion	10.00	2.00	1.12584	1.27985	0.15401
Clay	Phi	26.00	2.60	0.96758	1.45989	0.49231

σ*	0.094
μ_g	1.222
β	**2.366**
p_f	**8.98E-03**

* See equation in Section 3.3.4 of the report

3. Low & Tang (2004) FORM analysis in the normalised space of correlated nonnormals (Report section 3.3.5):

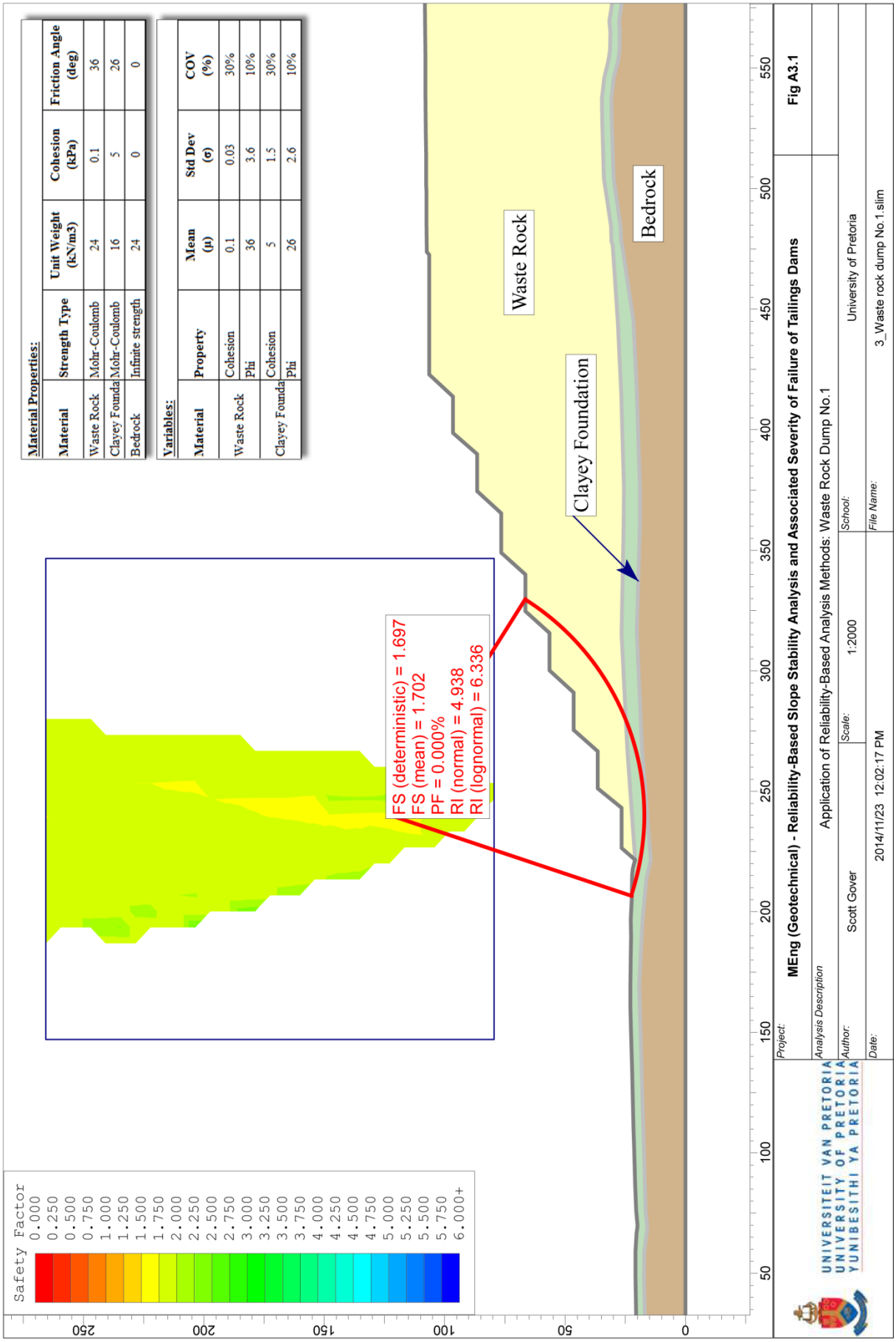
Material	**Property**	**Distribution**	**μ**	**σ**	***x***	**μ^N**	**σ^N**	**$(x-\mu^N)/\sigma^N$**	**ϕ_1**	**c_1**	**ϕ_2**	**c_2**	**g(x)**	**β**
Embankment	Phi	Normal	36.00	3.60	31.23	36.00	3.60	-1.326	1	-0.4	0	0	2E-07	**2.628**
Embankment	Cohesion	Normal	5.00	1.00	5.42	5.00	1.00	0.423	-0.4	1	0	0		
Clay	Phi	Normal	26.00	2.60	20.46	26.00	2.60	-2.132	0	0	1	-0.4		**Prob.Fail**
Clay	Cohesion	Normal	10.00	2.00	10.30	10.00	2.00	0.150	0	0	-0.4	1		**4.29E-03**
						Equivalent parameters		Optimised	Correlation matrix [R]					

4. Low & Tang (2007) FORM analysis in the original space of correlated nonnormals (Report section 3.3.6):

Material	**Property**	**Distribution**	**μ**	**σ**	**Para3**	**Para4**	**xi***	**ni**	**ϕ_1**	**c_1**	**ϕ_2**	**c_2**	**g(x)**	**β**
Embankment	Phi	Normal	36.00	3.60			31.22	-1.326	1	-0.4	0	0	9E-08	**2.628**
Embankment	Cohesion	Normal	5.00	1.00			5.42	0.421	-0.4	1	0	0		
Clay	Phi	Normal	26.00	2.60			20.46	-2.132	0	0	1	-0.4		**Prob.Fail**
Clay	Cohesion	Normal	10.00	2.00			10.30	0.149	0	0	-0.4	1		**4.29E-03**
								Optimised	Correlation matrix [R]					

© University of Pretoria

UNIVERSITEIT VAN PRETORIA
UNIVERSITY OF PRETORIA
YUNIBESITHI YA PRETORIA



© University of Pretoria

Analysis: **Application of Reliability-Based Analysis Methods: Waste Rock Dump No.1** **Fig A3.2**

1. FOSM Method (Report Section 3.3.3):

Material	Waste Rock		Clayey Foundation	
Property	Cohesion	Phi	Cohesion	Phi
Std Dev (σ)	0.03	3.60	1.50	2.60
2Δx	0.00367	0.44080	0.18368	0.31840
ΔSF	0.00002	0.01356	0.00129	0.01163
$\sigma_{Xi}^2\left(\frac{\Delta SF}{2\Delta x_i}\right)^2$	2.667E-08	1.226E-02	1.110E-04	9.019E-03
$\rho(X_i,X_j)\sigma_{Xi}\sigma_{Xj}\frac{\Delta SF}{2\Delta x_i}\frac{\Delta SF}{2\Delta x_j}$	-0.0000072		-0.0004002	
Total	2.10E-02			
$\sigma = \sqrt{\text{Total}}$	0.145			
μ_g	1.713			
β	**4.919**			
p_f	**4.35E-07**			

2. Simplified FOSM Method (Report Section 3.3.4):

Material	**Property**	**Mean (μ)**	**Std Dev (σ)**	**Min SF**	**Max SF**	**ΔSF**
Waste Rock	Cohesion	0.10	0.03	1.69642	1.69724	0.00082
Waste Rock	Phi	36.00	3.60	1.39344	2.07605	0.68261
Clayey Found	Cohesion	5.00	1.50	1.66504	1.72847	0.06343
Clayey Found	Phi	26.00	2.60	1.42132	1.99765	0.57633

σ*	0.148
μ_g	1.713
β	**4.819**
p_f	**7.22E-07**

* See equation in Section 3.3.4 of the report

3. Low & Tang (2004) FORM analysis in the normalised space of correlated nonnormals (Report section 3.3.5):

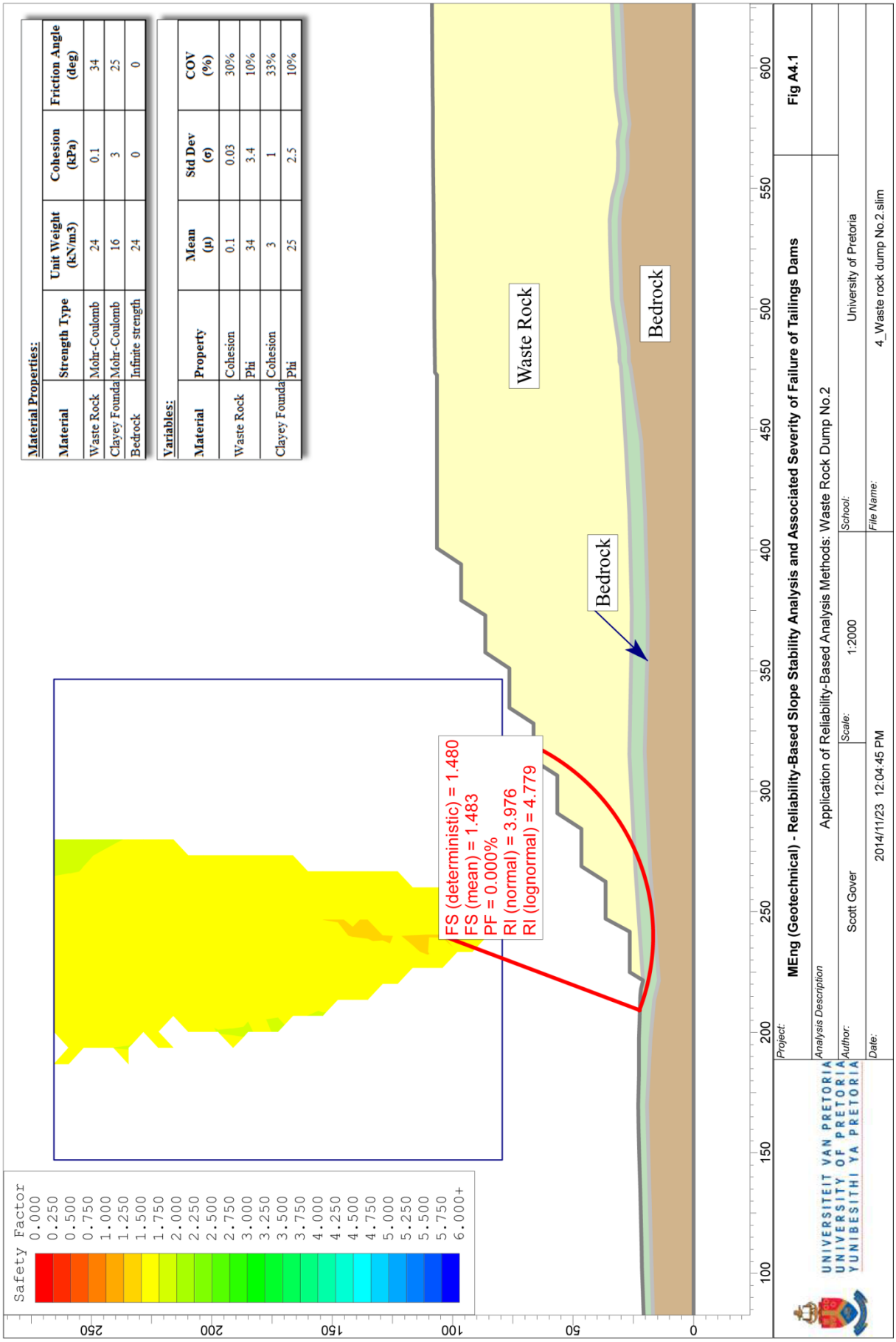
Material	**Property**	**Distribution**	**μ**	**σ**	***x***	**μ^N**	**σ^N**	**$(x-\mu^N)/\sigma^N$**	**ϕ_1**	**c_1**	**ϕ_2**	**c_2**	**g(x)**	**β**
Waste Rock	Phi	Normal	36.00	3.60	21.28	36.00	3.60	-4.088	1	-0.4	0	0	-3E-07	**5.540**
Waste Rock	Cohesion	Normal	0.10	0.03	0.15	0.10	0.03	1.630	-0.4	1	0	0		
Clayey Foundati	Phi	Normal	26.00	2.60	16.35	26.00	2.60	-3.711	0	0	1	-0.4		**Prob.Fail**
Clayey Foundati	Cohesion	Normal	5.00	1.50	6.60	5.00	1.50	1.067	0	0	-0.4	1		**1.51E-08**
						Equivalent parameters		Optimised	Correlation matrix [R]					

4. Low & Tang (2007) FORM analysis in the original space of correlated nonnormals (Report section 3.3.6):

Material	**Property**	**Distribution**	**μ**	**σ**	**Para3**	**Para4**	**xi***	**ni**	**ϕ_1**	**c_1**	**ϕ_2**	**c_2**	**g(x)**	**β**
Waste Rock	Phi	Normal	36.00	3.60			21.28	-4.088	1	-0.4	0	0	-9E-08	**5.540**
Waste Rock	Cohesion	Normal	0.10	0.03			0.15	1.630	-0.4	1	0	0		
Clayey Foundati	Phi	Normal	26.00	2.60			16.35	-3.711	0	0	1	-0.4		**Prob.Fail**
Clayey Foundati	Cohesion	Normal	5.00	1.50			6.60	1.067	0	0	-0.4	1		**1.51E-08**
								Optimised	Correlation matrix [R]					

© University of Pretoria

UNIVERSITEIT VAN PRETORIA
UNIVERSITY OF PRETORIA
YUNIBESITHI YA PRETORIA



© University of Pretoria

1. FOSM Method (Report Section 3.3.3):

Material	Waste Rock		Clayey Foundation	
Property	Cohesion	Phi	Cohesion	Phi
Std Dev (σ)	0.03	3.40	1.00	2.50
2Δx	0.00367	0.41640	0.12244	0.30620
ΔSF	0.00002	0.01082	0.00079	0.01075
$\sigma_{Xi}^2\left(\frac{\Delta SF}{2\Delta x_i}\right)^2$	2.667E-08	7.805E-03	4.163E-05	7.703E-03
$\rho(X_i,X_j)\sigma_{Xi}\sigma_{Xj}\frac{\Delta SF}{2\Delta x_i}\frac{\Delta SF}{2\Delta x_j}$	-0.0000058		-0.0002265	
Total	1.53E-02			
$\sigma = \sqrt{\text{Total}}$	0.124			
μ_g	1.498			
β	**4.023**			
p_f	**2.87E-05**			

2. Simplified FOSM Method (Report Section 3.3.4):

Material	**Property**	**Mean (μ)**	**Std Dev (σ)**	**Min SF**	**Max SF**	**ΔSF**
Waste Rock	Cohesion	0.10	0.03	1.47925	1.47995	0.00070
Waste Rock	Phi	34.00	3.40	1.23227	1.77430	0.54203
Clayey Found	Cohesion	3.00	1.00	1.46026	1.49886	0.03860
Clayey Found	Phi	25.00	2.50	1.22312	1.75523	0.53211

σ*	0.126
μ_g	1.498
β	**3.957**
p_f	**3.79E-05**

* See equation in Section 3.3.4 of the report

3. Low & Tang (2004) FORM analysis in the normalised space of correlated nonnormals (Report section 3.3.5):

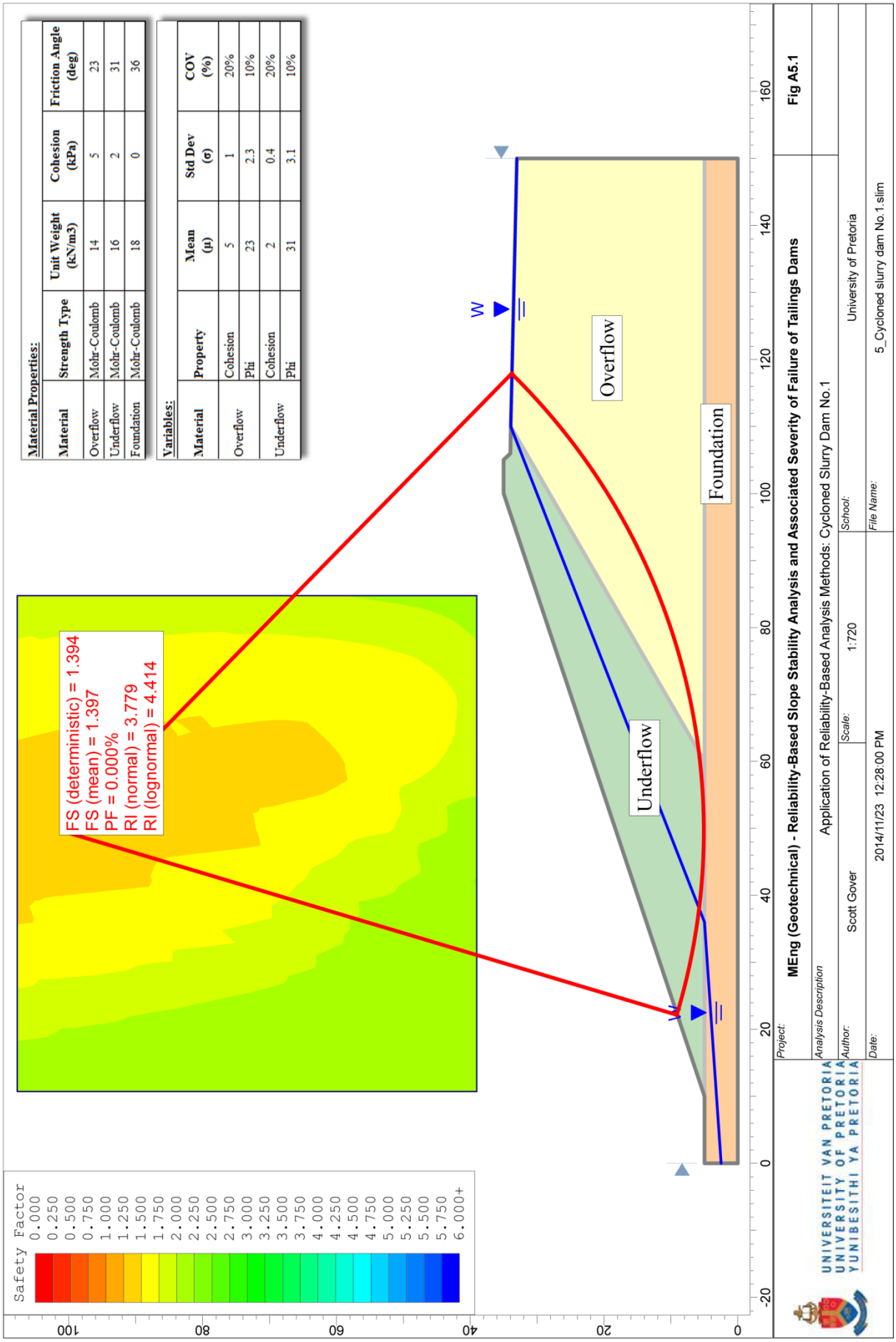
Material	**Property**	**Distribution**	**μ**	**σ**	***x***	**μ^N**	**σ^N**	**$(x-\mu^N)/\sigma^N$**	**ϕ_1**	**c_1**	**ϕ_2**	**c_2**	**g(x)**	**β**
Waste Rock	Phi	Normal	34.00	3.40	23.75	34.00	3.40	-3.015	1	-0.4	0	0	-3E-07	**4.343**
Waste Rock	Cohesion	Normal	0.10	0.03	0.14	0.10	0.03	1.202	-0.4	1	0	0		
Clayey Foundati	Phi	Normal	25.00	2.50	17.21	25.00	2.50	-3.117	0	0	1	-0.4		**Prob.Fail**
Clayey Foundati	Cohesion	Normal	3.00	1.00	4.03	3.00	1.00	1.027	0	0	-0.4	1		**7.03E-06**
						Equivalent parameters		Optimised	Correlation matrix [R]					

4. Low & Tang (2007) FORM analysis in the original space of correlated nonnormals (Report section 3.3.6):

Material	**Property**	**Distribution**	**μ**	**σ**	**Para3**	**Para4**	**xi***	**ni**	**ϕ_1**	**c_1**	**ϕ_2**	**c_2**	**g(x)**	**β**
Waste Rock	Phi	Normal	34.00	3.40			23.75	-3.015	1	-0.4	0	0	-2E-08	**4.343**
Waste Rock	Cohesion	Normal	0.10	0.03			0.14	1.202	-0.4	1	0	0		
Clayey Foundati	Phi	Normal	25.00	2.50			17.21	-3.117	0	0	1	-0.4		**Prob.Fail**
Clayey Foundati	Cohesion	Normal	3.00	1.00			4.03	1.027	0	0	-0.4	1		**7.03E-06**
								Optimised	Correlation matrix [R]					

© University of Pretoria

UNIVERSITEIT VAN PRETORIA
UNIVERSITY OF PRETORIA
YUNIBESITHI YA PRETORIA



© University of Pretoria

1. FOSM Method (Report Section 3.3.3):

Material	Overflow		Underflow	
Property	Cohesion	Phi	Cohesion	Phi
Std Dev (σ)	1.00	2.30	0.40	3.10
2Δx	0.12244	0.28160	0.04898	0.37960
ΔSF	0.00160	0.00816	0.00048	0.01068
$\sigma_{Xi}^2\left(\frac{\Delta SF}{2\Delta x_i}\right)^2$	1.708E-04	4.442E-03	1.537E-05	7.607E-03
$\rho(X_i,X_j)\sigma_{Xi}\sigma_{Xj}\frac{\Delta SF}{2\Delta x_i}\frac{\Delta SF}{2\Delta x_j}$	-0.0003484		-0.0001368	
Total	1.17E-02			
$\sigma=\sqrt{\text{Total}}$	0.108			
μ_g	1.400			
β	**3.688**			
p_f	**1.13E-04**			

2. Simplified FOSM Method (Report Section 3.3.4):

Material	**Property**	**Mean (μ)**	**Std Dev (σ)**	**Min SF**	**Max SF**	**ΔSF**
Overflow	Cohesion	5.00	1.00	1.35448	1.43304	0.07856
Overflow	Phi	23.00	2.30	1.20081	1.60384	0.40303
Underflow	Cohesion	2.00	0.40	1.38206	1.40525	0.02319
Underflow	Phi	31.00	3.10	1.15123	1.68461	0.53338

σ*	0.110
μ_g	1.400
β	**3.632**
p_f	**1.40E-04**

* See equation in Section 3.3.4 of the report

3. Low & Tang (2004) FORM analysis in the normalised space of correlated nonnormals (Report section 3.3.5):

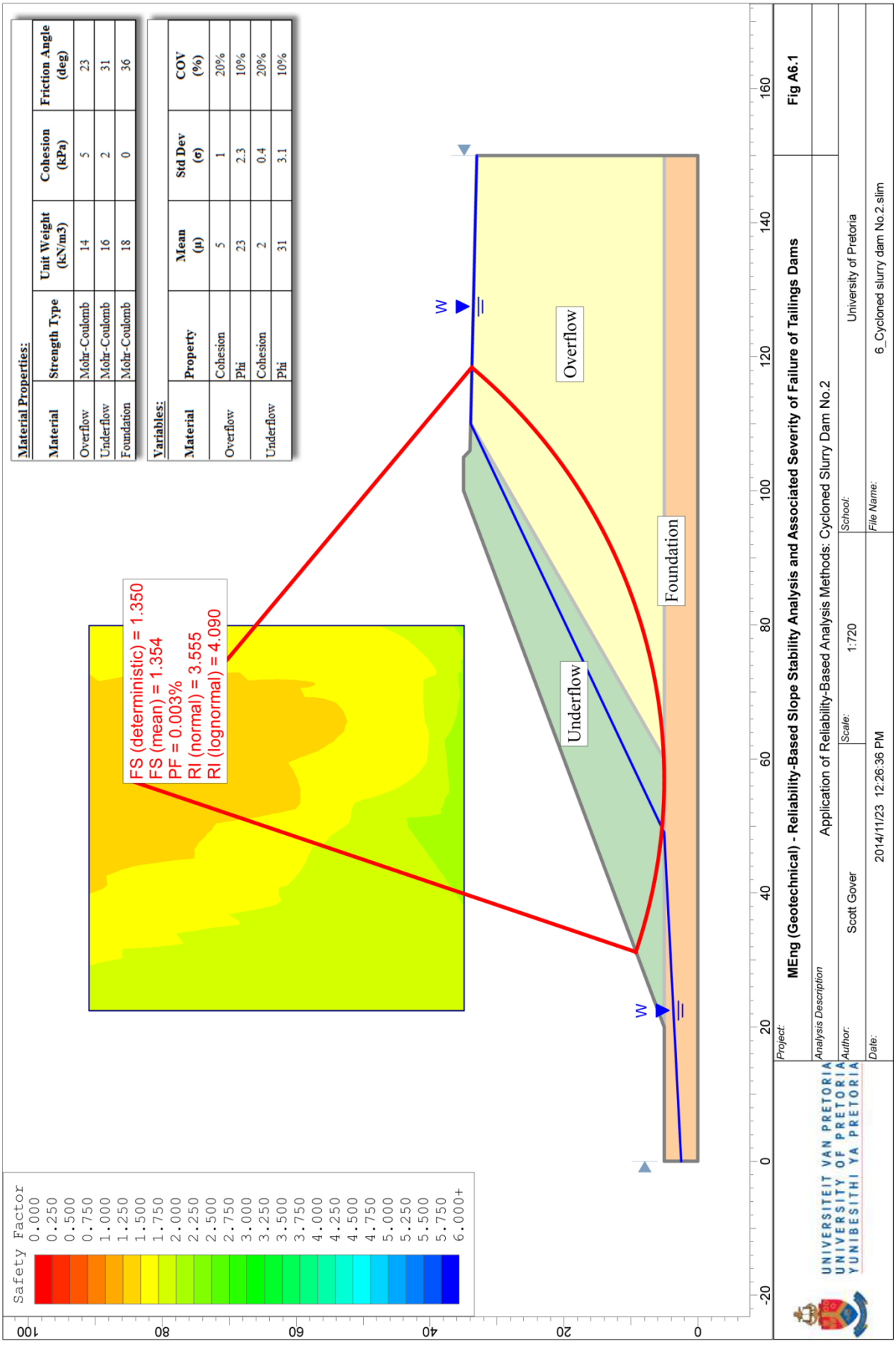
Material	**Property**	**Distribution**	**μ**	**σ**	***x***	**μ^N**	**σ^N**	**$(x-\mu^N)/\sigma^N$**	**ϕ_1**	**c_1**	**ϕ_2**	**c_2**	**g(x)**	**β**
Overflow	Phi	Normal	23.00	2.30	17.36	23.00	2.30	-2.450	1	-0.4	0	0	1E-07	**4.029**
Overflow	Cohesion	Normal	5.00	1.00	5.50	5.00	1.00	0.501	-0.4	1	0	0		
Underflow	Phi	Normal	31.00	3.10	21.23	31.00	3.10	-3.151	0	0	1	-0.4		**Prob.Fail**
Underflow	Cohesion	Normal	2.00	0.40	2.45	2.00	0.40	1.119	0	0	-0.4	1		**2.80E-05**
						Equivalent parameters		Optimised	Correlation matrix [R]					

4. Low & Tang (2007) FORM analysis in the original space of correlated nonnormals (Report section 3.3.6):

Material	**Property**	**Distribution**	**μ**	**σ**	**Para3**	**Para4**	**xi***	**ni**	**ϕ_1**	**c_1**	**ϕ_2**	**c_2**	**g(x)**	**β**
Overflow	Phi	Normal	23.00	2.30			17.36	-2.451	1	-0.4	0	0	1E-07	**4.029**
Overflow	Cohesion	Normal	5.00	1.00			5.50	0.501	-0.4	1	0	0		
Underflow	Phi	Normal	31.00	3.10			21.23	-3.151	0	0	1	-0.4		**Prob.Fail**
Underflow	Cohesion	Normal	2.00	0.40			2.45	1.119	0	0	-0.4	1		**2.80E-05**
								Optimised	Correlation matrix [R]					

© University of Pretoria

UNIVERSITEIT VAN PRETORIA
UNIVERSITY OF PRETORIA
YUNIBESITHI YA PRETORIA



© University of Pretoria

Analysis: **Application of Reliability-Based Analysis Methods: Cycloned Slurry Dam No.2** **Fig A6.2**

1. FOSM Method (Report Section 3.3.3):

Material	Overflow		Underflow	
Property	Cohesion	Phi	Cohesion	Phi
Std Dev (σ)	1.00	2.30	0.40	3.10
2Δx	0.12244	0.28160	0.04898	0.37960
ΔSF	0.00167	0.00957	0.00037	0.00851
$\sigma_{Xi}^2\left(\frac{\Delta SF}{2\Delta x_i}\right)^2$	1.860E-04	6.110E-03	9.130E-06	4.830E-03
$\rho(X_i,X_j)\sigma_{Xi}\sigma_{Xj}\frac{\Delta SF}{2\Delta x_i}\frac{\Delta SF}{2\Delta x_j}$	-0.0004264		-0.0000840	
Total	1.06E-02			
$\sigma=\sqrt{\text{Total}}$	0.103			
μ_g	1.359			
β	**3.478**			
p_f	**2.52E-04**			

2. Simplified FOSM Method (Report Section 3.3.4):

Material	**Property**	**Mean (μ)**	**Std Dev (σ)**	**Min SF**	**Max SF**	**ΔSF**
Overflow	Cohesion	5.00	1.00	1.30950	1.39167	0.08217
Overflow	Phi	23.00	2.30	1.12575	1.59829	0.47254
Underflow	Cohesion	2.00	0.40	1.34153	1.35939	0.01786
Underflow	Phi	31.00	3.10	1.15844	1.58318	0.42474

σ*	0.104
μ_g	1.359
β	**3.435**
p_f	**2.96E-04**

* See equation in Section 3.3.4 of the report

3. Low & Tang (2004) FORM analysis in the normalised space of correlated nonnormals (Report section 3.3.5):

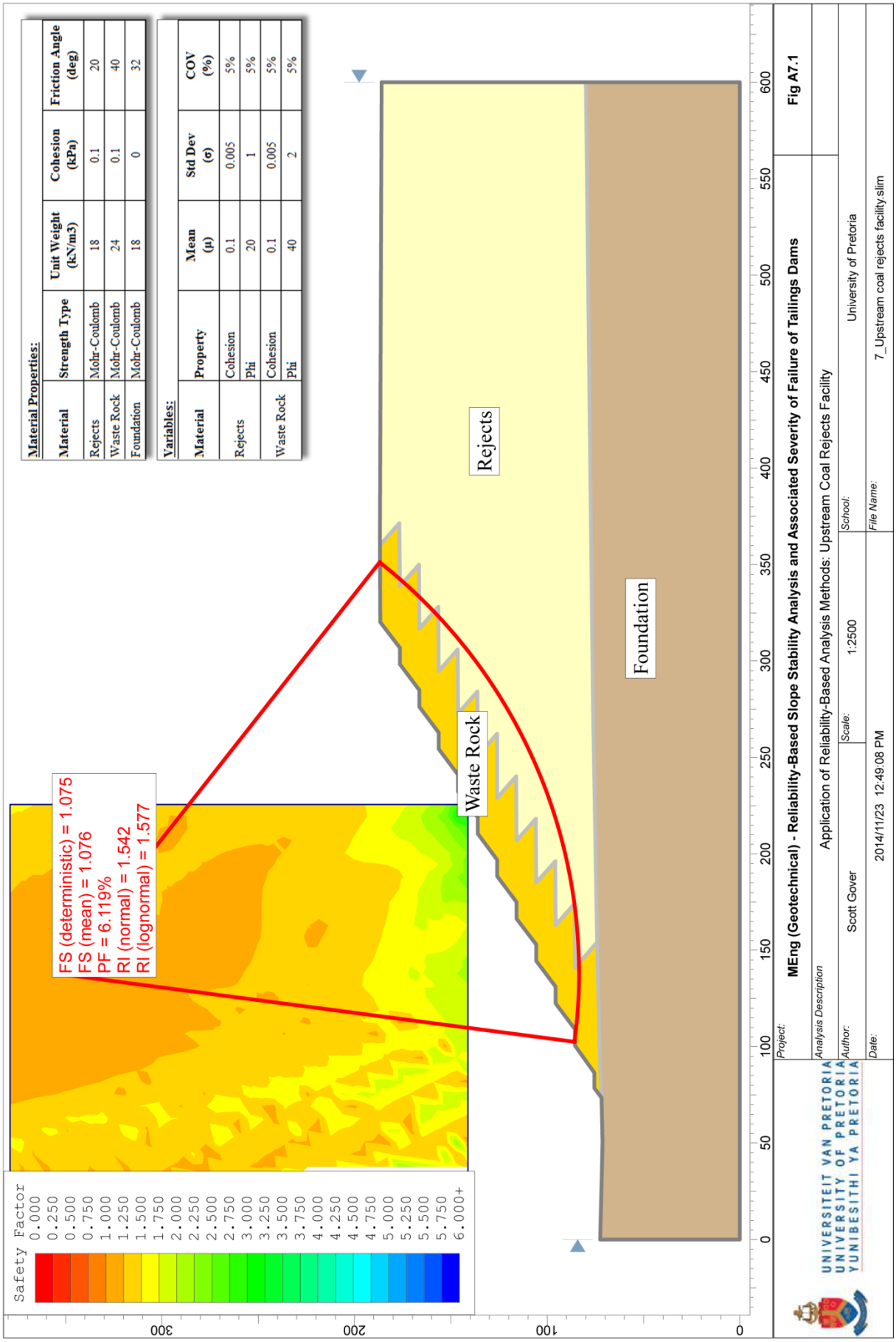
Material	**Property**	**Distribution**	**μ**	**σ**	***x***	μ^N	σ^N	$(x-\mu^N)/\sigma^N$	ϕ_1	c_1	ϕ_2	c_2	**g(x)**	**β**
Overflow	Phi	Normal	23.00	2.30	16.61	23.00	2.30	-2.779	1	-0.4	0	0	5E-08	**3.753**
Overflow	Cohesion	Normal	5.00	1.00	5.63	5.00	1.00	0.632	-0.4	1	0	0		
Underflow	Phi	Normal	31.00	3.10	23.36	31.00	3.10	-2.465	0	0	1	-0.4		**Prob.Fail**
Underflow	Cohesion	Normal	2.00	0.40	2.35	2.00	0.40	0.882	0	0	-0.4	1		**8.73E-05**
						Equivalent parameters		Optimised	Correlation matrix [R]					

4. Low & Tang (2007) FORM analysis in the original space of correlated nonnormals (Report section 3.3.6):

Material	**Property**	**Distribution**	**μ**	**σ**	**Para3**	**Para4**	**xi***	**ni**	ϕ_1	c_1	ϕ_2	c_2	**g(x)**	**β**
Overflow	Phi	Normal	23.00	2.30			16.61	-2.779	1	-0.4	0	0	3E-08	**3.753**
Overflow	Cohesion	Normal	5.00	1.00			5.63	0.632	-0.4	1	0	0		
Underflow	Phi	Normal	31.00	3.10			23.36	-2.465	0	0	1	-0.4		**Prob.Fail**
Underflow	Cohesion	Normal	2.00	0.40			2.35	0.882	0	0	-0.4	1		**8.73E-05**
								Optimised	Correlation matrix [R]					

© University of Pretoria

UNIVERSITEIT VAN PRETORIA
UNIVERSITY OF PRETORIA
YUNIBESITHI YA PRETORIA



© University of Pretoria

1. FOSM Method (Report Section 3.3.3):

Material	Rejects		Waste Rock	
Property	Cohesion	Phi	Cohesion	Phi
Std Dev (σ)	0.01	1.00	0.01	2.00
2Δx	0.00061	0.12240	0.00061	0.24480
ΔSF	0.00000	0.00585	0	0.00169
$\sigma_{Xi}^2\left(\frac{\Delta SF}{2\Delta x_i}\right)^2$	0.000E+00	2.284E-03	0.000E+00	1.906E-04
$\rho(X_i,X_j)\sigma_{Xi}\sigma_{Xj}\frac{\Delta SF}{2\Delta x_i}\frac{\Delta SF}{2\Delta x_j}$	0.0000000		0.0000000	
Total	2.47E-03			
$\sigma=\sqrt{\text{Total}}$	0.050			
μ_g	1.084			
β	**1.680**			
p_f	**4.64E-02**			

2. Simplified FOSM Method (Report Section 3.3.4):

Material	**Property**	**Mean (μ)**	**Std Dev (σ)**	**Min SF**	**Max SF**	**ΔSF**
Rejects	Cohesion	0.10	0.01	1.07494	1.07505	0.00011
Rejects	Phi	20.00	1.00	0.93403	1.22089	0.28686
Waste Rock	Cohesion	0.10	0.01	1.07498	1.07501	0.00003
Waste Rock	Phi	40.00	2.00	1.03549	1.12024	0.08475

σ*	0.050
μ_g	1.084
β	**1.677**
p_f	**4.68E-02**

* See equation in Section 3.3.4 of the report

3. Low & Tang (2004) FORM analysis in the normalised space of correlated nonnormals (Report section 3.3.5):

Material	**Property**	**Distribution**	**μ**	**σ**	***x***	**μ^N**	**σ^N**	**$(x-\mu^N)/\sigma^N$**	**ϕ_1**	**c_1**	**ϕ_2**	**c_2**	**g(x)**	**β**
Rejects	Phi	Normal	20.00	1.00	18.38	20.00	1.00	-1.621	1	-0.4	0	0	-3E-09	**1.686**
Rejects	Cohesion	Normal	0.10	0.01	0.10	0.10	0.01	0.648	-0.4	1	0	0		
Waste Rock	Phi	Normal	40.00	2.00	39.07	40.00	2.00	-0.465	0	0	1	-0.4		**Prob.Fail**
Waste Rock	Cohesion	Normal	0.10	0.01	0.10	0.10	0.01	0.186	0	0	-0.4	1		**4.59E-02**
						Equivalent parameters		Optimised	Correlation matrix [R]					

4. Low & Tang (2007) FORM analysis in the original space of correlated nonnormals (Report section 3.3.6):

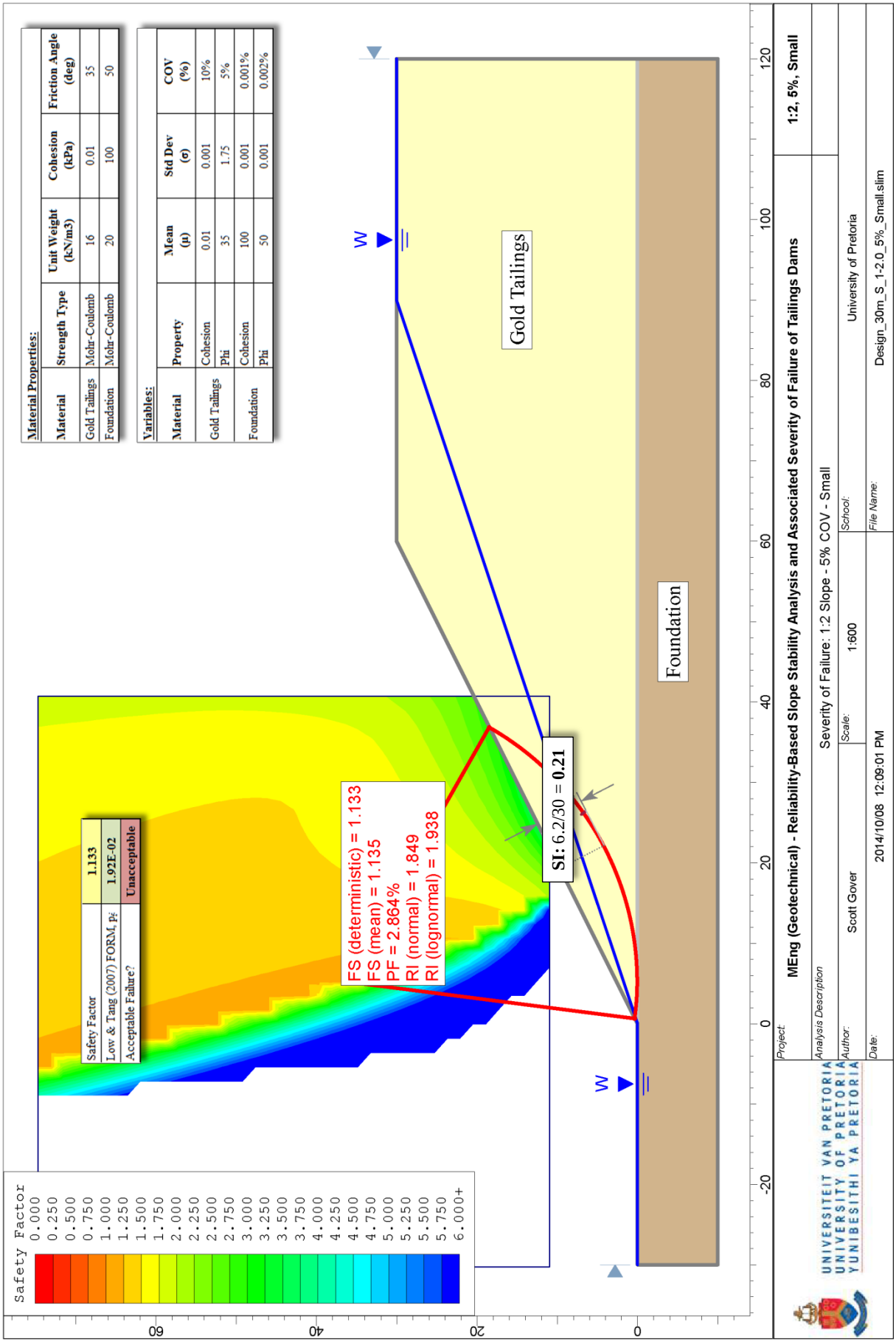
Material	**Property**	**Distribution**	**μ**	**σ**	**Para3**	**Para4**	**xi***	**ni**	**ϕ_1**	**c_1**	**ϕ_2**	**c_2**	**g(x)**	**β**
Rejects	Phi	Normal	20.00	1.00			18.38	-1.620	1	-0.4	0	0	2E-08	**1.686**
Rejects	Cohesion	Normal	0.10	0.01			0.10	0.648	-0.4	1	0	0		
Waste Rock	Phi	Normal	40.00	2.00			39.07	-0.465	0	0	1	-0.4		**Prob.Fail**
Waste Rock	Cohesion	Normal	0.10	0.01			0.10	0.186	0	0	-0.4	1		**4.59E-02**
								Optimised	Correlation matrix [R]					

© University of Pretoria

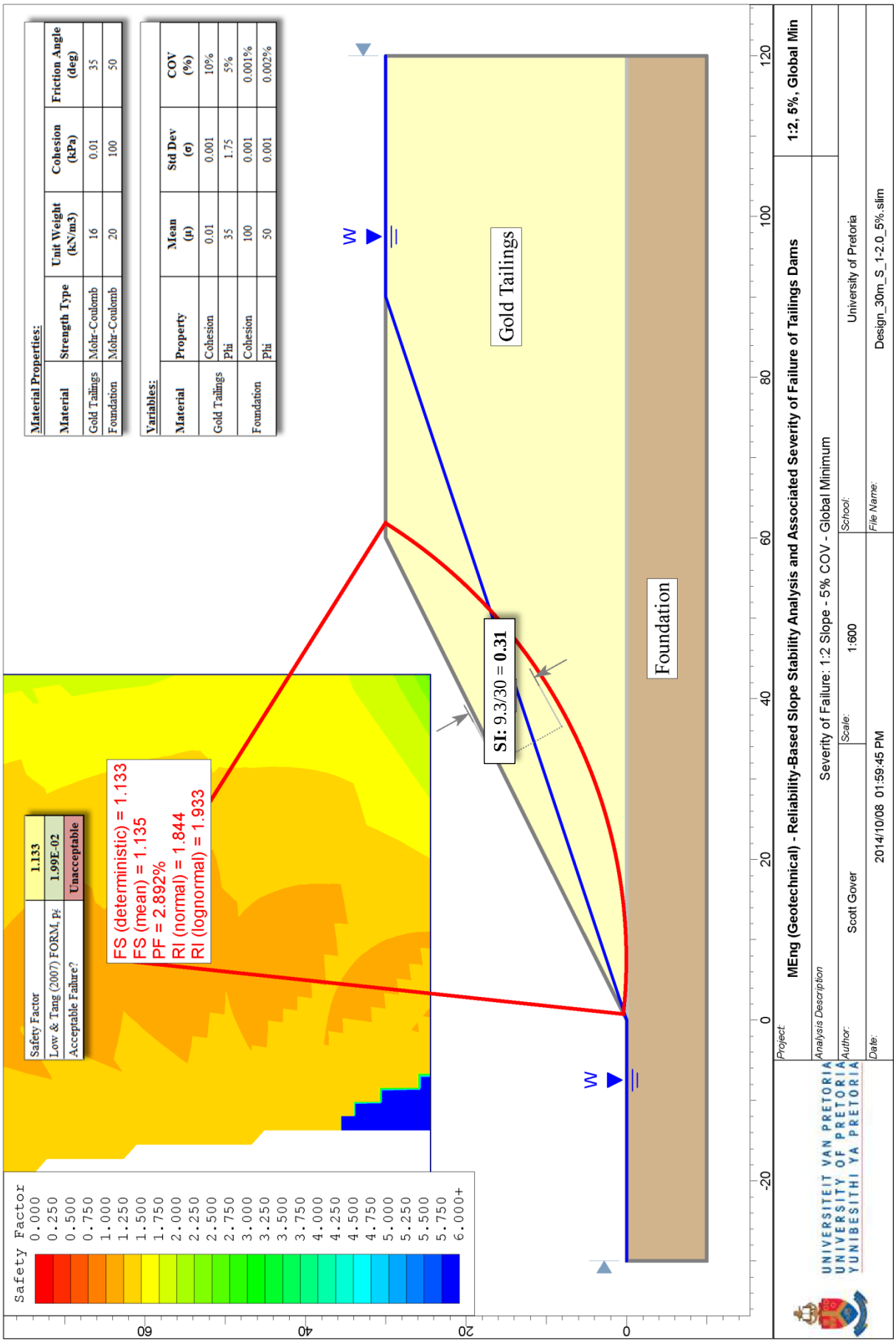
UNIVERSITEIT VAN PRETORIA
UNIVERSITY OF PRETORIA
YUNIBESITHI YA PRETORIA

APPENDIX B

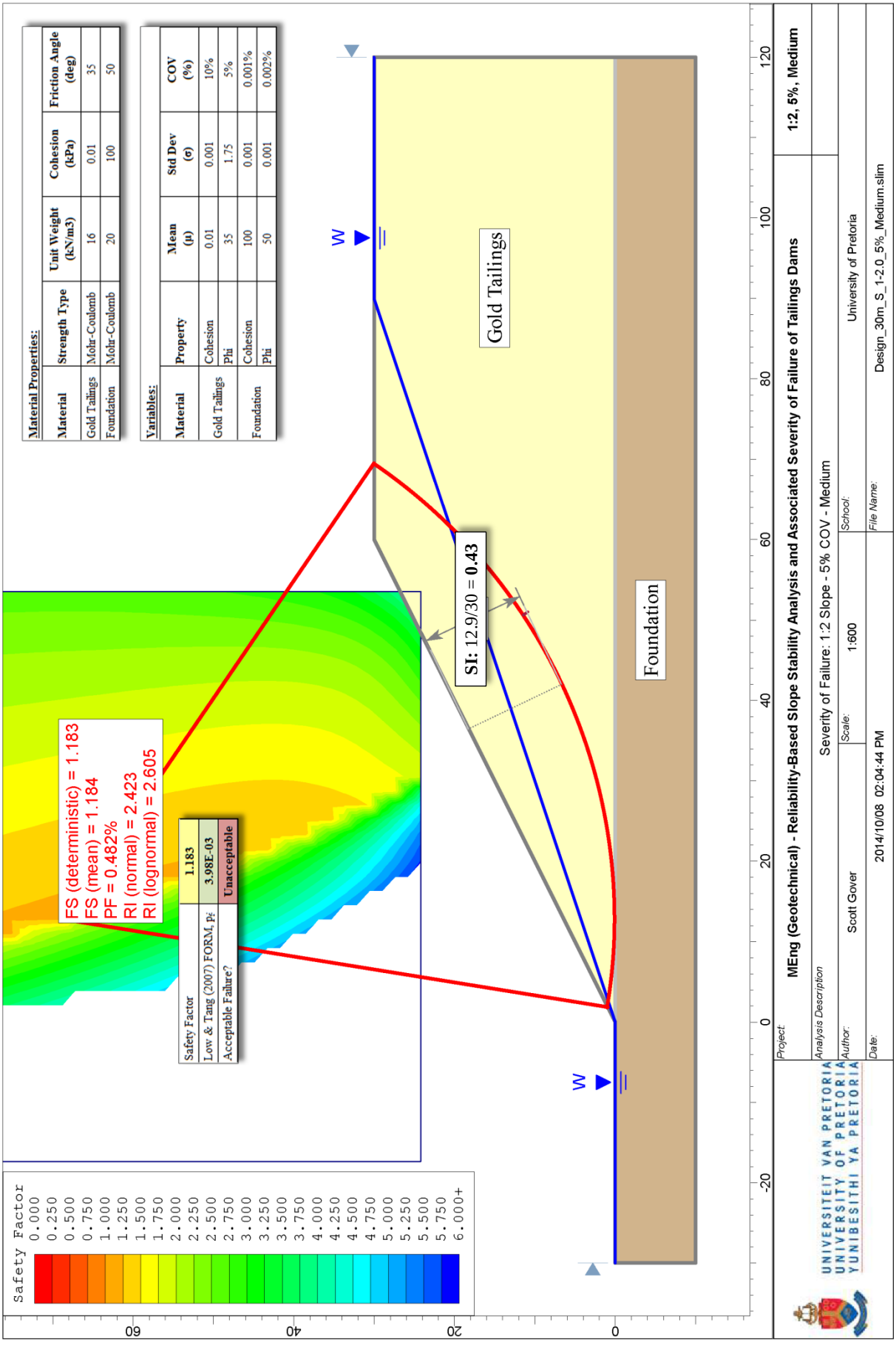
© University of Pretoria



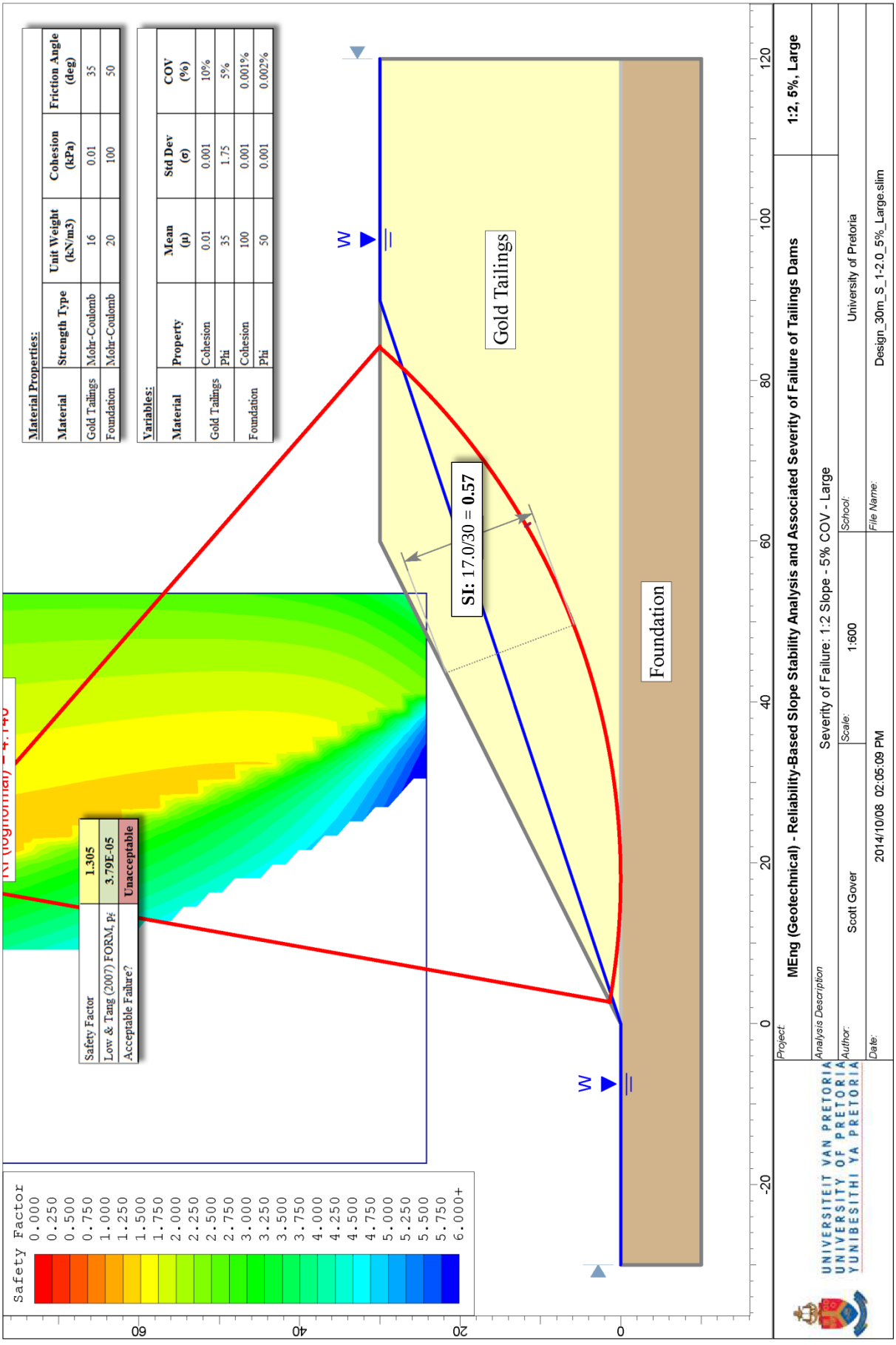
© University of Pretoria



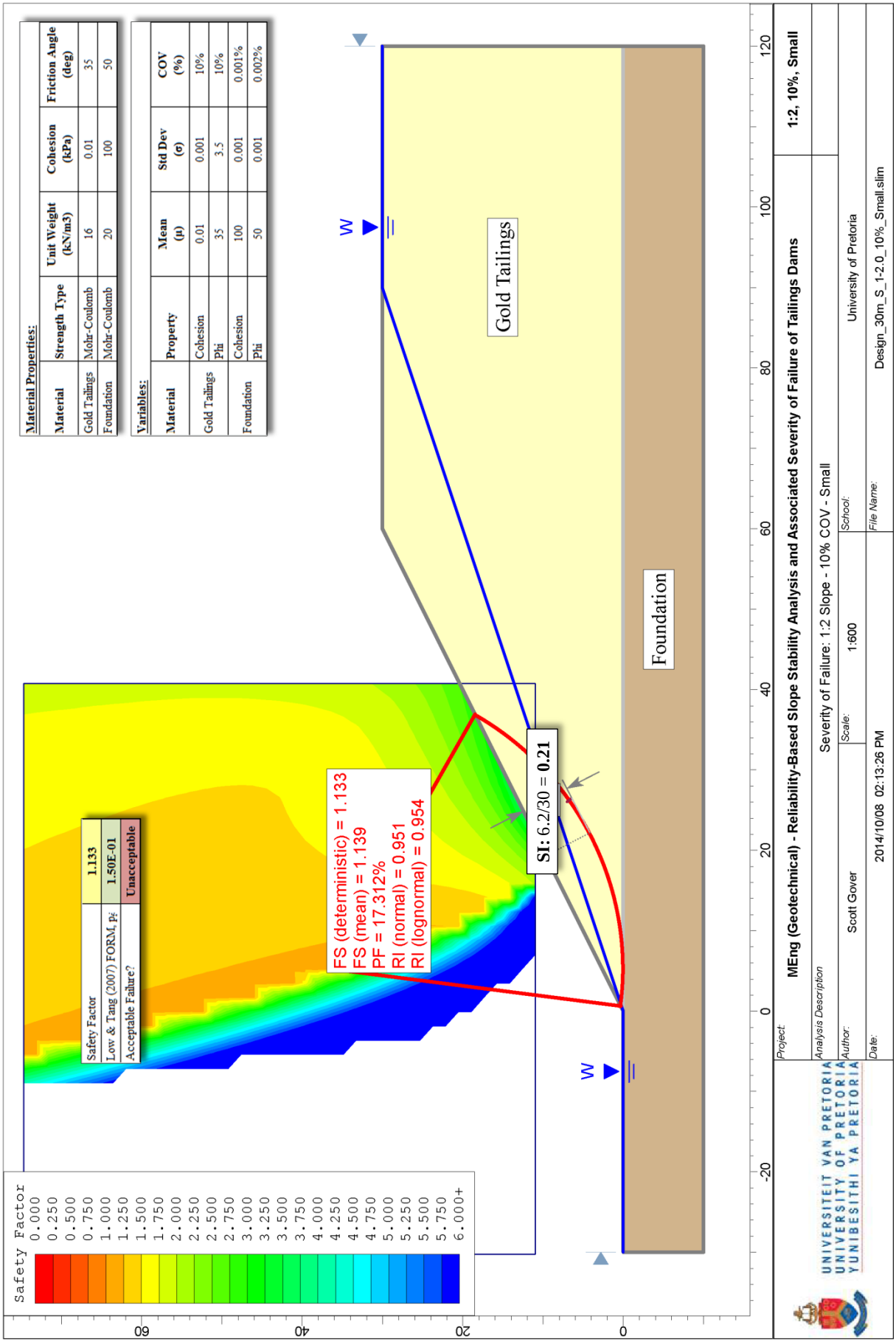
© University of Pretoria



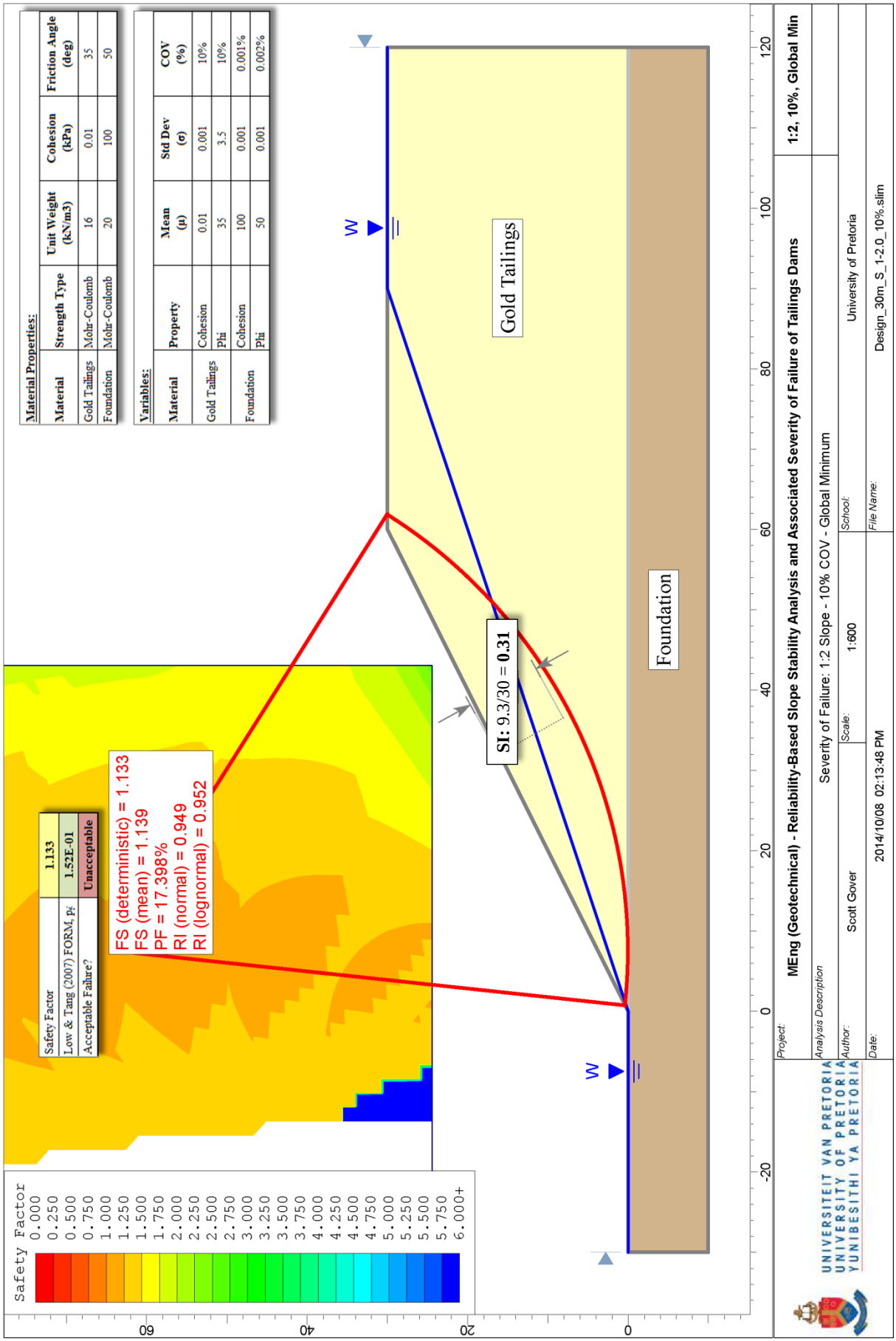
© University of Pretoria



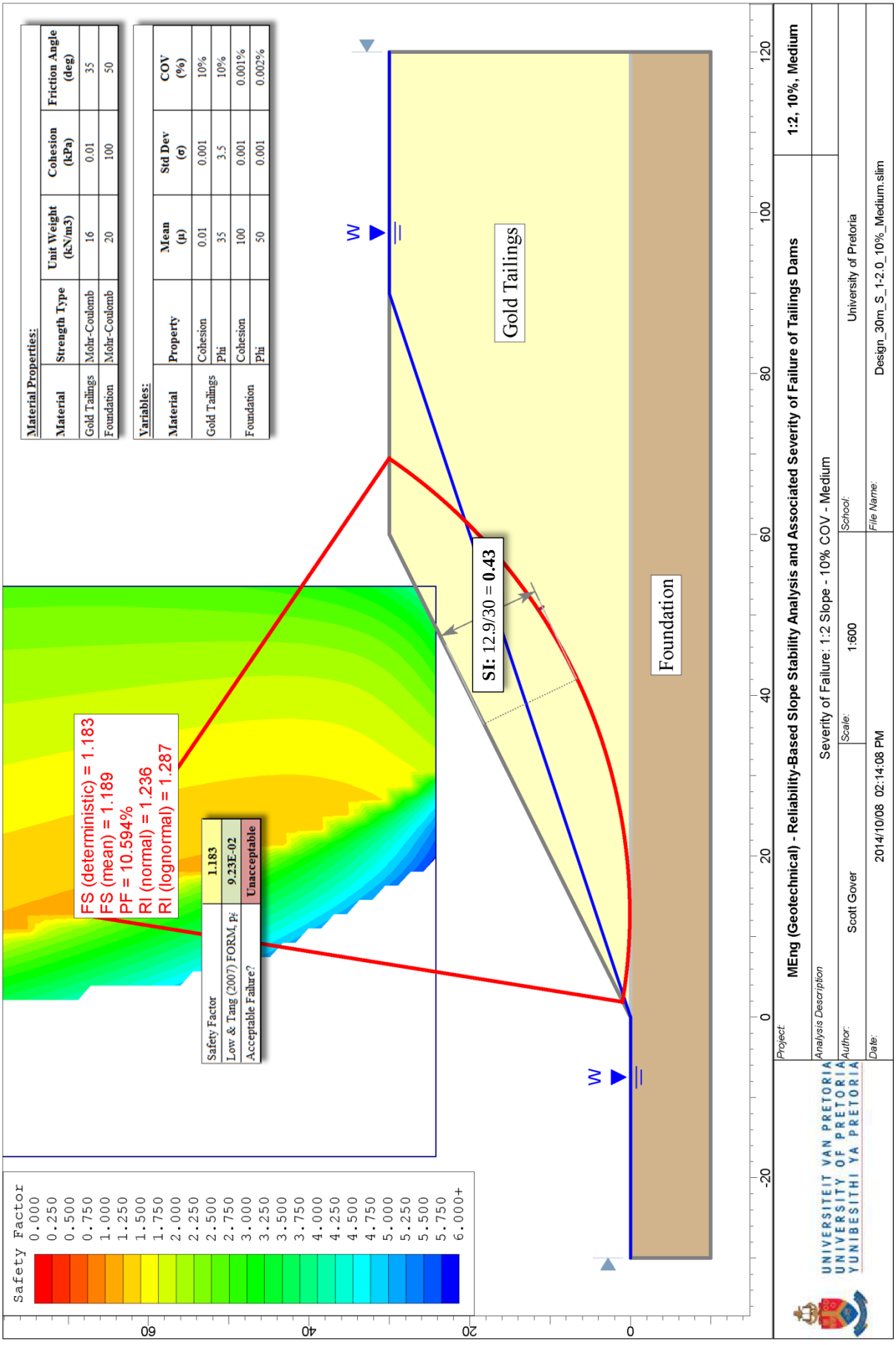
© University of Pretoria



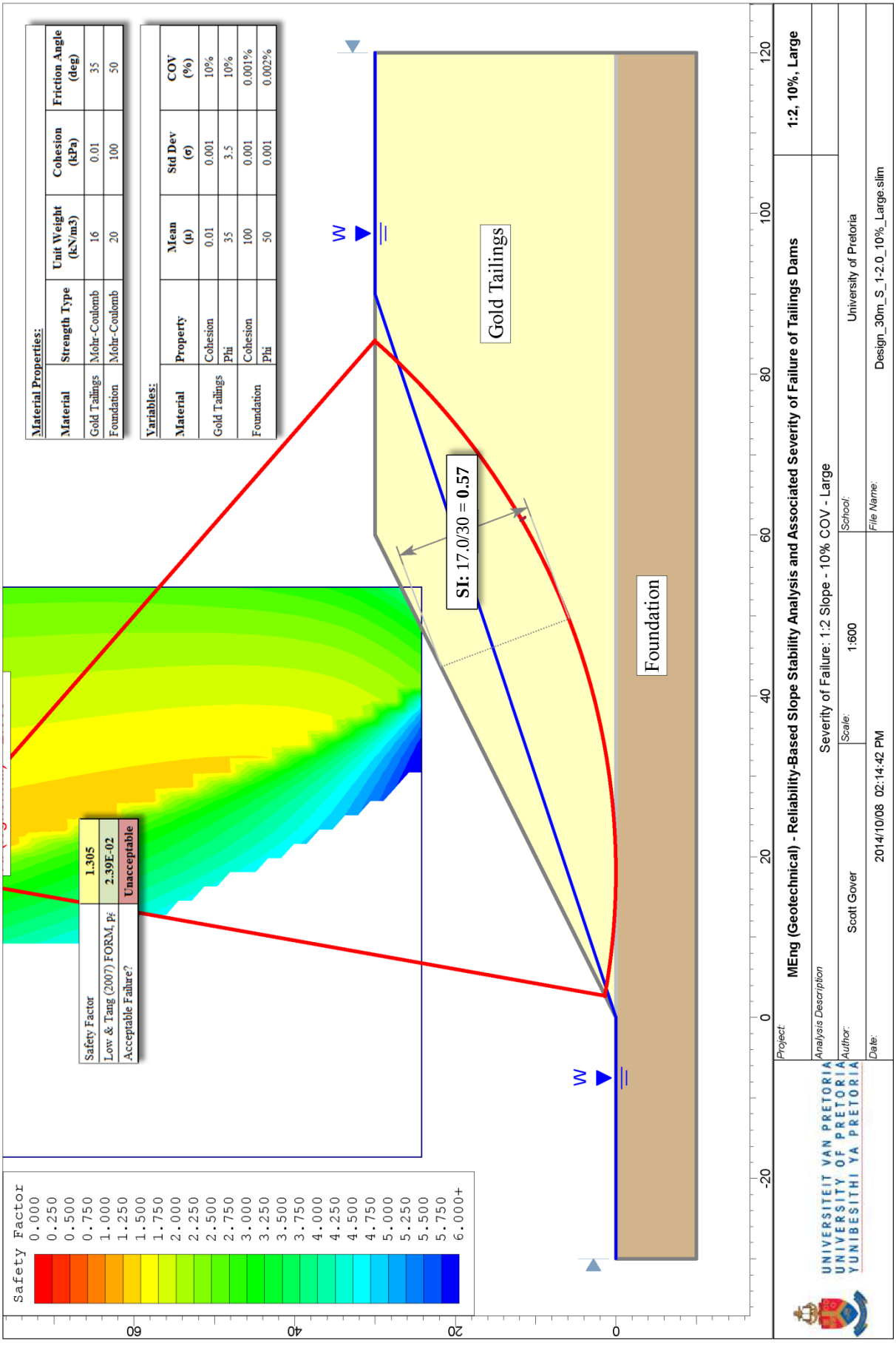
© University of Pretoria



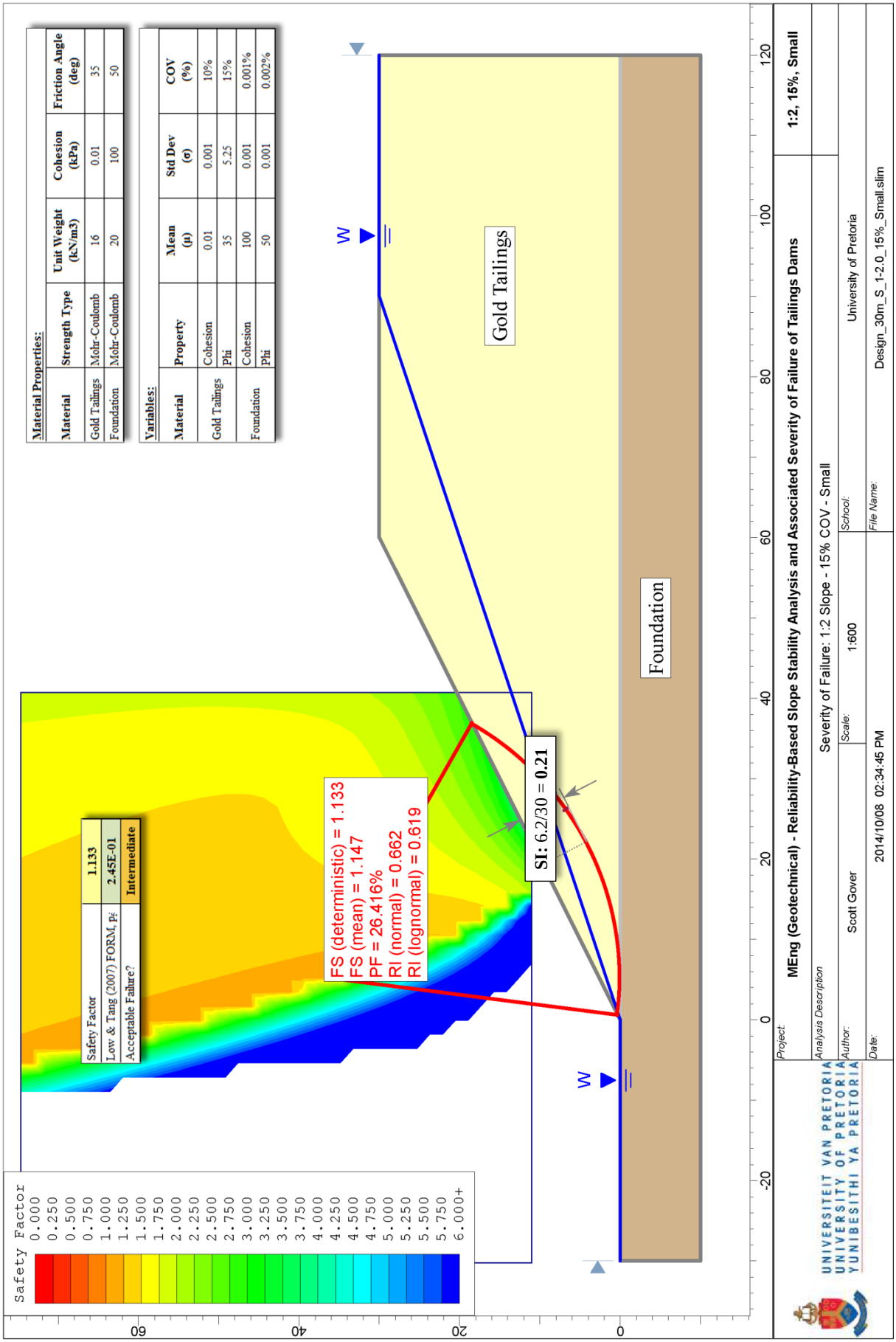
© University of Pretoria



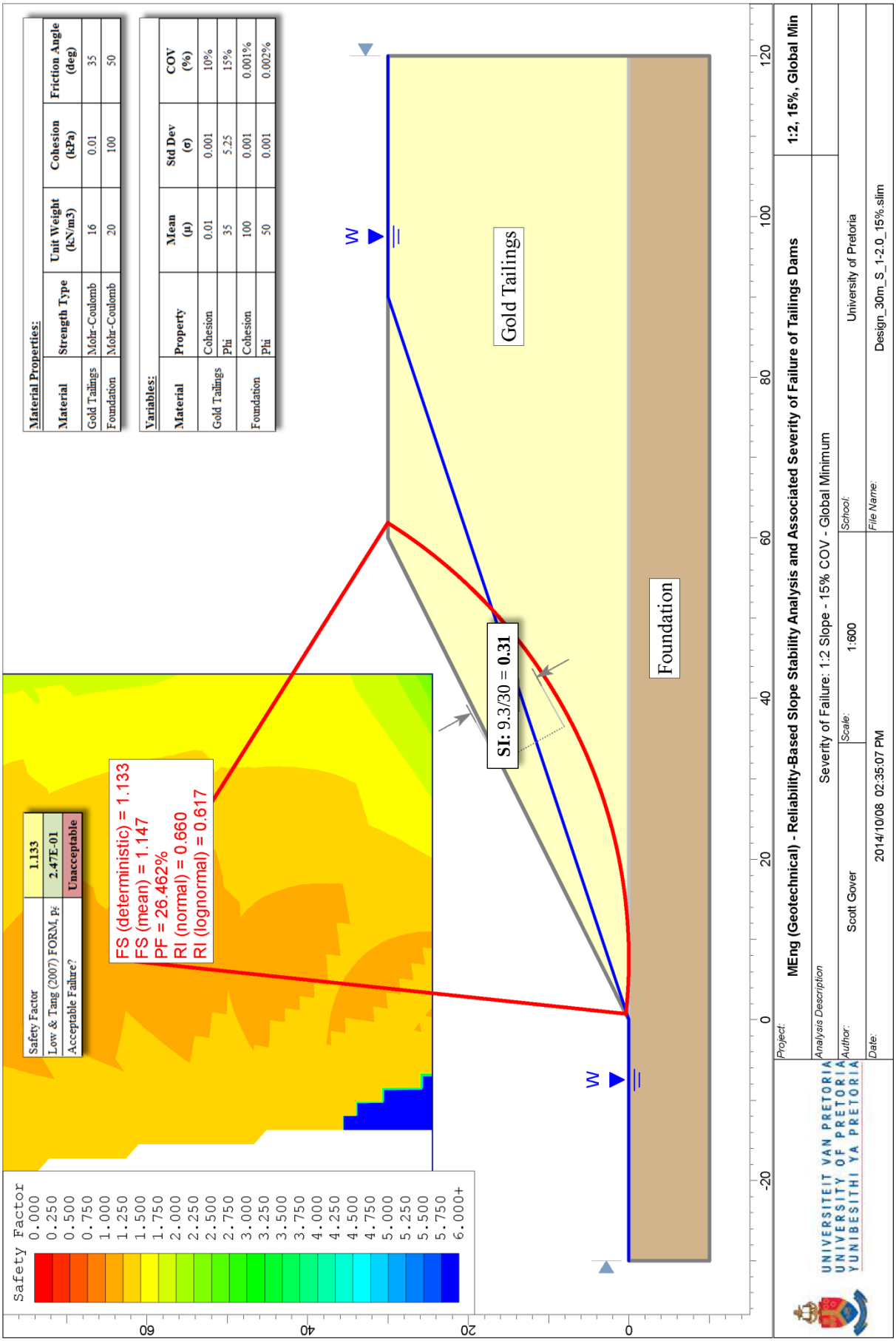
© University of Pretoria



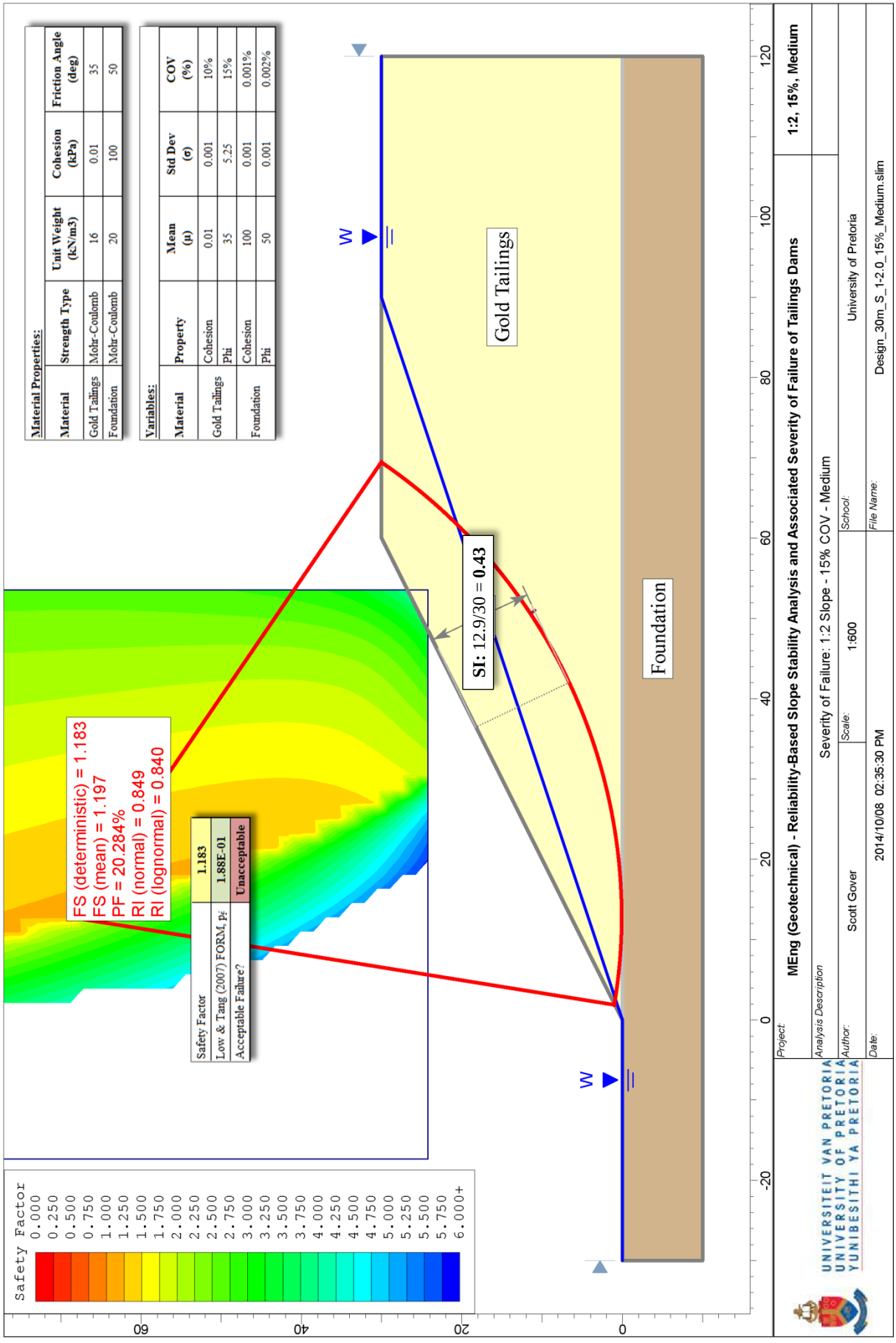
© University of Pretoria



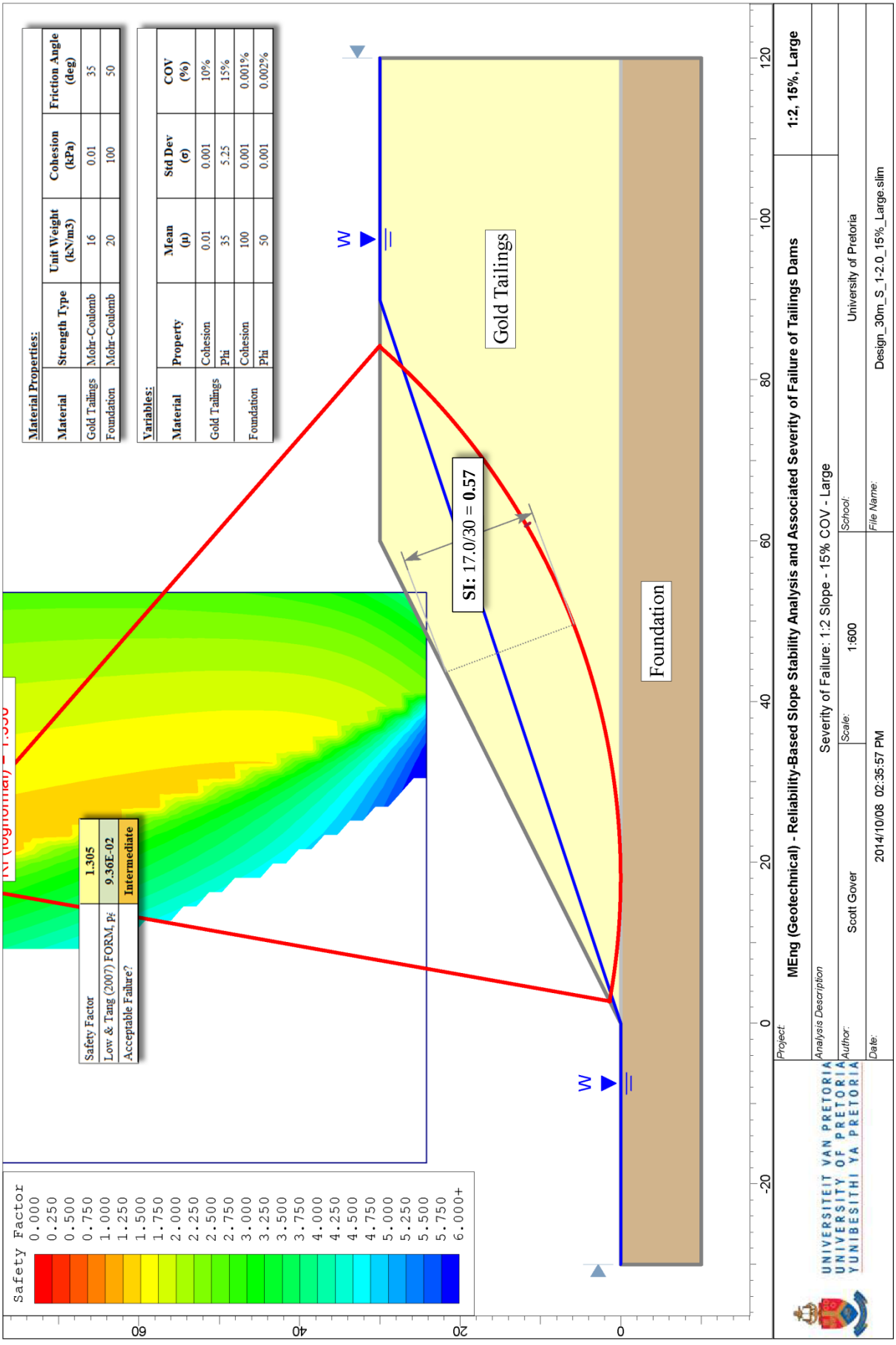
© University of Pretoria



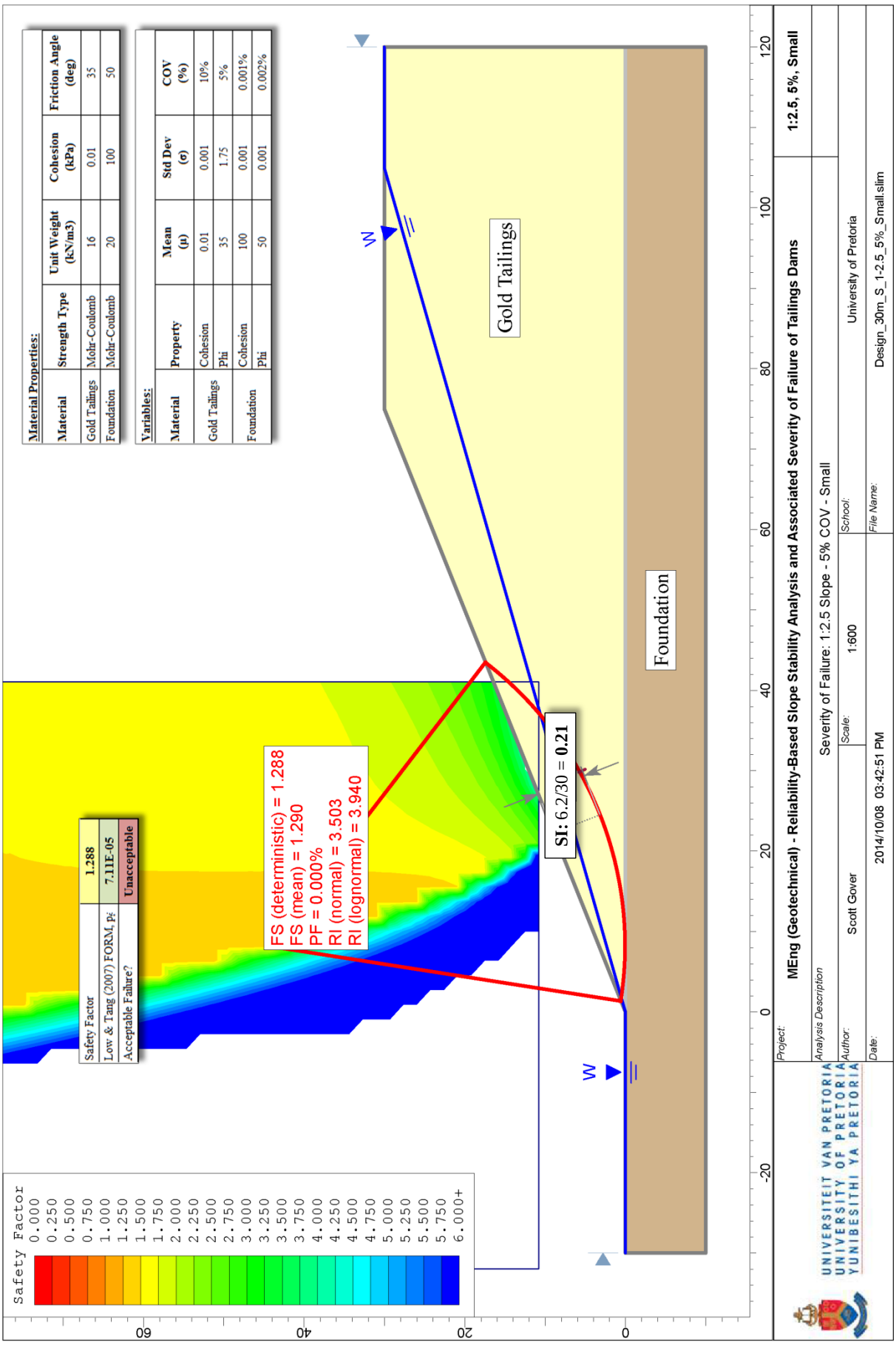
© University of Pretoria



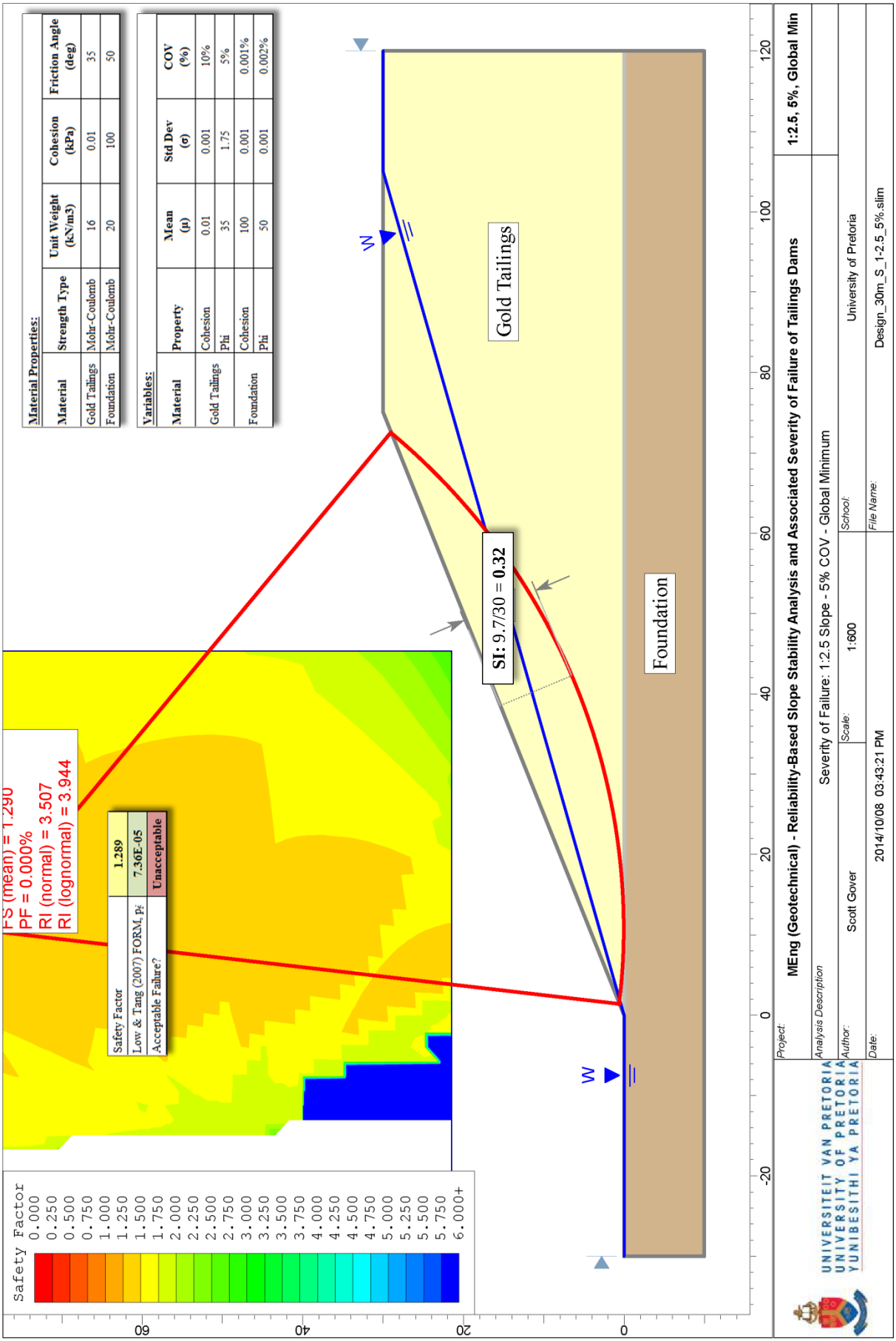
© University of Pretoria



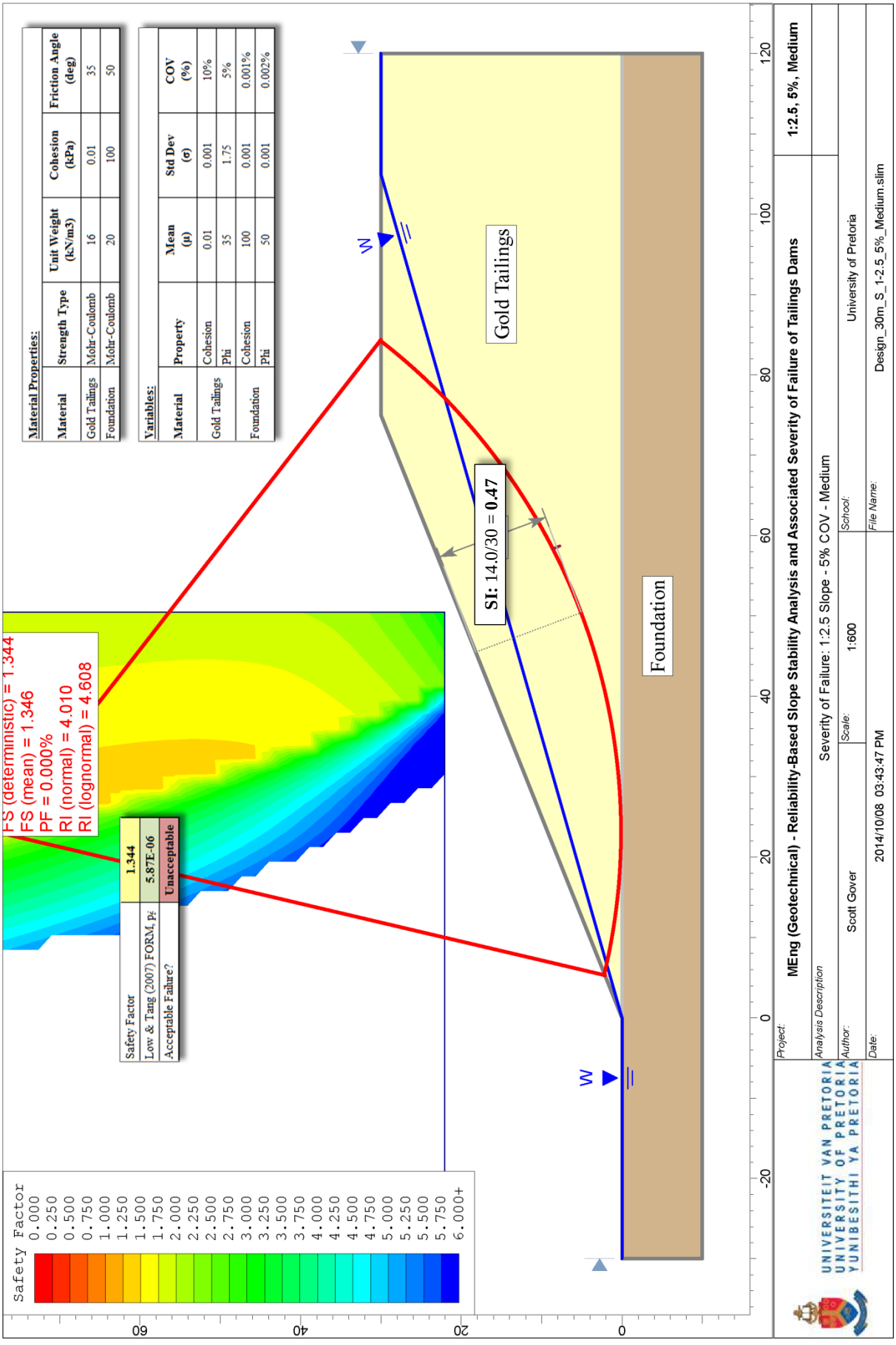
© University of Pretoria



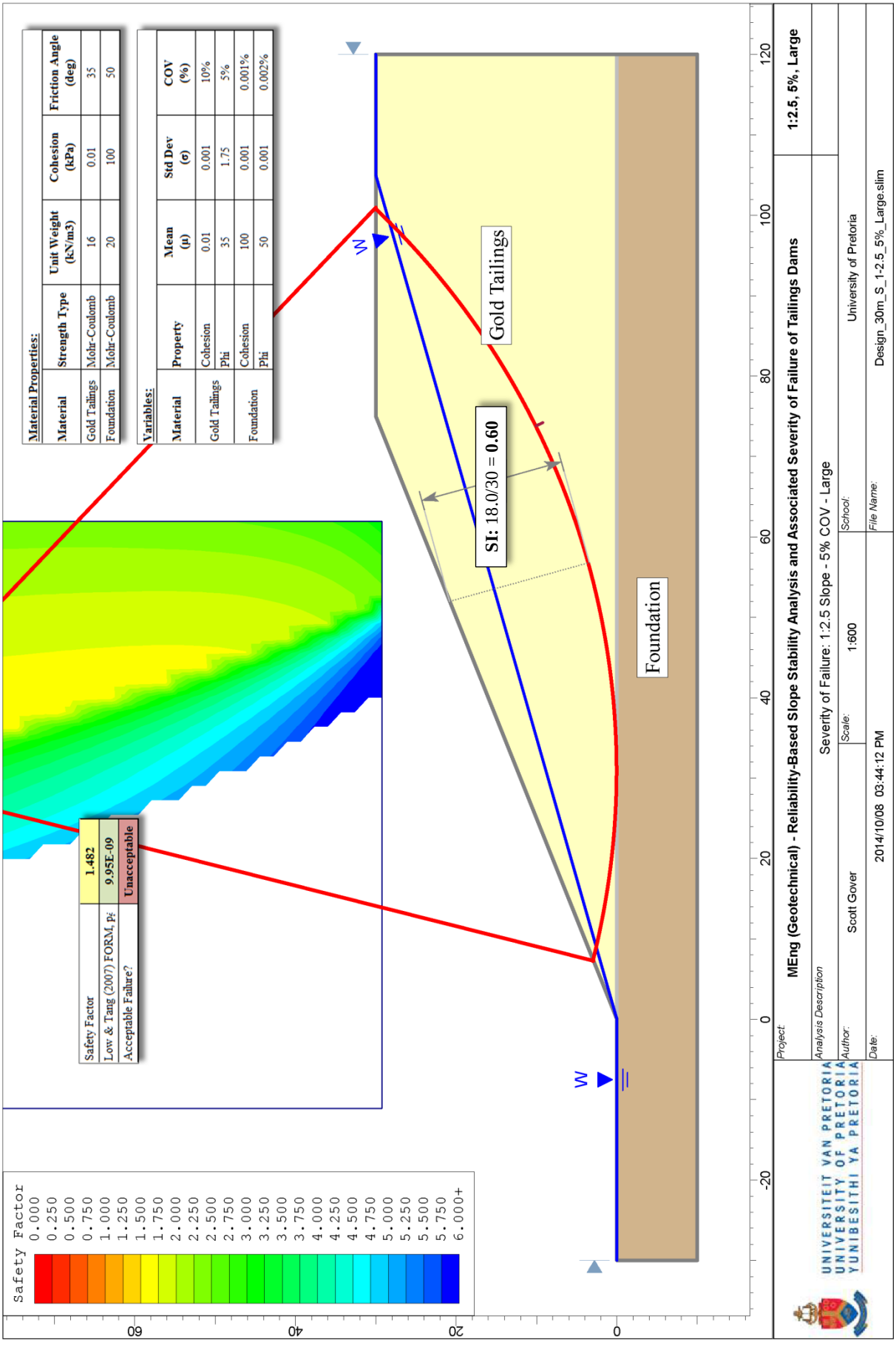
© University of Pretoria



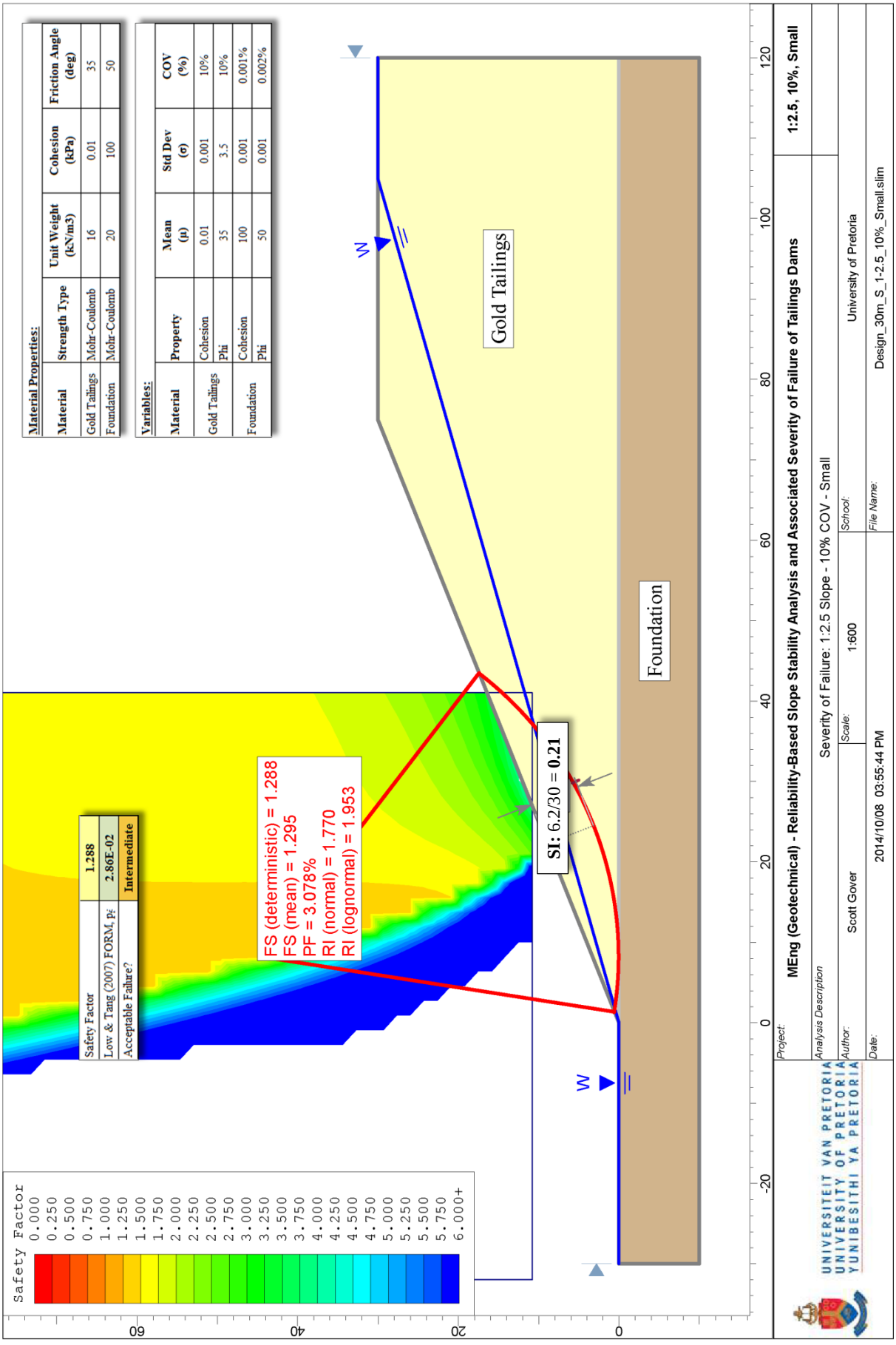
© University of Pretoria



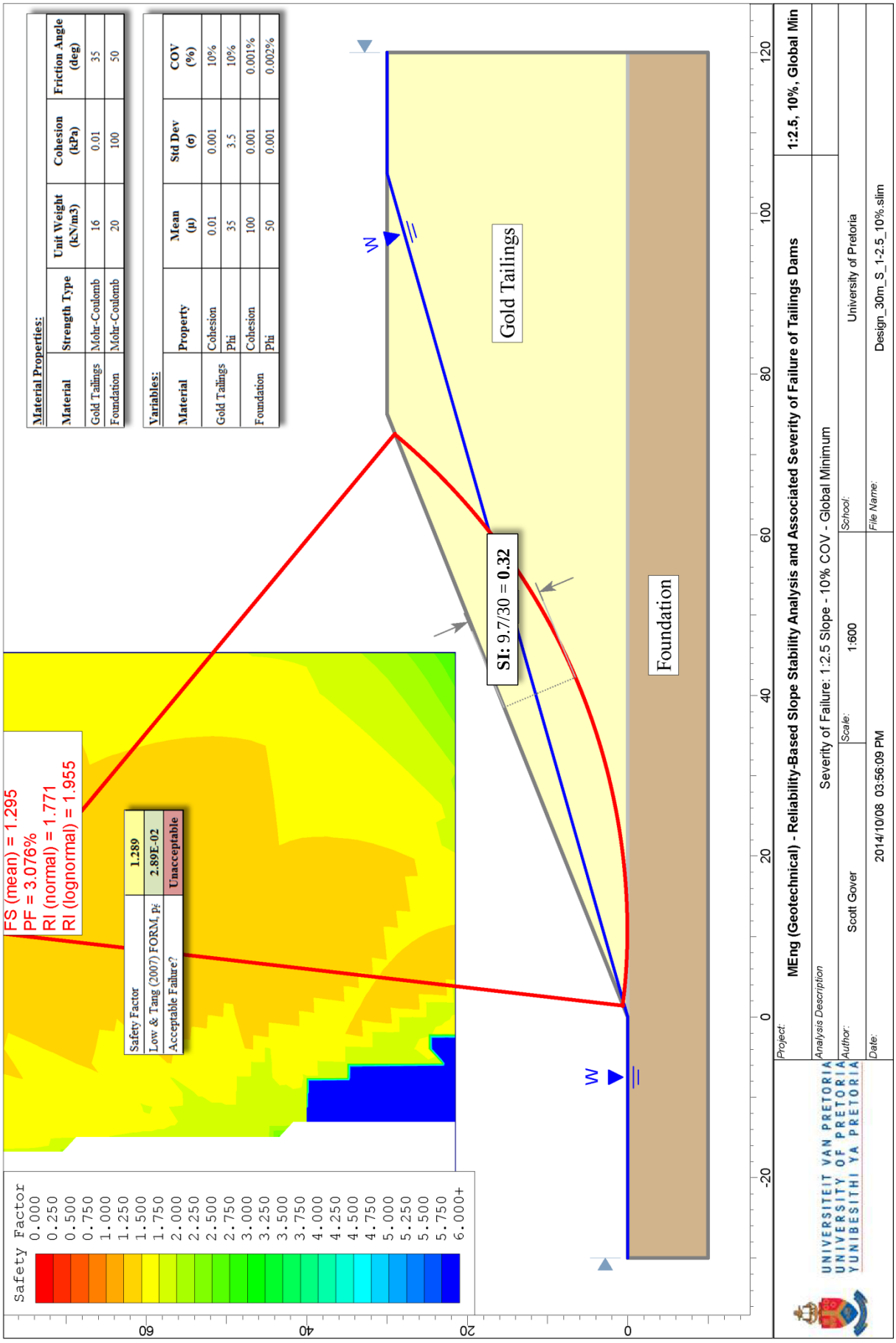
© University of Pretoria



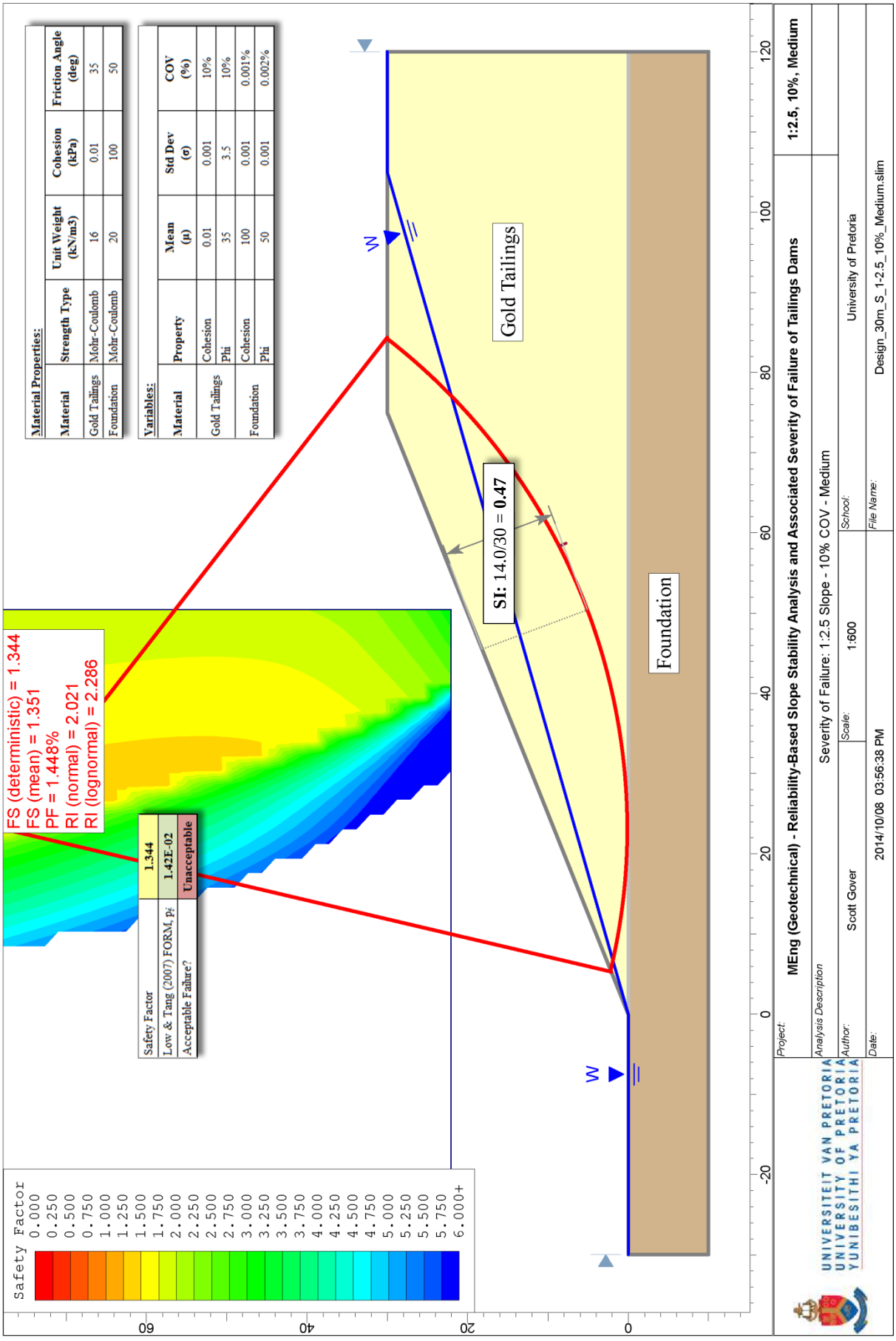
© University of Pretoria



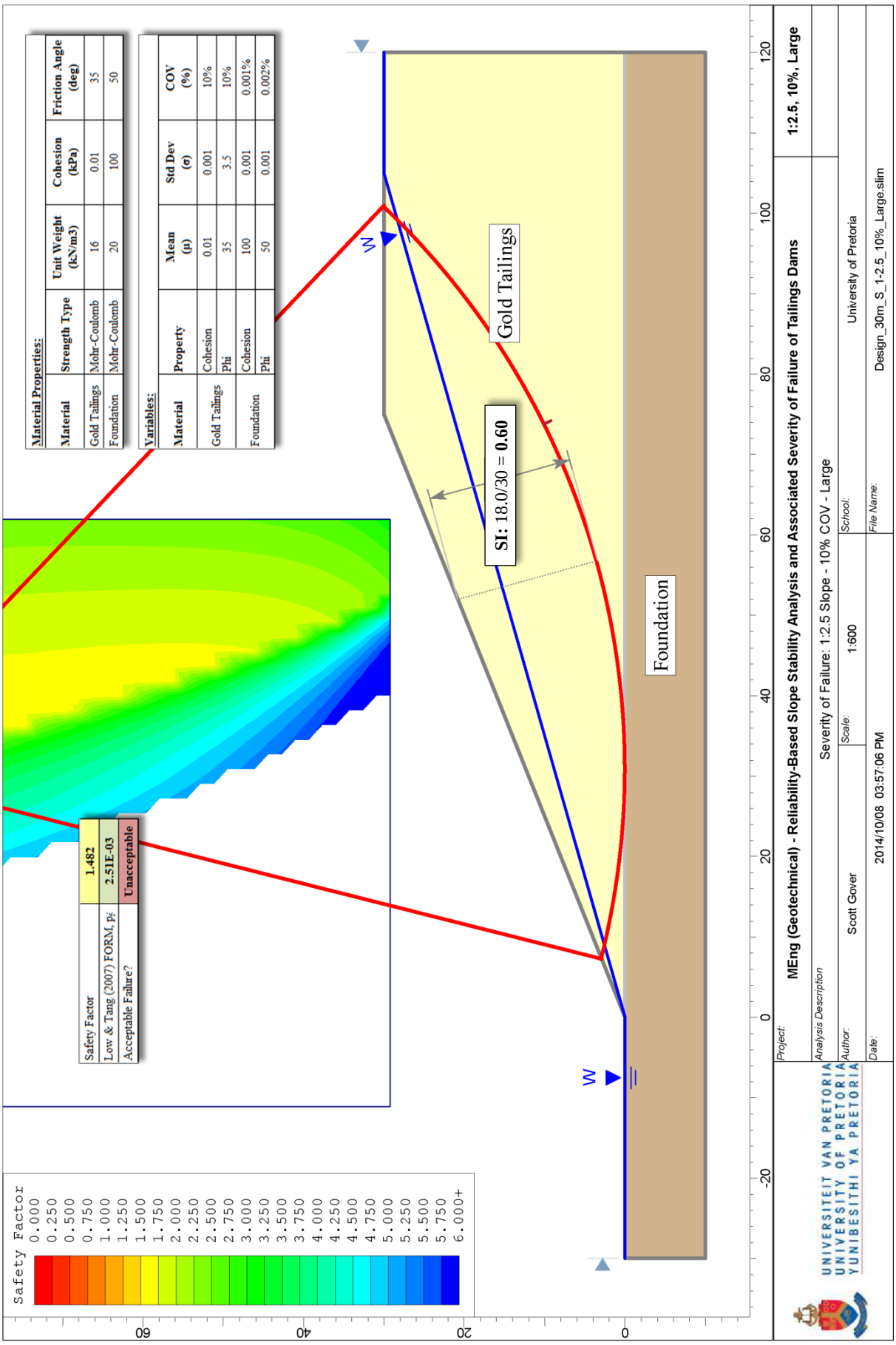
© University of Pretoria



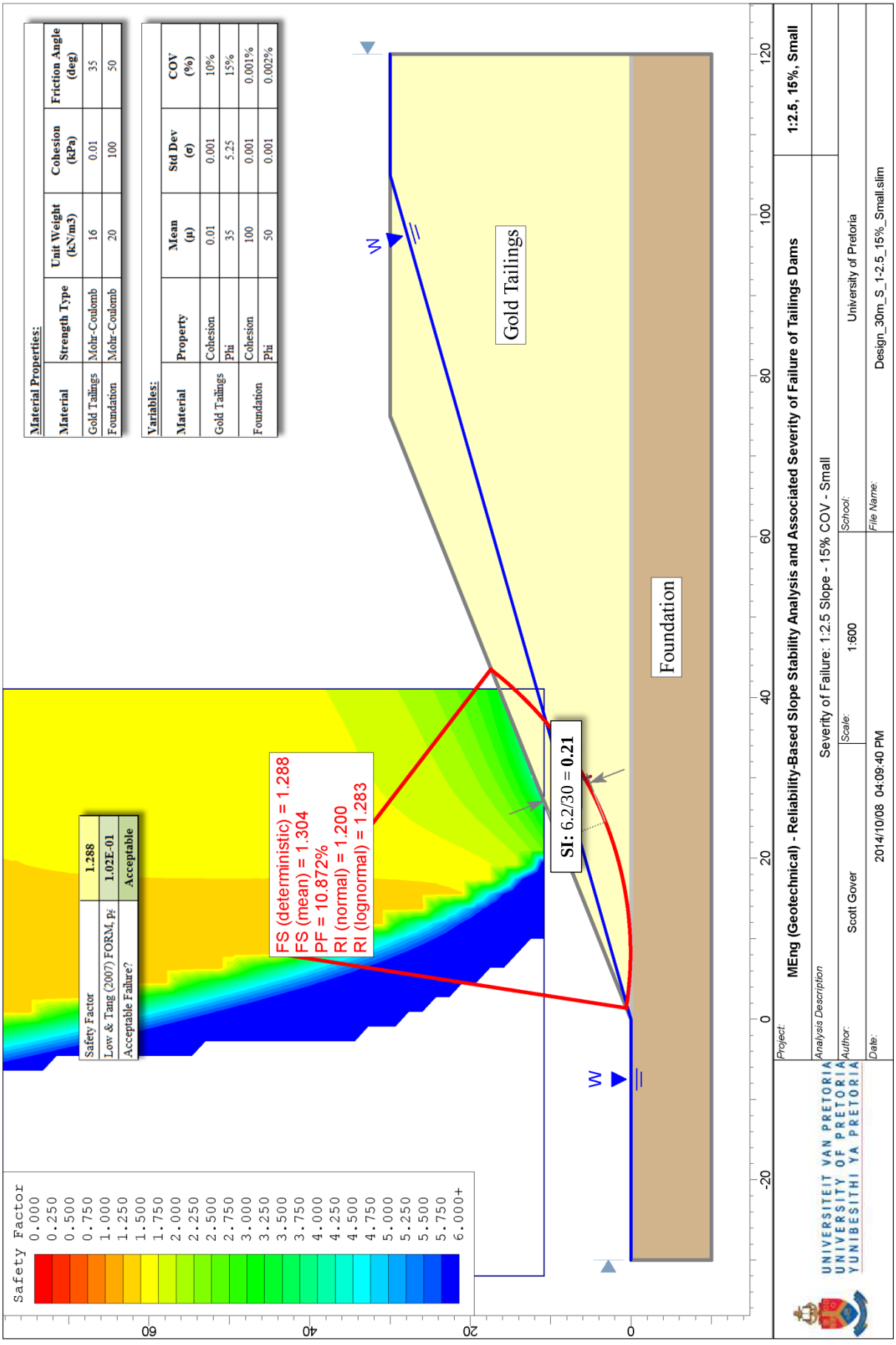
© University of Pretoria



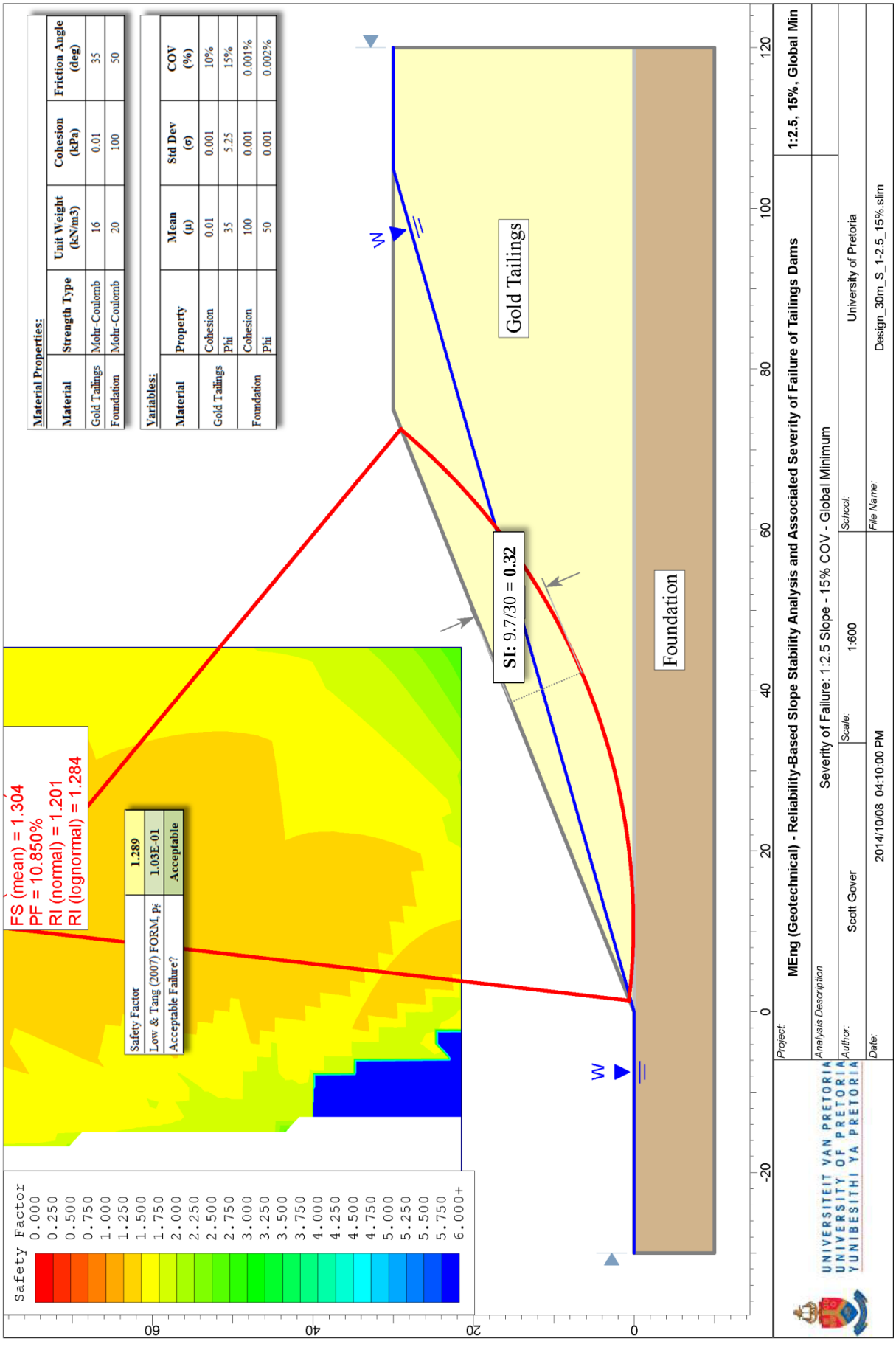
© University of Pretoria



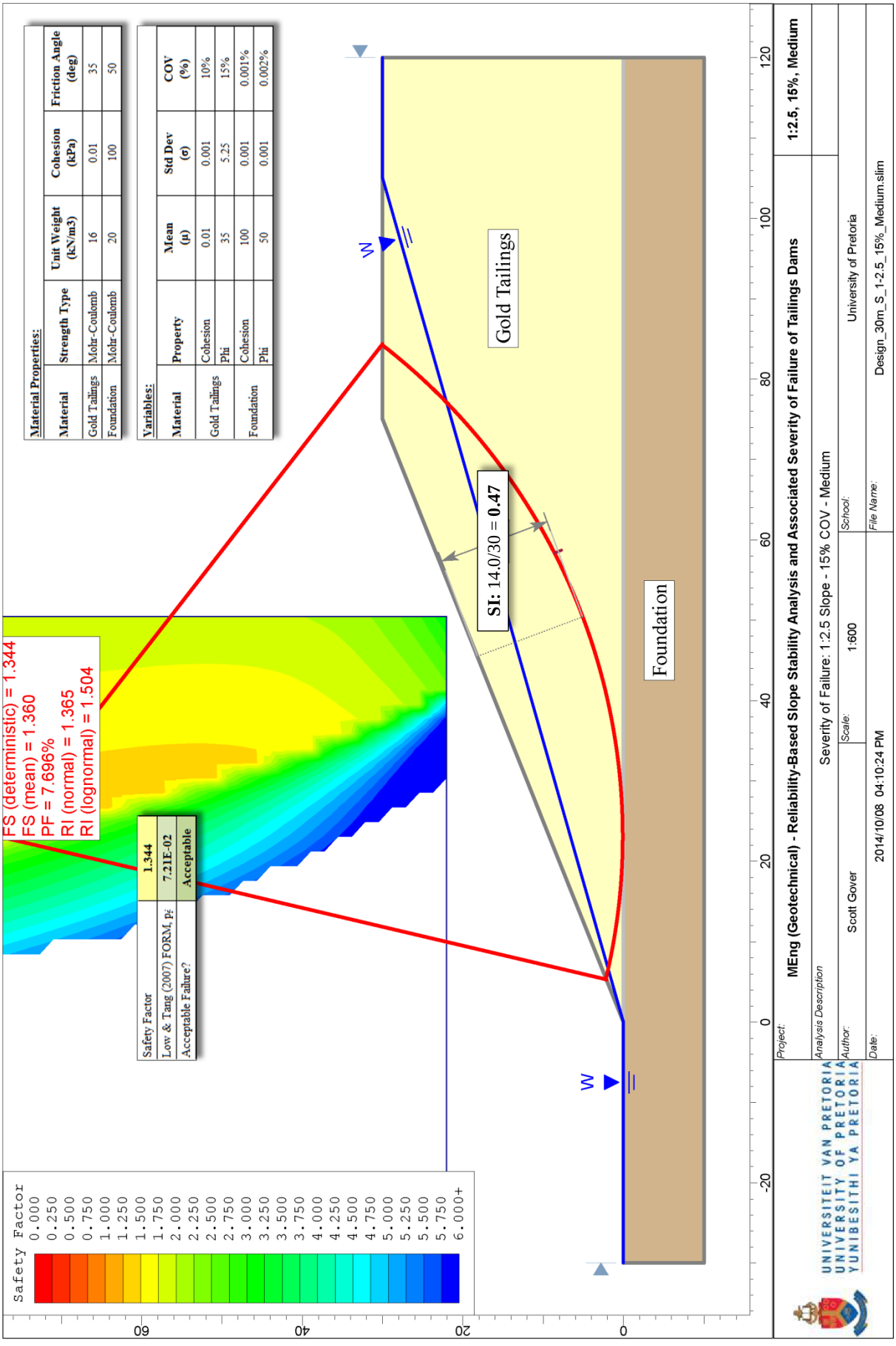
© University of Pretoria



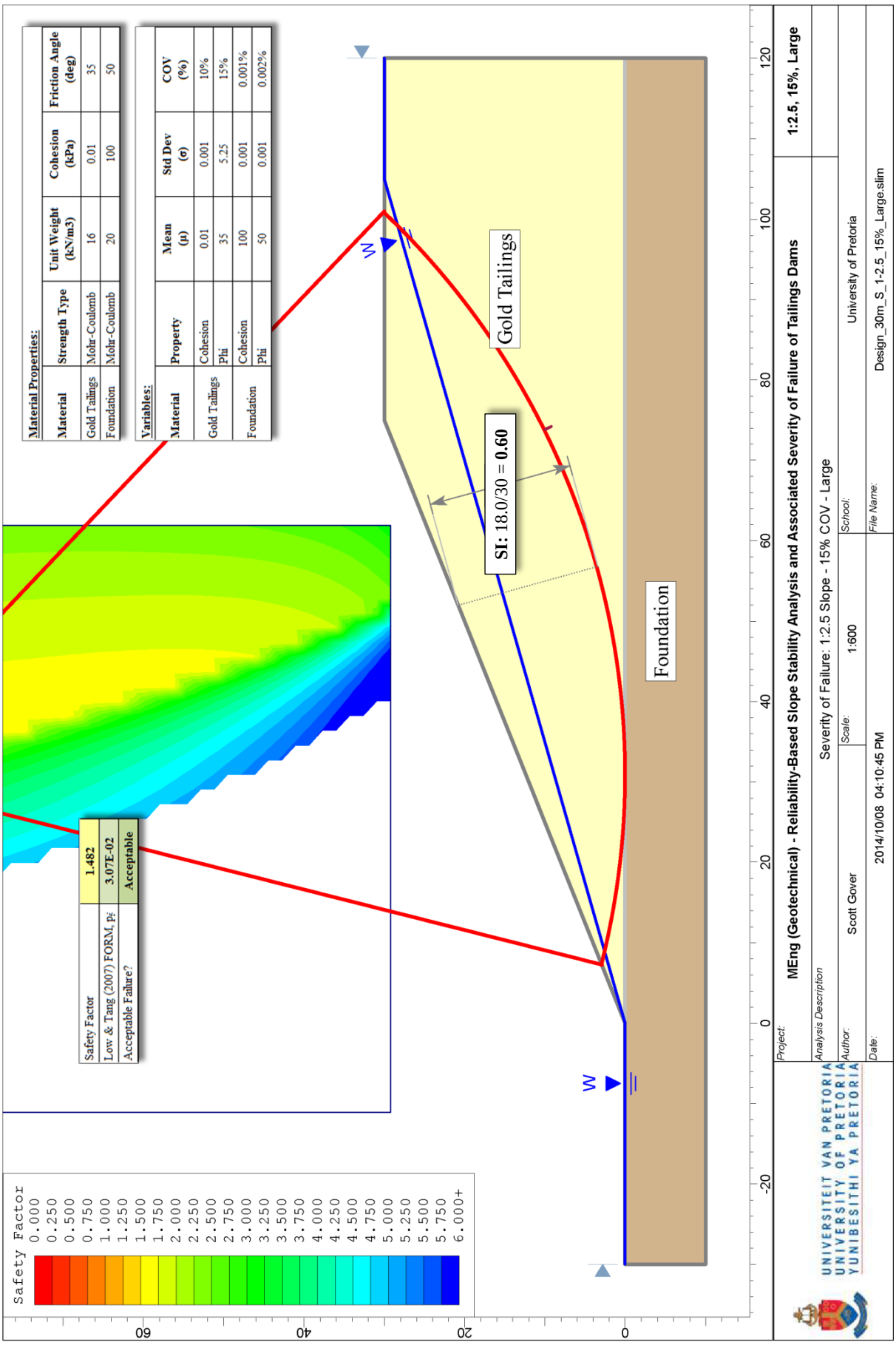
© University of Pretoria



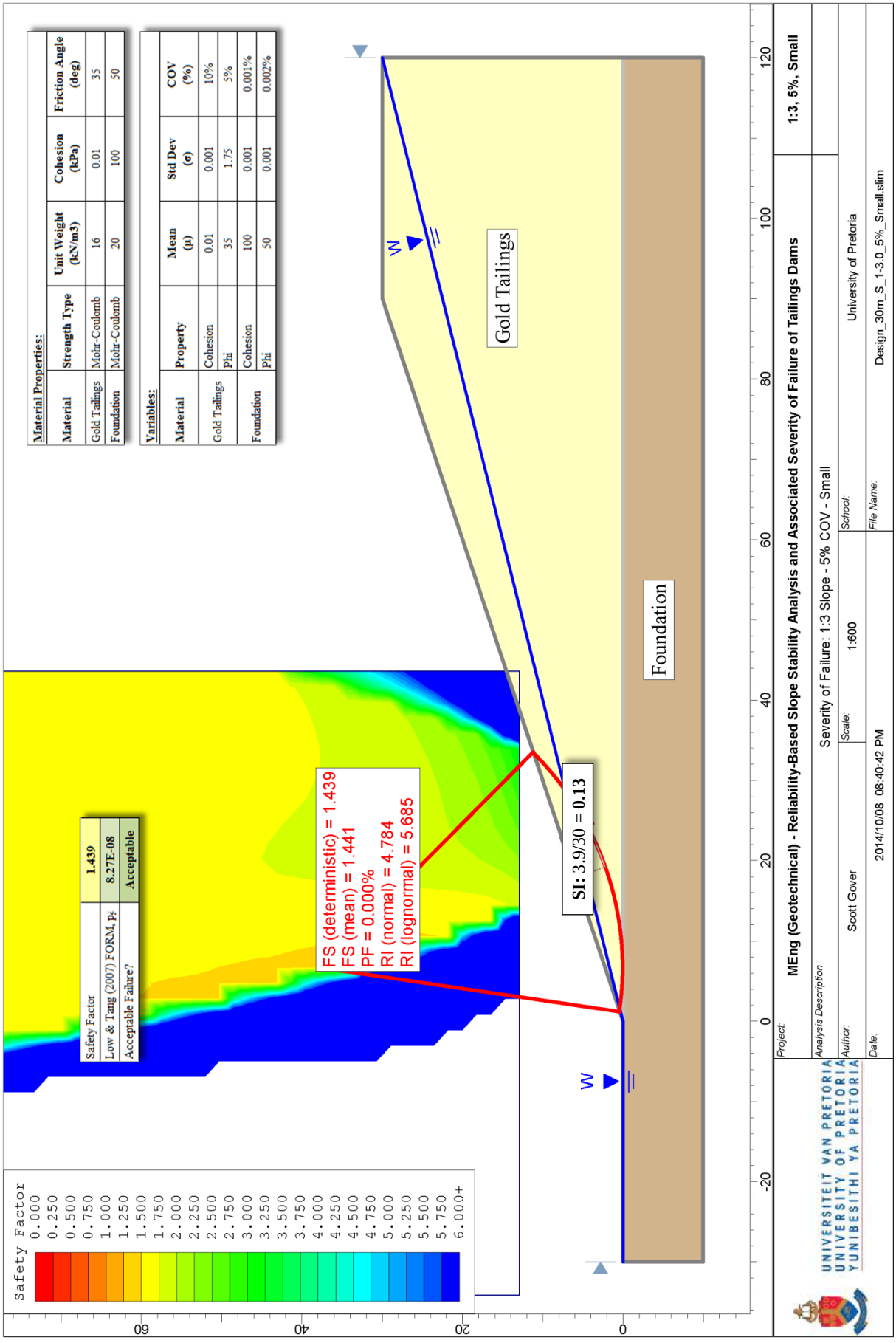
© University of Pretoria



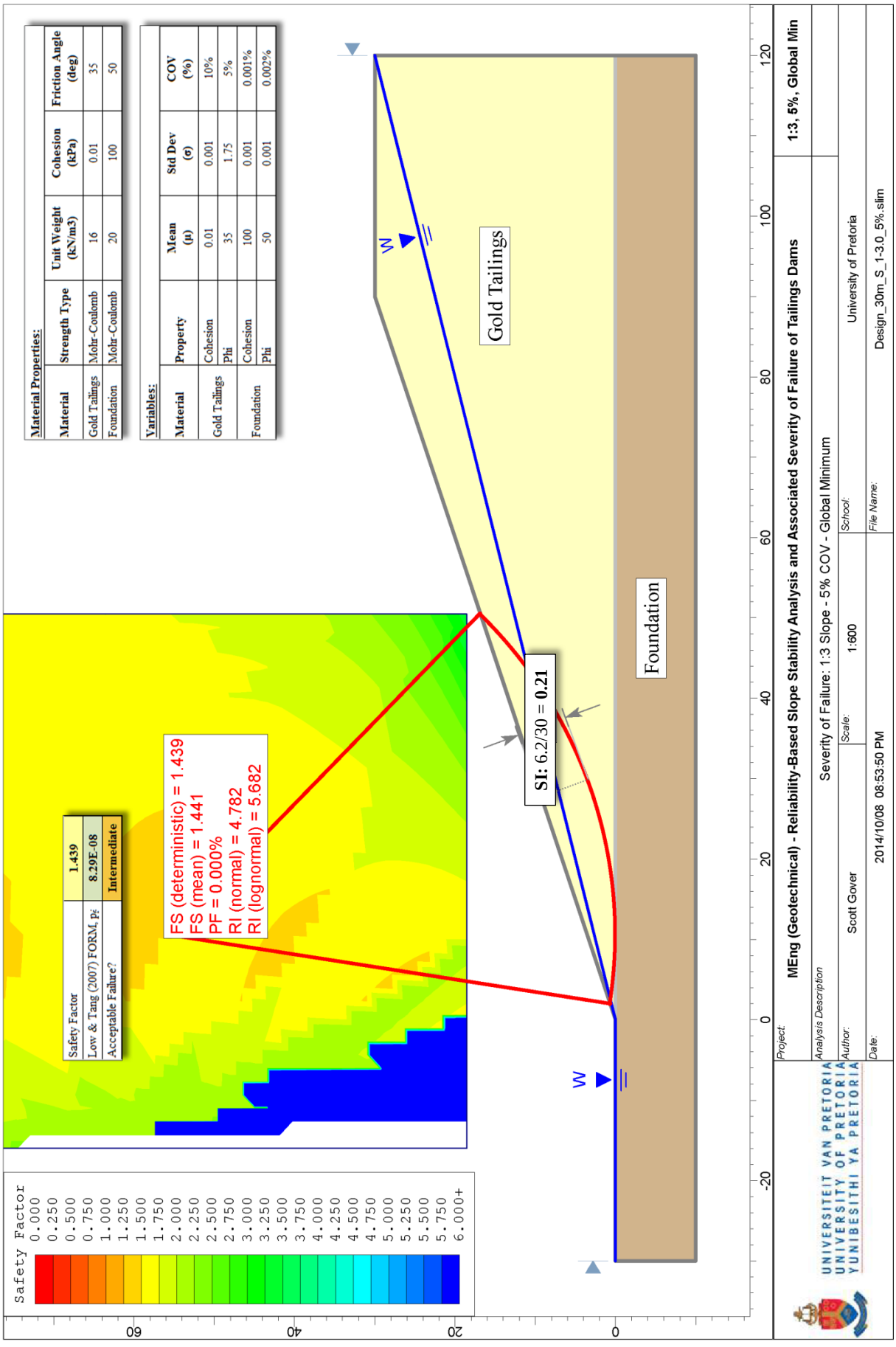
© University of Pretoria



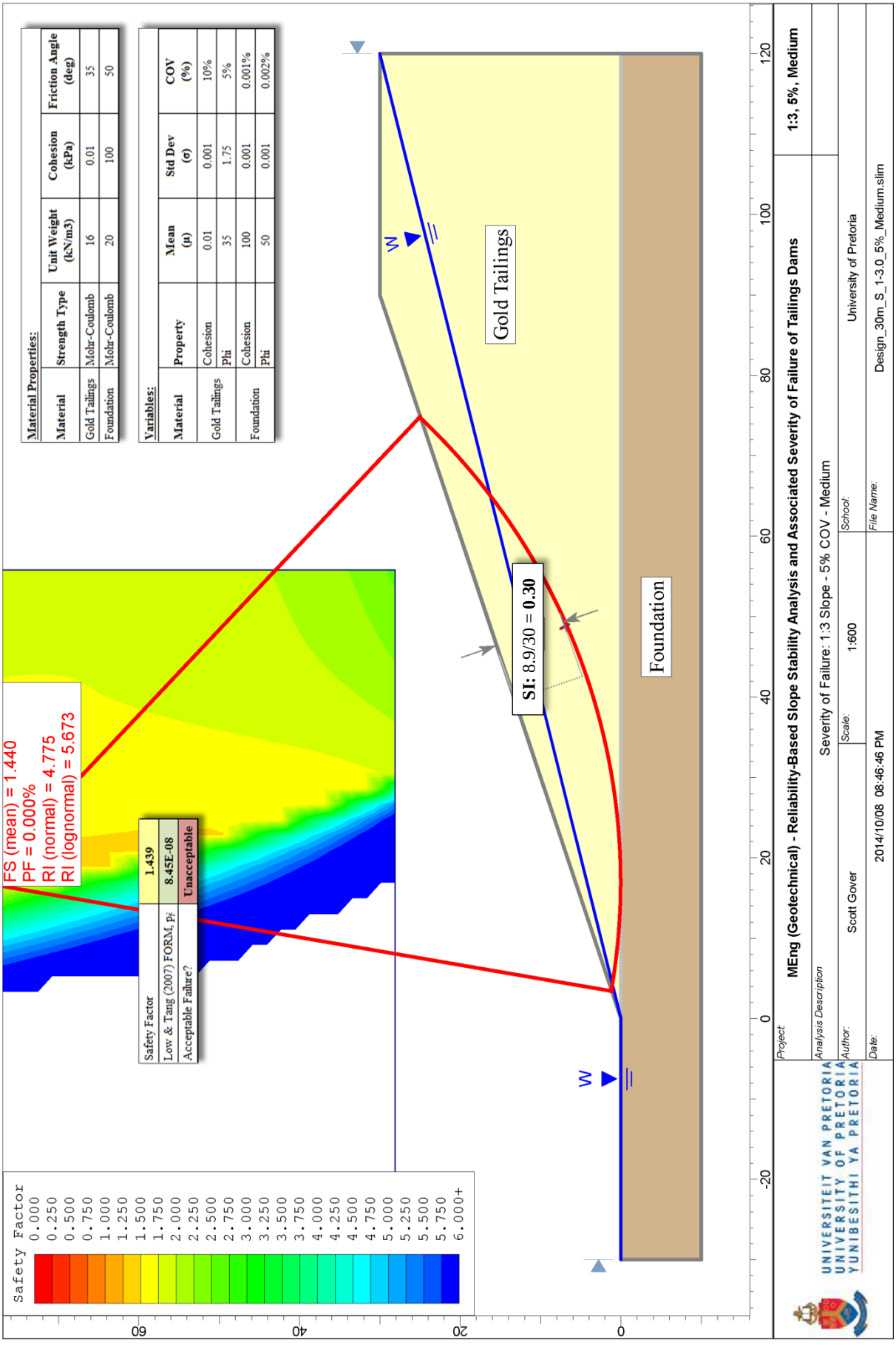
© University of Pretoria



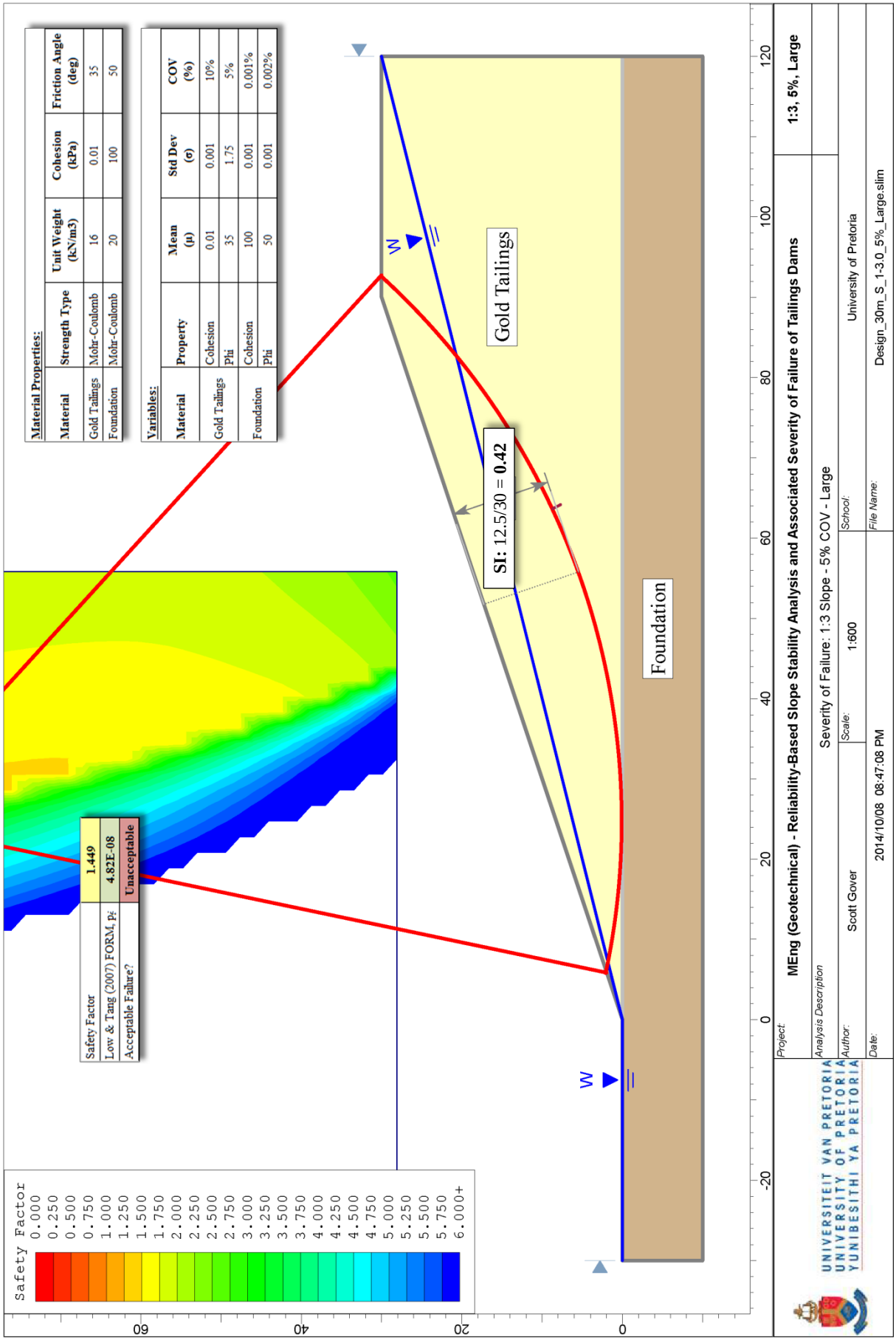
© University of Pretoria



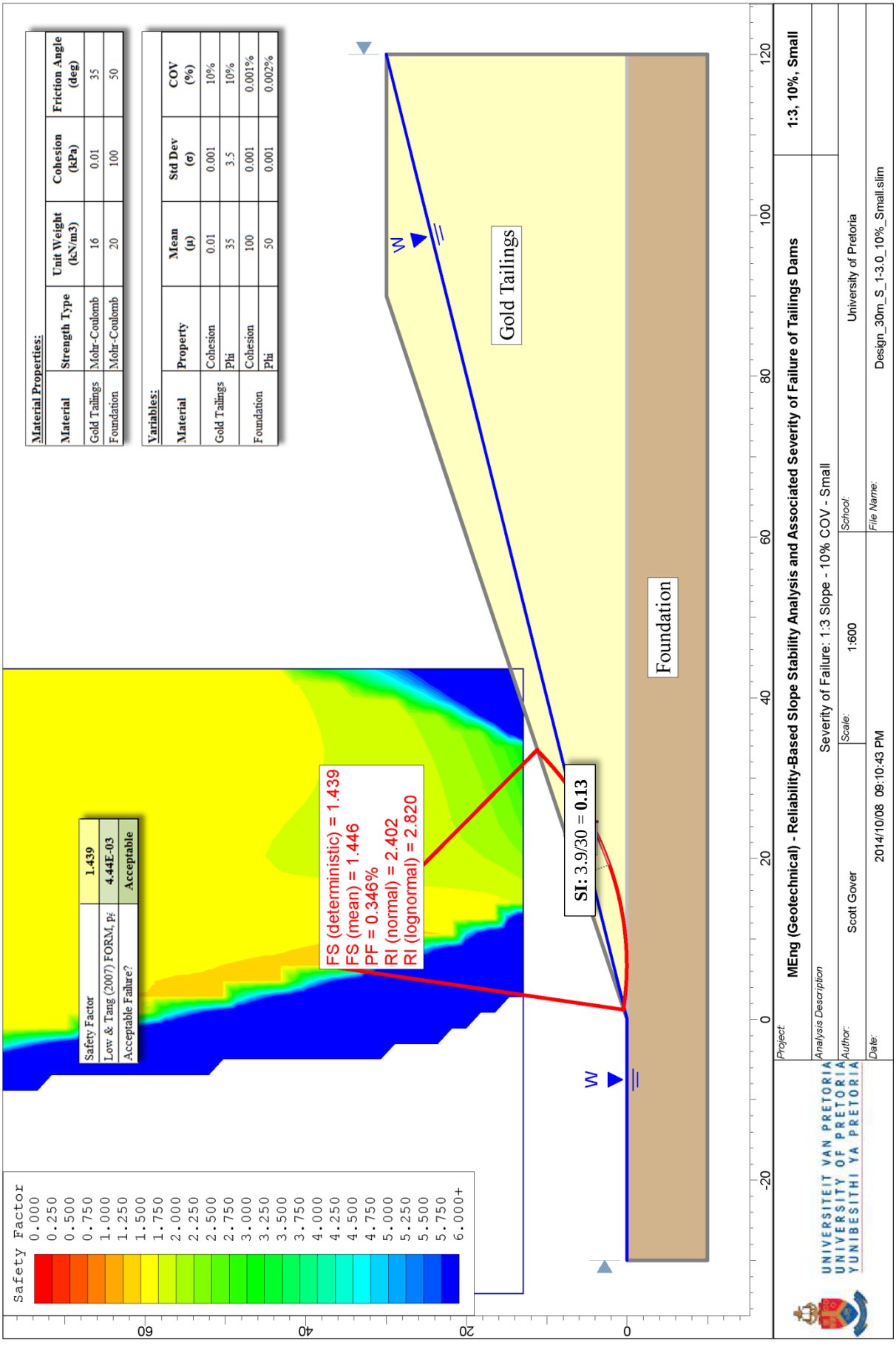
© University of Pretoria



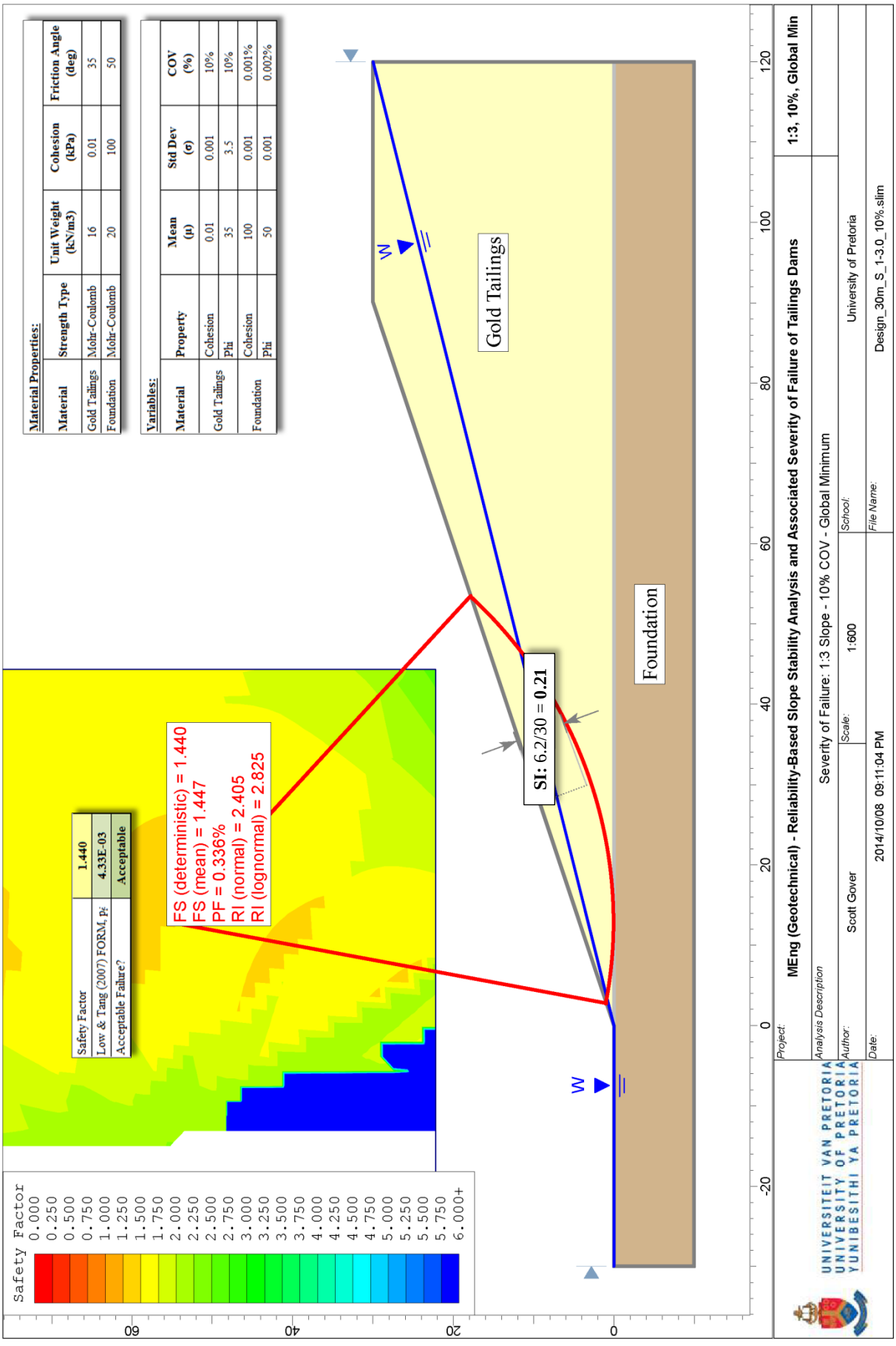
© University of Pretoria



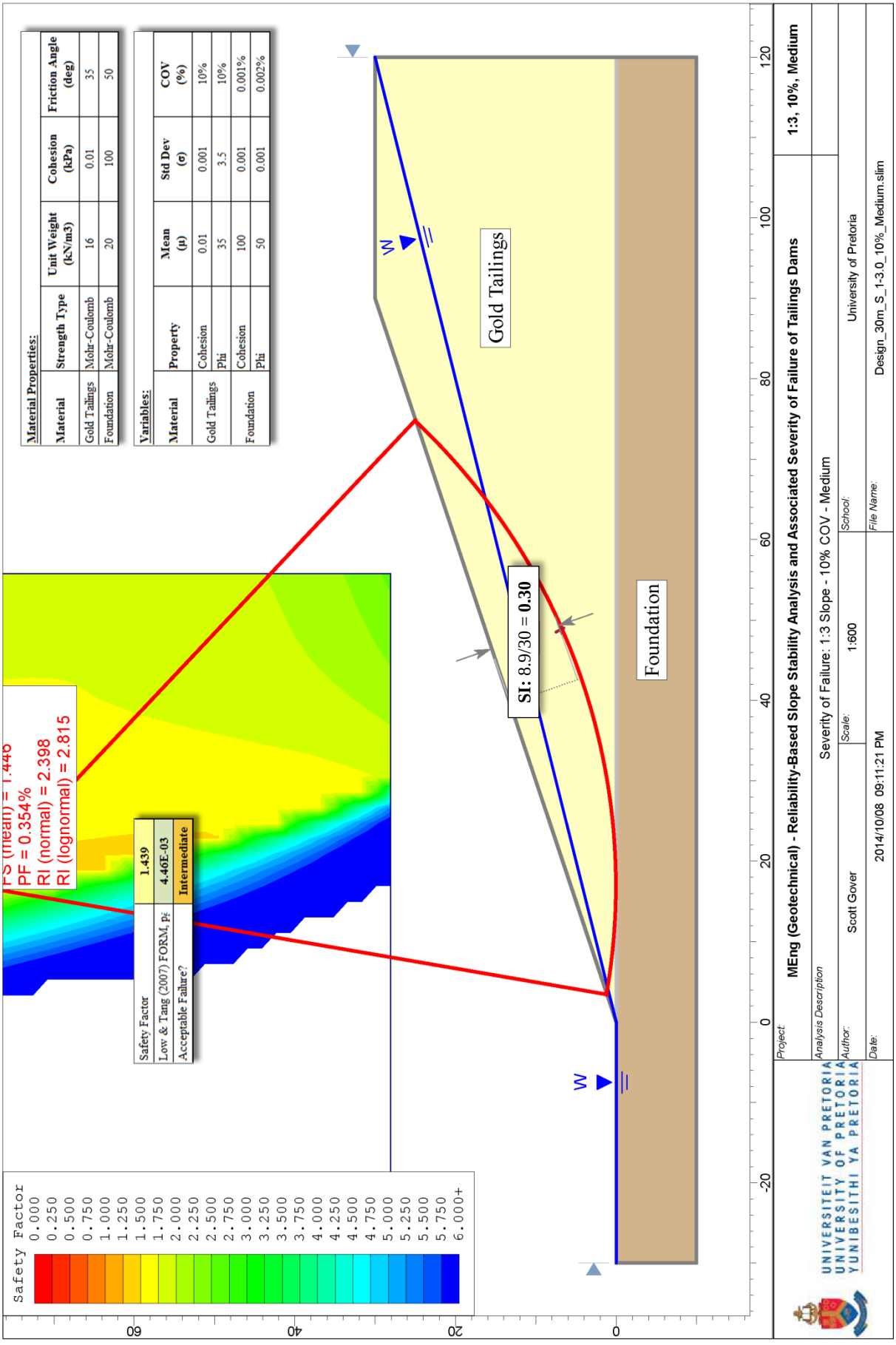
© University of Pretoria



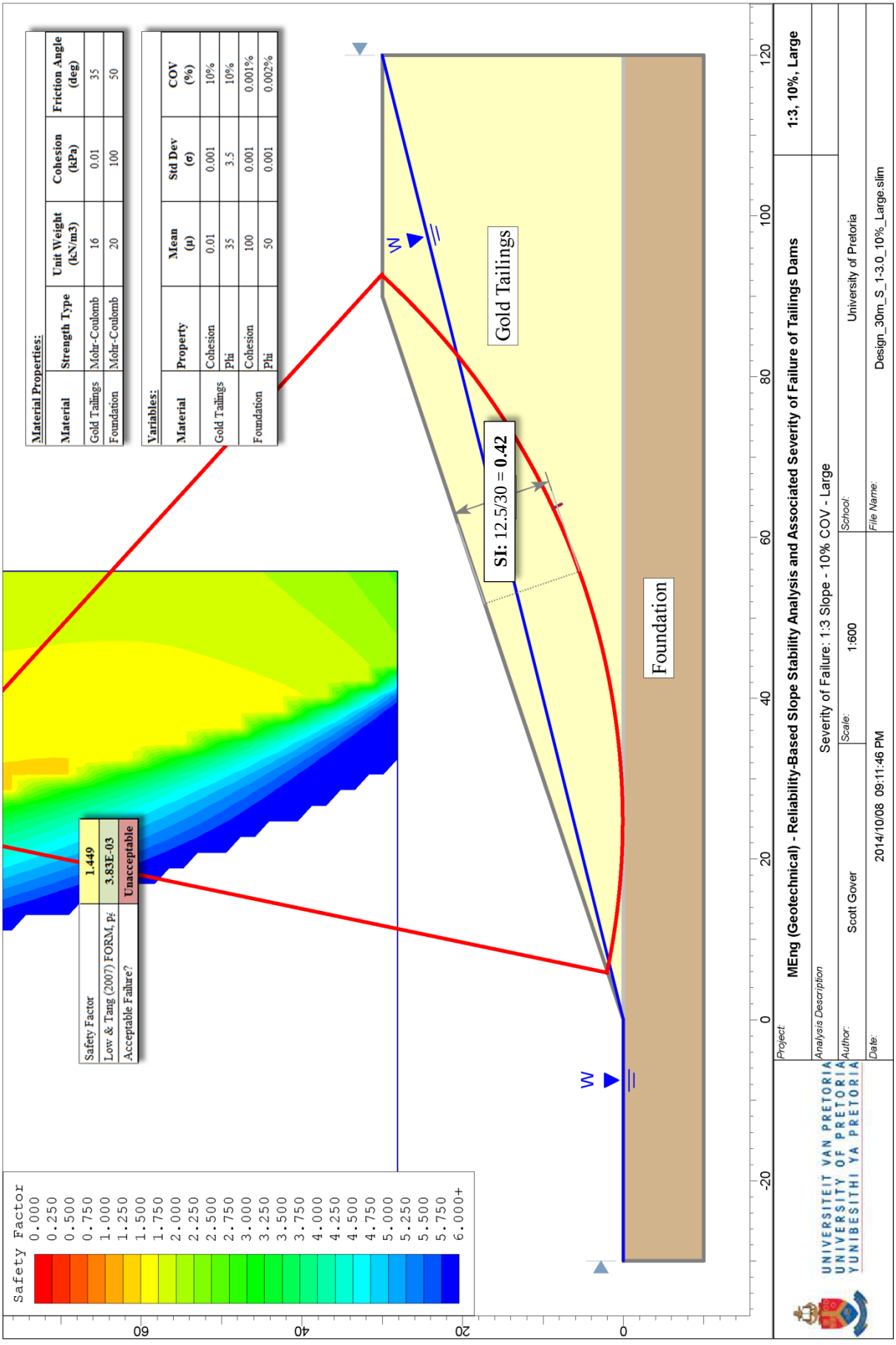
© University of Pretoria



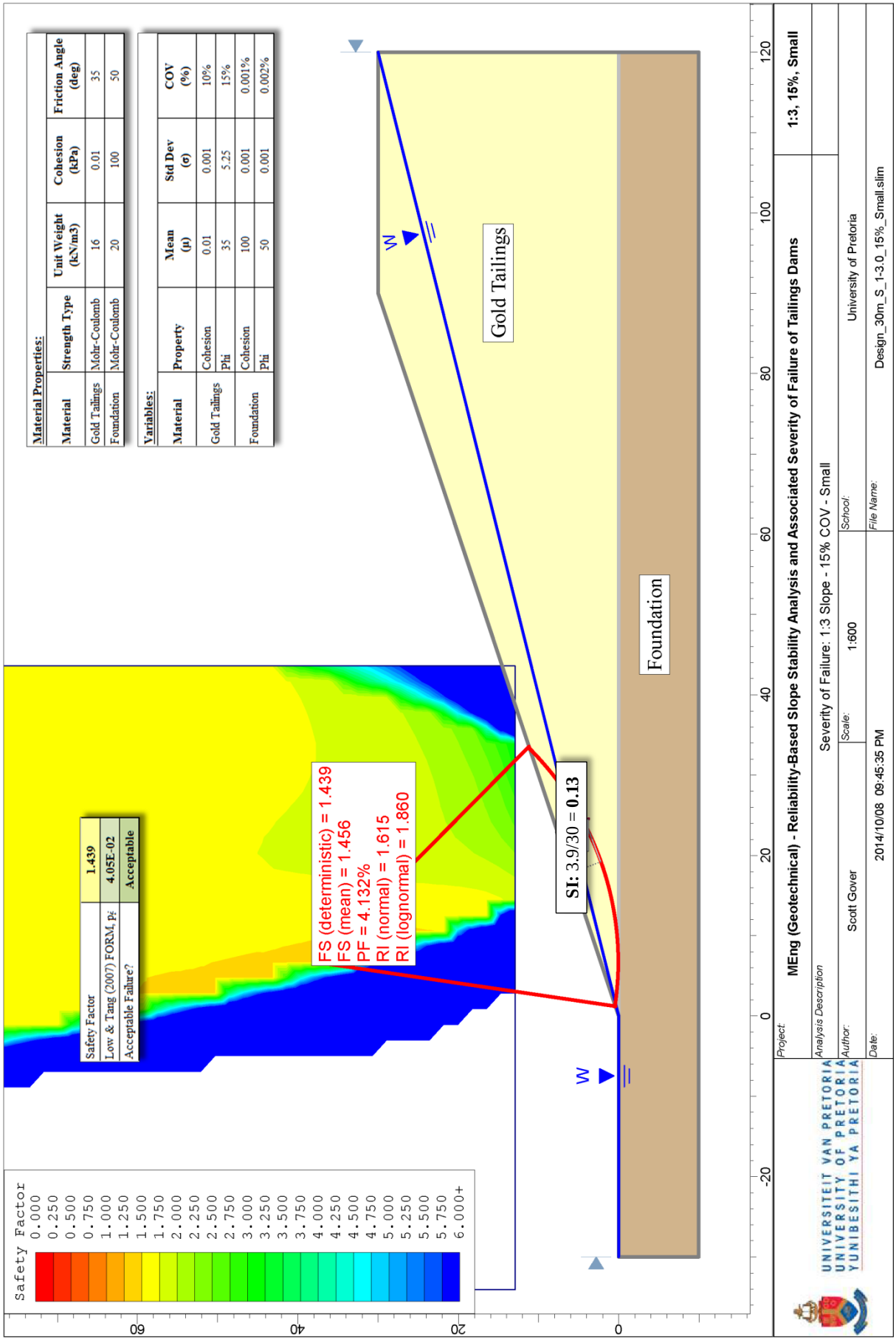
© University of Pretoria



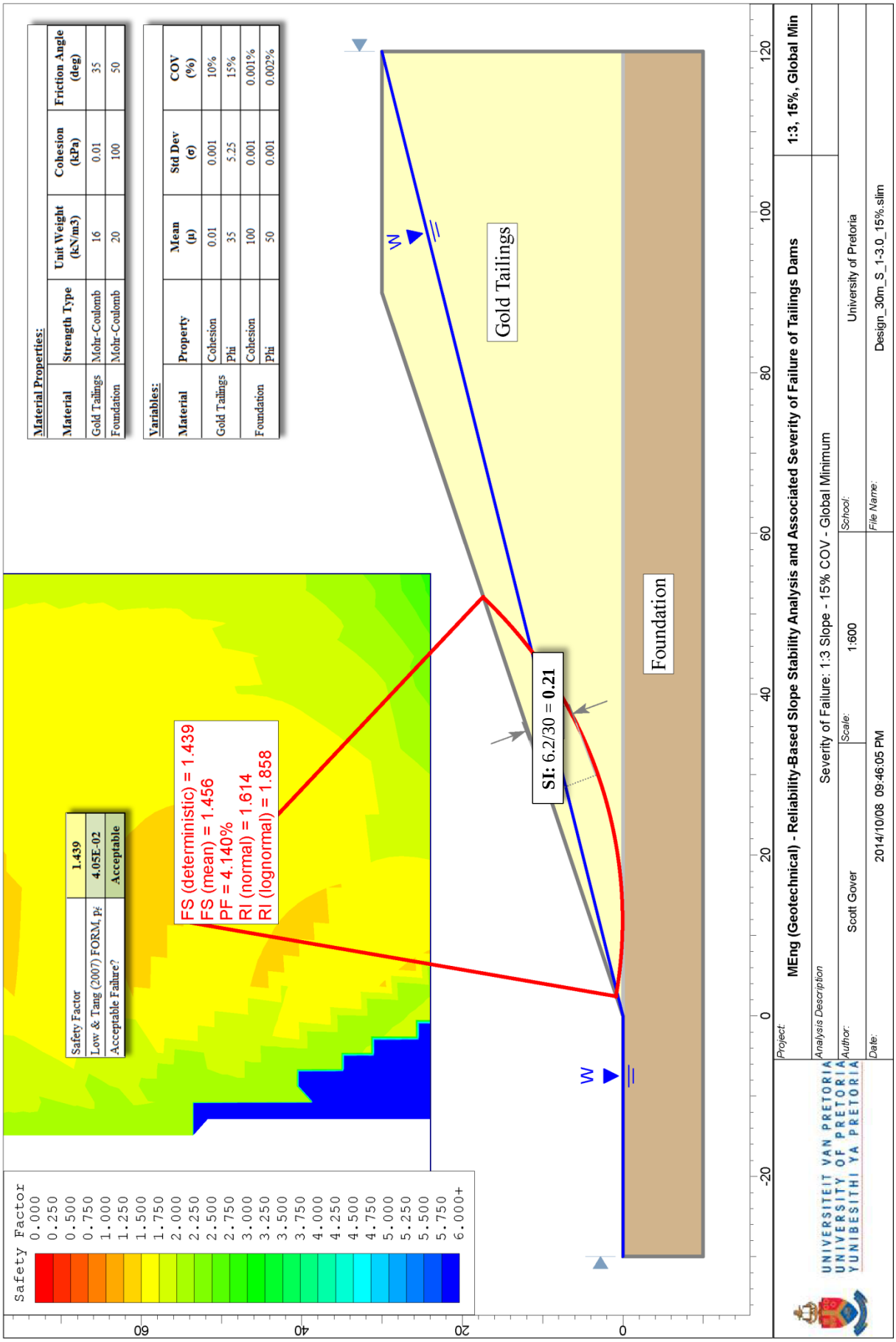
© University of Pretoria



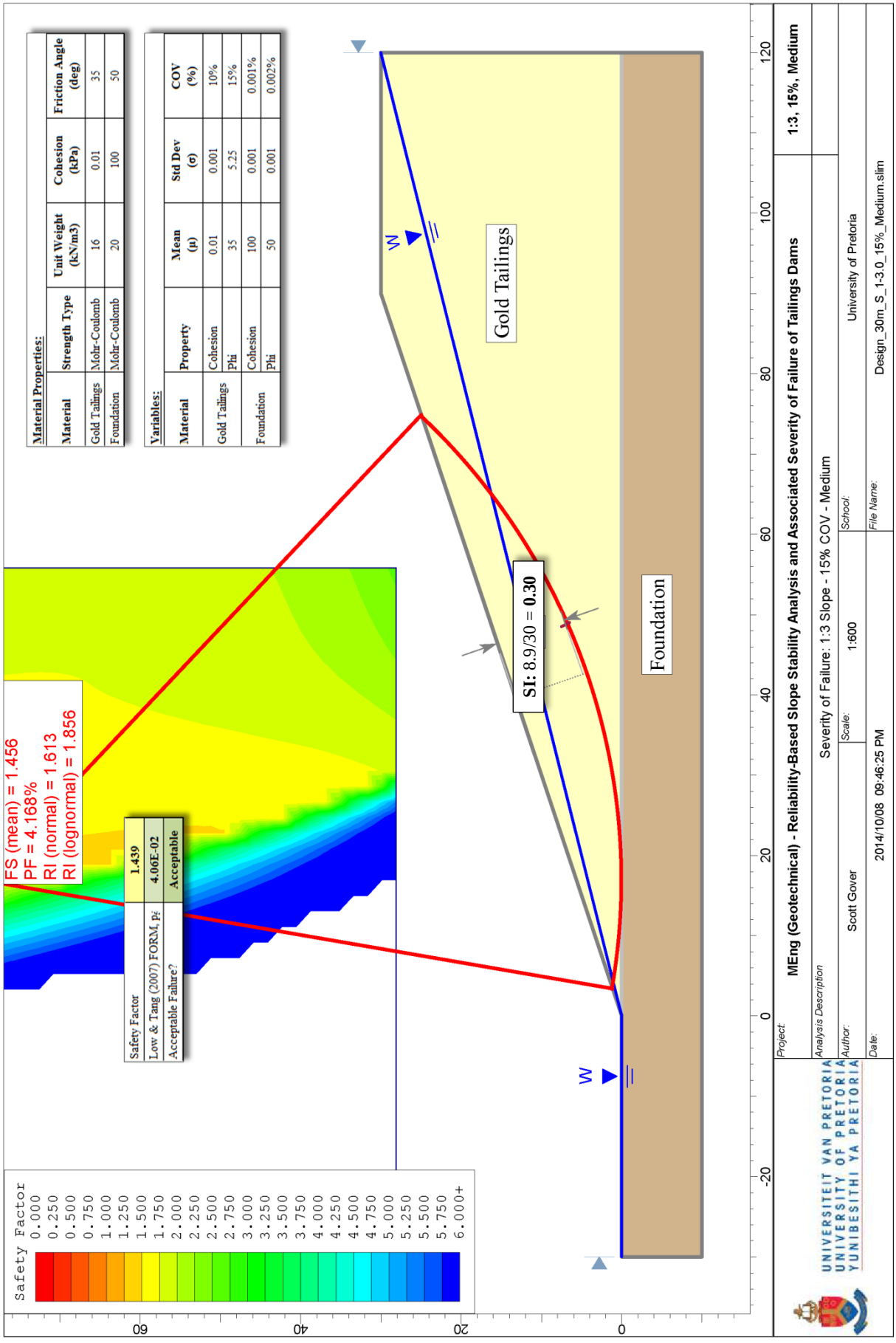
© University of Pretoria



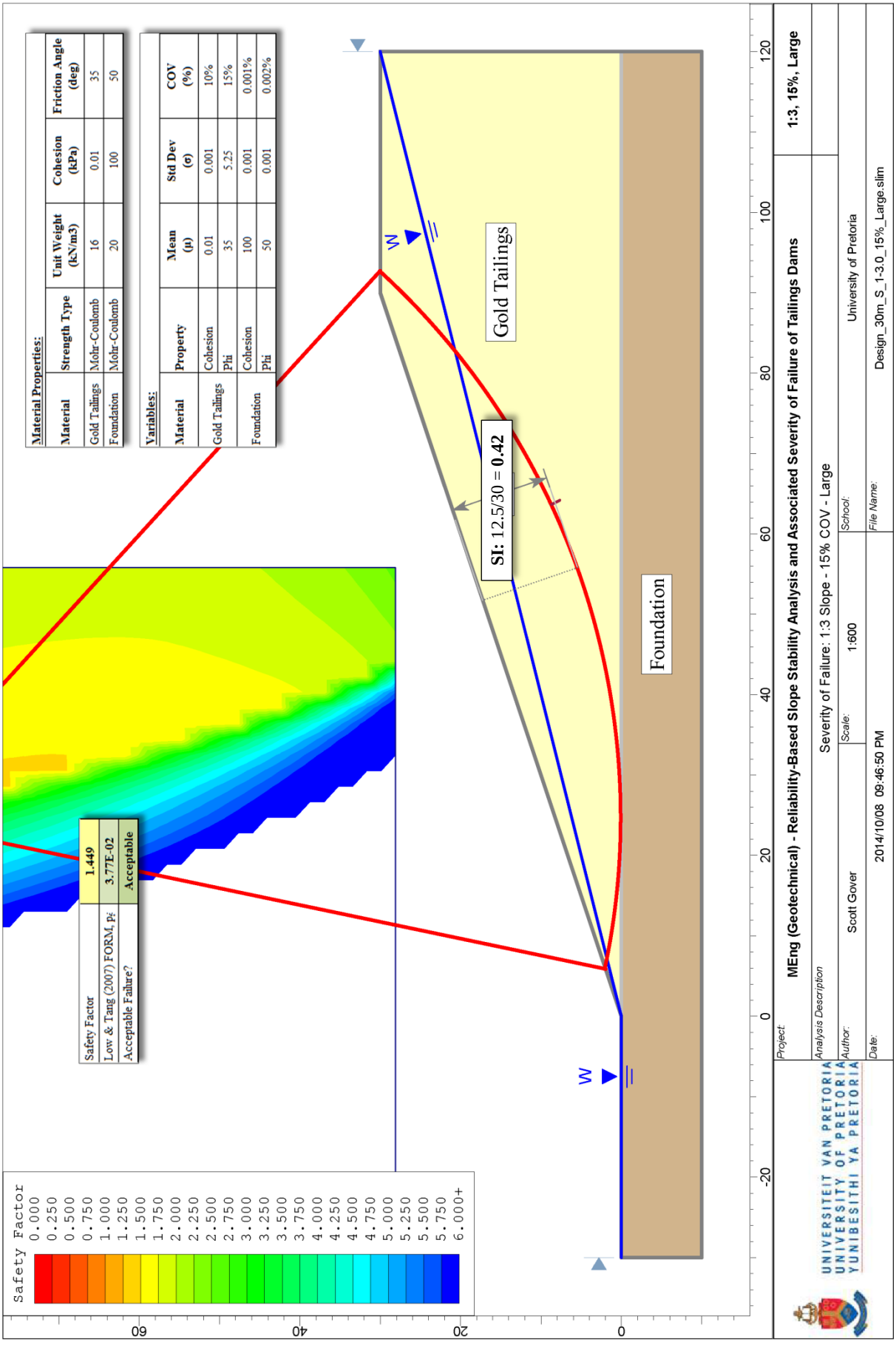
© University of Pretoria



© University of Pretoria



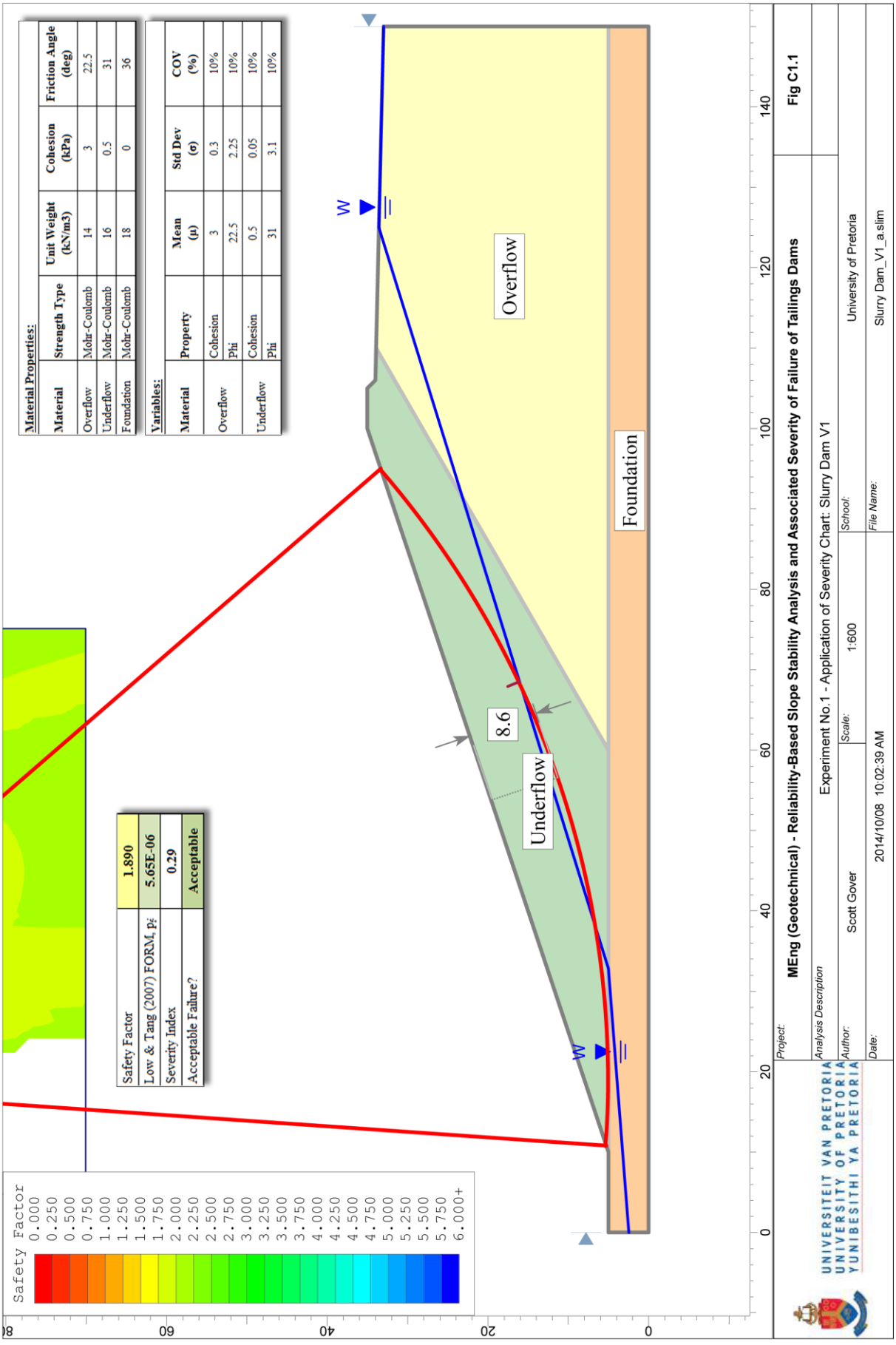
© University of Pretoria



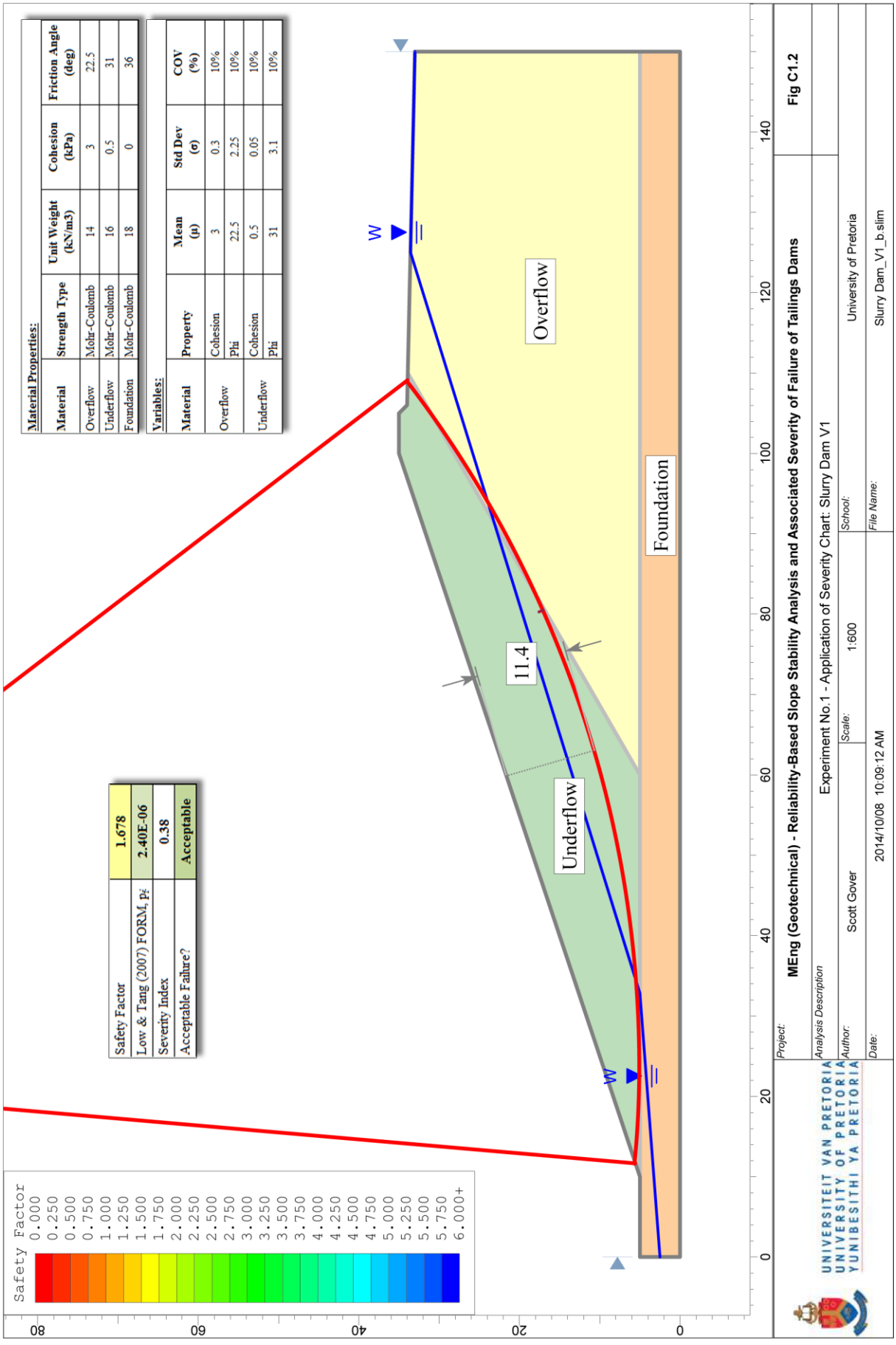
© University of Pretoria

APPENDIX C

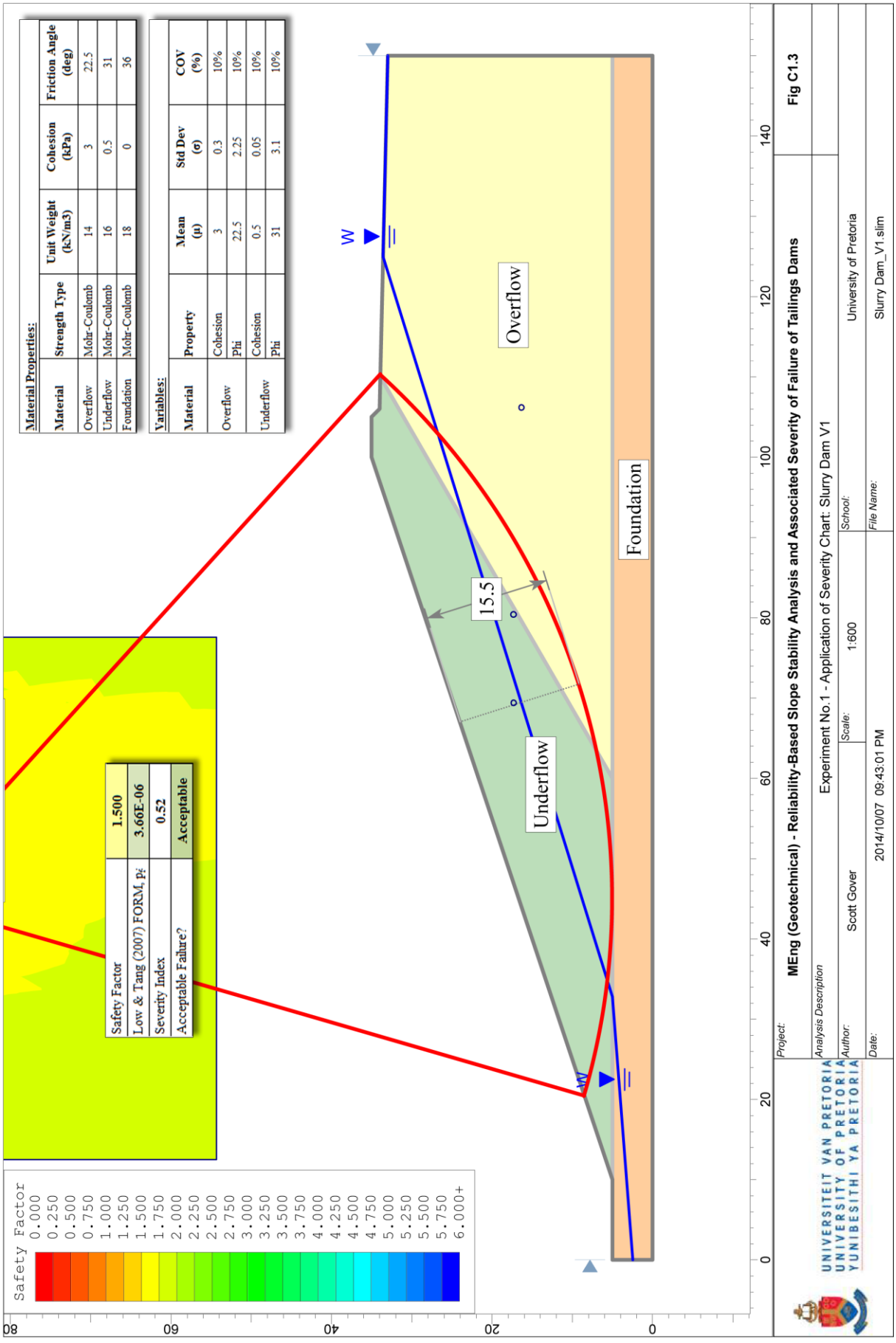
© University of Pretoria



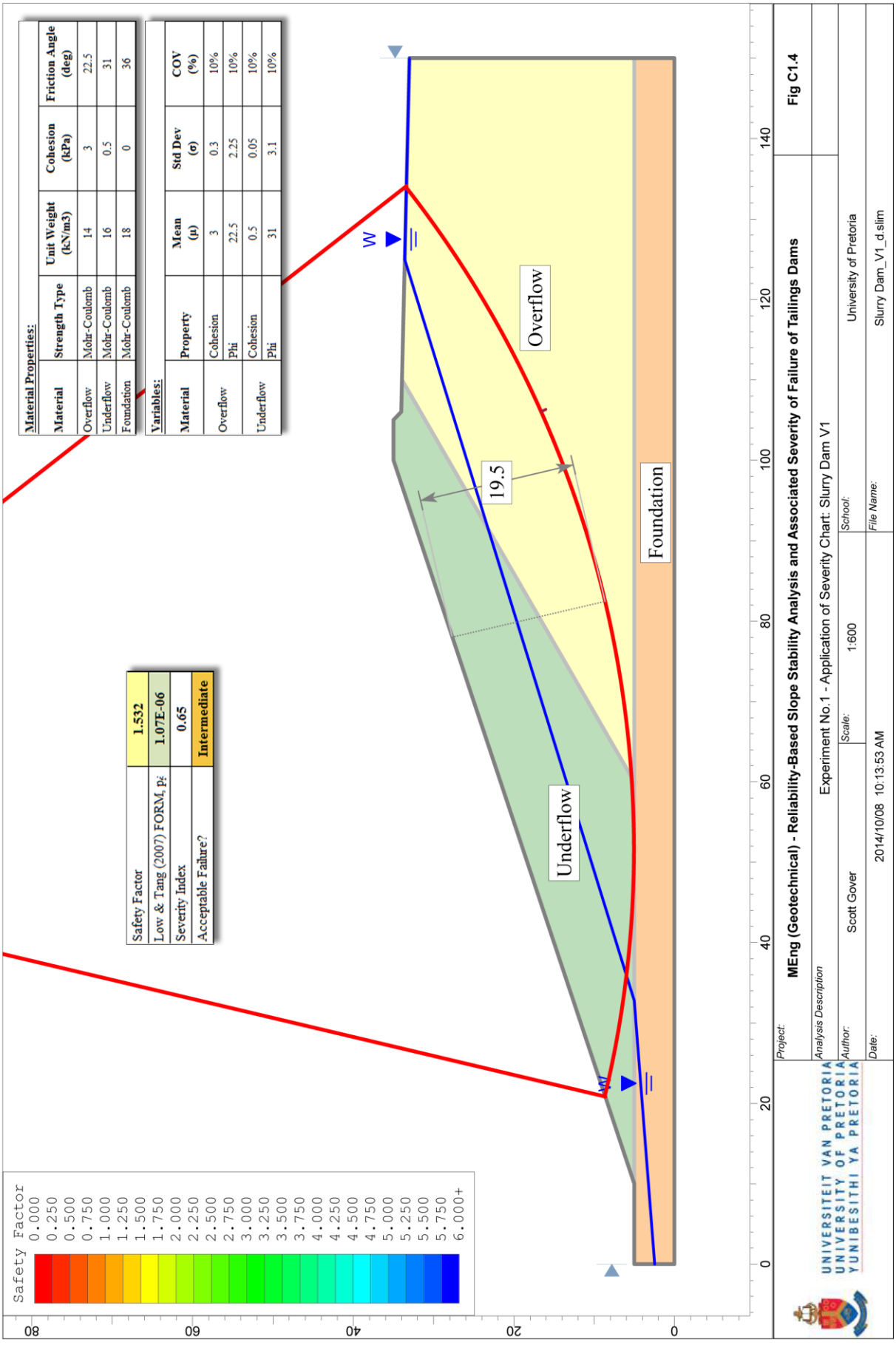
© University of Pretoria



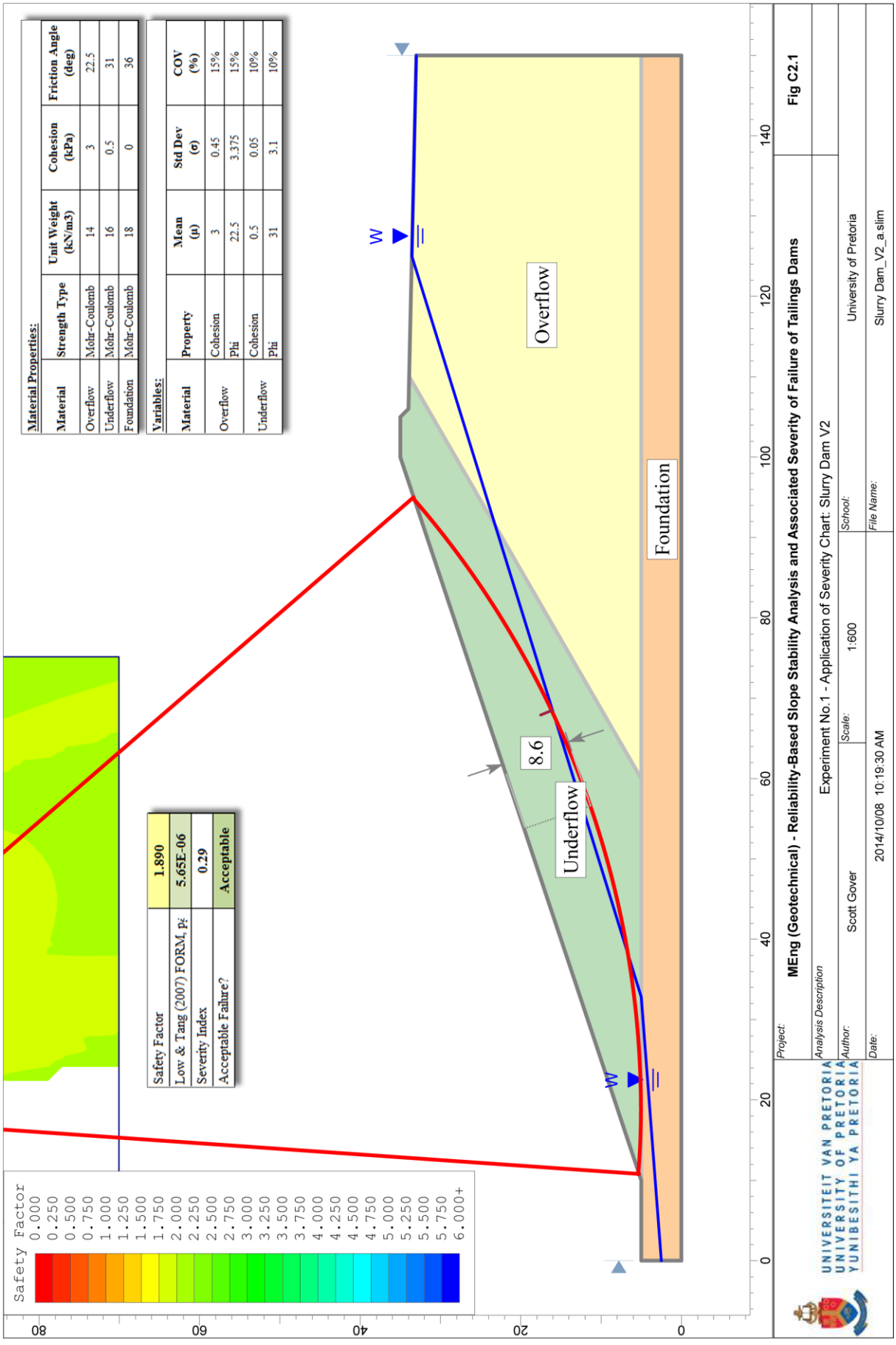
© University of Pretoria



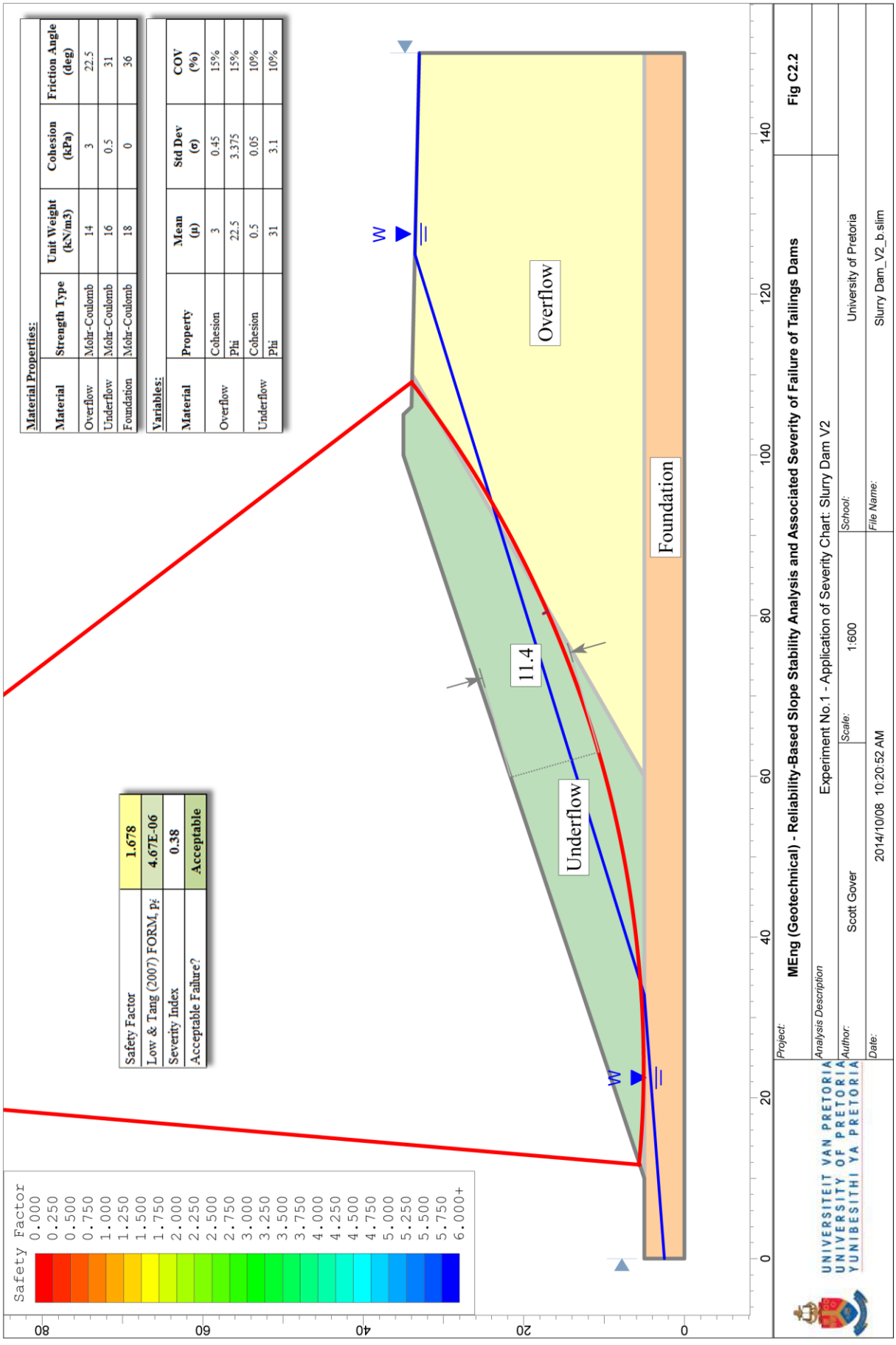
© University of Pretoria



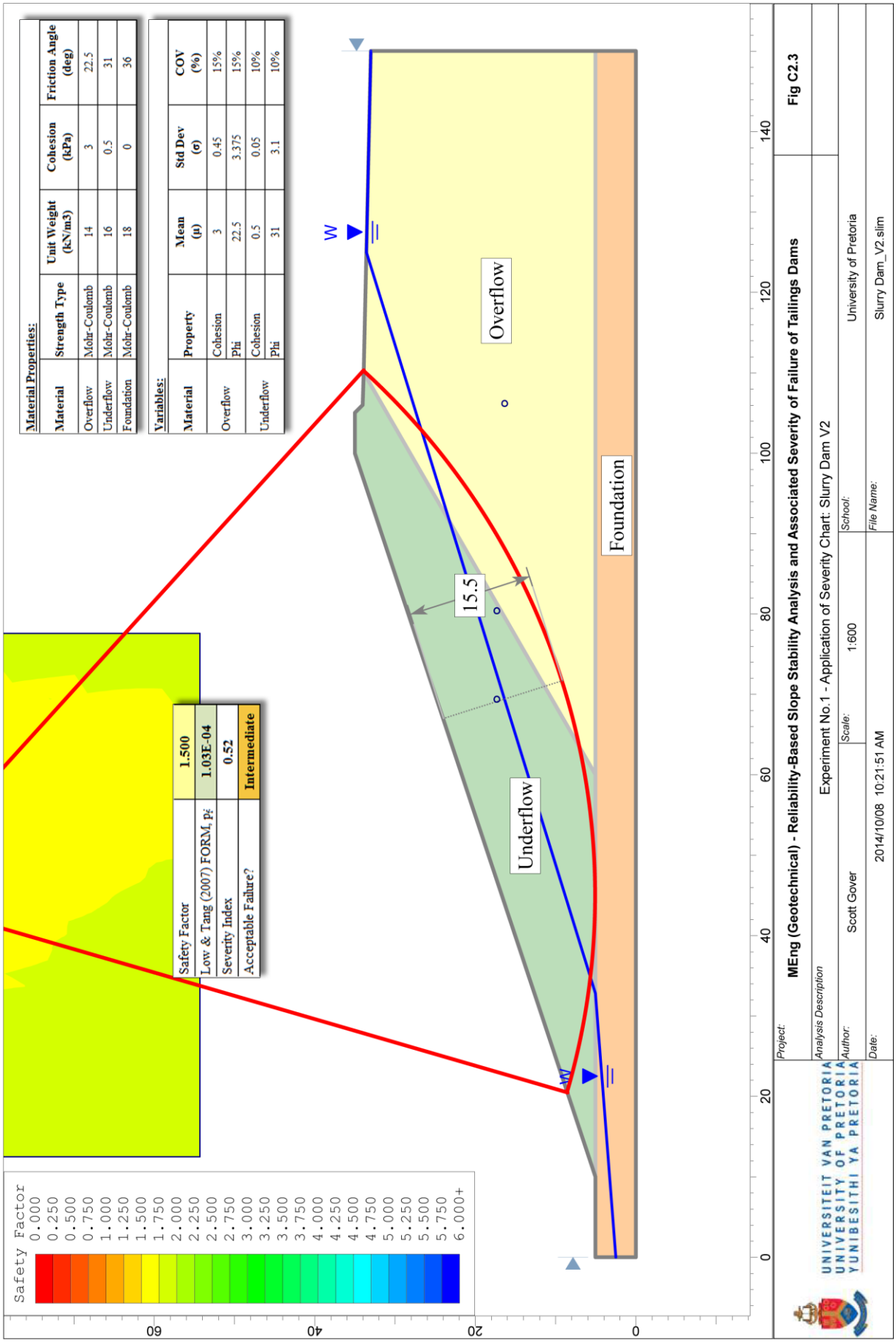
© University of Pretoria



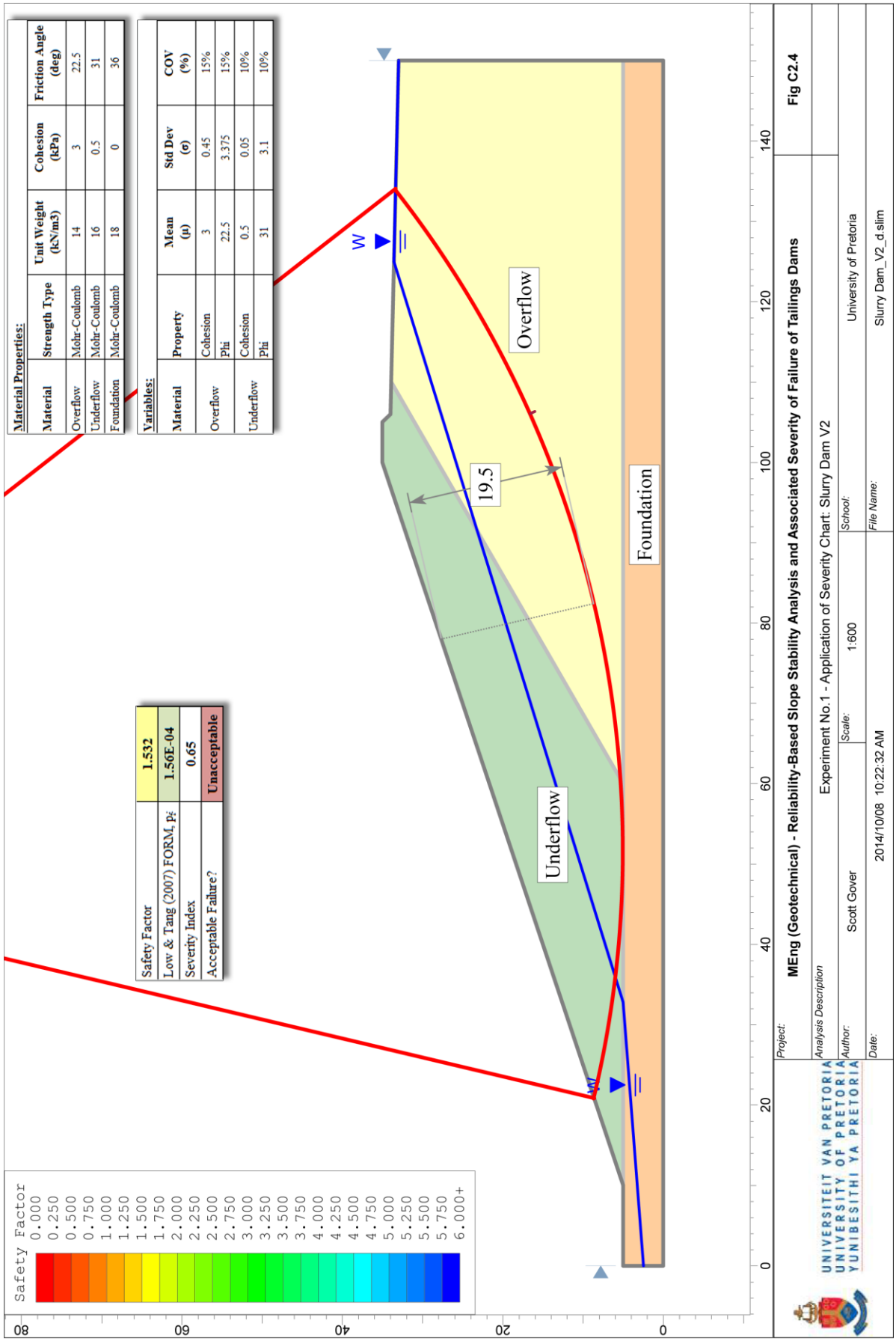
© University of Pretoria



© University of Pretoria



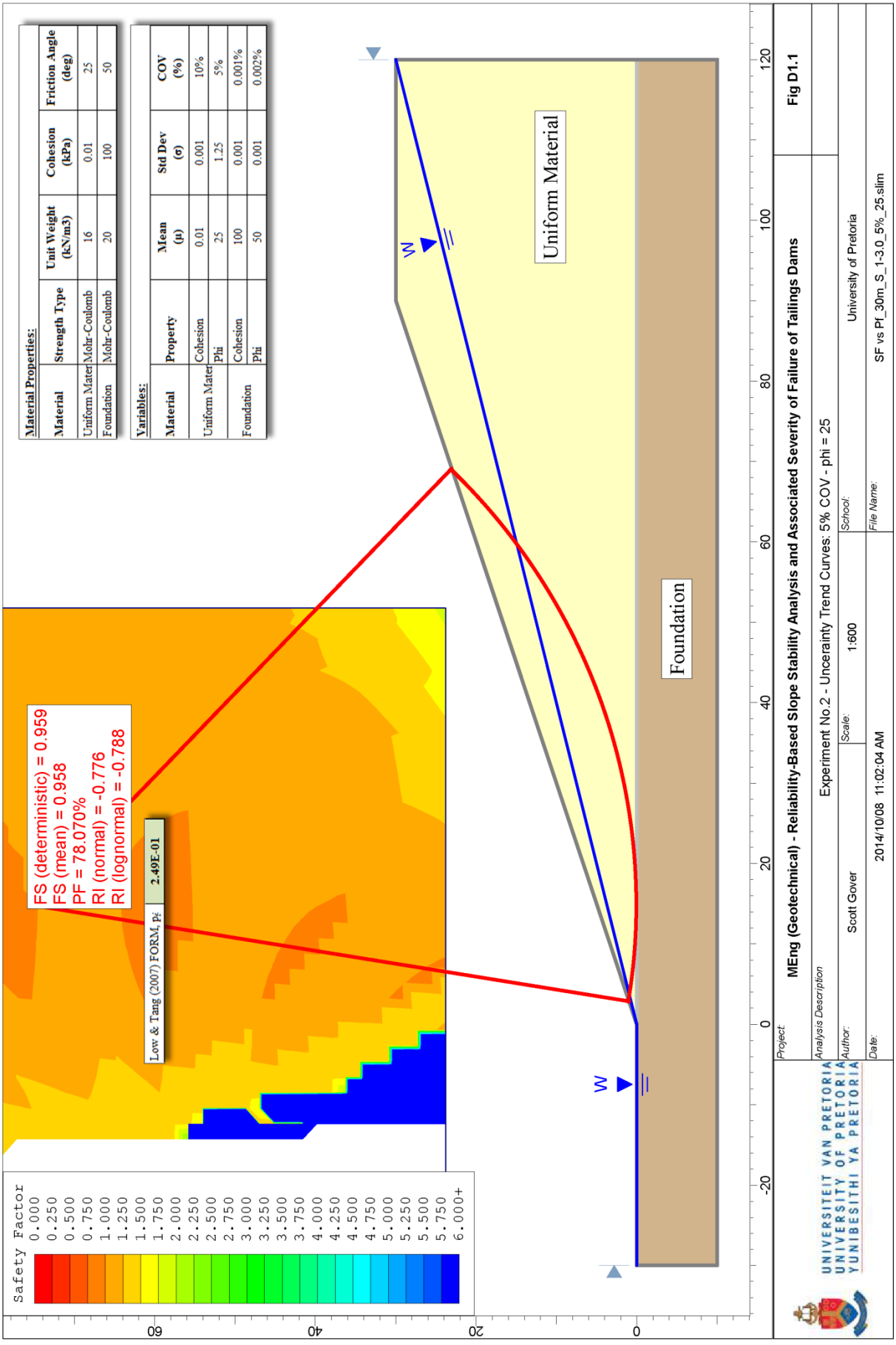
© University of Pretoria



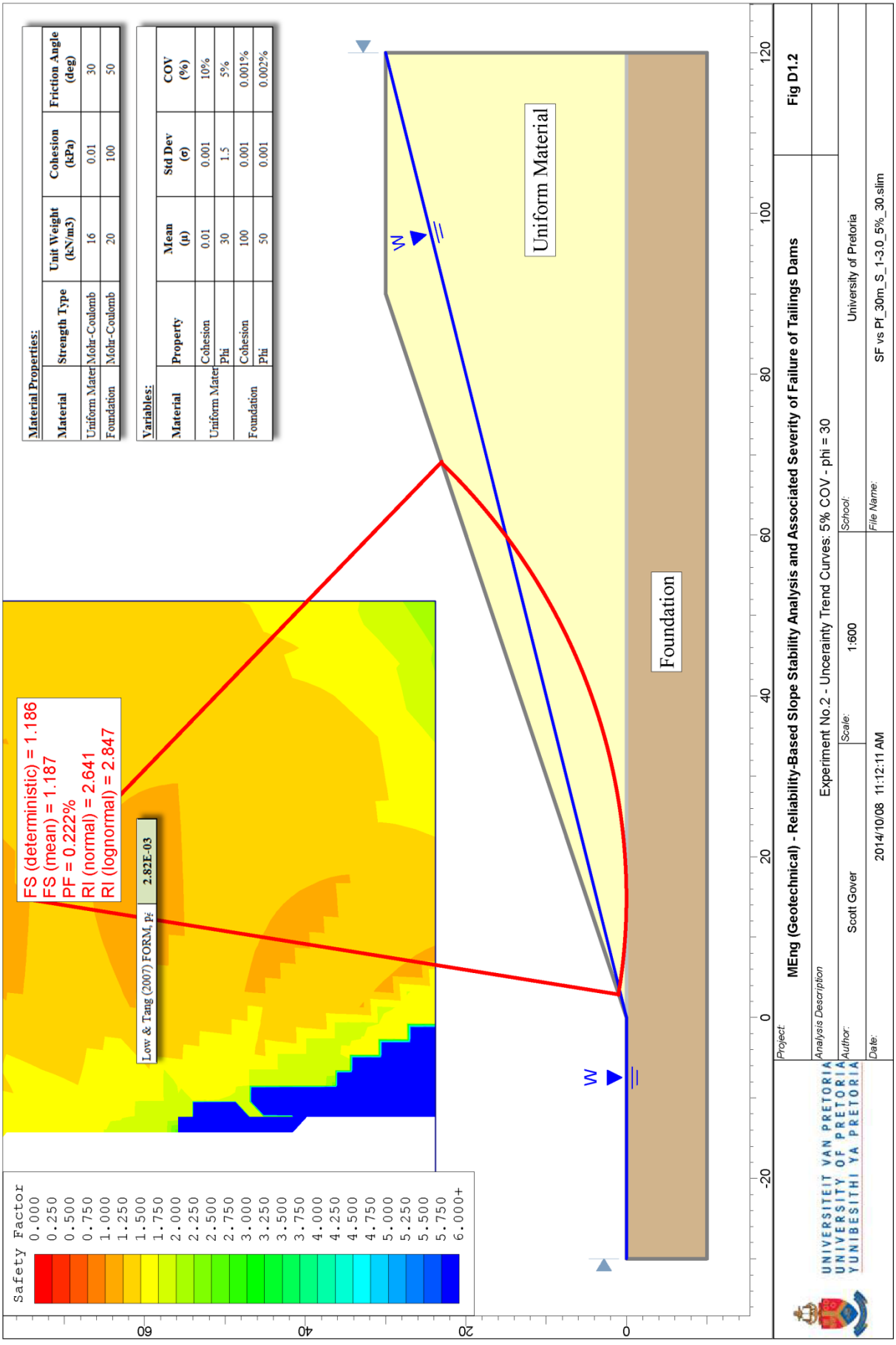
© University of Pretoria

APPENDIX D

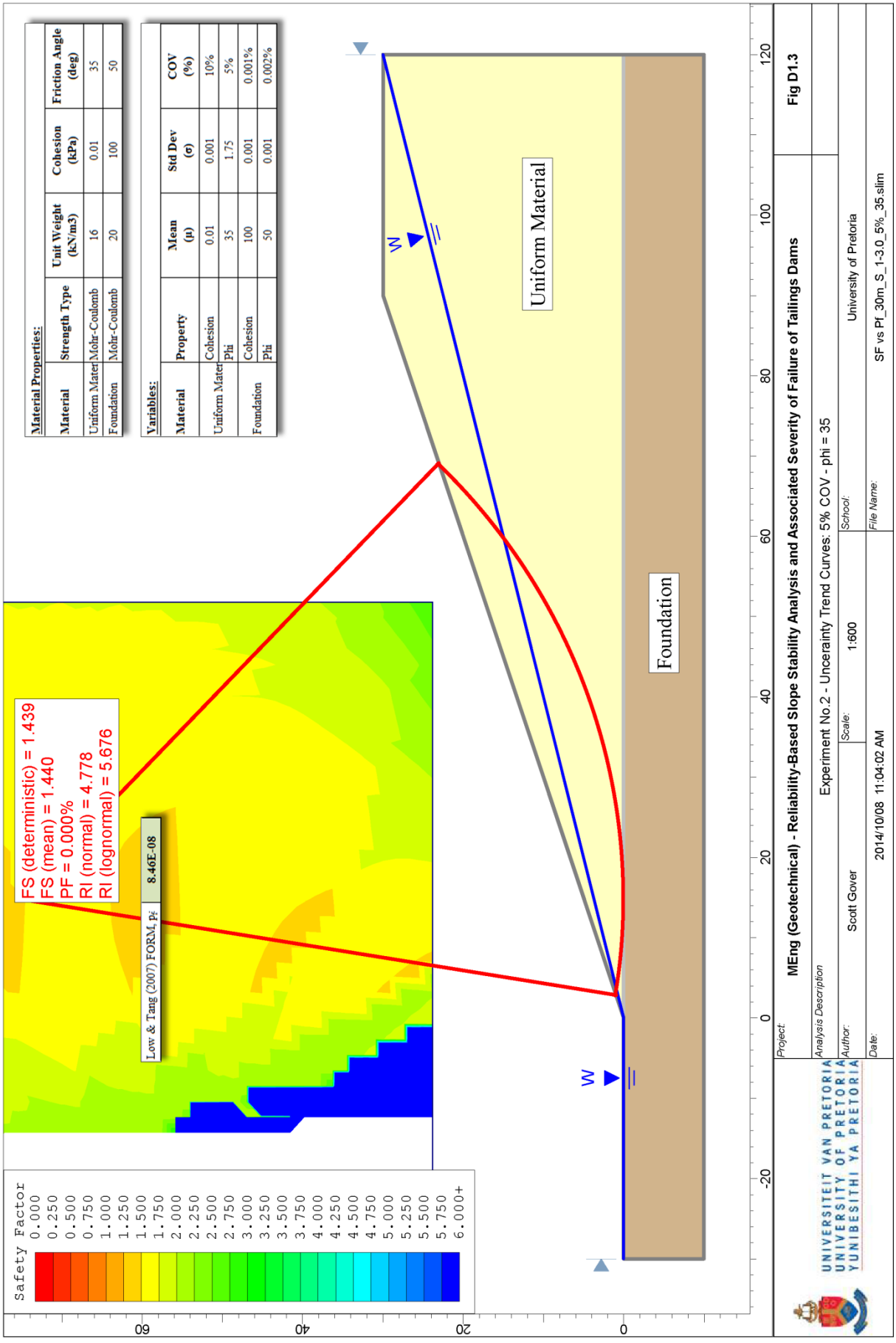
© University of Pretoria



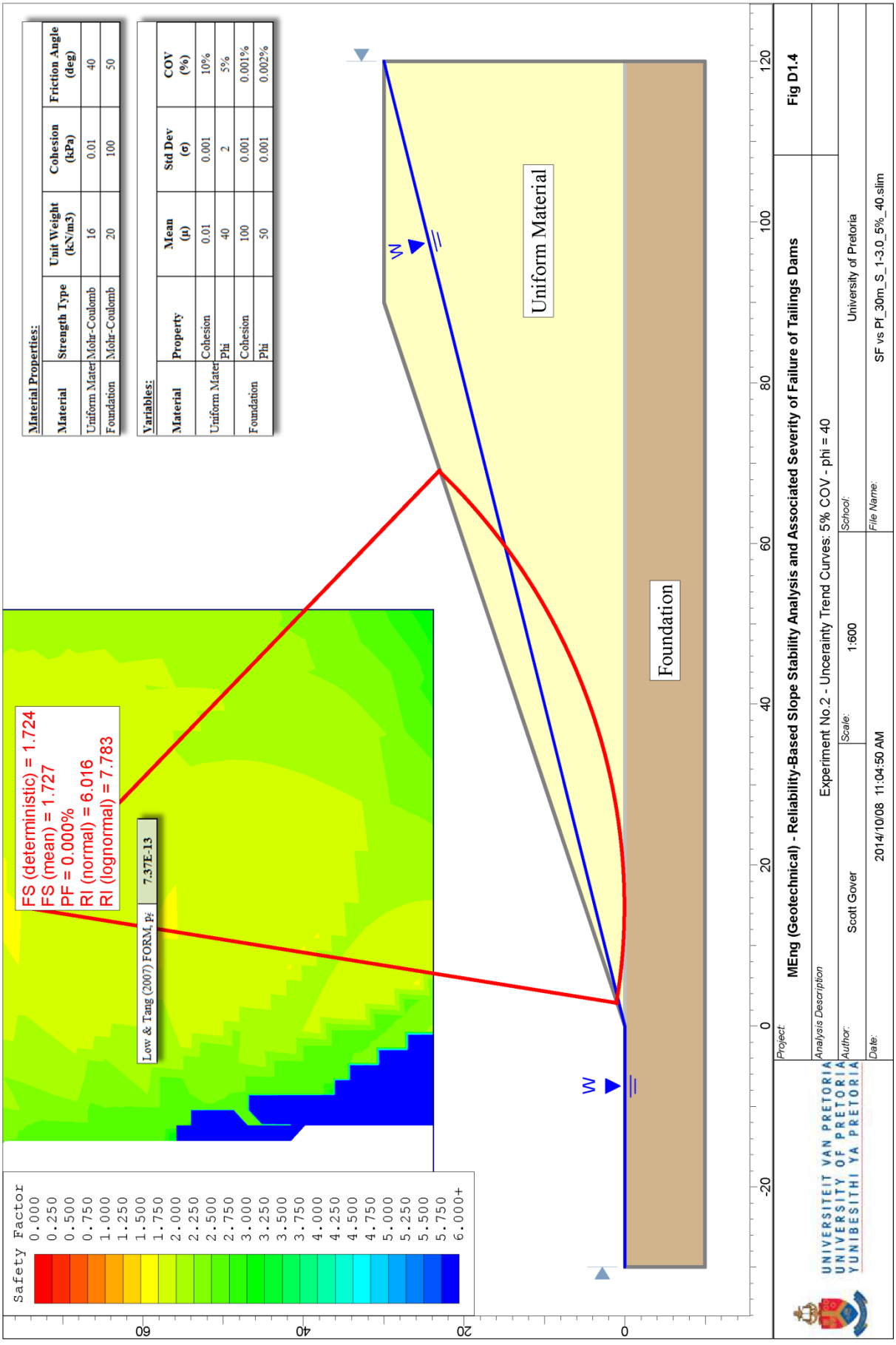
© University of Pretoria



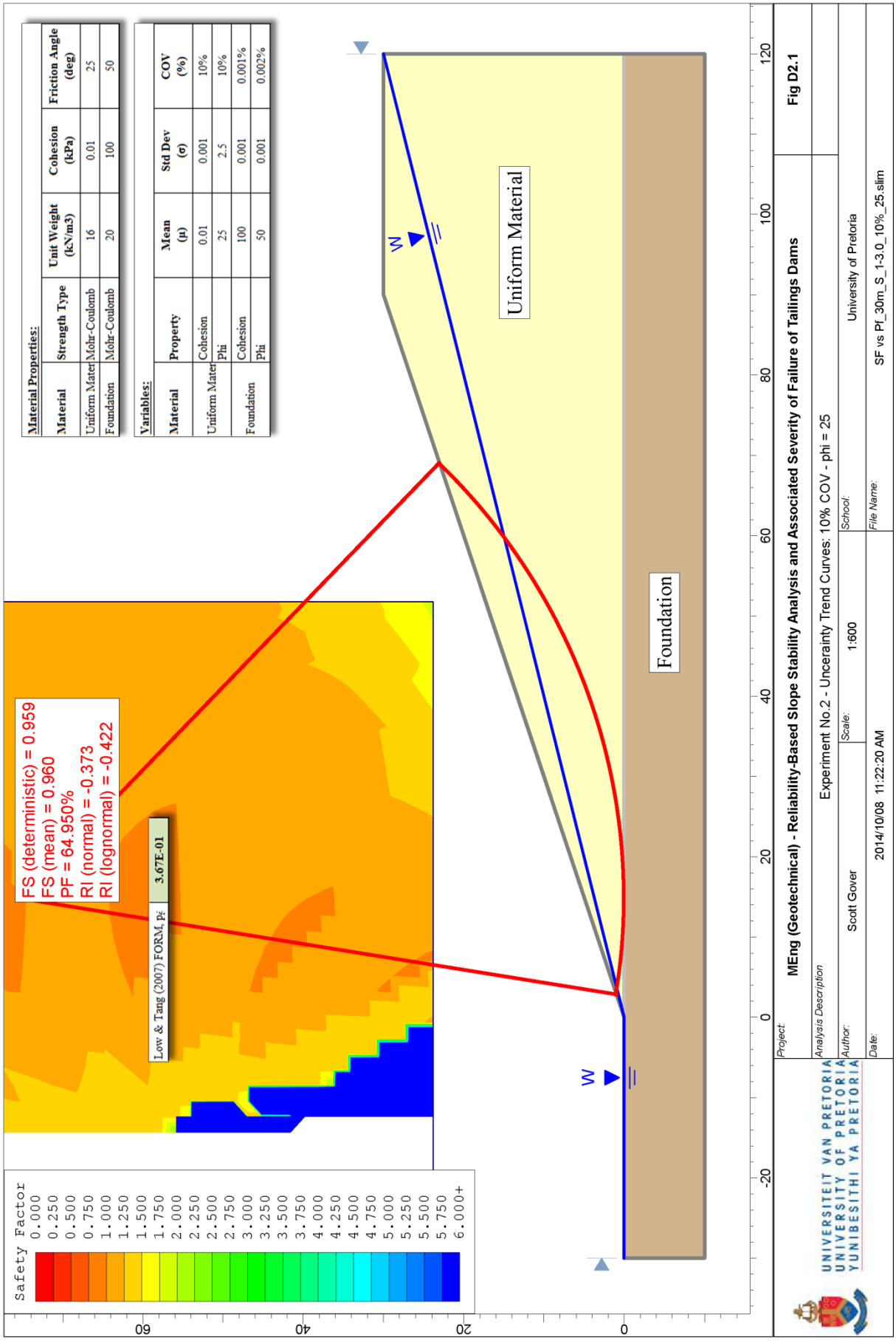
© University of Pretoria



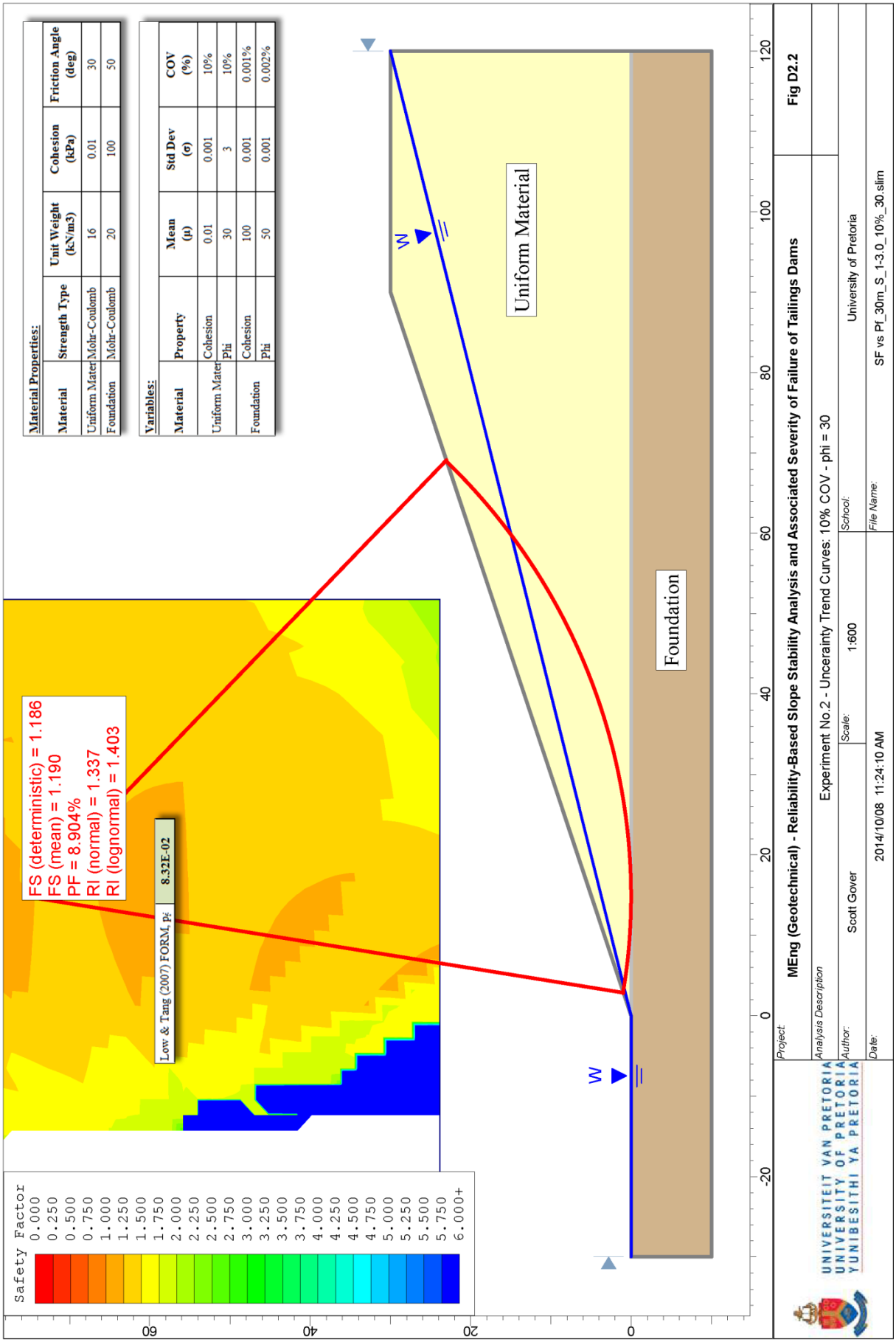
© University of Pretoria



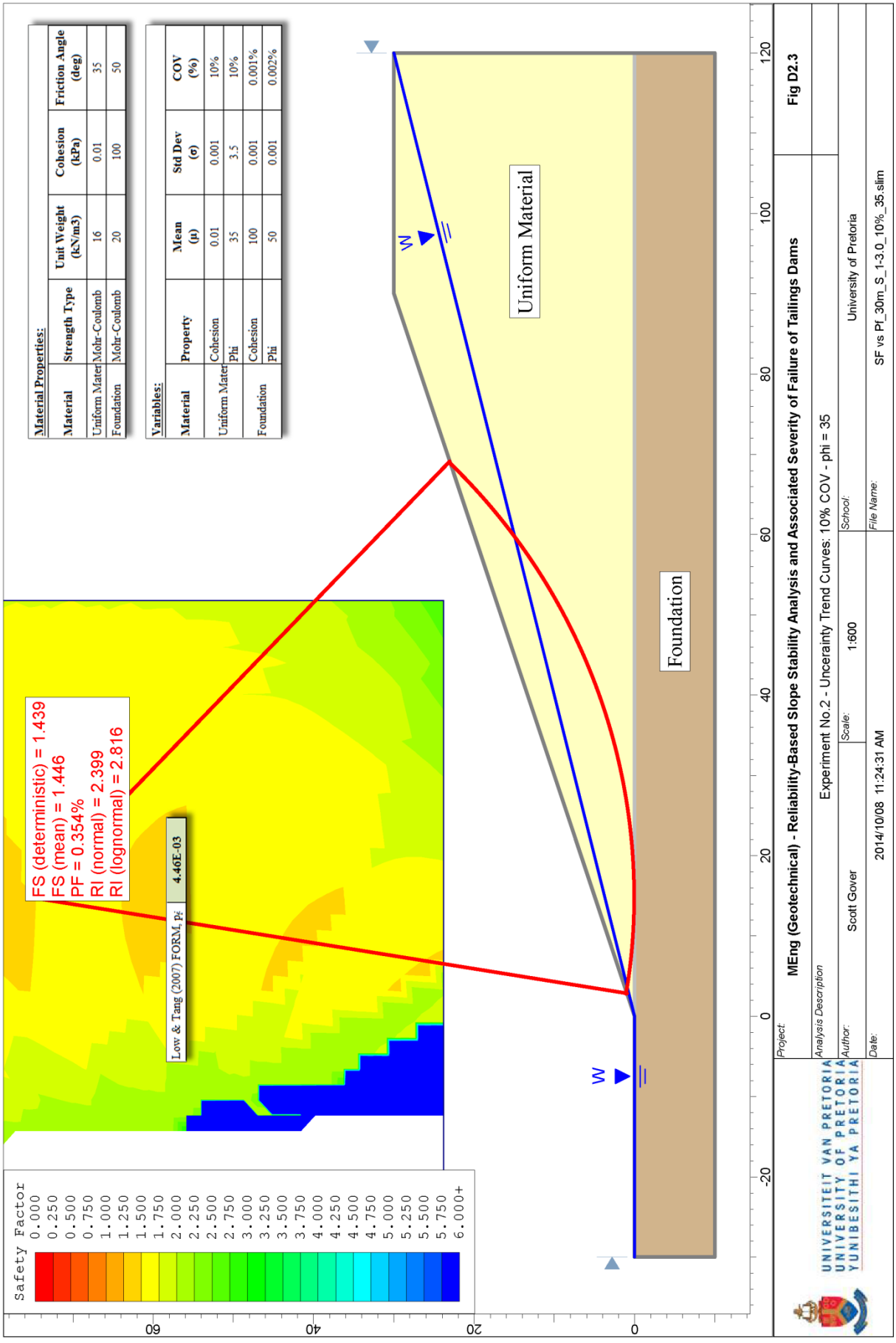
© University of Pretoria



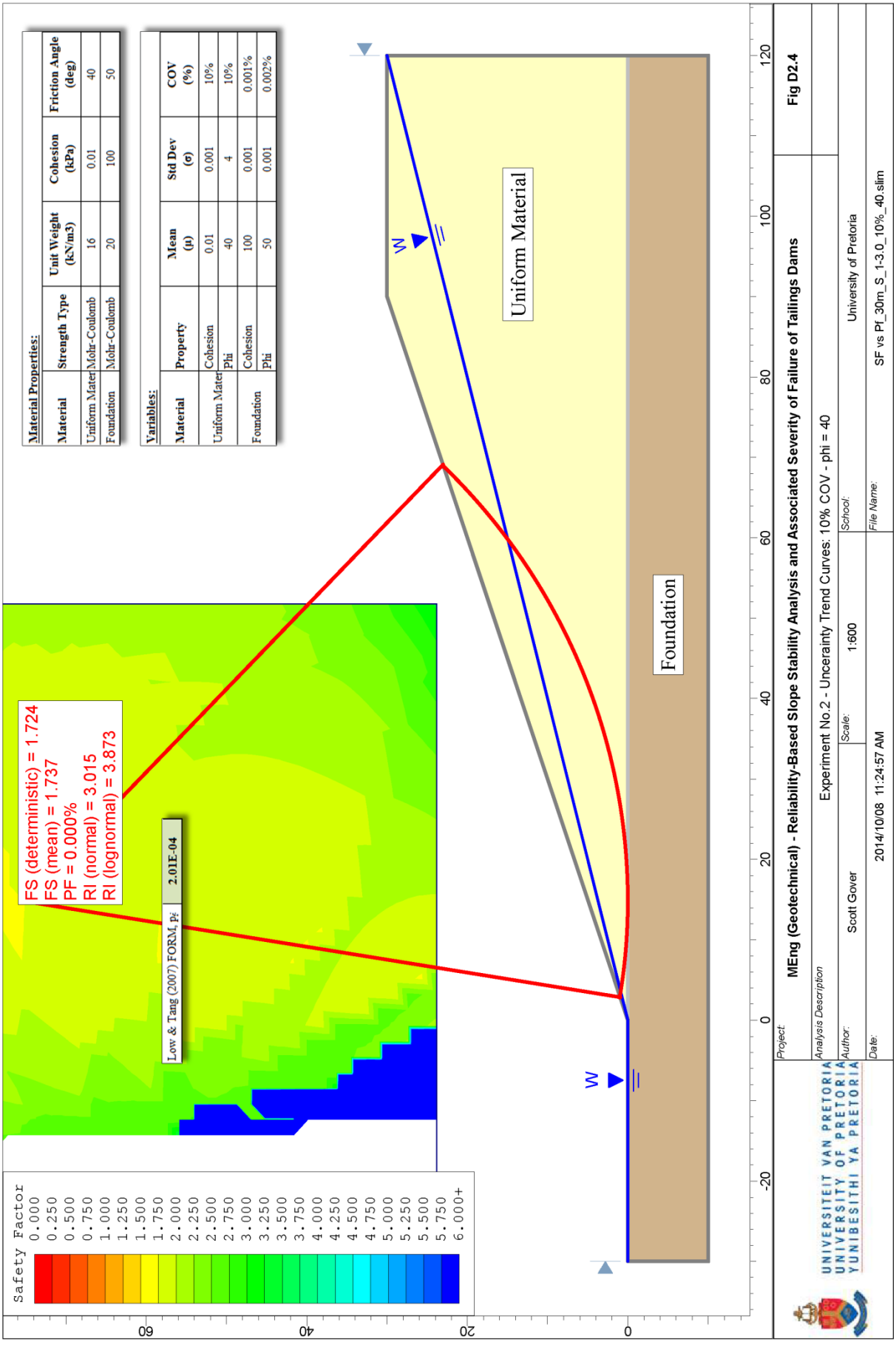
© University of Pretoria



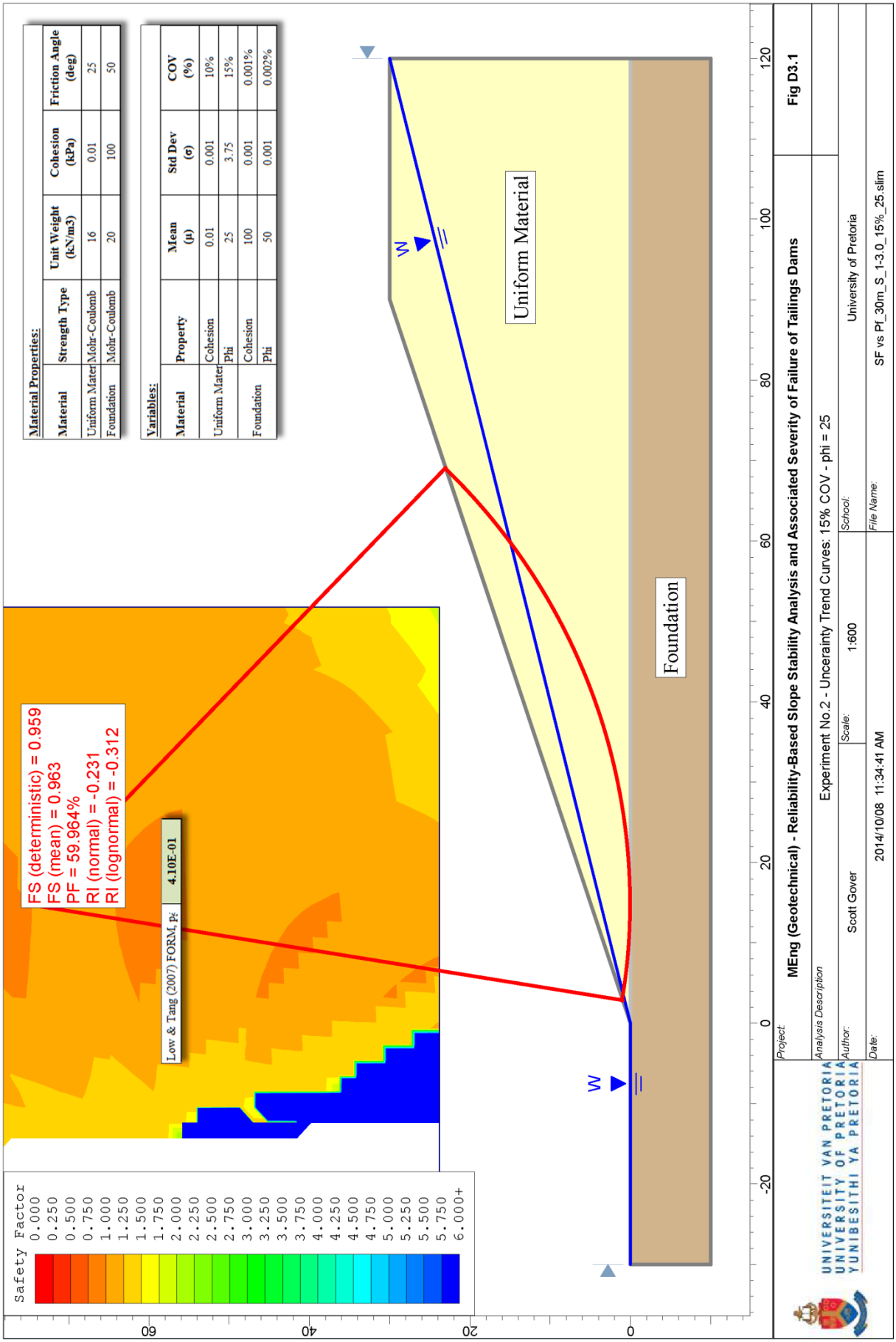
© University of Pretoria



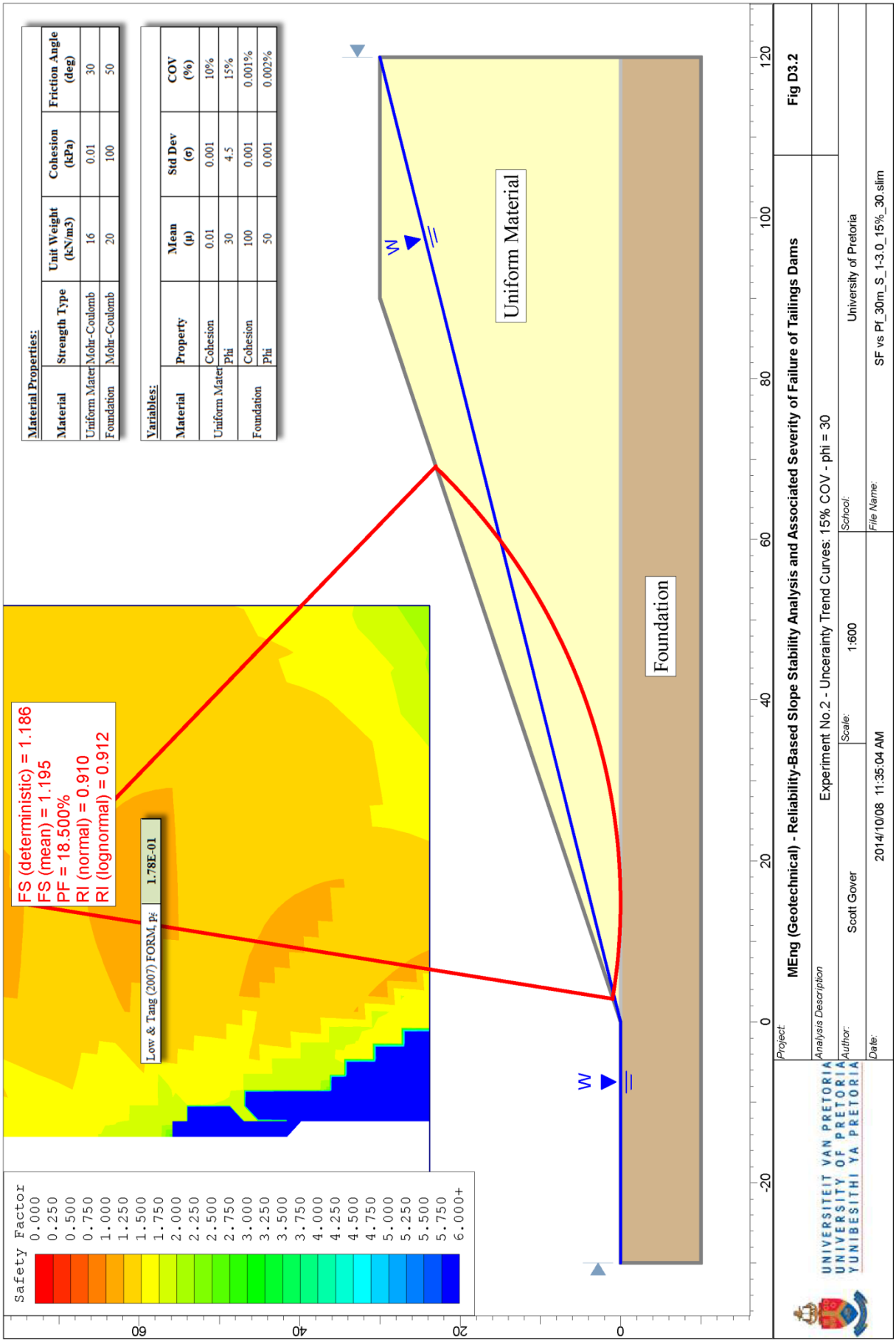
© University of Pretoria



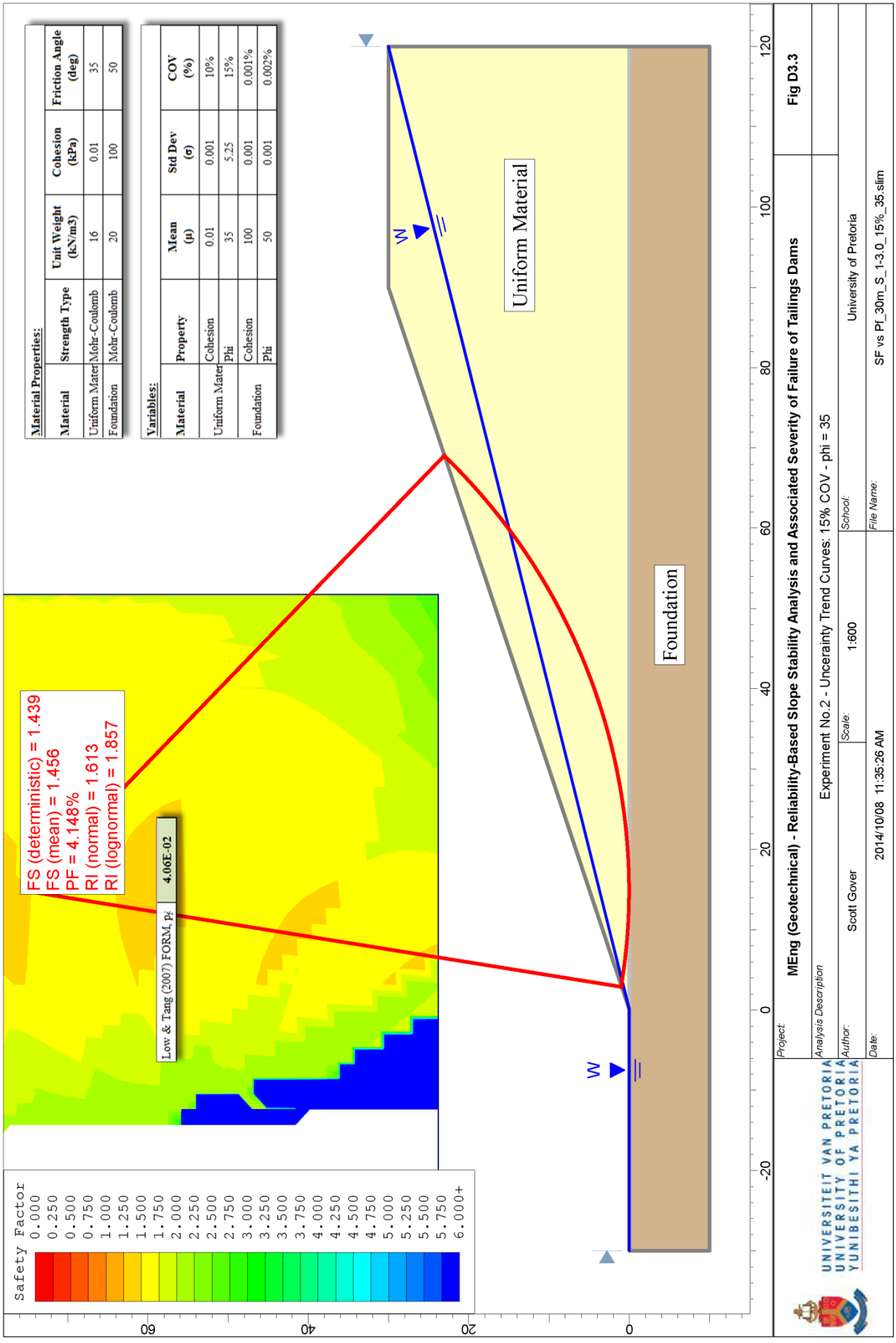
© University of Pretoria



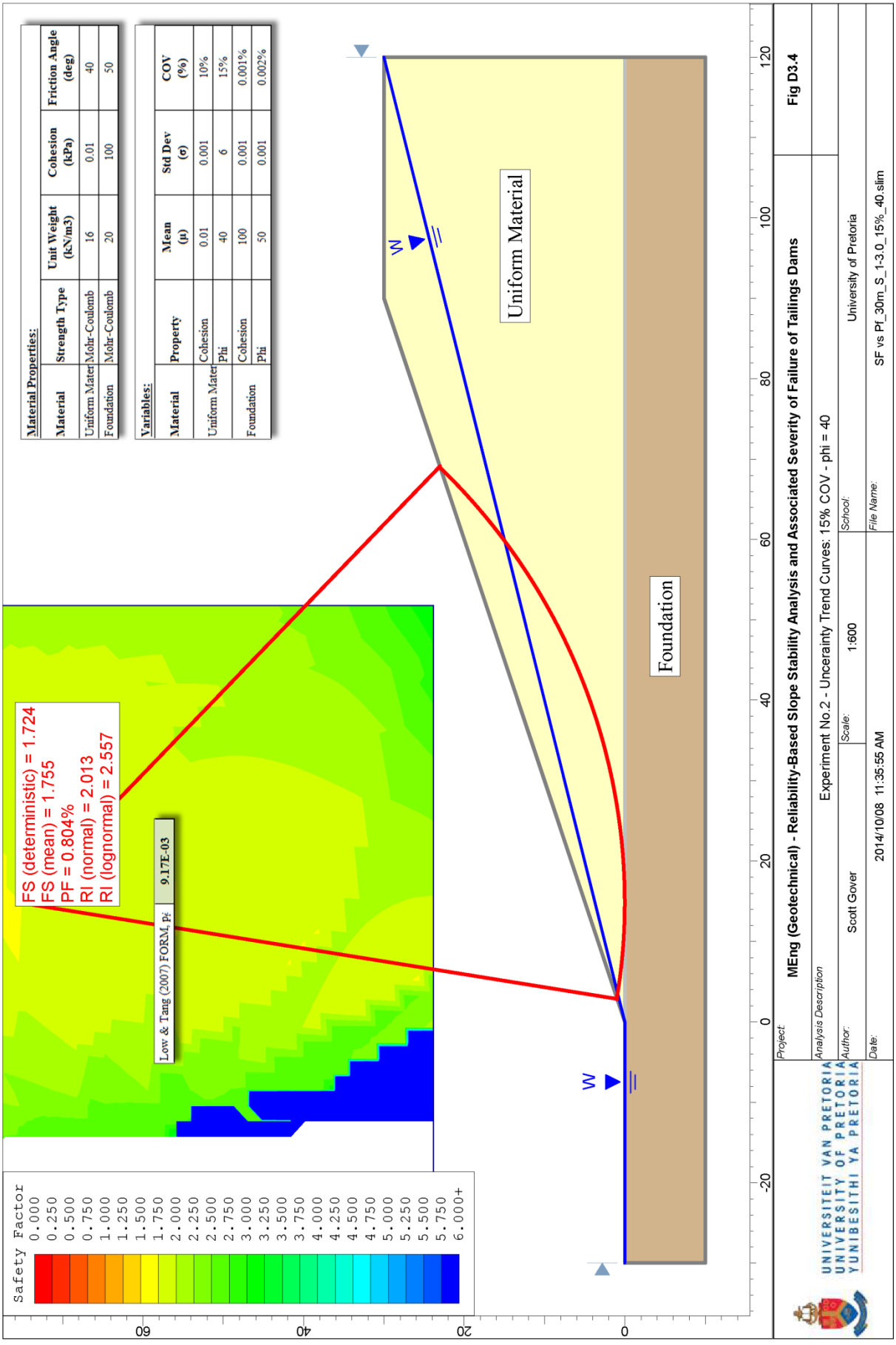
© University of Pretoria



© University of Pretoria



© University of Pretoria



© University of Pretoria